W. STUTZMAN

**NATIONAL ACADEMIES OF SCIENCES AND ENGINEERING**

**NATIONAL RESEARCH COUNCIL**

**of the**

**UNITED STATES OF AMERICA**

**UNITED STATES NATIONAL COMMITTEE**

**International Union of Radio Science**


# National Radio Science Meeting

**3–7 January 1995**

Sponsored by USNC/URSI

University of Colorado
Boulder, Colorado
U.S.A.

**Condensed Technical Program**

**Tuesday, 3 January**

*0855-1200*

| | | |
|---|---|---|
| B/E | EM IDENTIFICATION AND PARAMETER ESTIMATION | CR2-26 |
| D-1 | TUTORIAL SESSION ON RARE EARTH DOPED INTEGRATED OPTICS | CR1-46 |
| E/J | TECHNOLOGY AND REGULATORY INNOVATIONS: IMPACT ON SPECTRUM MANAGEMENT | CR0-30 |
| F-1 | REMOTE SENSING AND CHARACTERIZING THE TROPOSPHERE | CR1-9 |
| G-1 | INCOHERENT SCATTER RADAR AND MODELING STUDIES | CR2-6 |

*1335-1700*

| | | |
|---|---|---|
| E-1 | HIGH POWER ELECTROMAGNETICS | CR1-40 |
| F-2 | PROPAGATION AND ENVIRONMENTAL MEASUREMENT RELATED TO PROPAGATION | CR1-9 |

*1355-1700*

| | | |
|---|---|---|
| A-1 | TIME DOMAIN AND MICROWAVE MEASUREMENTS | CR1-42 |
| B/D-1 | LEAKY WAVES: THEORY AND APPLICATIONS TO HIGH-FREQUENCY INTEGRATED CIRCUITS | CR2-26 |
| F/G/J | EFFECTS ON RADIO SIGNALS FOR TRANSIONOSPHERIC PROPAGATION PATHS | CR0-30 |

*2000-2400*

| | |
|---|---|
| USNC-URSI Meeting | Broker Inn |

**Wednesday, 4 January**

*0815-1200*

| | |
|---|---|
| PLENARY SESSION | Math 100 |

*1335-1700*

| | | |
|---|---|---|
| A/B/K | BIOLOGICAL EFFECTS OF ELECTROMAGNETIC FIELDS | CR1-42 |
| B/F | ROUGH SURFACE SCATTERING | CR2-28 |
| D-2 | DEVICE, PACKAGING AND INTERCONNECTION ISSUES | CR1-46 |
| E-2 | SPECTRUM AND WIRELESS ISSUES FOR THE NII | CR1-40 |
| F-3 | RADAR AND RADIOMETER MEASUREMENTS OF HYDROMETEORS | CR1-9 |
| G/H-1a | IONOSPHERIC DISTURBANCES CAUSED BY LIGHTNING-I | CR2-6 |

*1335-1740*

| | | |
|---|---|---|
| J-1 | NEW US RADIO ASTRONOMY INSTRUMENTATION | CR0-30 |

*1700-1800*

| | |
|---|---|
| Commission A Business Meeting | CR1-42 |
| Commission D Business Meeting | CR1-46 |
| Commission E Business Meeting | CR1-40 |
| Commission F Business Meeting | CR1-9 |
| Commission H Business Meeting | CR2-6 |

**Thursday, 5 January**

*0835-1000*

| | | |
|---|---|---|
| G/H-1b | IONOSPHERIC DISTURBANCES CAUSED BY LIGHTNING-II | CR2-6 |

*0835-1200*

| | | |
|---|---|---|
| B-1 | EM THEORY | CR2-28 |
| D-3 | A TUTORIAL SESSION ON ACTIVE DEVICES | CR1-46 |
| F-4 | PASSIVE REMOTE SENSING OF THE ATMOSPHERE AND OCEAN | CR1-9 |
| G-2a | E- AND F-REGION IRREGULARITIES | CR2-26 |
| J-2 | VLBI POLARIZATION AND CALIBRATION | CR0-30 |

*0855-1020*

| | | |
|---|---|---|
| C-1 | RADAR SIGNAL PROCESSING | CR1-42 |

374 registrants

United States National Committee

INTERNATIONAL UNION OF RADIO SCIENCE

# PROGRAM AND ABSTRACTS

National Radio Science Meeting
3-7 January 1995

Sponsored by USNC/URSI

Copy

p. 33
p. 76-79
pp 201-210
190-192
237-241

127

NOTE:

Programs and Abstracts of the USNC/URSI Meetings are available from:

USNC/URSI
National Academy of Sciences
2101 Constitution Avenue, N.W.
Washington, DC 20418

at $5 for 1983-1995 meetings.

The full papers are not published in any collected format; requests for them should be addressed to the authors who may have them published on their own initiative. Please note that these meetings are national. They are not organized by the International Union, nor are the programs available from the International Secretariat.

## MEMBERSHIP

United States National Committee
INTERNATIONAL UNION OF RADIO SCIENCE

| | |
|---|---|
| Chair: | Dr. David C. Chang* |
| Vice Chair: | Dr. Charles M. Rush* |
| Secretary: | Dr. Susan K. Avery* |
| Immediate Past Chair: | Dr. Chalmers M. Butler* |

Members Representing Societies, Groups, and Institutes:

| | |
|---|---|
| American Geophysical Union | Dr. George C. Reid |
| IEEE Antennas & Propagation Society | Dr. Gary S. Brown |
| IEEE Microwave Theory and Techniques Society | Dr. A. A. Oliner |
| IEEE Geosciences and Remote Sensing Society | vacant |
| American Meterological Society | vacant |

| | |
|---|---|
| Members-at-Large: | Dr. Min-Chang Lee |
| | Dr. Robert J. Mattauch |
| | Dr. Yahya Rahmat-Samii |
| | Dr. Roland T. Tsunoda |
| | Dr. Edgeworth R. Westwater |
| | Dr. Donald Wilton |

Liaison Representatives from Government Agencies:

| | |
|---|---|
| National Telecommunications & Information Administration | Dr. Hans Liebe |
| National Science Foundation | Dr. Hugh Van Horn |
| Federal Communications Commission | Mr. John C.H. Wang |
| Department of the Navy | Mr. William J. Cook |
| Department of the Army | Mr. Earl J. Holliman |
| Department of the Air Force | Dr. Allen C. Schell |
| NASA | Dr. Erwin R. Schmerling |

Chairs of the USNC/URSI Commissions:

| | |
|---|---|
| Commission A | Dr. Sedki Riad |
| Commission B | Dr. Donald G. Dudley |
| Commission C | Dr. David J. Thomson |
| Commission D | Dr. Michael Shur |
| Commission E | Dr. Robert L. Gardner |
| Commission F | Dr. Julius Goldhirsh |
| Commission G | Dr. Sunanda Basu |
| Commission H | Dr. Paul A. Bernhardt |
| Commission J | Dr. Michael M. Davis |
| Commission K | Dr. James C. Lin |

* Member of USNC/URSI Executive Committee

Officers, Chairs and Vice Chairs of Commissions of URSI resident in the United States:

| | |
|---|---|
| Honorary President | Dr. William E. Gordon |
| Vice President | Dr. Thomas B.A. Senior |
| Vice Chair, Commission A | Dr. Motohisa Kanda |
| Vice Chair, Commission B | Dr. Chalmers M. Butler |
| Chair, Commission D | Dr. Tatsuo Itoh |
| Chair, Commission F | Dr. Richard K. Moore |
| Vice Chair, Commission G | Dr. Bodo W. Reinisch |
| Vice Chair, Commission K | Dr. James C. Lin |
| Foreign Secretary of the U.S. National Academy of Sciences | Sherwood Rowland |
| Honorary Members | Dr. Ernst Weber |
| Director, Board on Physics and Astronomy, National Research Council | Dr. Donald C. Shapero |
| Associate Director, U.S. Board on Physics and Astronomy, National Research Council | Dr. Robert L. Riemer |

# DESCRIPTION OF THE INTERNATIONAL UNION OF RADIO SCIENCE

The International Union of Radio Science is one of the world scientific unions organized under the International Council of Scientific Unions (ICSU). It is commonly designated as URSI (from its French name, Union Radio Scientifique Internationale). Its aims are (1) to promote the scientific study of radio communications, (2) to aid and organize radio research requiring cooperation on an international scale and to encourage the discussion and publication of the results, (3) to facilitate agreement upon common methods of measurement and the standardization of measuring instruments, and (4) to stimulate and to coordinate studies of the scientific aspects of telecommunications using electromagnetic waves, guided and unguided. The International Union itself is an organizational framework to aid in promoting these objectives. The actual technical work is largely done by the National Committee in the various countries.

The new officers of the International Union are:

| | |
|---|---|
| President: | Dr. P. Bauer (France) |
| Past President: | Prof. E.V. Jull (Canada) |
| Vice Presidents: | Prof. J. Bach Andersen (Denmark)<br>Prof. P.J.B. Clarricoats (U.K.)<br>Prof T. Okoshi (Japan)<br>Prof. T.B.A. Senior (U.S.A.) |
| Secretary-General: | Prof. P. Lagasse (Belgium) |
| Adjoint Secretary-General: | Prof. P. Van Daele (Belgium) |
| Administrative Secretary: | Mme. Iren Heleu (Belgium) |
| Honorary Presidents: | Sir G. Beynon (U.K.)<br>Dr. W. Dieminger (West Germany)<br>Prof. W. Christiansen (Australia)<br>Prof. W.E. Gordon (U.S.A.)<br>Dr. F.L.H.M. Stumpers (Netherlands) |

The Secretary-General's office and the headquarters of the organization are located at Avenue Albert Lancaster, 32, B-1180 Brussels, Belgium. The Union is supported by contributions (dues) from 38 member countries. Additional funds for symposia and other scientific activities of the Union are provided by ICSU from contributions received for this purpose from UNESCO.

The International Union, as of the XXIVth General Assembly held in Kyoto, Japan, August 25-September 3, 1993, has ten bodies called Commissions for centralizing studies in the principal technical fields.

Every three years the International Union holds a meeting called the General Assembly. The next is the XXVth, to be held in 1996, in Lille, France. The Secretariat prepares and distributes the Proceedings of the General Assemblies. The International Union arranges international symposia on specific subjects pertaining to the work of one or several Commissions and also cooperates with other Unions in international symposia on subjects of joint interest.

Radio is unique among the fields of scientific work in having a specific adaptability to large-scale international research programs, since many of the phenomena that must be studied are worldwide in extent and yet are in a measure subject to control by experimenters. Exploration of space and the extension of scientific observations to the space environment are dependent on radio for their research. One branch, radio astronomy, involves cosmic phenomena. URSI thus has a distinct field of usefulness in furnishing a meeting ground for the numerous workers in the manifold aspects of radio research; its meetings and committee activities furnish valuable means of promoting research through exchange of ideas.

*Tuesday Morning, 3 January, 0855-1200*

Session B/E, 0855-Tues., CR2-26
EM IDENTIFICATION AND PARAMETER ESTIMATION
Chairperson: L. Carin, Dept. of Electrical Engineering, Polytechnic Univ., 333 Jay St., Brooklyn, NY 11201

B/E-1 0900 **EDDY CURRENT RESPONSES OF CANONICAL METALLIC TARGETS, THEORY AND MEASUREMENTS**

Gary D. Sower
EG&G MSI Albuquerque Operations
Albuquerque, NM 87106

Previous papers derive the theory of magnetic field scattering from general conductive targets (C. E. Baum; "Low-Frequency Near-Field Magnetic Scattering from Highly, but not Perfectly, Conducting Bodies," Interaction Note 499, and "The Magnetic Polarizability Dyadic and Point Symmetry," Interaction Note 502, Phillips Laboratory). These results are here applied to bodies of simple geometric shapes (rotationally symmetric) for which the magnetic-polarizability dyadic is reduced to a simpler form, such as a diagonal tensor or even a scalar. These simple canonical shapes have simple natural resonances, which are negative real (damping only) which can be used to identify specific targets. Except for the very special case of a single filamental current loop (thin wire), the natural resonances form an infinite set of damping coefficients which are spaced infinitely closely and cannot be separated. However, the decay curve of the impulse response function is distinctive and unique. Test data are presented which show this impulse response decay function for some canonical shapes of various ferrous and non-ferrous conductors, with high and low conductivity.

B/E-2
0920

# LOW-FREQUENCY NEAR-FIELD MAGNETIC SCATTERING FROM HIGHLY, BUT NOT PERFECTLY, CONDUCTING BODIES

Carl E. Baum
Phillips Laboratory/WSR
3550 Aberdeen Dr. S.E.
Kirtland AFB, NM 87117-5776

This paper considers the properties of the quasi-magnetostatic scattering from permeable and highly conducting scatterers in terms of the magnetic-polarizability dyadic. This is treated in terms of the singularity expansion method (SEM). The natural frequencies are negative real and serve as identifiers of target type. The symmetric dyads which characterize the residues of the first order poles are comprised of real coefficients times real vectors which give the target aspect (orientation in space).

B/E-3
0940

# THE MAGNETIC POLARIZABILITY DYADIC AND POINT SYMMETRY

Carl E. Baum
Phillips Laboratory/WSR
3550 Aberdeen Dr. S.E.
Kirtland AFB, NM 87117-5776

In low-frequency target identification one approach involves quasi-magnetostatic illumination for determining the magnetic polarizability dyadic. For highly conducting permeable targets one can expand this in terms of a set of natural frequencies and modes as well as other limiting terms for identification. The targets of interest may have various point symmetries (rotation and reflection). Such symmetries simplify the forms that this dyadic and the associated modes can take, with the real unit vectors for the various modes aligning according to the symmetry planes and axes, thereby aiding in the identification of a particular target from a library of targets. All of the point symmetry groups are considered to give a complete categorization.

B/E-4
1020

## AN ORTHOGONALITY-BASED METHOD OF EXTRACTING CIRCUIT PARAMETERS FROM NUMERICAL CURRENT DISTRIBUTIONS IN A PLANAR TRANSMISSION LINE

Mike Spowart, Prof. E. Kuester
Department of Electrical Engineering
University of Colorado

A number of methods for extracting circuit parameters from numerical current distributions have been proposed. In most of these methods, current in the feedline is regarded as being expanded as a sum of modes with discrete complex propagation constants. The amplitudes of the froward and backward traveling waves, as well as their propagation constants, are found by solving a system of nonlinear equations. The system of equations may be overdetermined and solved in a least squares manner, e. g., nonlinear Gauss-Newton least squares, least squares Prony, and Pencil-of-Functions methods. A new method has been developed in which the Lorentz Reciprocity theorem and the related property of the orthogonality of independent modes in an arbitrary waveguide are used to de-embed the scattering parameters and propagation constants. Feedlines which are not necessarily electrically long may be used. The method is illustrated by application to planar microstrip transmission line.

Application of the orthogonality principle results in expressions containing products of mode amplitudes, and S-parameters are then obtained by taking ratios of these products. The method works well when products of the discrete mode amplitudes, am bm', am am', and bm bm' are much smaller than a1 b1', a1 a1', b1 b1' respectively. This will be the case when higher order modes have much smaller amplitudes than the fundamental quasi-static mode. These conditions are met when the feedlines are not too short. Comparisons with the three-point and least squares Prony methods show improved performance for de-embedding line lengths longer than 0.5 guide wavelengths. Examples of greater accuracy are: (1) attenuation constants closer to zero over wide frequency range, (2) end conductance, end susceptance, and reflection coefficient closer to expected values for the simple open-end line.

B/E-5
1040

## SHORT-PULSE PLANE-WAVE EXCITATION OF AN OPEN CAVITY: THEORY, SIGNAL PROCESSING, AND OPTOELECTRONIC MEASUREMENT

David R. Kralj and Lawrence Carin
Department of Electrical Engineering
Polytechnic University
333 Jay Street
Brooklyn, NY 11201
(718) 260-3876, FAX (718) 260-3906,
email:lcarin@stealth.poly.edu

Short-pulse plane-wave excitation of an open cavity is considered using an asymptotic model. The approximate asymptotic algorithm parametrizes the fields excited inside the cavity in terms of a concise set of observables. In particular, the time-domain fields excited in the cavity are parametrized in terms of a set of time-domain cavity modes, each of which is characterized at a given observation point by a time-dependent frequency. The wave physics is demonstrated clearly using time-frequency data processing, which extracts the time-domain modal dispersion relation from measured or computed data. Particular time-frequency distributions that are considered include the short-time Fourier transform and windowed superresolution algorithms (Prony, Matrix Pencil Method, etc.). Additionally, a unique set of measured data are presented and analyzed. The short-pulse time-domain data are measured optoelectronically using a pulsed laser to switch planar antennas photoconductively. The optical source is a mode-locked, pulse-compressed, frequency-doubled Nd-YLF CW laser and the antennas are miniature coplanar strip horns fabricated on silicon-on-sapphire. The optoelectronic measurements are performed by using optical fiber to guide the light to the transmitting and receiving antennas, and the small size of the receiving antenna allows it to be placed inside the cavity with minimal perturbation to the cavity fields. The results of the measurements are compared with the approximate theory and are processed as discussed above.

B/E-6 1100 METHOD-OF-MOMENT MODELING OF UWB GROUND-PENETRATING RADAR SCATTERING FROM ARBITRARILY ORIENTED WIRE TARGETS

Stanislav Vitebskiy and Lawrence Carin, Department of Electrical Engineering, Polytechnic University, 333 Jay Street, Brooklyn, NY 11201; (718) 260-3876, FAX: (718) 260-3906; Email: lcarin@stealth.poly.edu

The Method of Moments (MoM) is used to model three-dimensional ultra-wideband (UWB) time-domain scattering from wire targets embedded in various dispersive, lossy soil environments. The ground penetrating (GPEN) scattering is modeled by considering a geometry consisting of a planar interface between a semi-infinite air region and a semi-infinite ground region; the properties of the ground are simulated using published measured data for the dielectric constant and loss tangent of different types of soil and sand. To analyze electromagnetic scattering from general targets embedded in such an environment, we require the medium Green's function. This function is conventionally expressed in terms of highly oscillatory double spectral integrals which cannot be evaluated in closed form (and usually requires computationally expensive numerical algorithms). We have utilized an efficient scheme which represents the Green's function in terms of a compact set of analytic real and complex images, resulting in a significant reduction in computation time. This Green's function has been incorporated into the MoM analysis of UWB time-domain scattering from arbitrarily oriented wire scatterers buried in realistic soils. Several calculate results are presented in which we examine 1) pulse distortion due to soil dispersion and loss, 2) scattered fields from wire targets, 3) wire late-time resonant frequencies in the presence of the soil, and 4) the ability to perform late-time signal processing on GPEN radar scattering signatures.

---

B/E-7 1120 NATIONAL RESEARCH COUNCIL CONSIDERATION OF A POSSIBLE STUDY ON THE EFFICIENT USE OF THE RADIO SPECTRUM

Dr. R.L. Riemer, National Research Council, 2101 Constitution Avenue, Washington, D.C., 20418; and Mr. G.H. Hagn, SRI International, 1611 North Kent Street, Arlington,VA 22209

A Program Initiation Meeting was held at the National Research Council (NRC) in Washington, D.C., on 17 and 18 November 1994, under the auspices of the NRC Board on Physics and Astronomy to consider whether the NRC should undertake a study on "Efficient Use of the Radio Spectrum." Under the chairmanship of Prof. William E. Gordon (Honorary President of URSI), a group of 15 U.S. radio scientists and national spectrum managers from the Federal Communications Commission (FCC), the National Telecommunications and Information Administration (NTIA), and the National Science Foundation (NSF), discussed whether an NRC forum or study should be established on the science, mathematics, and engineering required to enable the efficient use of the radio spectrum. The group considered whether defining a research program in the area of spectrum efficiency would be useful to both the U.S. spectrum managers, the radio science community, and U.S. industry. The consensus of the Program Initiation group regarding such a study was positive. The group's discussions will be summarized and further NRC action will be described.

Session D-1, 0855-Tues., CR1-46
TUTORIAL SESSION ON RARE EARTH DOPED INTEGRATED OPTICS
Chairperson: Jacques Pankove, ECEN, Box 425, Univ. of Colorado at Boulder, Boulder, CO 80309-0425
Organizer: Alan Mickelson, Electrical and Computer Engineering, Univ. of Colorado at Boulder, Boulder, CO 80309-0425

D1-1
0900

# Rare Earth Integrated Optics

Alan Rolf Mickelson
Electrical and Computer Engineering
Campus Box 425
University of Colorado
Boulder, CO
80309-0425

This invited talk will provide an overview for the rest of this tutorial session. Discussion will first be given to the rare earth elements, their atomic structure, their spectroscopy, and then to the problems to which they have been applied, with emphasis given to lasers and optical amplifiers. Discussion will then turn to integrated optics, first the what and why, to be followed by reference to accomplishments achieved in the area before then moving on to the why not yet. This talk will conclude with a discussion of why the work to be presented in this session may be truly significant to present day technology.

D1-2
0920

**Integrated-Optical Devices in Rare-Earth-Doped Glass**

Kevin J. Malone
National Institute of Standards and Technology
Optoelectronic Manufacturing Group, 815.04
325 Broadway, Boulder, CO 80303-3328
(303) 497-3289

Integrated-optical devices made from rare-earth-doped glasses have emerged as an atttractive new technology that is on the verge of commercial insertion. In this presentation, I will give an overview of integrated-optical devices that use rare-earth-doped glasses. I will discuss achievements in device performance. I will also describe fabrication techniques for both thin-film and ion-exchanged devices. I will also comment on various analytical and diagnostic techniques that can be used to improve device performance. I will conclude with a discussion of some current topics in this field.

D1-3
1000

## LUMINESCENCE IN RARE EARTH DOPED SEMICONDUCTORS

R. J. Feuerstein and J. I. Pankove
Dept. of Electrical and Computer Engineering
University of Colorado
Boulder, CO 80309-0425

Since 1985 there has been interest in electrically-pumped rare earth doped semiconductors. The possibility of getting a light source with well defined optical characteristics, even in indirect gap materials such as silicon, has spurred this work on. We will review the advances since 1985 for erbium and neodymium doped Si, GaN, GaAs, InP, InGaP, InP and GaP. Theories explaining the decrease in luminescence as the temperature increases from 77K will be also discussed. Descriptions of the the pumping mechanisms for the rare earths, as well as the requirements for forming active devices, such as optical amplifiers, will be presented. Recent results from our work in Colorado will close the talk.

D1-4
1020

## Rare-Earth-doped Ferroelectric Waveguide Devices

J. Andrew Aust
National Institute of Standards and Technology
Optoelectronic Manufacturing Group, 815.04
325 Broadway
Boulder, Colorado 80303

Rare earth elements are interesting from an optics standpoint because of their technologically useful spectroscopic transitions. Many of these transitions are suited to provide optical gain for laser systems. Most notable of these are the ~1.06 Em emission of neodymium and the ~1.5 Em emission of erbium. Ferroelectric crystals are an attractive optical material because of their electro-optic, acousto-optic, and nonlinear properties. These properties allow control over optical fields in the form of switches, modulators, and frequency converters. Incorporation of rare earth elements into ferroelectric crystals provides for a unique opportunity to combine the properties of both materials in a single device. When the optical fields are confined to channel waveguides (having typical cross-sectional area of ~25 Em2) the increased optical power densities provide for higher gain and more efficient electro-optic, acousto-optic, and non-linear interactionscompared to bulk devices.

The first rare-earth-doped ferroelectric waveguide device was reported in 1989 when Lallier et al. [E. Lallier, J.P. Pocholle, M. Papuchon, C. Grezes-Besset, E. Pelletier, M. DeMicheli, M.J. Li, Q. He, and D.B. Ostrowsky, *Electron, Lett.*, vol. 25, pp. 1491-1492, 1989] successfully laser neodymium at 1.085 Em in MgO:LiNbO3. Since then many advances have been made in this field. Other rare earth elements have been lased and more complicated laser configurations have been realized. Among these achievements are the fabrication of a self-Q-switched laser for the production of high power pulses and a tunable wavelength filter with gain operating in the 1.5 Em range. Most recently, there has been great interest in utilizing the nonlinear properties of lithium niobate in conjunction with the lasing properties of the rare earths to obtain blue-green light. In order to avoid the tight requirements for standard phase matching, quasi-phase matching has evolved as the method of choice for performing second harmonic generation and sum frequency generation. Through proper design of the domain grating period, a wide range of particular wavelengths can be generated. A survey of past accomplishments will be presented along with an update of the work being done at NIST.

D1-5
1100

# Rare Earth Doped Polymers

Alan Rolf Mickelson
Electrical and Computer Engineering
Campus Box 425
University of Colorado
Boulder, CO
80309-0425

This review talk will discuss ongoing efforts to fabricate active devices in rare earth doped polymers. Already gain has been has been demonstrated by Chen in a photolime gelatin doped with rare earth salts. Such hygroscopic (water soluble) polymers, however are not the ones which, like polyimides, epoxies and acrylates, are the ones which are compatible with semiconductor processing. Both acrylates and polyimides have already shown to be excellent optical as well as electrooptical materials that can be used for electronic compatible integrated optics. Rare earth salts, however, do not exhibit sufficient solubility in the solvents which are used in the spin coating of such polymers. Work here in Colorado on the use of rare earth chelates to increase solubility will be discussed. Photoluminescence measurements of such chelates in various solutions and polmer hosts will then be presented. A prognosis for the success of such efforts in achieving a whole new class of integrated optical materials and devices will then be given.

Session E/J, 0855-Tues., CR0-30
TECHNOLOGY AND REGULATORY INNOVATIONS: IMPACT ON SPECTRUM MANAGEMENT
Chairperson: Richard Parlow, NTIA, Dept. of Commerce, Room 4099A, 14th and Constitution Ave. N.W., Washington, DC 20230
Organizers: Willem Baan, NAIC; and David Cohen, NTIA/OSM

E/J-1
0900

## RECENT REGULATORY INNOVATIONS WHICH IMPACT SPECTRUM MANAGEMENT

R.D. Parlow, Associate Administrator
National Telecommunications and Information Administration, Room 4099A
U.S. Department of Commerce
14th & Constitution Avenue, N.W.
Washington, D.C. 20230

Currently, there is rapid growth in wireless communications. Spectrum support for this rapid growth is being provided by several innovative spectrum related regulatory changes by Congress, NTIA, and the FCC. A summary of these innovative regulatory changes is presented along with a progress report on the implementation of the regulatory changes.

Among these regulatory innovations are: (1) the FCC reallocation of 140 MHz of spectrum for new personal communication services (2) the auctioning of spectrum (Congress, 1993 Budget), and (3) the Federal Government (NTIA) required to reallocate 200 MHz of its spectrum for non-government use (Congress, 1993 Budget).

Also to be presented is a synopsis of the actions of the recently completed International Telecommunications Union Plenipotentiary Conference. and a review of the agenda and issues for the upcoming 1995 World Administrative Radio Conference (WARC).

E/J-2
0920

## NEW RADIO SERVICES AND THEIR IMPACT ON RADIO ASTRONOMY

Tomas E. Gergely
Division of Astronomical Sciences
National Science Foundation
Arlington, VA, 22230

In the last decade, demand for radio spectrum based services has undergone an explosion, and it is expected that demand will continue to increase. The increased demand is particularly noticeable at frequencies above 1 GHz, which was relatively unexploited until the early eighties, due to the lack of technology.

Some of these new services, for example mobile satellites, share some bands with radioastronomy. Sharing between these satellite systems and radioastronomy presents extensive coordination problems. This is particularly true of non- geostationary mobile satellite systems, of which there are close to a dozen on the drawing board. These systems use a varying number of satellites, modulation schemes and other characteristics. A large number of astrophysically important lines can be found at mm wavelengths. Commercial activity is, however, also increasing. The mm-wave region may be particularly useful for short range transmissions, because it can be extensively reused, due to the high atmospheric absorption. Finally, the idea of Solar Power Satellites, which was abandoned in the early eighties has been raised again

I discuss the possible timetable for the introduction of these new services, and their potential impact on radio astronomy.

E/J-3
0940

## RADIO ASTRONOMY IN EUROPE: A PASSIVE SERVICE IN AN ACTIVE WORLD

T.A.Th.Spoelstra
Netherlands Foundation for Research in Astronomy
Postbus 2, 7990 AA Dwingeloo
THE NETHERLANDS (spoelstra@nfra.nl)

Radio astronomy as physics of the extra-terrestrial universe is a passive telecommunication service. The interests and characteristics of the applications of active services diverge completely from those of the Radio Astronomy Service. Radio astronomy is, therefore, very vulnerable to man-made interference and sensitive to regulatory issues.

The regulatory issues in Europe are reviewed briefly. The role of European organizations such as the European Community (EC), the European Telecommunications Standards Institute (ETSI) and the Conference Europeenne des Postes et des Telecommunications (CEPT) in this process is summarized. In 1996 the telecommunication legislation in the countries of the European Community has to follow the directives from Brussels. The ETSI works hard to set telecommunication standards. But though industry is well represented in ETSI, the interests of scientific frequency usage has low priority. The CEPT is preparing a European table of frequency allocations which should be effective before 2008. In this preparatory phase it carries out detailed spectrum investigations (DSIs).

The CEPT also works on standardization but in a regulatory manner. Pricing radio frequency use is becoming a hot issue. So far the different European countries have rather different opinions. A big threat for radio astronomy concerns the development and installation of mobile telephone systems and related applications, either terrestrial or spaceborne. Privatizing telecommunication services in politically fragmented Europe while the regulatory bodies are still governmental causes many difficult administrative problems, both nationally and internationally.

The Committee on Radio Astronomy Frequencies (CRAF) of the European Science Foundation (ESF) coordinates the representations made to various national and supranational radio regulatory bodies within Europe for the protection of the Radio Astronomy Service. CRAF activities both at an administrative and at a technical level are described. For instance, CRAF is concerned with setting up programmes of interference monitoring, and seeks to develop technical means for the protection of radio astronomical observations. CRAF also assumes an educational role in making others, particularly the active users of the radio spectrum , aware of the sensitivity and consequent need for protection of the RAS.

E/J-4
1020

# SPREAD SPECTRUM TECHNOLOGY TRENDS

Robert C. Dixon
Omnipoint Corporation
1365 Garden of The Gods Road
Colorado Springs, CO 80907

Spread spectrum technology is being applied today in applications that stretch its abilities (and inabilities) to the limits. Unfortunately, there is no magic, and techniques that provide acceptable performance in the military applications, that have historically been the venue of spread spectrum systems, do not meet the needs of a consumer product. Therefore, spread spectrum methods must be carefully weighed and judiciously employed, if the performance of more conventional techniques is to be equaled. That is, there are times when a spread spectrum approach is not warranted. In some cases a spread spectrum approach is advisable, if not mandated, however.

Spread spectrum methods are especially well adapted to those applications in which spectrum sharing is required. This is particularly true when spectrum is to be shared by multiple, non-cooperating systems, whose uses may vary from industrial heating, to critical communications. It is also true of systems for both government and private sector applications.

This paper addresses approaches applicable to systems intended to serve the needs of multiple users. This includes those that are cooperative and those that are completely oblivious to the existence of anyone or anything else in their little universe.

E/J-5
1100

## THE NEW TECHNOLOGY INNOVATIONS: IMPACT ON SPECTRUM SHARING

David J. Cohen
U.S. Department of Commerce
National Telecommunications and
Information Administration
179 Admiral Cochrane Drive
Annapolis, MD 21401

The projected growth in new radiocommunication services, such as the newly emerging personal communication services, is accompanied by the need for spectrum support. However, these new services can be provided "empty" spectrum only at higher frequencies or if a band is evacuated. The alternative to "empty" spectrum is that systems for these new services share the spectrum with existing systems, technologies and services. In some instances this sharing will be transitory and the existing services will move over time into alternative spectrum. In other instances the sharing is envisioned to be permanent.

This talk will identify and explain new innovative spectrum sharing techniques which have been suggested or adopted. The sharing innovations are technically based upon interference avoidance or spectrum overlays. New sharing of services to be reviewed include: PCS with microwave radio relay, random multiple access spectrum sharing among unlicensed PCS users, HDTV with NTSC television, ultra-wideband (UWB) spectrum overlays, CDMA with existing services and "mixed use" geographical/time sharing. Over the next several years the spectrum management community will have the opportunity to experience and assess with real users the effectiveness of these adopted or proposed spectrum sharing methods.

E/J-6
1120

SPREAD SPECTRUM AND DIGITAL MODULATION FROM THE RADIO ASTRONOMER'S VIEWPOINT.

A. R. Thompson
National Radio Astronomy Observatory
2015 Ivy Road, Suite 219
Charlottesville VA 22903

Direct-sequence spread spectrum and phase modulation of digital signals result in radio spectra which, if unfiltered, take the form of a sinc-squared function of s, the frequency measured from the RF carrier. The peak power levels in the sidebands fall away as $s^{-2}$, i.e. only 6 dB per octave in s, and can cause serious interference to radio astronomy at frequencies well removed from the carrier. In systems that employ such techniques it is generally true that only the central maximum of the transmitted spectrum is accepted by the IF filters of the receiver, so the additional sidebands are unwanted emissions.

A particularly troublesome example has been the Glonass radionavigation satellites which operate in the band 1597-1617 MHz. Severe interference has been caused to radio astronomy in the band 1610.6-1613.8 MHz by satellites for which the wanted emission is well outside this radio astronomy band, and serious interference from Glonass is experienced as far away as the 1660-1670 MHz radio astronomy band (J. Galt, Nature, 345, 483, 1990). Plans to eliminate the interference by a combination of moving the required frequencies away from the radio astronomy band and including additional filtering in the satellites have resulted from discussions between the Glonass Administration and IUCAF (Interunion Commission for the Allocation of Frequencies for Radio astronomy and Space Science), and first steps to relieve the situation have now been taken.

Elimination of the unwanted sidebands near the carrier by means of filters at the carrier frequency may be difficult or impracticable. The problem has been considered in detail by Ponsonby (Proceedings of IEEE Symposium on Spread Spectrum, Oulu, Finland, July 1994), who points out that the decrease of the sideband power will vary as $s^{-6}$ (18 dB per octave) if the phase modulation function is continuous in the first derivative with respect to time. Implementation of this improvement involves rounding off the sharp phase transitions produced by the spectrum-spreading or digital waveforms, and should not significantly change the information content of the wanted central maximum of the spectrum. Ponsonby has devised a method of implementing such modulation, and has demonstrated the expected rate of sideband reduction in a low-frequency laboratory model.

Attenuation of the unwanted sidebands in spread spectrum and digital modulation is becoming critically important because of the increasing use of these techniques. For example, the WARC-1992 allocation of the band 1452-1492 MHz to sound broadcasting includes digital transmission from satellites. Sidebands of such transmissions falling within the 1400-1427 MHz radio astronomy band, if not filtered or otherwise attenuated, could exceed the harmful interference threshold for radio astronomy. The 1400-1427 MHz band is of particular importance to radio astronomy, not only for the hydrogen line but also because its exclusive allocation to passive services allows the highest possible sensitivity to be utilized.

F1-1
0900

## RETRIEVAL OF RAINDROP SIZE DISTRIBUTIONS USING TWO DOPPLER WIND PROFILERS: MODEL RESULTS

W.B. Maguire II and S.K. Avery
University of Colorado, Boulder
Cooperative Institute for Research in Environmental Science
Campus Box 216
Boulder, CO 80309-0216

The behavior of precipitation is of great importance in obtaining a better understanding of heat transport estimates and global processes in the atmosphere. Precipitation behavior as a function of height, with high time resolution, has not been satisfactorily studied. Our work involves improvements to the raindrop size distribution model of Currier *et al.* (Geophys. Res. Letters, 19, 1017–1020, 1992) that utilizes two Doppler wind profilers to obtain accurate measurements of rainfall properties at various altitudes. A UHF Doppler wind profiler provides the precipitation return while a VHF Doppler wind profiler provides information on the vertical clear-air, which is necessary to account for the spectral effects of the mean clear-air vertical velocity and turbulence.

The improved raindrop size distribution (DSD) model has the ability to model the drop size distribution with any number of different functions, including exponential, gamma, and Gaussian. Model improvements include the use of spectral point variances in the nonlinear least-squares minimization to improve fitting abilities, and an improved method of calculation involving the use of the Fast Fourier Transform that greatly increases model speed.

The DSD model is extensively tested at various sites operated by the National Oceanic and Atmospheric Administration's Aeronomy Laboratory. The model is tested on rainfall data from the Flatland Atmospheric Observatory in Flatland, Illinois, Manus Island, Christmas Island, and Darwin Australia. A comparison between tropical rainfall at Christmas Island (2°N, 157°W) and Darwin (12°S, 131°E) is presented that analyzes raindrop size distribution as a function of height and rainfall behavior. Each site has at least one full year of archived rainfall events that are used for model analysis.

F1-2
0920

## A GENERAL EXPRESSION FOR THE SPACE-TIME CORRELATION FUNCTION FOR SPACED-ANTENNA RADARS

R. J. Lataitis[1] and R. J. Doviak[2]
[1]NOAA/Environmental Technology Laboratory
325 Broadway,
Boulder, CO 80303
[2]NOAA/National Severe Storms Laboratory
1313 Halley Circle,
Norman, OK 73068

We present a single-integral expression for the space-time, backscattered-field cross-correlation function applicable to most vertically-pointing, spaced-antenna radar systems. The result only requires that the scatterers be horizontally isotropic and that the receiving antennas lie reasonably close to the transmitting antenna. The integration is over the transverse wavenumber of the scattering irregularities, and the integrand comprises a product of an arbitrary refractive index spectrum and a spectral sampling function.

By associating each transverse wavenumber with a thin refractive phase screen the integral over wavenumber can be interpreted as an integral over zenith angle. The connection between wavenumber and zenith angle arises from an angular spectrum decomposition of the transmitted field and the observation that a plane wave incident on a thin phase screen is scattered into preferred angles (J. A. Ratcliffe, Rep. Progr. Phys., 19, 188-267, 1956). Our result is therefore consistent with an expression for the spatial correlation function derived by Briggs (J. Atmos. Terr. Phys.,54, 153-165, 1992), with his scattering aspect sensitivity function clearly identifiable as the three-dimensional refractive index spectrum evaluated at a vertical wavenumber 2k, where k is the radar wavenumber.

The correlation integral cannot be evaluated analytically for power-law spectra that are most appropriate for scatter from atmospheric turbulence. The approach of many authors has been to use a Gaussian form for the refractive index spectrum (Liu et al., Radio Science, 25, 551-563, 1990). We demonstrate that results obtained using a vertically anisotropic, Kolmogorov-type spectrum differ from those obtained using a Gaussian spectrum. In particular, predicted field correlation scales are equivalent only if the Bragg wavelength (i.e., one half the radar wavelength) is greater than the vertical correlation length of the scatterers.

By using a Gaussian approximation for the Kolmogorov spectrum sampled at a vertical wavenumber of 2k, we are able to obtain a general closed-form solution for the space-time correlation function valid for a Kolmogorov-type refractive index spectrum. A general expression for the field correlation scale is also derived.

F1-3
0940

## STATISTICAL MODELS FOR TROPOSPHERIC RANDOM REFRACTIVITY

Dr. J. Gozani
Cooperative Institute for Research in Environmental Sciences
University of Colorado at Boulder
Boulder, Colorado 80309-0449

Recent in-situ temperature measurements by aircraft, and balloons, revealed that the medium is randomly layered, highly irregular and anisotropic [NASA¡ UCLA Workshop on Laser Propagation in Atmospheric Turbulence, February, 1994]. Consequently, it became apparent that we are confronted with challenging new research, because of the following reasons: (1) The known theory of wave propagation in random media, which was developed for homogeneous and isotropic medium is not applicable to such conditions. (2) To define the problem, new models that describe the inhomogeneous medium are required. (3) New data measurements and processing that are applicable to inhomogeneous medium are necessary. (4) Higher complexity than before indicates that the problem is more computer intensive, than propagation in homogeneous random medium.

The theory for (1) was already formulated by Gozani [Opt. Lett. 17, 559 (1992)], [SPIE, Vol. 1971, 15 (1992)], [Proceedings of the NASA-UCLA Workshop on Laser Propagation in Atmospheric Turbulence, February, 1994. Editors: A.V. Balakrishnan and R. Butts].

The presentation will address to (2), whereas (3), and (4) are still open. The paper suggests heuristic models based on generalizations of the Poisson process, which is flexible in emulating realistic media. We will show how a turbulent atmospheric boundary layer flow that includes coherent structures can be simulated, and discuss possible generalizations.

F1-4
1020

## STUDY OF ECHOES OBSERVED DURING BIRD MIGRATION BY PROFILING RADARS OPERATING ON THREE DIFFERENT FREQUENCIES

J. M. Warnock, W. L. Clark, W. L. Ecklund, and T. E. VanZandt
Aeronomy Laboratory, NOAA/ERL, Boulder, CO 80303
W. R. Evans
Cornell Laboratory of Ornithology, Ithaca, NY 14850

During conditions favorable for bird migration, UHF and higher frequency radars frequently detect very strong echoes apparently due to migrating birds. In some cases these bird echoes may dominate the radar signals, so that the wind profiling capability of a radar may be compromised. In order to help distinguish and characterize the bird echoes from other sources such as insects, hydrometers, and clear air, we conducted a field campaign from 28 September to 7 October 1994 at the Flatland Atmospheric Observatory (FAO), located near Urbana-Champaign, IL. A unique sensitive bird-call listening and recording system developed by one of the authors (Evans) was installed at the site and operated eight hours each night beginning at 18:45 CDT. This equipment frequently detected bird calls during nights when the wind and other meteorological conditions were favorable for migration. Profiling radars operating at 50, 915, and 2835 MHz (6 m, 32 cm, and 10 cm wavelength, respectively) were operated nearly continuously during the campaign and both the spectra and moments were displayed in real time and recorded. Both the 915 and 2835 MHz radars are very sensitive to bird echoes, whereas the 50 MHz radar is insensitive to them. Because the relative sensitivity of echoes from competing sources for the three radars are usually different from the bird ones, it may be possible under some conditions to identify the bird echoes and help establish criteria for their detection by a single radar. Preliminary results will be given at the meeting.

F1-5
1040

# MUELLER MATRIX CHARACTERIZATION OF ELECTROMAGNETIC WAVES SCATTERED FROM IRREGULAR STRATIFIED MEDIA --FULL WAVE SOLUTIONS

Ezekiel Bahar and Yuzhi Zhang
Department of Electrical Engineering
University of Nebraska-Lincoln
Lincoln, NE 68588-0511

The scattered electromagnetic waves from random rough surfaces can be fully characterized by the (41) Stokes vectors. The scattered Stokes vectors are related to incident Stokes vectors through the (44) Mueller matrix for the rough surfaces. The Mueller matrix characterization of electromagnetic fields scattered from irregular stratified media can be applied to the problems of remote sensing, thin film analysis, and communications in stratified media. To this end, the Mueller matrix elements are derived based on the full wave solutions for the vertically and horizontally polarized fields scattered from an irregular stratified structure consisting of three distinct media, air, coating material and substrate. The upper and lower interfaces are two dimensionally random rough surfaces. The thickness of the coating material is uniform. The waves are depolarized upon scattering, since the normal to the rough surface is not restricted to the reference plane of the incidence. The full wave solutions satisfy the duality and reciprocity relationships in electromagnetic theory and the surface element scattering coefficients are invariant to coordinate transformations (E. Bahar, Radio Science, 23, 5, 749-759, 1988, E. Bahar and M.- A. Fitzwater, IEEE Trans. on AP, Vol. 37, No. 12, 1609- 1615, 1989).

The terms of the full wave solutions for the scattered fields from the irregular three media structure have simple physical interpretations. The first term is associated with waves scattered upon reflection from the upper interface. The second term is associated with waves that make multiple round trips in medium 1 before being scattered upon transmission into medium 0 from medium 1. The third term is associated with waves that are scattered upon transmission into medium 1 from medium 0 and make multiple round trips in medium 1 before they are transmitted back to medium 0. The fourth term is associated with waves that make multiple round trips in medium 1 before being scattered upon reflection from below the upper interface and then make multiple round trips in medium 1. The fifth term is associated with waves that are scattered upon reflection from the lower interface. These waves are multiply reflected in medium 1 before and after they are scattered by the surface element.

In this work the Mueller matrix elements for the coated rough surfaces are evaluated for the backscatter case. The results show that the non zero Mueller matrix elements are more sensitive to the changes in the surface slopes than the surface heights. Some of the Mueller matrix elements are more sensitive to the changes in the thickness of the coating material than others.

G1-1
0900

## FIRST RESULTS FROM SPECTRAL MEASUREMENTS OF INCOHERENT-SCATTER OBTAINED BY ALTAIR

R. T. Tsunoda, R. C. Livingston, and M. Mendillo
Geoscience and Engineering Center
SRI International
Menlo Park, CA 94025

ALTAIR, an incoherent-scatter (IS) radar located in the Kwajalein Atoll, Marshall Islands, was outfitted in 1990 with a data acquisition and processing system that enabled it to obtain spectral measurements for the first time. Because ALTAIR is not only fully steerable but also the only radar at equatorial latitudes that can obtain IS returns from below 200-km altitude, it is capable of providing information about the electrodynamics of the equatorial ionosphere as a function of altitude and latitude, a capability that has never before been available. We present some of the first results of such measurements, including example profiles of plasma density, electron and ion temperatures, and ion velocity. We also discuss how this new measurement capability can address some of the outstanding questions in equatorial physics.

G1-2
0920

## HIGH-RESOLUTION ISR OBSERVATIONS OF LAYER AND WAVE STRUCTURES IN THE 80-200 KM ALTITUDE REGION ABOVE ARECIBO: INITIAL RESULTS AND INTERPRETATIONS

J. D. Mathews[1] and M. P. Sulzer[2], P. Perillat[2]
Communications and Space Sciences Laboratory
[1]The Pennsylvania State University
University Park, PA, USA 16802
[2]Arecibo Observatory
National Astronomy and Ionosphere Center
Arecibo, Puerto Rico 00613

The Arecibo 430 MHz Incoherent Scatter Radar (ISR) is being used with an 88 baud, 1 ms/baud code to observe electron concentrations in the 80-280 km altitude region of the ionosphere at 150 m and 10 s height and time resolutions, respectively. We report initial results from these electron concentration observations that reveal the presence of layers and waves at scales approaching or equaling the resolution limits. Specifically, tidal ion layers and sporadic E layers in the 100-110 km altitude region often display significant peaks and edges that appear in only one range gate. Ion layering events similar to the Complex Layer Structures observed during the AIDA-89 campaign and associated with sporadic sodium layers, have been observed to involve the presence of considerable wave activity--with apparent periods as short as 2 minutes--and as many as five layers in the 90-100 km region. Waves with approximately 12 minute apparent period have been observed extending from about 105 km to above 280 km. These waves have an apparent vertical wavelength of 30 km below 155 km altitude and 90 km above this height, respectively. We offer an interpretation of this observed shift in apparent wavelength along with an updated view of the layering process in the presence of intense, small-scale wave activity.

G1-3
0940

## COMPOSITION OF TIDAL ION LAYERS IN THE E REGION

M. W. Lemon and K. L. Miller
Center for Atmospheric and Space Sciences
Utah State University
Logan, UT 84322-4405

Incoherent scatter radar observations of descending tidal ion layers in the upper E region were made using the 430-MHz radar at the Arecibo Observatory. Continuity arguments were used to determine if the measurements are consistent with layer composition being ambient NO+ and O2+ or consistent with metallic ions. A tidal layer was observed on the night of April 30, 1994, which descended from the base of the F region to an altitude of about 120 km. Changes in the column density of the layer suggest that its composition is primarily ambient ions. Changes in the column density of a simultaneously occurring sporadic-E layer suggest a layer dominated by metals. The formation of a smaller layer immediately below the tidal layer appears to be correlated with changes in the larger layer. The formation of the small layer is preceded by fluctuations in the shape of the larger layer. Measurements of changes of the ionization profile suggest that winds generated by interference between the semi-diurnal tide and a gravity wave scavenge ionization from the bottom of the tidal layer to form the smaller layer. Theory and discussion are presented.

G1-4
1000

## FULL PROFILE ANALYSIS OF MILLSTONE HILL INCOHERENT SCATTER E REGION DATA COLLECTED DURING THE AUGUST 10-16, 1994 CADITS/MLTCS CAMPAIGN

J. M. Holt
MIT Haystack Observatory
Westford, MA 01886

Millstone Hill observations during the August 10-16, 1994 CADITS/MLTCS campaign yielded daytime E and F region and nighttime F region data. E region coverage was limited to the daytime due to low nightime electron densities. A 16-baud alternating code was used for the E region spectral measurements. Previous experiments using this technique had yielded good incoherent scatter spectra down to 100 km. During the August experiment, many spectra were also measured between 90 and 100 km, providing the first extensive set of Millstone Hill spectral measurements in this region.

Below about 120 km, ion-neutral collisons have an important effect on the incoherent scatter spectrum, and must be taken into account when analyzing the data. Between 100 and 120 km, both temperature and collision frequency can be determined from a single spectrum, though this becomes increasingly difficult as the altitude decreases and collisions become more important. Below 100 km, the spectrum is collision dominated, and only one parameter, which dependes both on collision frequency and temperature, can be determined from a single spectrum.

However, both temperature and collision frequency can be determined by means of a full profile analysis in which all the E region spectra are analyzed simultaneously. The full profile analysis is able to make use of the assumption that the collision frequency follows a diffusive equilibrium distribution corresponding to the derived temperature and average neutral mass. Temperature and collision frequency results using this analysis technique are presented for the August campaign.

G1-5
1020

## BI-STATIC INCOHERENT AND COHERENT SCATTER RADAR EXPERIMENTS AT MILLSTONE HILL

J. C. Foster[1], J. M. Holt[1], A. D. Pailes[1], D. R. Moorcroft[2], H. Atkinson[2] and B. Jackel[2]
[1]MIT Haystack Observatory
Westford, MA 01886
[2]University of Western Ontario
London, Ontario, Canada N6A 3K7

A new radar receiver has been constructed to support bi-static ionospheric experiments using the Millstone Hill UHF radar. The project was undertaken by the MIT Haystack Observatory with supplementary funding provided by the Canadian Network for Space Research and the MIDAS-C receiver is now operated by the University of Western Ontario. With a low system noise temperature and sophisticated signal processing capabilities, MIDAS-C can be used as an incoherent scatter radar receiver when used with an antenna of appropriate gain. Operated monostatically during tests at Millstone Hill, the system successfully detected incoherent scatter signals. A wide dynamic range combined with a variable attenuation stage also allows the system to be used for observing E region coherent scatter. Bi-static auroral echoes have been seen while using the 2 MW transmitter and 42-m dish at Millstone Hill, and a 2-m dish at the University of Western Ontario. Planned future research includes bi-static F region incoherent scatter observations using the Millstone Hill transmitter, and a 46-m receiving antenna at the Algonquin Space Complex in Algonquin Park, Ontario. An further possibility is the simultaneous observation of coherent and incoherent scatter from the same volume of the E region plasma.

G1-6
1100

## IMPROVING IRI90 LOW LATITUDE IONOSPHERIC SPECIFICATION

D. T. Decker (Institute for Space Research, Boston College, 885 Centre St., Newton, MA 02159; 617-377-5194; decker@plh.af.mil)
D.N. Anderson (Phillips Laboratory/GPIM, Hanscom AFB, MA 01731)
A.J. Preble (Phillips Laboratory, Laser and Imaging Directorate, Kirkland AFB, NM, 87117)

At low latitudes a number of comparisons between the IRI90 model of F-region electron density profiles with observed profiles measured by the Jicamarca incoherent scatter radar indicate that during the daytime, the observed profile shape is much broader in altitude than that specified by IRI90 while at night, just after sunset, observed Hmax values are significantly higher. This is especially true during periods of high solar activity. The theoretically-derived ionospheric parameters such as Hmax, Nmax and profile shape which are contained in the Parameterized Ionospheric Model (PIM) have been shown to be in better agreement with Jicamarca observations. This paper describes an attempt to improve IRI90 at low latitudes by calculating three ionospheric parameters, the profile half thickness, Nmax, and Hmax from PIM as a function of latitude, longitude, and solar local time for a variety of solar cycle, seasonal and geomagnetic conditions. The generation of electron density profiles using these three parameters will be presented as well as a description of how these expressions might be implemented into the IRI90 model. Finally, we discuss the degree of improvement which has been achieved by comparing these profile parameters with a number of ionospheric observations not only at the magnetic equator but also at higher magnetic latitudes near the crests of the equatorial anomaly.

G1-7
1120

## IONOSPHERIC EFFECTS ON LOW LATITUDE NEUTRAL DYNAMICS AND COMPOSITION

W.S. Borer and D.N. Anderson
Phillips Laboratory, PL/GPIM, Hanscom AFB, MA 01731
T.J. Fuller-Rowell and M.V. Codrescu
CIRES, University of Colorado/NOAA Space Environment Lab., Boulder, CO 80303

Anomalies in the temperature, winds, and densities of the low latitude thermosphere have been observed with satellite sensors (Raghavarao, et al, Geo Res Let, 18, 1193-1196, 1991 and Hedin and Mayr, J Geo Res, 78, 1688-1691, 1973). The spatial and temporal location of these anomalies correlate well with features of the well known equatorial anomaly in the ionosphere. First-principles calculations of the coupled neutral composition and dynamics have recently been completed using a global three-dimensional thermosphere model (Fuller-Rowell and Rees, J Atmos Sci, 37, 2545-2567, 1980 and Plan Spac Sci, 37, 1209-1222, 1983) incorporating a Parameterized Ionosphere Model(PIM) to specify the electron density. The equatorial anomaly is well-described by PIM so this approach offers a promising way to investigate the effects of the low latitude ionosphere on neutral densities and dynamics. Results show that several of the neutral composition and dynamical anomalies are seen only when the equatorial anomaly is evident. The ability of the model to simulate all the observed features and elucidate their origin will be discussed.

G1-8
1140

## IONOSPHERIC ELECTRON DENSITIES CALCULATED USING DIFFERENT EUV FLUX MODELS AND CROSS SECTIONS: COMPARISON WITH RADAR DATA

M. J. Buonsanto[1], P. G. Richards[2], W. K. Tobiska[3], S. C. Solomon[4], J. A. Fennelly[5], and Y.-K. Tung[1,6]

The recent availability of the new EUVAC (P. G. Richards et al., J. Geophys. Res., 99, 8981–8992, 1994) and EUV94X (W. K. Tobiska, Solar Physics, 152, 207–215, 1994) solar flux models and new wavelength bin averaged photoionization and photoabsorption cross section sets led us to investigate how these new flux models and cross sections compare with each other and how well electron densities ($N_e$) calculated using them compare with actual measurements collected by the incoherent scatter radar at Millstone Hill (42.6°N, 288.5°E). In this study we use an updated version of the photochemical model of Buonsanto et al. (J. Geophys. Res., 97, 10513–10524, 1992). For the *F2*-region, this model is coupled with determinations of the motion term in the $N_e$ continuity equation obtained from nine-position radar data. We also include two simulations from the FLIP model of P. G. Richards et al. All the model results underestimate the measured $N_e$ in the *E* region, except that the EUV94X model produces reasonable agreement with the data at the *E*-region peak because of a large Lyman β (1026 Å) flux, but gives an unrealistically deep *E-F1* valley. The photochemical model predicts that the $O_2^+$ density is larger than the $NO^+$ density in the *E* region, while numerous rocket measurements show a larger $NO^+$ density. Thus the discrepency between the photochemical model and the radar data in the *E* region could be due to an incomplete understanding of the $NO^+$ chemistry. In the *F2* region, the photoionization rate given by EUV94X is significantly larger than that given by the EUVAC and earlier models. This is due to larger EUV fluxes in EUV94X compared to EUVAC over the entire 300–1050 Å wavelength range, apart from some individual spectral lines. In the case of EUVAC, this is partly compensated for by larger photoelectron impact ionization due to the larger EUV fluxes below 250 Å.

1. Massachusetts Institute of Technology, Haystack Observatory, Westford, MA 01886.
2. Computer Science Dept. and Center for Space Plasma and Aeronomic Research, The University of Alabama, Huntsville, AL 35899.
3. Jet Propulsion Laboratory, Pasadena, CA 91109-8099.
4. Laboratory for Atmospheric and Space Physics, University of Colorado, Boulder, CO 80309-0392.
5. Center for Space Plasma and Aeronomic Research, The University of Alabama, Huntsville, AL 35899.
6. Physics Dept., University of California, Berkeley, CA 94720.

G1-9
1200

## STORM TIME DEPENDENCE OF LOW LATITUDE F REGION ZONAL PLASMA DRIFTS

Ludger Scherliess and Bela G. Fejer
Center for Atmospheric and Space Sciences
Utah State University
Logan, UT 84322-4405

Incoherent scatter radar observations from Jicamarca and Arecibo are used to study the effect of magnetic activity on low latitude zonal plasma drifts. We show that these perturbation velocities change considerably with storm time. The short time responses, proportional to rapid changes in the high latitude current system, result from the prompt penetration of high latitude electric fields to low latitudes. The longer term effects are due to the dynamo action of storm time winds driven by enhanced energy deposition into the high latitude ionosphere. We use a new data analysis technique to separate the disturbance drifts associated with these prompt penetration and delayed effects. This technique is also used for quantitative comparisons between the experimental data and results from global convection and storm time thermospheric circulation models.

G1-10
1220

## AVERAGE REPRESENTATIVE PROFILES FROM IONOGRAMS

Xueqin Huang and Bodo W. Reinisch
University of Massachusetts Lowell Center
for Atmospheric Research
450 Aiken Street, Lowell, MA 01854, USA

For comparison with ionospheric models it is useful to define an RAverage Representative ProfileS (ARP) for a given month and time of day, derived from the individual vertical electron density profiles obtained from ionograms. A robust algorithm has been developed that calculates ARP from any set of profiles. The method is based on the Huang-Reinisch [1983] profile inversion technique that presents each ionospheric layer in the form h = hm + gl/2 SUM[Ai Ti*(g)]. The ARP function is represented in the same form. The method is applied to ionogram data from Jicamarca, Arecibo and Millstone Hill, and the hourly ARP curves are compared with the corresponding IRI profiles.

Session A-1, 1355-Tues., CR1-42
TIME DOMAIN AND MICROWAVE MEASUREMENTS
Chairperson: M. Kanda, NIST, Boulder, CO; and S. Riad, VPI, Blacksburg, VA

A1-1
1400

## Time-Domain Impulse Testing of an Anechoic Chamber

**Robert T. Johnk**
**Arthur R. Ondrejka**
**Motohisa Kanda**

**National Institute of Standards and Technology**
**Boulder, Colorado**

During the past five years, there has been much interest here at NIST in the time-domain measurement of pyramidal absorber reflectivity. This effort has been driven by the need to predict the performance of anechoic chambers that utilize these materials. The measurements have been quite effective in the assessment of the performance of pyramidal absorbers. However, the past effort has been limited only to the characterization of absorptive materials. While the ability to measure reflectivity is important for the prediction of the performance of anechoic chambers, it is essential to measure the performance of a chamber once it is constructed to see how it actually behaves.

A study has been performed on the NIST anechoic chamber using a time-domain measurement system consisting of an impulse generator, a sampling scope, two TEM horns, and a computer for signal processing. The chamber performance has been studied using a combination of time windowing and FFT's in order to construct the cumulative decay spectrum for the chamber. The results indicate cavity-like behavior with a moderate amount of reverberation at the low frequencies. As the frequency increases, the cavity-like behavior disappears rapidly as the pyramidal absorber reflectivity decreases. Depending on the frequency range of interest, the signal processing methodology has to be modified in order to account for changing absorption.

A1-2
1420

# DIELECTRIC CHARACTERIZATION OF CONCRETE SLABS USING TEM HORN ANTENNA

*Wansheng Su, Raqibul Mostafa*
*Sedki. M. Riad, and Imad L. Al-Qadi*
The Bradley Department of Electrical Engineering
Virginia Polytechnic Institute and State University
Blacksburg, Virginia 24061-0111
Phone: 703-231-4463 Fax: 703-231-3362

Nondestructive techniques to evaluate the condition of concrete structures, such as bridges and highway, are important to determine the servability and the need for repairs to these structures. Electromagnetic approaches are currently under evaluation to test voids, cracks and deteriorations in a concrete wall. This paper focuses on tests performed on concrete slab specimens under laboratory conditions using TEM horn antennae. TEM horn antennae are used due to their wideband performance [1]. An impulse is used as exciting signal and the response is acquired using a wideband sampling oscilloscope. Time domain techniques are used to extract the material properties which is correlated to the concrete mechanical properties. Due to the heavy weight of the slab specimen, it is rebutted using steel rods. A 1'x1' spacing between the rods is designed to reduce the effects of the steel rods to the characterization. Preliminary test results of the characterization are shown over the frequency range from 500 MHz to 10 GHz.

Reference

[1] A. R. Ondrejka, J. M. Ladbury, and H. W. Medley, "TEM Horn Antenna Design Guide", NIST Internal Preliminary Report.

A1-3
1440

## IMPROVED MULTILINE TRL CALIBRATION OF A TIME DOMAIN NETWORK ANALYZER

Roger B. Marks, Leonard A. Hayden, and Jeffrey A. Jargon
National Institute of Standards and Technology
Mail Code 813.06, 325 Broadway
Boulder, CO 80303

A time domain network analyzer (TDNA) measures frequency-dependent network parameters using a transient source. Accurate TDNA measurements require a calibration to remove the effects of cables and connectors, nonideal source and sampler response, and source and sampler mismatch.

Recently (R. B. Marks, D. F. Williams, and F. Williams, "Multiline Through-Reflect-Line Calibration of a Time Domain Network Analyzer," XXIVth URSI General Assembly, Kyoto), we applied the multiline through-reflect-line (TRL) method (R. B. Marks, *IEEE Trans. Microwave Theory Tech.*, **39**, 1205-1215, 1991) to TDNA calibration. TRL uses transmission lines as fundamental calibration standards and thereby obviates the need for characterized transfer standards. The multiline version of TRL takes advantage of the broadband nature of the instrument by permitting calibration over a wide frequency band. The method properly accounts for the frequency-dependent characteristic impedance $Z_0$ of the calibration transmission lines and full characterizes them.

Here we report an improved calibration resulting from control of and correction for drift in the time base. TDNA is particularly susceptible to this error because slight variations in the time of the incident step lead to large inaccuracies at all frequencies. Here we consider internal TDR calibration methods as well as an external method of drift correction. We illustrate the results by comparing TDNA to a conventional frequency-domain network analyzer (FDNA).

The results show that the multiline TRL calibration is effective for TDNA. The figure shows a comparison of the real part of the effective relative permittivity of coplanar waveguide on GaAs using TDNA and FDNA.

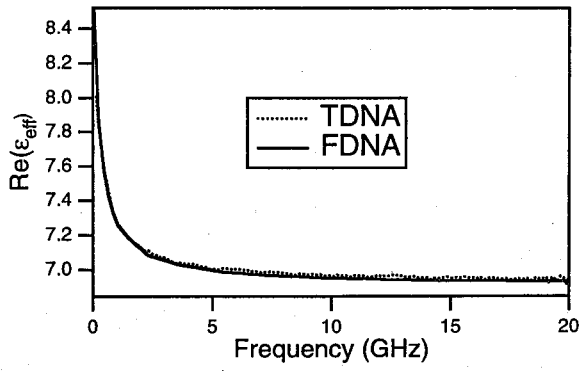

A1-4
1500

**MEASUREMENTS OF SHIELDING EFFECTIVENESS AND CAVITY CHARACTERISTICS OF AIRPLANES**

D.A. Hill, R.T. Johnk, A.R. Ondrejka, and D.G. Camell
Electromagnetic Fields Division
National Institute of Standards and Technology
Boulder, CO 80303

The possibility of electromagnetic interference to aircraft electronics from high intensity radiated fields (HIRF) has been under study for several years. Because the shielding effectiveness of aircraft skins is not well characterized, the interior fields that excite aircraft electronics are not well characterized even if the incident field is known. The National Institute of Standards and Technology (NIST) has recently developed a theoretical model for the shielding effectiveness (SE), quality factor (Q), and time constant of electrically large cavities with apertures and has validated the model with measurements on a loaded rectangular cavity with an aperture (D.A. Hill, M.T. Ma, A.R. Ondrejka, B.F. Riddle, M.L. Crawford, and R.T. Johnk, IEEE Trans. Electromag. Compat., 37, 169-178, 1994).

The purpose of this talk is to describe the measurement techniques that were used and results that were obtained on three small (twin-engine) airplanes. Two of the airplanes were fully equipped for flight and are thought to be representative of twin-engine planes currently in use. The third airplane was less representative because it had been partially stripped for parts. Both cw and pulse measurement methods were used to obtain SE, Q, and time constant. The frequency range was from 400 MHz to 18 GHz to correspond to the range where the potential HIRF field amplitudes are high.

For both cw and pulse measurements, the main cabin of the airplane under test was instrumented with a receiving antenna and a mechanical mode stirrer (paddle wheel). The measured quantities were averaged over stirrer position, but the cumulative distributions were also examined. For measurements of Q and time constant, the transmitting antenna was located inside the main cabin. Comparisons of Q and time constant obtained by cw and pulse measurements were made with theory. The measured Q values increase with frequency in an irregular manner, but are on the order of 200. For SE measurements, the transmitting antenna was located 15 m from the airplane at a number of aspect angles. The measured SE values are variable, but are on the order of 15 dB. For incidence from the rear of the airplane, the SE values are higher because the windows are shadowed.

A1-5
1540

# COMPLEX PERMITTIVITY MEASUREMENTS OF LIQUIDS USING A SHIELDED OPEN CIRCUIT

Michael D. Janezic and James Baker-Jarvis
National Institute of Standards and Technology
Electromagnetic Fields Division, 813.08
Boulder, CO 80303 U.S.A.

This paper presents an improved method of measuring the complex permittivity of liquids using a shielded open circuit, shown below. An advantage of the shielded open circuit is the simplicity of sample installation, broad frequency coverage, and strong electric field in the sample region. In the past, only a dominant TEM mode analysis was used to characterize the shielded open circuit (H.E. Bussey, *IEEE Trans. Instrum. Meas.*, vol. 29, pp. 120-124., June 1980). However, as both the frequency and the sample permittivity increase, higher-order modes are excited, and the single-mode TEM analysis becomes inadequate. In our formulation of the problem, a TEM mode is assumed to propagate in the coaxial region of the open circuit. At the transition between the coaxial region to the circular waveguide region, a TEM mode is reflected and higher-order $TM_{0n}$ modes are excited.

Complex permittivity measurements of several liquids, using a 14 mm shielded open circuit operated between 10 MHz and 1 GHz, are presented. These include deionized water, isopropyl alcohol, and methyl alcohol.

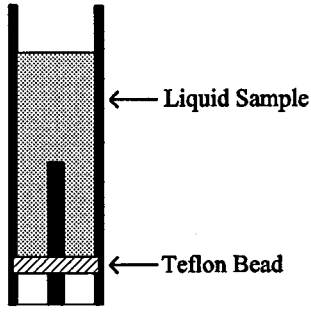


Shielded Open Circuit Holder

A1-6
1600

## THE CHARACTERISTICS OF INTERFERENCE PATTERNS PRODUCED BY ULTRA-WIDEBAND ARRAYS

Jodi L. Schwartz and Bernard D. Steinberg
Valley Forge Research Center
University of Pennsylvania
Philadelphia, PA

This short paper addresses interesting problems in the design of verylarge, widely-spaced, ultra-wideband antenna arrays. It is shown that for such an array the common picture of the radiation pattern is no longer adequate for describing the interference of the pulses emitted from the array, and that aperture taper not only ceases to be an effective method for controlling the sidelobe level in the distant sidelobe region of the interference pattern but SNR is needlessly sacrificed by its unsuccessful attempt at sidelobe control. The characteristics of the interference pattern are related to array parameters such as size, bandwidth, number of elements, element spacing, and scan angle.

A1-7 1620

# THE UNCERTAINTY IN Y-FACTOR MEASUREMENTS

Sunchana P. Pucic
Electromagnetic Fields Division
National Institute of Standards and Technology
Boulder, CO 80303

The noise powers as measured by the NIST noise calibration systems are on the order of 1 mW, with a dynamic range of $\approx$ 10 dB for typical hot sources with the ENR of 15 dB. The measurements are performed in quick succession by the dc substitution technique, using a single dual-element thermistor mount connected to the NIST Type IV power meter. The relative standard uncertainty in the noise temperature of the unknown noise source $T_x$ due to the uncertainty in the measurement of the Y-factor $Y = (P_x/P_a - 1)/(P_s/P_a - 1)$ is

$$\frac{\partial T_x}{T_x} = \left|\frac{T_s - T_a}{T_x}\right| \partial Y, \tag{1}$$

where the subscripts $s, a, x$ stand for the cryogenic standard, the ambient standard, and the unknown noise source. The uncertainty $\partial Y$ has the following sources:

1. The dominant bolometer uncertainty is the dual element substitution uncertainty, a decrease (G.F.Engen, IEEE Trans. Instr. Meas. 13, 58-64, 1964) in the effective efficiency of the thermistor mount with increasing power levels. This dependency on power is modelled by a linear relationship $\eta_e = \eta_{e0} + kP$, where $\eta_0$ is the effective efficiency at zero power level, and $k$ is a negative coefficient. The bolometer uncertainty is the largest uncertainty affecting the Y-factor measurements.

2. The uncertainty due to the limitations of operational amplifiers and resistors making up the NIST Type IV power meter is negligible in comparison to the bolometer uncertainty (N.T.Larsen, IEEE Trans. Instr. Meas. 25, 58-64, 1976).

3. The Type B uncertainty of the laboratory-quality voltmeter used in the calibration system is also negligible. The Type A uncertainty associated with the voltmeter is accounted for in the overall experimental uncertainty.

4. The uncertainty due to drift is caused by temperature changes in the radiometer components and the environment. Temperature-controlled water circulating through water jackets keeps the drift negligible during a measurement.

Assuming the uncertainty in the slope of the effective efficiency and the uncertainty in the intercept are uncorrelated, the Y-factor uncertainty is

$$\partial Y \approx \frac{1}{(Y_s - 1)^2(\eta_{e0} - kP_a)^2} \left\{ \frac{P_x}{P_a}(Y_s - 1)\left[P_a(\eta_{e0} - kP_x) - P_x(\eta_{e0} - kP_a)\right] - \frac{P_s}{P_a}(Y_x - 1)\left[P_a(\eta_{e0} - kP_s) - P_s(\eta_{e0} - kP_a)\right] \right\} \partial k, \tag{2}$$

where $k$ has been estimated to be on the order of $10^{-4}$ (F.R.Clague, NCSL Symp., 291-297, 1994) with a standard uncertainty of $10^{-4}$, and $\eta_{e0} \approx 0.992$. For a typical noise source, the relative uncertainty in the noise temperature traceable to the Y-factor uncertainty is 0.09 %.

A1-8
1640

## MEASUREMENT OF ABSOLUTE EM FIELD MAGNITUDES USING IR THERMOGRAMS

J. Norgard(*), R. Sega(**), M. Seifert(***), A. Pesta(***)
(*)USAF Academy, Colorado Springs, CO 80840
(**)NASA/JSC, Houston, TX 77058
(***)USAF Rome Laboratory, Griffiss AFB, NY 13441

The purpose of this paper is to develop appropriate theory and experimental practices to permit the absolute determination of electric and magnetic field intensities from thermographic images (IR thermograms) of microwave fields.

Initial empirical results from anechoic chamber tests indicate that the induced temperature distribution (IR thermogram) in a properly designed, lossy, planar IR detection screen placed in the area over which an electromagnetic (EM) field is to be mapped can be calibrated to measure the incident EM wave using the Joule heating of the screen material.

The relative accuracies of the field intensities measured by the IR thermograms taken with the IR scanner were determined using numerical computer codes to predict the normalized field intensities for the same geometries. The relative accuracies were usually no greater than 7% in error. These errors occurred at the minimum (null) field intensity positions in the thermograms, where the effect of thermal conduction (bleeding) from adjacent hot spots tends to fill in the nulls somewhat. Therefore, the technique has the potential to produce extremely accurate field intensity measurements, much less than +/- 1 dB in error.

To determine the absolute electric or magnetic field strengths from IR thermograms, the IR scanning detectors and detector screens must be calibrated, i.e the broad-band frequency dependence of the complex constitutive electrical and thermodynamic parameters of the IR detection screen materials must be determined.

A theory has been developed for the microwave interaction with a lossy/complex thermal absorber material. The electric/magnetic field distributions can then be predicted for well-known, theoretically tractable problem geometries. These predictions are verified experimentally to validate the measurement accuracy for each problem geometry.

Session B/D-1, 1355-Tues., CR2-26
LEAKY WAVES: THEORY AND APPLICATIONS TO
HIGH-FREQUENCY INTEGRATED CIRCUITS
Chairperson: D.R. Jackson, Dept. of Electrical and Computer Engineering, Univ. of Houston, Houston, TX 77204-4793
Organizers: D.R. Jackson; A.A. Oliner, Polytechnic Univ., Brooklyn, NY; and E. Towe

B/D1-1
1400

## LEAKY MODES ON PRINTED-CIRCUIT TRANSMISSION LINES

**Arthur A. Oliner**
Polytechnic University, Brooklyn, NY

Recent work on integrated circuits employing printed-circuit transmission lines, such as microstrip line, coplanar waveguide, or slot line, has shown that two initially unexpected features can occur: (a) the dominant modes on these lines become ***leaky*** when the conditions are right (which usually means above a critical frequency), and (b) ***new dominant modes*** have been found, some of which are always leaky. Both of these features produce crosstalk and power loss that may seriously disturb and even ruin circuit performance. An even stranger new effect has been found, namely, a ***spectral gap*** at the transition between bound and leaky modes, within which the solutions are ***nonphysical.***

The leakage occurs in the form of ***surface waves*** that propagate away at an angle from the axis of the transmission line. (Surface waves are also excited at circuit discontinuities, but that mechanism is completely different.)

This basically tutorial and survey talk will begin with a brief review of printed-circuit transmission lines, and with a general discussion of the properties of leaky waves. The conditions under which bound modes can become leaky will then be presented, and several examples will be given of such modes on printed-circuit transmission lines. We will also consider what happens to a leaky mode when the line is placed inside a closed package. Finally, we will consider the newest effects, i.e., spectral gaps and new leaky dominant modes.

The transition between bound and leaky solutions is not smooth and simple but contains some very interesting fine structure. On closer examination, this transition region turns out to be ***nonphysical***, and it is therefore called a "spectral gap". Much is already understood about these spectral gaps, but there are still some unanswered questions.

Under certain conditions, these spectral gaps change their character and give rise to ***new*** and ***unexpected*** leaky dominant modes. Two classes of such new modes will be presented. The first class occurs on microstrip line and on stripline with an air gap, and is associated with a semi-infinite spectral gap. The other occurs when, as the line parameters are varied, the spectral gap gradually disappears and the bound and leaky solutions overlap and are present ***simultaneously*** over a frequency range which can become very large. The phenomenon is quite general, but it will be illustrated for conductor-backed coplanar strips. The presence of these new modes has been confirmed experimentally.

**Acknowledgment:** The material to be presented has been drawn from several extensive investigations in which the author has collaborated with two independent groups: Professors H. Shigesawa and M. Tsuji of Doshisha University, Kyoto, Japan, and Mr. D. Nghiem and Professors J. T. Williams and D. R. Jackson of the University of Houston, TX, USA.

B/D1-2
1440

# THE CHOICE OF INTEGRATION PATH IN THE SPECTRAL-DOMAIN SOLUTION OF LEAKY MODES

*David Nghiem, Jeffery T. Williams, and David R. Jackson*
Department of Electrical and Computer Engineering
University of Houston
Houston, TX 77204-4793

*Krzysztof A. Michalski*
Department of Electrical Engineering
Texas A & M University
College Station, TX 77843-3128

Recently, considerable attention has been devoted to the study of leaky modes on a variety of waveguiding structures. Many of these waveguiding structures are characterized by one or more conducting strips residing within a layered structure. A few examples of the structures that have been investigated are stripline, microstrip line, coplanar waveguide, and coplanar strips. For any of these structures, the spectral-domain method is a powerful and convenient tool for analyzing the propagating modes. In a typical analysis the method of moments is used, in which the current on the conducting strips is represented in terms of basis functions, and the electric field integral equation is enforced on these strips. This leads to a determinantal equation ($det[Z(k_{z0})] = 0$) for the unknown complex propagation constant $k_{z0} = \beta - j\alpha$. The elements of the $Z$ matrix, corresponding to the reactions between basis functions, are in the form of spectral-domain integrals, and thus involve an integration over $(-\infty, \infty)$ in the transverse spectral wavenumber $k_x$. In a conventional analysis, the path of integration is chosen as the real axis for these integrals. Such a path always recovers the *bound* modal solutions, i.e., the modes whose fields decay transversely away from the strip in either the $x$ or $y$ directions. Such solutions are well known.

As opposed to the bound mode solutions, leaky-mode solutions have a field behavior that *increases* in either or both the $x$ and $y$ directions. This field behavior corresponds, in general, to leakage of power from the strip, which may be in the form of leakage into a guided mode of the background structure (surface wave), leakage into a space wave, or both. These leaky solutions are found from the spectral-domain formulation by choosing a path of integration that is different from the real axis. In particular, the path is chosen to detour around one or more poles of the integrand if the leakage occurs into one or more surface waves, or through the branch cut if the leakage is in the form of a space wave.

This talk will summarize the reasoning behind the choice of integration path for the leaky mode solutions, and will explore the physical meaning associated with the choice of such paths. The physical meaning of the modes will be discussed in connection with a leakage condition, which says that, to first order, leakage into a particular background guided mode (or space wave) should occur only when the leaky mode has a phase constant $\beta$ that is less than the wavenumber of the background guided mode (or space wave). This leakage condition is closely connected to the concept of the *spectral gap* that occurs when a leaky mode is in transition from a physically meaningful mode to one that has no physical meaning.

B/D1-3
1500

## LEAKY-WAVE AND RADIATION MODES OF INTEGRATED DIELECTRIC WAVEGUIDES

Dennis P. Nyquist
Department of Electrical Engineering
Michigan State University
East Lansing, Michigan 48824

Open dielectric waveguides support both spectral (discrete and continuous) and non-spectral leaky-wave modes. Although the bound surface-wave modes of practical integrated dielectric waveguides (e.g., dielectric strip, channel and rib guides) have been studied extensively, the discrete leaky-wave modes and continuous spectra of those configurations have not been adequately conceptualized nor quantified. Consequently, the latter wave types are known for only a few canonical open dielectric waveguides. Studies of EM wave excitation, coupling and scattering on integrated open waveguides depend critically, however, upon those wave components. Recent efforts by Rozzi and his colleagues [e.g., Mongiardo and Rozzi, IEEE MTT Trans., Aug. 1993] have studied the continuous spectrum of open waveguides using a differential-operator (Sturm-Liouville) based mode-matching method. The research exposed here provides an alternative approach, and studies the leaky-wave modes and continuous spectrum as pole and branch-point contributions to a singularity expansion of the total field, based upon an exact spectral-domain integral-operator description for the open waveguide.

An integrated dielectric guide with cross section $CS$ is immersed in a layered background environment. The total guiding-region field is $\vec{E} = \vec{E}^i + \vec{E}^s$, where $\vec{E}^i$ is the impressed field due to primary currents and $\vec{E}^s$ is the scattered field maintained by guiding-region polarization currents. The guiding region with refractive index $n_g$ is immersed in a cover layer of index $n_c$, leading to index contrast $\delta n^2 = n_g^2 - n_c^2$. Coordinates are chosen with $x,z$ tangential and $y$ normal to the planar interfaces, where $z$ is the waveguiding axis. All field quantities are axially Fourier transformed, e.g., $\mathcal{F}_z\{\vec{E}(\vec{r})\} = \vec{e}(\vec{\rho},\zeta)$, with $\vec{\rho} = \hat{x}x + \hat{y}y$ the 2-D position vector and $\zeta$ the axial transform variable. Transforming the total field, and expressing the scattered field in terms of the polarization current which maintains it, leads to the spectral-domain integral equation

$$\vec{e}(\vec{\rho},\zeta) - \int_{CS} \frac{\delta n^2(\vec{\rho}')}{n_c^2} \bar{\bar{g}}^e(\vec{\rho}\,|\,\vec{\rho}';\zeta)\cdot\vec{e}(\vec{\rho}',\zeta)\,dS' = \vec{e}^i(\vec{\rho},\zeta) \quad \ldots \forall\ \vec{\rho} \in CS$$

where $\bar{\bar{g}}^e$ is the electric Green's dyad (with 1-D Sommerfeld-integral representation in transverse transform variable $\xi$) which describes the layered environment.

Integrands in the electric Green's dyad representation have $\xi$-plane singularities consisting of branch points and surface-wave poles which are contributed by the layered background environment. Those singularities migrate in the complex $\xi$-plane as $\zeta$ is varied in the complex $\zeta$-plane. To assure a strip of convergence in the $\xi$-plane, which minimally includes the real axis, branch cuts in the $\zeta$-plane must be selected to prevent the migration of $\xi$-plane singularities across the real axis. Violating the $\zeta$-plane cuts leads to leaky discrete modes, and deforming the $\zeta$-plane inversion contour about them (to remain on the top sheet of a four-sheeted Riemann surface) leads to the continuous spectrum of the guiding structure. A natural classification of the propagation modes into spectral (discrete and continuous) and non-spectral leaky-wave components consequently evolves. Leaky-wave modes of the guiding structure are associated with $\zeta$-plane pole singularities which occur off the top Riemann sheet, while the continuous spectrum is defined by solutions to the above integral equation at points along the $\zeta$-plane branch cuts. Dielectric strip/rib waveguide configurations are studied based upon numerical solutions to the above integral equation, and extensive numerical results are obtained.

B/D1-4
1540

# THE PROPERTIES OF THE SPECTRAL GAP AT THE TRANSITION BETWEEN BOUND AND LEAKY MODES

**Arthur A. Oliner* and David R. Jackson****

*Polytechnic University, Brooklyn, NY
**University of Houston, Houston, TX

It was recognized over 30 years ago that the transition region between bound and leaky modes contains some very interesting fine structure, and that in fact the guided-mode (eigenvalue) solution is ***nonphysical*** over a small frequency range. The structures on which these effects were noted at that time were dielectric layers and open periodic surfaces. No attempts were made until very recently to understand the behavior in such regions, however. In fact, in many papers, even recent ones, these transition regions were either simply presented without explanation or interpretation as part of a total solution, or they were assumed to be an artifact of the numerical calculation and were therefore treated as an error and smoothed over completely.

Recently, in the context of printed-circuit transmission lines (such as microstrip line, slot line and coplanar waveguide) and also some leaky-wave antennas, these transition regions have again been found, but this time they are being examined carefully in an attempt to understand their nonphysical nature. They are now called "***spectral gaps***" because there exists a frequency range, or gap, over which the solution is ***nonphysical.*** This gap in frequency is usually, but not always, small. These spectral gaps seem to occur on all guiding structures that have inhomogeneous dielectric material (such as layers) in the cross section, and are open in a transverse direction.

We now understand ***why*** the fine structure must have the form that it does, and we will present that explanation in the talk. We also understand much about the behavior within these initially mysterious spectral gaps, but not everything yet. There are still some open questions.

On the ***bound*** mode side of these spectral gaps, the guided-mode solution changes into a pair of ***improper real*** solutions which are obviously ***nonphysical.*** The solution, as frequency changes, then turns into a pair of ***improper complex*** solutions, of which one grows exponentially in the propagation direction and is therefore clearly always nonphysical, and the other is a ***leaky mode*** that is physical outside the spectral-gap region. However, the leaky-mode region ***within*** the spectral gap requires further examination. There are good reasons to regard this leaky-mode region as nonphysical, but there are also other good reasons to make us believe that this region is really physical, or at least that physical meaning is lost only gradually as the region is entered. The resulting ***dilemma*** produced by these contradictory arguments will be addressed in this talk and in the next one.

B/D1-5
1600

# THE INFLUENCE OF LEAKY WAVES ON THE FIELDS OF A GUIDING STRUCTURE

**H. Ostner**
Lehrstuhl für Hochfrequenztechnik
Technische Universität München, 80290 München, Germany
**D. R. Jackson**
Department of Electrical and Computer Engineering
University of Houston, Houston, TX 77204–4793, USA

Planar structures consisting of multiple dielectric layers over a ground plane are capable of supporting weakly attenuated leaky waves, and can be used as efficient leaky-wave antennas at millimeter-wave frequencies. In addition, such structures serve as canonical geometries for investigating the role of leaky waves in determining the total fields of a guiding structure, and for investigating the influence of leaky-wave poles on the radiation pattern of a leaky-wave antenna. The results of such an investigation are presented here, for the specific case of a line source excitation inside a layered structure.

The leaky waves launched by the line source correspond to the poles of the spectral-domain Green's function, located on the improper Riemann sheet. Depending on the chosen scan angle these poles are either to the left of the extreme steepest-descent path (ESDP) (in the fast-wave region) or to the right of the ESDP (in the slow-wave region). When the dominant leaky-wave pole is located within the fast-wave region, the beam angle and the phase constant of the leaky wave are closely related, and the aperture field can also be predicted quite accurately via the residue of the leaky-wave pole. As the frequency (or equivalently, the scan angle) increases, the leaky-wave pole moves toward the ESDP path, and eventually crosses it, entering the spectral-gap region. In this region the aperture field and the leaky-wave field diverge, and consequently there no longer exists a simple relation between the beam angle and the phase constant. It is customarily said that the pole looses physical meaning in this region.

In the first part of this presentation it will be shown how the aperture field can be decomposed into a leaky-wave field and a space-wave field in various ways. The influence of the leaky-wave pole on the aperture field will then be investigated as the pole moves through the spectral-gap region. The generalized pencil of functions (GPOF) method is used to quantify this influence. Finally, an examination of how the radiation pattern changes as the pole moves through the spectral gap will be made.

B/D1-6
1620

# Engineering Applications of Electromagnetic Leakage Phenomena in Microwave Integrated Circuits

Y. Liu and T. Itoh
UCLA
Electrical Engineering Department
405 Hilgard Avenue
Los Angeles, CA 90024-1594

During the past several years, following by a warning from Professor Oliner that there potentially exist leaky waves in many planar transmission line configuration, a number of studies have been made. In some cases, these leaky waves are natural part of the dominant mode so that the latter always leaks while, in other cases, the onset of the leakage is frequency dependent. These studies investigated causes of the leakage, physical explanation, and mathematical and numerical analyses. Some work has been carried out to find a mechanism and/or modifications of the structures to prevent leakage. In most cases, these leakage phenomena are considered something undesirable and detrimental. This is because they seriously undermine the performance of the microwave circuits designed based on the non-leaky dominant mode transmission lines.

The purpose of this talk is to introduce an alternative view toward these leakage phenomena and to seek possible engineering applications of such phenomena. There are two leading causes to find such an applications. One is that, as the frequency is increased, the conventional circuits may become very small and the processing can become expensive. This is true at Terahertz region. In such cases, we need to find a way to increase the size of the circuit. The leakage phenomena referred to above have a potential, because the wave can be transmitted in a transverse direction to the waveguide for a considerable distance without decay. Second, the leakage phenomena have a potential to create a two-dimensional planar circuit which has electrically large dimensions in both longitudinal and transverse directions. Obvious complications of such a large circuit is the multi-mode problem which requires careful design, particularly if active devices are involved.

An example for the engineering applications is the leaky wave directional coupler. (Y. Liu, T. Hirota and T. Itoh, Coupling Phenomena in Conductor-Backed Slotline Structures, IEEE MTT Sympoisum, pp.1203-1206. June 1993.) In this structure, two slotlines far apart is coupled by way of the lateral leakage mechanism provided only between the two slot lines. To this end, an additional ground plane is provided on the lower side of the substrate only between the two slotlines. Therefore, the two slotlines are coupled by the leakage mechanism. No leakage occurs outside the region bounded by the two slotlines.

There are several possible configurations which may enjoy the use of lateral leakage to develop new types of circuit configurations. Some of them are reflection type amplifiers where the devices are distributed away from the "main" waveguide for easier heat sinking. Another possible examples are two dimensional frequency selective mechanism. These structures are still conjectures. However, this talk will emphasize the importance of the departure of the microwave circuit design concept from the traditional waveguide based approach.

B/D1-7
1640

## PHYSICAL INTERPRETATION OF TIME-DOMAIN LEAKAGE FROM PRINTED-CIRCUIT TRANSMISSION LINES

Lawrence Carin
Department of Electrical Engineering
Polytechnic University
333 Jay Street
Brooklyn, NY 11201
(718) 260-3876, FAX (718) 260-3906,
Email:lcarin@stealth.poly.edu

Leaky modes supported by planar transmission lines have been the focus of significant research over the last several years. Most of these previous studies have been for frequency-domain operation and have concentrated on calculating the complex wavenumber as well as field profiles. Although much of the current trend in monolithic integrated circuits is toward high-speed pulsed operation, very little work has been performed concerning the effects of leakage on short-pulse, time-domain operation. This issue was addressed for the first time in a recent paper by Tsuji, Taniguchim, and Shigesawa [MTT Trans., vol. 41, pp. 1017-1023, June/July 1993] using the Finite Difference Time Domain Method. The purpose of the present talk is to provide a physical interpretation of time-domain leakage from planar transmission lines. In particular, we will observe the time-dependent leaked fields at a fixed point away from the transmission-line guiding region. The time-dependent fields will be characterized in terms of time-dependent frequencies as follows. The transient leaked energy propagates at a time-dependent angle to the observer. Further, it is well known from the frequency-domain point of view that the angle of leakage away from the strip/slot depends on the frequency of operation. Thus, the time-dependent angle of leakage (with respect to the point of observation) can be linked via the frequency dependence of the leakage angle to yield an observed time-dependent frequency. In other words, although the pulse traveling down the transmission line consists of a wide instantaneous frequency spectrum, it can be shown that the time-dependent leaked energy observed at a given point in space can be represented at any given time by a dominant narrow-band frequency component; the particular narrowband component varies as a function of time. Thus, while the pulse on the transmission line has wide instantaneous frequency, the observed leaked energy will consist of a chirped waveform with narrow but time-dependent instantaneous frequency. The above considerationswill be shown explicitly by performing an asymptotic analysis of the time-dependent leaked radiation, and the associated wave physics will be demonstrated clearly using time-frequency distributions (windowed Fourier transforms, for example).

B/D1-8 Discussion
1700

E1-1
1340

# IMPEDANCES OF COPLANAR CONICAL PLATES IN A UNIFORM DIELECTRIC LENS AND MATCHING CONICAL PLATES FOR FEEDING A PARABOLOIDAL REFLECTOR

Carl E. Baum
Joseph J. Sadler
Phillips Laboratory
PL/WSR, KAFB
Albuquerque, NM 87117
Alexander P. Stone
Department of Mathematics and Statistics
University of New Mexico
Albuquerque, NM 87131

In this paper we investigate impedance characteristics of coplanar conical plate geometries which pass through a lens boundary. The plates are initially in a dielectric lens matching to exterior conical plates which serve as a paraboloidal reflector feed. The lens impedance $Z_{in}$, is a function of the "half-angle", $\alpha'$, of the interior conical plates, but is independent of the ratio, $F/D$, of focal length to reflector diameter. Various practical choices of this ratio are made and impedances, $Z_{out}$, of the exterior region are calculated. As $\alpha' \longrightarrow 0$, the ratio $Z_{out}/Z_{in}$ approaches $\sqrt{\epsilon_r}$, where $\epsilon_r$ is the relative permittivity of the lens region. As $\alpha'$ increases, the impedance ratio also increases. Numerical and graphical impedance results are presented as a function of $F/D$, so that one can trade off the various performance characteristics.

E1-2
1400

# DESIGN, FABRICATION AND TESTING OF A REFLECTOR ANTENNA AND PULSER SYSTEM FOR IMPULSE-LIKE WAVEFORMS

I.D.Smith and D.W.Morton, Pulse Sciences,Inc., San Leandro, CA
D.V.Giri and H. Lackner, Pro-Tech, Lafayette, CA
C.E.Baum and J.R.Marek, Phillips Laboratory, Kirtland AFB, NM

## ABSTRACT

In this paper, we present our results on the design, fabrication and testing of a radiating system for impulse-like waveforms. The antenna consists of a paraboloidal reflector fed by a pair of conical TEM lines. Several aspects of an impulse radiating antenna (IRA) such as TEM feed configurations, aperture efficiencies, prepulse, far fields, etc. have been studied in the past by various researchers. The present work will focus on the actual design and implementation of prior analytical work.

The pulse generator that feeds the TEM structures incorporates the following elements, (a) an electromagnetic lens in the wavelaunching region to ensure a near-ideal spherical TEM wavelaunch, (b) a high voltage ($\geq$ 120 kV), high pressure (100 atm) hydrogen switch and risetimes (10-90%) of the order of 120 ps, operating in a burst mode at a prf of up to 200 Hz, (c) a pulse forming network that results in an exponential decay of 15ns. Two orthogonal TEM conical lines in air, connected in parallel present a 200 Ohm impedance to the generator. The lines are terminated through a matching network to the edges of the parabolic reflector, which is 3.66m in diameter. The aperture antenna produces a waveform which is the time derivative of the double exponential [(120ps, 33ns) 10-90% rise and fall] waveform supplied by the pulser.

The key elements in the pulser are the high-pressure hydrogen switch and an electromagnetic (EM) lens. The switch is charged by the differential output of a center-tapped iron core pulse transformer and the charging circuit is completed via the antenna. the wavelauncher, capacitors and the switch are immersed in oil, making the insulation relatively easy. The oil medium used in insulation, also serves the purpose of an EM lens when the oil container is shaped to ensure that the exit-waves at the oil-air interface have a spherical wavefront. The design and performance details of the pulser and the antenna are discussed. Risetime, near field measurements and far field estimates will be presented.

This work was sponsored by Phillips Laboartory/WSR under a Govt. Contract F29601-93-C-0185 (SBIR Phase II Program) awarded to Pro-Tech with Pulse Sciences, Inc., as a subcontractor.

E1-3
1420

# A HIGHLY-DIRECTIONAL, ULTRA-WIDEBAND, BINARY-TREE TEM HORN ANTENNA

Dr. Robert A. Koslover
Phillips Laboratory / WST
3550 Aberdeen Ave, SE
Kirtland AFB, NM 87117-5776

100% of $f_c$

The generation of a highly-directional beam of RF energy from an antenna driven by a short (≤ a few ns) high-power (multi-GW) pulse is especially challenging. Conventional narrowband high-gain (G > 20 dBi or more) long-pulse and/or continuous-wave (cw) antennas typically achieve high directionality by either forming an interference pattern from multiple radiating elements (most useful at low frequencies) or using quasi-optical reflectors (most useful at high frequencies). In the former, under cw conditions, elements can be driven by signals delayed relative to one another by integral multiples of a wave period, since the driving signal is invariant under such a temporal shift. This method fails for a short-pulse UWB signal, since the entire signal may persist only one or two cycles. Driving this class of antenna with such a short-pulse severely reduces directionality, which can fall to as low as that of a single-element (~ 3 dBi) in the limiting case of single-cycle excitation. Reflector and lens-type antennas do not suffer from this problem, but are heavy and unwieldy at longer wavelengths. Reflector antenna feeds may exhibit breakdown at multi-GW powers. In contrast, conventional TEM horns with parallel-plate feeds offer both extremely high power handling and excellent short pulse behavior, but exhibit peak directionality of only ~20 dBi in practice. One new approach[1] is a compact array of TEM horns flaring from a single parallel-plate feed in a binary-splitting arrangement. An "n-stage" design yields $2^n$ adjacent apertures (n=0,1,2,3...) in the E-plane. This provides superior gain relative to an equivalent-size TEM horn, by dramatically reducing the E-plane phase error (along with a minor decrease in H-plane phase error). The ability to handle extremely high peak power and the short-pulse response characteristics are preserved. Predicted antenna performance and measured data showing behavior of the tapered transmission-line splittings are presented. Also discussed are rule-of-thumb formulas and a computer program[2] used to rapidly estimate radiation patterns, angular dependence of specific waveforms radiated, and radiated energy densities. The discussion presented for binary-tree horns can also be applied to ordinary TEM horns, as "n=0" special cases.

---

[1] U.S. Patent # 5,323,169. This work was performed by the author while previously employed at Voss Scientific, Albuquerque, NM. Patent rights retained by Voss Scientific.
[2] Available from Voss Scientific, Albuquerque, NM.

E1-4
1440

## ULTRA-WIDEBAND HIGH-POWER BALUN DESIGN

Everett G. Farr*, Gary D. Sower**, and C. Jerald Buchenauer†
*Farr Research, 614 Paseo Del Mar NE, Albuquerque, NM, 87123
**EG&G, Inc, 2450 Alamo Ave. SE, Albuquerque, NM 87106
†Phillips Laboratory, 3550 Aberdeen Ave., Kirtland AFB, NM 87117

A number of high-power ultra-wideband (UWB) sources provide output into a large coaxial transmission line, providing an unbalanced signal. However most antenna designs such as TEM horns and reflector or lens Impulse Radiating Antennas (IRAs) require a balanced source for proper operation. This provides the impetus for investigating a balun that can operate with high power, while preserving risetimes in the range of less than 150 ps. The design of a balun with these properties is a considerable challenge. There is a tradeoff between the peak voltage one can sustain, and the risetime one can preserve through a length of transmission line. We consider here several candidate balun designs, and we find that a classical coaxial unzipper balun to be preferable in this application.

We consider here a relationship between the risetime and peak voltage that is sustainable in the coaxial unzipper balun. This is based on both a simple theory, and on comparisons to existing coaxial unzipper transitions, in particular, that at the ARES test EMP test facility.

We also provide a two-dimensional analysis of slices through a coaxial unzipper balun. This allows one to determine the impedance as a function of position on the unzipper. These calculations were carried out using Ansoft Corporation's *Maxwell* 2-D Finite element solver.

There is a rationale for keeping the impedance as low as possible through the transition. It turns out that coupling to the common mode is reduced when the transition occurs at lower impedances.

We consider a ferrite/dielectric sandwich for reducing the common mode even more than what can be achieved with a simple solid ferrite sleeve. Practical considerations (size, weight, and cost of the ferrite) may limit the usefulness of ferrites in high-power devices, but may be useful in smaller devices.

Finally, we consider the radiated field one can achieve with such a device using a lens IRA.

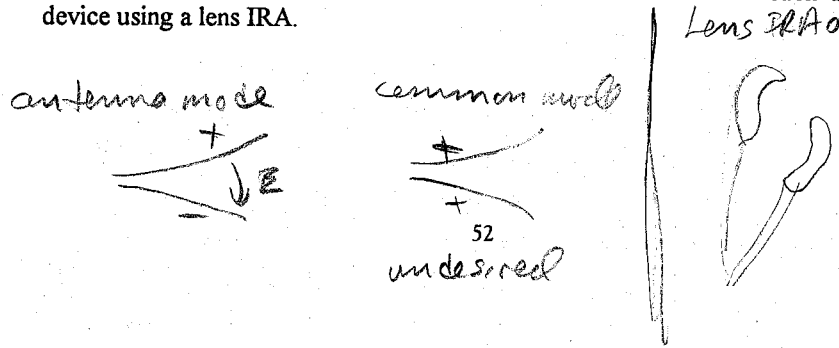

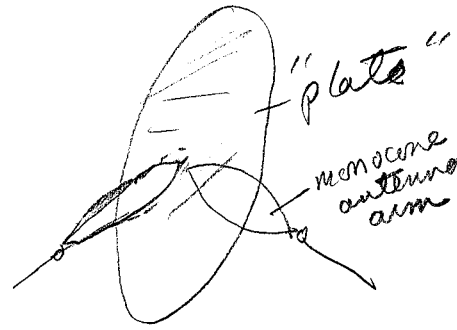


E1-5
1500

# THE BALANTENNA, PART II

Carl E. Baum
Phillips Laboratory, WSR
3550 Aberdeen Ave SE
Albuquerque, NM 87117-5776

Donald P. McLemore
Kaman Sciences Corp
6400 Uptown Blvd., NE
Albuquerque, NM 87110

two 100Ω TLs in parallel on input (50Ω) and in series on output (200Ω), giving 4:1

A balantenna has been proposed as a matching device for the feed section of the ELLIPTICUS antenna. The design of this matching device is intended to give a 4:1 increase over the feed line impedance across a very wide frequency range, reaching upper frequencies of 3 GHz or better. This device is also designed so that it integrally fits into the "worm-hole" feed scheme of the ELLIPTICUS antenna.

The original design incorporated a single apex design in the center of the balantenna. Subsequent experiments with the loading ferrites have shown that heating effects (above the Curie temperature) due to small ferrite volumes in regions of high current densities could be a drawback to this first design. To counter these heating effects, a new design is proposed which does not require such extensive shaping of the ferrite material and uses a larger ferrite cross section near the center of the balantenna where surface currents are expected to be large. In order to accommodate this change, a new double apex design is also required for the feed transition inside the balantenna.

This design should also improve the high frequency performance for the balantenna with the elimination of an inherent "dispersion distance" in the first design. Below is a figure which gives the impedance of the balantenna feed as a function of the angle of depression from the horizontal ($\alpha$) and the half-angle ($\beta$) for each of the conical arms of the antenna. These conical arms and the center assembly of the balantenna form the biconical feed for the antenna.

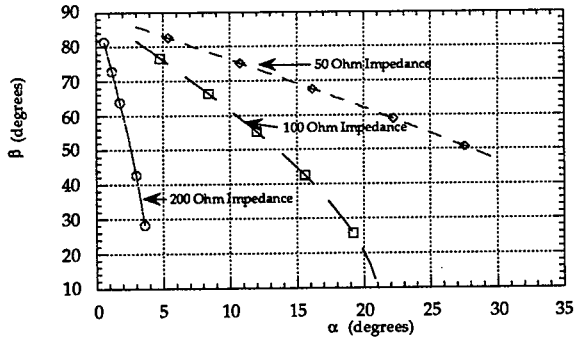

E1-6
1540

## ANALYSIS METHODS APPLIED TO THE CALCULATION F THE PENETRATION OF HIGH FREQUENCY ELECTROMAGNETIC WAVES DEEP INTO COMPLEX SYSTEMS

Robert L. Gardner
Phillips Laboratory/WST
3550 Aberdeen SE
Kirtland AFB, NM 87117-5776

This paper considers the probelm of specfication of the electromagnetic topology of complex systems and methods to calculate the pentration of high frequency electromagnetic waves into those systems. The paper depends to a large degree on the results of a workshop on the same subject held at Phillips Laboratory in November 1993 by the URSI Commission E Working Group on High Power Electromagnetics (Proceedings of the Workshop on the Penetration of High Frequency Waves Deep Into Complex Systems: Fulmen 6, R. L. Gardner, ed, EMP Note Series, Kirtland AFB, NM). Various direct methods of calculation are considered including numerical modeling and topological decomposition. Applications of statistics in such models are alos considered. It is found that statistics gathered by enumeration are ineffective in calculation of the behavior of complex electromagnetic systems models, but the use of statistical electromagnetics may be of some value in these calculations.

E1-7
1600

# DAMPING TRANSMISSION-LINE AND CAVITY RESONANCES

Carl E. Baum
Phillips Laboratory/WSR
3550 Aberdeen Dr. S.E.
Kirtland AFB, NM 87117-5776

In the interaction of electromagnetic fields with complex electronic systems there are often low-loss resonances associated with conductors (transmission-line modes) and cavities. These resonances can allow the effective transmission of undesirable signals through the systems at the resonance frequencies. This paper discusses techniques for suppressing (damping) such resonances. These involve various spatial distributions of resistors ( in some cases with inductors (chokes)).

E1-8
1620

## ELECTROMAGNETIC FIELD PATTERNS FROM A SURFACE EXCITED BY PULSE AND CW LASER RADIATION

Dr William E. Page
Phillips Laboratory / WST
3550 Aberdeen Ave, SE
PL/WST KAFB New Mexico 87117-5776

Laser beams incident on a metallic surface can produce an electron emission boundary layer that may be modelled as a dipole sheet. .The non linear dynamics of this layer has previously been analyzed in a one dimensional approximation. These results have been applied to a finite flat metallic plane. The resulting electromagnetic fields produced by this surface have been studied in the approximation where edge diffraction effects are ignored. Field patterns for near, far, and intermediate zones have been calculated. The cases of CW, pulsed, and repetitively pulsed laser illumination have been studied. The phasing relationship of the induced dipole distribution and it's time behavior have been used to determine the resulting field distributions in the vicinity of the surface. In the CW case results vary from specular reflection at small wavelengths to an elemental dipole pattern for modulation wavelengths large compared to the surface dimensions. The pulsed and repetitively pulsed cases have also been analyzed to illustrate the spectral content and spatial variations in intensity distribution of the induced electromagnetic fields.

F2-1
1340

## APPLICATION OF RADAR PROFILER MIXING HEIGHTS TO RADIO PROPAGATION PREDICTIONS

Richard A. Paulus
Ocean and Atmospheric Sciences Division
NCCOSC RDT&E DIV 543
53170 WOODWARD ROAD
SAN DIEGO CA 92152-7385

The NOAA Environmental Technology Laboratory (ETL) installed and operated three 915 MHz profilers in the southern California area for the Variability of Coastal Atmospheric Refractivity (VOCAR) experiment. They were located at Point Loma in San Diego, on San Clemente Island, and at Point Mugu near Oxnard. For the period 23 August to 3 September 1993, ETL analyzed the profilers' radar reflectivity data and extracted hourly estimates of the mixing depth of the planetary boundary layer. The mixing depth is the height of the base of the temperature inversion. In the southern California coastal region, the temperature inversion is highly correlated with a trapping layer. Thus the temporal variation of mixing depth indicates temporal variation of the height of the trapping layer.

The mixing layer depth data, along with statistics of refractive layer gradients and thicknesses, are used to construct modified refractivity profiles for input to the Radio Physical Optics propagation model. Predictions of propagation loss for the VOCAR radio links, with a temporal resolution of one hour, are compared to the measured radio signals.

F2-2
1400

## LIMITATIONS ON THE ACCURACY OF PATHLOSS ESTIMATES DETERMINED FROM TIME SERIES OF MEASURED PATHLOSS VALUES

L. Ted Rogers
Ocean and Atmospheric Sciences Division
NCCOSC RDT&E DIV 543
53170 WOODWARD ROAD
SAN DIEGO CA 92152-7385

In practice, environmental observations used to develop pathloss estimates are not available continuously, but rather at discrete times. Use of pathloss estimates however, tends to be uniform over time. The error of pathloss estimates as a function of lag time between the time of an environmental observation and the time of the use of the estimates is therefore of as much interest as the error at the time of an observation. The error as a function of lag for pathloss estimates on a given path that are exact at zero-lags can be calculated from radio measurements performed on that path. The error of the estimator that is exact at zero lags is a lower bound on the error of the best possible propagation model pathloss estimates for all lag values.

Pathloss error as a function of lag time is examined using a parabolic equation model with horizontally homogeneous refractivity profiles. Radio data and environmental observations are derived from the Variability Of Coastal Atmospheric Refractivity experiment. At lag times of greater than one hour, the error of the described propagation estimates is observed to be only marginally greater than that seen with estimates that are exact at zero lags. It is concluded that a substantial decrease in the error of propagation estimates, through the use of horizontally varying refractivity profiles as inputs to propagation models, will only be realized if the time intervals between obtaining the refractive profiles is on the order of an hour or less.

F2-3
1420

# CRITERIA FOR CHOOSING VERTICAL, LATERAL, AND TEMPORAL MEASUREMENT RESOLUTIONS FOR ASSESSING COASTAL PROPAGATION CONDITIONS

G. Daniel Dockery, Julius Goldhirsh
The Johns Hopkins University, Applied Physics Laboratory
Johns Hopkins Road, Laurel, Maryland, 20723-6099

This paper addresses the fundamental question, "What are the vertical, lateral, and temporal measurement resolutions required in the execution of in-situ and remote sensing of atmospheric refractive index for the assessment of coastal propagation conditions?" We address this question by examining the extent to which the accuracy of the propagation factor predictions at frequencies between 1 and 10 GHz diminish when we inject measured refractive index data, which are spoiled in spatial and temporal measurement resolutions, into a broadly accepted propagation model. These results are compared with "truth" calculations corresponding to the original high resolution data set. The refractive index data, which were collected with a helicopter along the east and west coasts of the United States, were culled from a set of thousands of atmospheric profiles. The propagation model used is known as the Tropospheric Electromagnetic Parabolic Equation Routine (TEMPER), which is based on a Fourier split-step numerical solution of the parabolic wave equation. The raw measured helicopter data are first processed by an algorithm called the "Large-scale Atmospheric Refractivity Range Interpolator," (LARRI). Preliminary results at 10 GHz and 3 GHz have demonstrated the following for data collected in a California coastal region having a dual surface duct feature with the lowest duct height being approximately at 36 m: (1) Refractive index profiles derived with a 6 m vertical resolution (or smaller) give acceptable smoothed propagation factor versus height profiles up to a height of 40 m at 10 GHz and 110 m at 3 GHz. (2) Refractive index profiles derived with 18 m resolution intervals and larger give unacceptable propagation factor versus height profiles at heights above 20 m at 10 GHz and 50 m at 3 GHz. These results clearly indicate a diminished sensitivity in the required measurement resolution accuracy at 3 GHz vis-a-vis 10 GHz. Preliminary results associated with required lateral resolutions have demonstrated the following employing the same west coast example: (1) Errors in the smoothed propagation factor which approach 15 dB may arise at heights in excess of 30 m by making the common assumption of lateral uniformity in the refractivity profile. (2) Assuming an 18 km lateral measurement resolution interval, accuracies are generally acceptable up to heights of 40 m at 10 GHz and 50 m at 3 GHz. This paper amplifies on the above results and presents general criteria derived from multiple example cases.

F2-4
1440

# FADING CHARACTERISTICS ON TERRESTRIAL MICROWAVE COMMUNICATIONS SYSTEMS

Alan R. Webster and Thang Tieu,
Faculty of Engineering Science,
The University of Western Ontario,
London, ONT. N6A 5B9.

Observations on the nature and characteristics of signal fading have been carried out on several typical microwave communications links in Southern Ontario for a number of years using a wide-aperture array. This system allows the identification of individual rays in a multipath situations and gives directly the amplitude and angle-of-arrival (AOA) of each of these components (see A.R. Webster and T.S. Merritt, IEEE Trans. Comm., 38, 25-30, 1990). Recent observations have been supplemented by acoustic sounding measurements intended to probe for the existence of layers in the atmosphere which lead to such multipath propagation and hence to signal fading.

Two main mechanisms have been identified as producing multipath propagation leading to frequently selective fading. In either case, interference between weak ground reflected rays and reduced amplitude non-reflected ray(s) causes short deep fades. The more common scenario appears to be reduction in amplitude of the single direct atmospheric ray due to the existence of a nocturnal ground based layer, which results in a characteristic depression of the median amplitude over periods of many hours. On the other hand, elevated atmospheric layers can produce two or more essentially normal amplitude rays which interfere to produce a net signal which may be reduced or enhanced in strength. This situation is characterized by close to normal median amplitude with rapid enhancements of several dB and deep fades of 10s of dB. All of this is directly confirmed by the results generated by the experimental systems mentioned above.

A detailed look is taken into several aspects of the fading data including the cumulative distribution for each of the mechanisms described above, together with the behaviour on a second-by-second basis of the amplitude and AOA of the individual components. Included here are statistics related to the fade duration and the rate of change of fade depth.

F2-5
1500

## CONTINUOUS MONITORING OF ATMOSPHERIC WATER VAPOR USING THE GLOBAL POSITIONING SYSTEM

Russell B. Chadwick and Seth I. Gutman
Demonstration Division, Forecast Systems Laboratory
NOAA Environmental Research Laboratories
Boulder, Colorado 80303-3288

Water vapor is one of the most important constituents of the free atmosphere since it is the principle mechanism by which moisture and latent heat are transported and cause "weather". A knowledge of the spatial and temporal distribution of water vapor in the atmosphere is essential to climate and weather research, as well as short-term weather prediction, but our capabilities in these areas are severely limited by the lack of timely water vapor data.

Since 1992, experiments conducted by the University NAVSTAR Consortium (UNAVCO), North Carolina State University, and NOAA's Environmental Research Laboratories (ERL), have demonstrated that data from the Global Positioning System (GPS) can be used to monitor precipitable water vapor (PWV) with millimeter accuracy and sub-hourly temporal resolution. Other results indicate that information derived from GPS observations will be useful for sensing and monitoring global climate change, and that accurate, high resolution measurements of PWV used in conjunction with wind profiler data can significantly increase short-term cloud and precipitation forecast accuracies.

ERL has initiated a program to continuously monitor atmospheric water vapor at NOAA wind profiler sites. By the end of 1994, 6 sites will be instrumented and provide data to a central data processing hub located at the Profiler Control Center in Boulder, Colorado. Data will be processed retrospectively and made available to researchers and forecasters for analysis. This initial effort will demonstrate the value of continuous PWV data and network operations, and support the Global Energy and Water Cycle (GEWEX) Research Program's water vapor project (GVaP) in 1995. The possible deployment of 8 additional systems at profiler sites in the Mississippi River Valley will provide basic data for global climate change studies.

In the longer term, ERL plans to continue to expand the network of GPS PWV systems and is collaborating with UNAVCO to develop the techniques necessary to acquire and process GPS water vapor data in real-time. This effort, which will include "on-the-fly" calculation of improved satellite orbits (required for measuring PWV), will benefit numerous scientific and engineering disciplines outside of the meteorological and global climate communities. Some of these areas include: geophysics, global tectonics, earth quake monitoring and prediction, ionospheric monitoring, volcano research, surveying and mapping, air navigation, and national defense.

This paper describes the techniques used to measure atmospheric water vapor with GPS, and provides some examples from recent field experiments.

F2-6
1540

## TEST OF THE GPS/MET QUICK-LOOK SOFTWARE USED TO RECOVER REFRACTIVITY FROM OCCULTATION MEASUREMENTS

Michael L. Exner
UCAR-GPS/MET Program Office
3300 Mitchell Lane, Suite 245B
Boulder, CO 80301

The main goal of the GPS/MET Program is to demonstrate the utility of GPS derived radio occultation observations for the production of improved weather forecasts. Occultation measurements taken by a special GPS receiver on the MicroLab-1 satellite, due to be launched Fall 1994, will be processed using a complex set of software modules designed to recover atmospheric refractivity profiles. The refractivity data will be used in a forecast model using four dimensional data assimilation (4DDA) techniques to determine the impact of this new data type on the quality of the forecast.

To test the refractivity inversion software prior to launch, a 3D ray trajectory program was used to generate simulated observations for several model atmosphere cases. Day and night time ionospheric cases were included for wet and dry, polar and tropical atmospheres. The effect of various sources of measurement and processing noise was tested. A discussion of the results is presented, including the implications for projected temperature and moisture recovery errors.

F2-7
1600

## SEASCATTER MODULATIONS FROM X-BAND PROPAGATION THROUGH STANDING WAVES ON THE MARINE INVERSION

R.J. Zamora and R.A Kropfli
NOAA Environmental Technology Laboratory
Boulder, CO 80303

During the San Clemente Island Ocean Probing Experiment (SCOPE), a 9.3 GHz radar developed by the NOAA Environmental Technology Laboratory (ETL) was operated from an elevated site (573 m AGL) on San Clemente Island to study atmospheric influences on microwave scatter from the ocean. On several occasions radar images of the ocean had dramatic patterns which we do not believe could have been caused directly by ocean waves. For example, at a 2 deg grazing angle we observed a linear echo having a normalized radar cross-section (NRCS) of -35 dB approaching the radar at 17 m/s. A second example is that of a wave-like echo having a "wavelength" of about 2 km. Many wavelengths are evident in the image. The echo had no apparent movement over its 15 minute coherence time. Doppler velocity patterns for both of these cases was bland, showing none of the structure observed in NRCS. These features were generally the same at horizontal and vertical polarization. No unusual wave disturbances were reported by observers on nearby research vessels.

We hypothesize that these patterns were caused by disturbances on the marine inversion located below the height of the radar. These disturbances caused variations in curvature of the radar beam resulting in small changes in grazing angle at the surface. Since at these small grazing angles (about 2 deg) NRCS is very sensitive to small variations in grazing angle, we speculate that a standing wave on the inversion resulted in a periodicity in grazing angle with distance from the radar. For this case MBL flow was directly across the axis of the island and nearby soundings did confirm that the marine inversion was below the height of the radar.

To test this hypothesis we performed a ray trace calculation with software provided by the Naval Command Control Ocean Surveillance Center (NCCOSC). The Engineer's Refractive Effects Prediction System (EREPS) ray tracing program allowed us to compute the effect of propagation through a wavy inversion. In our presentation we will show the results of ray tracing through a refractivity field constructed from a nearby sounding with the MBL inversion height modulated in space by a wavelength similar to that observed in the NRCS image. The synoptic conditions that produced the background refractivity profile will also be discussed.

F2-8
1620

## ENHANCED TROPOSCATTER FROM ELEVATED LAYERS

Herbert V. Hitney
Ocean and Atmospheric Sciences Division
NCCOSC RDTE DIV 543
53170 WOODWARD ROAD
SAN DIEGO CA 92152-7385

Tropospheric scatter radio propagation models usually account for refractive-index fluctuations associated with a normal or standard atmosphere. These models typically give good long-term results and they also give good short-term results when the refractive conditions are well characterized by a standard atmosphere. In the case of elevated trapping layers, substantial increases in signal level are often observed beyond the horizon that normally can be modeled with waveguide or parabolic equation methods based on the mean refractivity profile (Hitney, *Radio Sci.*, 27, 6, 893-898, 1992). However, it is conjectured that enhanced refractive-index turbulence associated with the elevated layer can also contribute to these increased signal levels.

The parabolic equation portion of the Radio Physical Optics (RPO) model has recently been modified to account for normal troposcatter (Hitney, *IEEE Trans. Antennas & Propagat.*, 41, 7, 905-909, 1993). This model assumes an effective median refractive-index structure parameter given by $C_{ne}^2 = 3.9 \times 10^{-15} e^{-z/2000}$ where $z$ is height in meters (Doviak, et al., *IEEE Trans. Geosci. Remote Sens.*, 21, 25-33, 1983). Radar measurements have indicated structure parameters as high as $10^{-12}$ in elevated layers (Gossard, et al., *J. Climate Appl. Meteor.*, 23, 474-490, 1984). The troposcatter model in RPO was modified to increase the structure parameter arbitrarily to $10^{-12}$ for altitudes corresponding to elevated trapping layers. The figure below compares results from the enhanced troposcatter model to normal and no troposcatter models and to measurements for an elevated trapping layer at 600 m. In this case the inclusion of enhanced troposcatter is seen to decrease the propagation loss up to 10 dB at some ranges. It is concluded that enhanced troposcatter is a potentially important propagation mechanism for some cases.

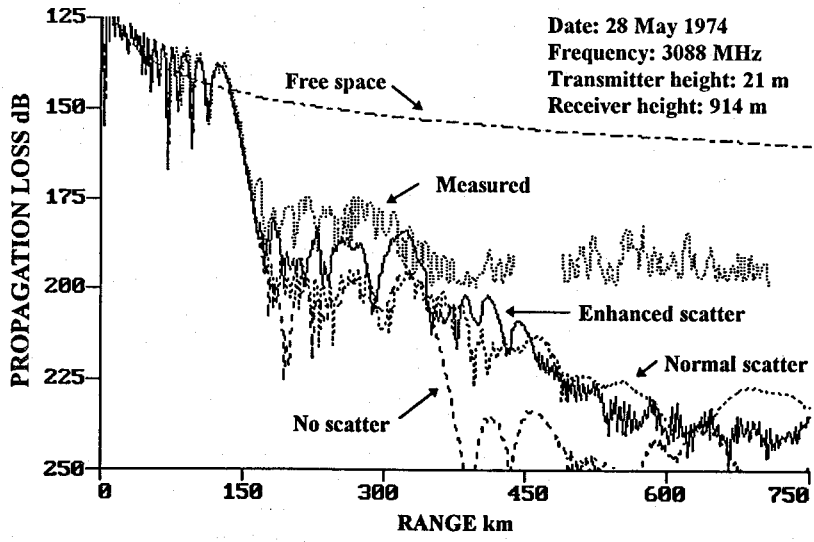

F2-9
1640

# AN APPROXIMATE METHOD FOR MODELING VEGETATION EFFECTS OVER TERRAIN

Amalia E. Barrios
Ocean and Atmospheric Sciences Division
NCCOSC RDTE DIV 543
53170 WOODWARD ROAD
SAN DIEGO CA 92152-7385

There are currently several models that have been validated that can model radiowave fields over terrain (R.J. Luebbers, *IEEE Ant. and Prop.*, 951-955, 1984, S. Ayasli, *IEEE Ant. and Prop.*, 1013-1023, 1986, A.E. Barrios, *IEEE Ant. and Prop.*, 90-98, 1994). While these models perform adequately when the terrain path is absent of any major vegetation such as trees and large brush, they fail to adequately account for the increased attenuation observed when vegetation is present.

A simple method, implemented in a terrain split-step parabolic equation model (TPEM), is presented in which the ground is modified to approximate the vegetation. The method consists of simply increasing the ground elevation by the height of the intervening trees or brush. This method is particularly useful when the topography of the terrain path is poorly described, in which case the ground elevation can then be adjusted by an average value along the entire path.

An example is shown below in which fields were measured over a 6 km long terrain path at a frequency of 910 MHz (K.A. Chamberlin, R.J. Luebbers, *IEEE Ant. and Prop.*, 1093-1098, 1982). Signals were measured under two conditions, one in which the terrain path was clear, and one in which a grove of trees blocked the propagation path.

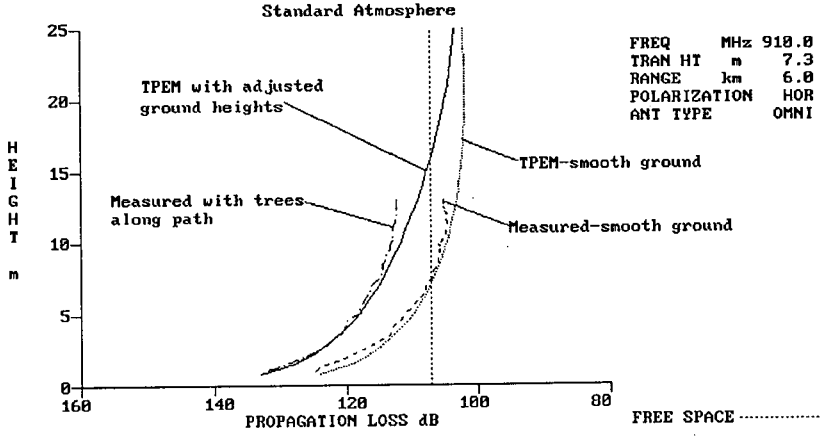

F2-10 THE ARCTIC UNATTENDED PROPAGATION EXPERIMENT
1700

Edward J. Kennedy & Michael A. Rupar
Naval Research Laboratory, Code 5550
4555 Overlook Ave., SW
Washington, DC 20375-5337

A system to study terrestrial radiowave propagation has been implemented on the northern Alaskan coastline. Signal strength measurements are taken of radiated signals from dedicated test beacons operating in the VHF and UHF frequency bands, as well as signals of opportunity in the MF and HF bands. These measurements have been conducted nearly continuously since September 1993. Measurements are correlated with local environmental conditions and with weather information from the US Navy's NODDS system. The paths are all coastal/maritime, with open water during a portion of the year, leading to wide variation in the near-surface atmospheric properties. Some correlation has been observed with both temperature and season.

Session F/G/J, 1355-Tues., CR0-30
EFFECTS ON RADIO SIGNALS FOR TRANSIONOSPHERIC PROPAGATION PATHS
Chairperson: Santimay Basu, Phillips Laboratory/GPIA, 29 Randolph Road, Hanscom AFB, MA 01731
Organizers: S. Basu; J. Goldhirsh, APL/JHU; and M. Davis, NAIC

F/G/J-1
1400

## TROPOSPHERIC EFFECTS ON EARTH-SPACE PROPAGATION AT VHF-EHF

Ernest K. Smith and Warren L. Flock
Electrical and Computer Engineering Department
University of Colorado at Boulder
Boulder, CO 80309-0425

The magnitude and severity of tropospheric impairments to earth-space transmissions are reviewed for the frequency range 30 MHz to 30 GHz (roughly the region where both tropospheric and ionospheric effects need to be examined). This is done for absorption, ray curvature, depolarization and scintillation as a function of frequency, elevation angle, humidity and rain rate.

While ionospheric effects per se are not the focus of this paper, the relative importance of the ionospheric impairments as compared to those of the neutral atmosphere will be treated.

F/G/J-2 1420 COMBINED EFFECTS OF SENSING THE ATMOSPHERE AND IONOSPHERE WITH SPACE BASED GPS RECEIVER

D. R. Schropp, Jr. and Y. T. Chiu
Lockheed Palo Alto Research Laboratory
Palo Alto, California 94304
Tel: (415) 354-5631;
Internet: schropp@agena.space.lockheed.com

Remote ionospheric and atmospheric sensing using occultation type geometry from a space-based GPS receiver depends upon measuring and interpreting the propagation effects on GPS's transmitted signals. The ionospheric and atmospheric modifications to the index of refraction are responsible for these propagation effects, which include ray path spatial deviation, carrier and group phase shifts, and amplitude shifts. Detailed calculation of these quantities are needed for studying and developing atmospheric inversion algorithms for retrieval of spatial density and temperature information. We have performed very accurate numerical integrations of signal rays transmitted from a GPS satellite through both the atmosphere and ionosphere. Results obtained demonstrate that the ionosphere affects the vertical resolution of the retrieved atmosphere at the level of ~1.5 km, necessitating knowledge of ionospheric refraction to realize the 0.5 km vertical resolution goal of atmospheric measurements. Furthermore, significant effects of the ionosphere on the accuracy of atmospheric density and temperature retrieval using an algorithm based on bending angle data are shown, indicating that spatial density information of the ionosphere is required to properly retrieve atmospheric parameters.

F/G/J-3
1440

# SPACE WEATHER EFFECTS ON SATELLITE COMMUNICATION AND NAVIGATION SYSTEMS

Santimay Basu and Gregory J. Bishop
Phillips Laboratory/GPIA
29 Randolph Road
Hanscom AFB, MA 01731
Sunanda Basu
Atmospheric Sciences Division
National Science Foundation
4201 Wilson Blvd
Arlington, VA 22230

The weather in the earth's near space plasma environment, commonly known as the ionosphere, dictates the quality and accuracy of satellite radio communication and navigation systems that operate in the VHF-UHF range of frequencies. Under stable weather conditions, the ionized near earth space environment behaves as free space for VHF-UHF radio waves. When unstable weather conditions develop, the prevailing turbulent processes create electron density irregularities in this region. It is shown that these irregularities can become sufficiently strong to scatter radio signals in the frequency range of 250 MHz to 4 GHz and introduce unacceptable message errors, particularly, near the magnetic equator. The GPS navigation systems operating at 1.2/1.6 GHz not only suffer data loss and cycle slips due to intense fading but may also lose phase lock in the presence of rapid changes of phase caused by electron density structures, and the relative motions of these satellites and the ionosphere. The confinement of equatorial irregularities in latitudinally extended and longitudinally discrete structures provides a unique set of constraints/ advantages to the use of GPS satellites in this region. It is pointed out that the day-to-day variability of weather in the near space environment is primarily controlled by internal forcing functions such as the electric field, gravity waves and the neutral wind rather than transient solar phenomena such as solar flares, and energetic particle events. The present state of near earth space weather models is also discussed in the context of systems requirements.

F/G/J-4
1500

## RECENT IMPROVEMENTS TO A MODEL OF IONOSPHERIC F-LAYER IRREGULARITIES

J. A. Secan, R. M. Bussey, E. J. Fremouw
Northwest Research Associates, Inc.
Bellevue, WA 98009
Sa. Basu
USAF Phillips Laboratory, GPIA
Hanscom AFB, MA 01731

The WBMOD ionospheric scintillation model has been extensively modified over the past three years to include improved specification of variations in scintillation in both the equatorial and high-latitude regimes. Previous versions of the model were based primarily on data collected from the Wideband satelliteat three stations: Poker Flat, Alaska at high latitudes; and Ancon, Peru, and Kwajalein Atoll in the equatorial region. In addition to being spatially limited, the data were limited in local time as the Wideband satellite was in a sun-synchronous orbit. In the present upgrade, we have used data from three additional equatorial stations (Huancayo, Peru; Manila, Philippines; Ascension Island) provided by the USAF Phillips Laboratory Geophysics Directorate, and four additional high-latitude stations (Bellevue, Washington; Ft. Churchill, Canada; Tromso, Norway; Sondre Stromfjord, Greenland) from the Hi-Lat/Polar BEAR satellite experiments. These data sets have provided not only spatial diversity, but full coverage in local time as well.

The new models for the height-integrated spectral strength, $C_kL$, are more complex than in previous versions of WBMOD. The model of the equatorial region now provides for higher scintillation levels near the anomaly crests than at the (dip) equator, and uses an algorithm for the onset time near sunset based on current understanding of the physics underlying the generation of ionization depletion "bubbles" in the post-sunset equatorial $F$-region. The high-latitude section of the model has also undergone extensive modification based on analysis of the extensive HiLat/Polar BEAR data sets, and now includes a separate polar-cap region, a more complex transition from the benign mid-latitude region into and through the auroral region, and a longitude-dependent variation with season.

The propagation model has been modified as well, and now includes a corrected algorithm for two-way $S_4$ calculation, calculation of the SI(dB) index, and the capability to calculate either the scintillation levels at a given probability of occurrence or the percent of the time that a user-specified scintillation level is exceeded.

F/G/J-5 PROPAGATION IN RANDOMLY STRUCTURED IONIZATION
1540

L. J. Nickisch
Dennis Knepp
Mission Research Corporation
2300 Garden Road, Suite 2
Monterey, CA 93940-5326

The natural ionosphere of the earth, though often treated as a smooth or slowly varying medium, frequently exhibits structure at scales which diffract or scatter radio waves. When passing through such regions, the phase of the radio wave is modulated by the ionization structure resulting in scintillation (amplitude fluctuations) and loss of signal coherence both spatially and temporally. This review talk will consider several computational methods for analyzing propagation in ionization structure. The characteristics of naturally occurring ionization structure will be briefly addressed. Examples of the effects on radiowave propagation due to structured ionization on trans-ionospheric VHF signals and bottomside HF signals will be shown. Several methods for computing signal decorrelation times, frequency coherence bandwidths, and signal correlation lengths will be examined. These include analytic parabolic equation approaches, multiple phase screen approaches, and the Finite-Difference Time-Domain method.

F/G/J-6
1600

# IONOSPHERIC PROPAGATION EFFECTS ON CYCLOSTATIONARY SIGNALS

William A. Brown
and
Dennis L. Knepp
Mission Research Corporation
2300 Garden Road, Suite 2
Monterey, CA 93940-5326

Cyclostationary signal processing techniques are useful for detection of signals buried in noise, measurement of carrier frequency, baud rate, time-difference-of-arrival, direction-of-arrival, and other applications. In particular, the spectral correlation function (SCF), which gives a complete description of the second-order signal statistics, is distinct for different transmitted signal types, and is therefore useful in the above applications. However, for cases of radio propagation through the ionosphere the random nature of the channel can modify the cyclostationary properties of the received signal. This paper presents an analytic formulation that characterizes the effect of ionospheric scintillation on the received signal's SCF.

Under conditions of worst-case scintillation, the parabolic wave equation may be used to compute the two-position, two-frequency mutual coherence function (MCF) which describes the correlation function of the received electromagnetic field, given that a constant amplitude sine wave is transmitted through a disturbed ionospheric layer. Motion of the line-of-sight through the irregularities comprising the ionosphere convert the spatial variations calculated in the MCF to temporal variations of interest here.

The mutual coherence function is used in a straightforward manner to relate the ionospheric communications channel to the channel impulse response correlation function $\langle h(\nu_1, \tau_1) h^*(\nu_2, \tau_2) \rangle$. This correlation function is expressed in terms of the MCF, and is shown to be uncorrelated in doppler $(\nu_1 - \nu_2)$ and in delay $(\tau_1 - \tau_2)$. Thus the ionospheric channel is a wide-sense stationary uncorrelated scattering channel.

The general expression for the received signal SCF depends on the MCF and the SCF of the transmitted signal. This expression is used to provide examples of the SCF for BPSK and MSK signals after propagation through realizations of a strong-scattering ionospheric channel. These simulations are shown to agree with the analytic calculations.

F/G/J-7
1620

## THE EFFECT OF TRANSIONOSPHERIC PROPAGATION ON VLBI OBSERVATIONS

Carl Gwinn and Maria Jose Ojeda
Physics Department
Broida Hall
University of California
Santa Barbara, CA 93106

We describe effects of transionospheric propagation on geodetic very-long baseline interferometry (VLBI) observations, as a function of the length of interferometer baseline, time of day, and phase of solar cycle. We find that the effects are largest for long baselines, during day at one antenna and night at the other, near or just after solar maximum. These conclusions are based on measurements of the dispersive part of the differential delay between antenna pairs, from a database of dual-frequency VLBI observations spanning a solar cycle. We compare these observations with measurements of ionospheric TEC as inferred from measurements of the ionospheric Faraday rotation of satellite signals, over the period that such observations are tabulated, and find that this reproduces most of the correction. We discuss the accuracy for ionospheric corrections that might be obtained from dual-frequency GPS receivers co-located at VLBI antennas.

F/G/J-8 INTERPLANETARY SCINTILLATION

1640 John W. Armstrong
Mail Stop 238-737
Jet Propulsion Laboratory
Pasadena CA 91109

Interplanetary scintillation (IPS) has been used as a diagnostic of solar wind speed and interplanetary plasma turbulence, allowing inference of speed and electron density power spectrum close to the sun and out of the ecliptic. In that context, IPS is "signal" and provides scientifically interesting data. IPS is also of interest because amplitude and phase perturbations imposed on radio waves are "noise" for telemetry and precision Doppler tracking of deep space probes and for some radio astronomical observations.

In this talk I briefly review the connection between scattering observables and the electron density power spectrum. The main part of the talk emphasizes IPS-as-noise, with examples drawn from scintillation observations using the Galileo, Mars Observer, and Pioneer spacecraft. Interplanetary phase scintillation on time scales of 100-10,000 seconds is an important noise in mass determinations of small solar system bodies during space-probe flybys and in searches for low-frequency gravitational radiation. (Interplanetary phase scintillation at S-band limit the sensitivity of gravity wave experiments and are more than an order of magnitude higher than the precision of the hydrogen masers driving the Doppler system.) Amplitude scintillation, which degrades space probe telemetry performance for some tracking geometries, is also of practical interest. Examples of amplitude scintillation for near-sun tracking are given, along with the predicted scintillation environment for Galileo at Jupiter orbit insertion and for the proposed Solar Probe, which will pass to within 4 solar radii from the sun.

## *Wednesday Morning, 4 January, 0815-1200*

0815-Wed., Math 100
PLENARY SESSION

0815 Introduction

0825 Student Paper Competition

0930 Break

0945 Invited Plenary Lectures

1145 Student Paper Award

Session A/B/K, 1335-Wed., CR1-42
BIOLOGICAL EFFECTS OF ELECTROMAGNETIC FIELDS
Chairperson: James C. Lin, Univ. of Illinois at Chicago, M/C 154, 851 S. Morgan St., Chicago, IL 60607-7053
Organizers: James C. Lin; and Moto Kanda, NIST, Boulder, CO

A/B/K-1
1340

## A REVIEW OF THEORETICAL BIOELECTROMAGNETIC DOSIMETRY

Carl H. Durney
Departments of Electrical Engineering and Bioengineering
University of Utah
Salt Lake City, UT 84112

Work in theoretical dosimetry began to accelerate in the 1960s as concern intensified over the ever increasing exposure of people to a wide variety of electromagnetic (EM) field sources. In the early work, calculations were made primarily in planar and spherical models irradiated by planewave EM fields.

By the end of the 1970s, a combination of analytical and numerical techniques had been used to get extensive data for whole-body average SARs for models of humans and experimental animals over a frequency range from the 60 Hz region up to hundreds of GHz. For a man model in free space, the whole-body average SAR for planewave incidence showed a strong resonance with frequency at about 80 MHz, at which a half-wavelength is about equal to the length of the model. For an average rat, this resonance occurs at about 600 MHz, which significant difference emphasizes the need for dosimetry in extrapolating the results of biological EM effects in experimental animals to those expected in humans.

In the 1980s, calculations were extended to include some near-field irradiation and to study distribution of the internal fields in addition to calculating the average SARs. Then advances in numerical EM techniques led to extensive use of newer methods, the finite-difference time-domain method, for example. As computing power has increased, calculations have been made in increasingly more sophisticated models, such as that of a man derived from magnetic-resonance images consisting of hundreds of thousands of mathematical cells. As the technology advances, more attention is being paid to calculations for exposure to relevant sources, such as cellular telephones, and less to planewave exposure.

Advances in numerical EM techniques and increased computing power will allow still more meaningful calculations of internal fields, but will require advanced methods of generating realistic biological models. Significant effort, for example, is required to determine the permittivity and conductivity of each mathematical cell in a model of the human body consisting of hundreds of thousands of such cells. Methods should be developed for generating such models and making them generally available to those who want to make calculations of internal fields. Another need is to extend dosimetry to the micro scale. For example, as biological techniques for making measurements on biological cells advance, micro-circuit methods should be used to model cells and to apply fields, and induced fields should be calculated on a micro scale.

A/B/K-2
1420

# BIOEFFECTS AND PUTATIVE HEALTH RISKS OF ELF FIELDS FROM POWER LINES AND OTHER SOURCES

Howard Wachtel(1) and Robert Pearson(2)
(1) Dept. of Electrical and Computer Engineering
University of Colorado, Boulder, CO 80309-0425
(2) Radian Corporation, Denver, CO

The present public concern over putative adverse health effects of 60 Hz (ELF) fields from power lines stems in large part from the studies of Wertheimer and Leeper (1979) who devised "wire codes" as surrogates for direct magnetic field measurements in a pioneering study of childhood cancer risk based in the Denver/Boulder area. More recent studies having improved exposure assessment methodologies include Savitz, Wachtel, Barnes, John, and Trvdik (1988) who spot measured magnetic (and electric) fields in homes in the Denver/Boulder area as well as using wire codes as "surrogates"; London et al, (1991) who measured magnetic fields over 24-hours or longer intervals as well as using spot measurements and wire codes in Los Angeles County and Feychting and Ahlbom (1992) who estimated magnetic field exposure near transmission lines in Sweden using distance and historic line loading data and also made magnetic field measurements.

In all these studies the surrogate indicator (wire codes or distance) showed an association with childhood cancer risk but the magnetic field measurements did not. This paradoxical finding has led us to explore other factors that may underly the linkage between wire codes and childhood cancer.

We recently reported that several "Residential Environment and Lifestyle" (REL) factors are strongly associated with certain wire code categories used by Savitz et al as a derivation of the original Wertheimer and Leeper formulation. In particular we found that "very high current configuration" (VHCC) homes were predominantly found in rectangular street layout neighborhoods located close to city centers, were generally built prior to 1972 and tended to be occupied by renters. In contrast, homes having buried distribution lines, which was the wire code referent group in the Savitz et al, study, were located almost exclusively in "cul de sac" street layout neighborhoods located in the suburban outskirts of the Denver metro area, were generally built after 1971 and tended to be owner occupied. These associations between wire code categories and REL factors suggest the possibility of a linkage between wire codes and childhood cancer risk through pathways that are plausible alternatives to magnetic fields.

Some of the biophysical research that we have carried out at the University of Colorado and elsewhere suggests that fields induced in and around cells by 60 Hz magnetic fields on the order of 1μT flux density, are quite small compared to ambient bioelectric fields and would therefore be unlikely to have carcinogenic actions. However, we have also found that under certain conditions neurons (such as Aplysia pacemakers) can be influenced by such fields and that specialized "electroreceptors" in sharks (and related species) can be even more sensitive to ELF fields. Therefore there are sensory bioeffects of low level ELF fields, but it seems that such effects are unlikely to lead to adverse health outcomes (such as cancer).

A/B/K-3
1520

## BEHAVIORAL STUDIES AND RADIOFREQUENCY FIELD EXPOSURE

Mary Ellen O'Connor,
Psychology Department,
The University of Tulsa,
Tulsa, OK 74104

The history of the study of possible health effects from exposure to radiofrequency fields always has included the question of behavioral effects. Some of the earliest reports of possible adverse effects from working with radiofrequency fields included psychological observations on humans and other animals. In fact behavioral studies were part of the core of cooperative efforts between the former Soviet Union and the U.S. The threshold for the establishment of the current IEEE recommendations for exposure to radiofrequency fields is derived from behavioral observations of rodents and primates in laboratory studies. These behavioral studies formed the threshold for the recommendation when the specific absorption rate (SAR) and frequency dependency were first included in the rationale for establishment of radiofrequency exposure guidelines. The behavioral guidelines have been upheld in subsequent revisions. Behavioral studies have decreased in frequency in the last two decades, as have most studies in the radiofrequency range. The few behavioral studies that have been reported in recent years support the continutation of the IEEE recommendation with some possible question regarding millimeter wave exposure and high peak power conditions.

A/B/K-4
1600

**HUMAN EXPOSURE STANDARDS FOR RADIO FREQUENCY FIELDS**

James C. Lin
EECS Department (M/C 154)
University of Illinois at Chicago
851 South Morgan Street
Chicago, IL 60607-7053

The fact that exposure to continuous, sinusoidal, time-varying, radio frequency fields can produce untoward biological effects in human beings have been acknowledged for some time. In October 1968, the U. S. Congress adopted the "Radiation Control for Health and Safety Act (PL 90-602)," to protect the public from unnecessary exposure to potentially harmful radiation, including radio waves emitted by electronic products. Together with the former Soviet Union's far more conservative standards for long term exposure, this Act had posed new questions on the adequacy of the existing knowledge of biological effects of radio frequency fields and of the protection afforded the public from the harmful effects of these fields.

The resulting research has produced a large data base of literature, which was used by several national and international organizations to develop safety standards and exposure guidelines. However, this discussion shall cover only the standard recently published by the Institute of Electrical and Electronic Engineers (IEEE) and recognized by American National Standards Institute (ANSI) as an American national standard (IEEE/ANSI C95.1-1992).

The ANSI/IEEE Standard for safe human exposure to 3 kHz - 300 GHz radio frequency fields includes extensive revisions of earlier versions of these standards. It presents recommendations for prevention of adverse or harmful effects in humans. However, it is a voluntary standard and thus provides only guidelines for maximum permissible exposure (MPE) limits on electric and magnetic fields or current and power densities under normal environmental conditions.

Among the various new revisions are:(1) The expansion of frequency range from 3 kHz to 300 GHz to include quasi-static and quasi-optic fields; (2) Contact and induced-current limits to deter shock and burn hazard; (3) Two-tiered MPE to distinguish between occupational vs. general public exposures; (4) Peak power limits to prevent unintentional high-power exposure; (5) Relaxation of MPE limits for partial body exposures; (6) Relaxation of MPE limits for low-frequency magnetic fields; (7) Frequency-dependent averaging times.

B/F-1
1340

## FREQUENCY AND ANGULAR CORRELATIONS OF ELECTROMAGNETIC WAVES SCATTERED BY ROUGH SURFACES

Lynn Ailes-Sengers, Akira Ishimaru and Yasuo Kuga
Department of Electrical Engineering
University of Washington
Seattle, WA 98195

There has been an increasing interest in the frequency and angular correlations of acoustic and electromagnetic waves scattered by rough surfaces. Frequency correlations, called the "two-frequency mutual coherence function," are the correlations of the scattered waves at two different frequencies for given incident and scattering angles and represent the coherence bandwidth of the scattered waves. The inverse Fourier transform of the two-frequency mutual coherence function is the scattered pulse shape in the time domain and illustrates the pulse broadening. On the other hand the angular correlation functions represent the correlation of the waves at different scattering angles for different incident angles at a given frequency. The angular correlations show the "memory effects" and are also used in the inverse problems of remote sensing of rough surface characteristics. These correlations are useful in characterizing ocean acoustic scattering channels and in SAR remote sensing of earth surfaces.

We present analytical expressions for the two-frequency mutual coherence function and the angular correlation function based on the first and second order Kirchhoff approximations with angular and propagation shadowing corrections. This theory is valid for scattering from very rough, high slope, two-dimensional surfaces, which are defined as the surfaces whose rms slopes are of the order of unity and whose rms heights are of the order of a wavelength. This is the region where conventional Kirchhoff approximations and perturbation theories are not applicable. The second order Kirchhoff approximations include the ladder and cross terms and give the enhanced backscattering. The second order terms are given by four fold integrals which are evaluated approximately giving double integrals.

Scattered pulse shapes in time are calculated as the Fourier transform of the two-frequency mutual coherence function and illustrate the pulse broadening due to the rough surface. The angular correlation results are presented in the form of the "angular memory signatures," which reveal the "memory effects." The "memory effects" refer to the strong correlation observed when the difference in the transverse wave numbers is the same for the incident and the scattered wave. Therefore, the change in the direction of the incident wave on a random medium is "remembered" by the scattered wave in the angular correlation characteristics. Millimeter wave scattering experiments are performed on two-dimensional, perfectly conducting rough surfaces in the frequency range of 75-100 GHz. The experimental data show good agreement with the analytical results.

B/F-2
1400

## INTEGRAL EQUATIONS ON SCATTERING AMPLITUDES FOR ROUGH SURFACE SCATTERING

John A. DeSanto
Department of Mathematical and Computer Sciences
Colorado School of Mines
Golden, CO 80401

We treat the acoustic problem of a two-dimensional rough interface separating two different semi-infinite media. The scattering from such surfaces can be described using boundary values of the field and its normal derivative. The latter arise from the solution of boundary integral equations in coordinate space. The reflection and transmission coefficients are determined from the boundary values using an integration over the surface.

Here we discuss a method, using the boundary integral equations in coordinate-space, to generate coupled integral equations directly on the reflection and transmission in Fourier transform space. The general case will be discussed as well as the restricted examples of the Dirichlet and Neumann integral equations.

B/F-3
1420

## THE ONSET OF MULTIPLE SCATTERING AT INTERMEDIATE FREQUENCIES AS SURFACE ROUGHNESS STEEPENS

Donald E. Barrick
CODAR Ocean Sensors
1000 Fremont Avenue
Los Altos, CA 94024

High-frequency approximations like physical optics often carry caveats that disclaim their validity when the surface profile becomes sufficiently steep so that multiple scattering is expected to contribute. Recent interest has focused on 'enhanced backscatter', where a somewhat increased return observed in the backscatter direction is attributed to multiple scatter. Bahar has studied this effect theoretically with full-wave theory as applied to statistically rough surfaces. The introduction of randomness and statistics, however, obscures the fundamental mechanisms at play and makes it difficult to assess the validity and applicability of approximate methods.

A computationally efficient, exact, unified modal methodology is used to examine the subject of normal-incidence backscatter from a large-scale periodic deterministic surface as the profile steepens, while keeping its spatial period and the radio wavelength constant. Both polarizations are studied. First, we examine the surface-induced currents based on: (i) the singly incident-ray tangent-plane assumption; (ii) the surface current produced by both singly and doubly incident rays (derived by Holliday); (iii) our exact method. The singly incident-ray current is seriously in error as the surface steepens; the doubly incident-ray addition helps as the slopes approach the 45°corner-reflector condition, especially for horizontal polarization.

The backscattered field using the singly incident-ray current with physical optics becomes essentially meaningless (compared to the exact backscatter) for slopes that exceed even 20°. The doubly-incident multiple-scatter correction to physical-optics currents fails to predict backscatter correctly when slopes exceed 45°, even though the high-frequency asymptotic assumptions are reasonably well satisfied. These findings are important when one considers 'patching up' physical or ray optics by including a double-bounce contribution.

B/F-4
1440

# NUMERICAL CALCULATIONS OF RANDOMLY ROUGH AND PERIODIC SURFACE SCATTERING USING A VARIATIONAL PRINCIPLE

D. J. Donohue
Applied Physics Laboratory
Johns Hopkins University
Johns Hopkins Road
Laurel, MD 20723

As an alternative to the Method of Moments, we investigate the application of a Schwinger variational principle (SVP) to rough surface scattering calculations. The SVP is an approximate method requiring an initial approximation to the field and/or its normal gradient at the scattering surface. We use the well-studied Kirchhoff or tangent-plane approximation with a correction for geometric optics shadowing. The work is directed towards ocean surface scattering, particularly at low grazing angles, where the Kirchhoff approximation breaks down. One of the issues investigated is the effectiveness of the SVP at correcting the Kirchhoff approximation for shadowing and multiple scattering effects that are known to be significant at near-grazing angles. A numerical code has been developed to calculate the far-field scattering from arbitrary surface height profiles. Stochastic surfaces are considered by averaging the calculation over repeated deterministic surface realizations. Results are calculated from various surface profiles, including periodic, sinusoidal and hemi-cylindrical, and Gaussian rough surfaces. The results are analyzed for both accuracy and computational time requirements. It is shown that given the lack of an apriori error estimate, the method must be cautiously applied over certain surface features such as wave cusps or crests. Nevertheless, the method does appear to be promising for considering a wide range of surface descriptions and scatter geometries.

Research sponsored by the Aegis Shipbuilding Program, PMS-400, under Navy contract #N00039-94-C-0001.

B/F-5
1500

# A SIMPLE MODEL OF THE KNOTTS-MICHEL-O'DONNELL ONE-DIMENSIONAL, RANDOMLY ROUGH, NON-GAUSSIAN SURFACE

E. R. Méndez
Division de Fisica Aplicada
Centro de Investigacion Cientifica y de
Educacion de Ensenada
Apdo. Postal 2732
Ensenada, Baja California, Mexico

A. A. Maradudin
Department of Physics
University of California
Irvine, CA 92717

In recent work Knotts, Michel, and O'Donnell (J. Opt. Soc. Am. **10**, 928 (1993)) measured and calculated the independent elements of the Stokes matrix for a one-dimensional, randomly rough, metal surface. They found that the agreement between computer simulation and experimental results for these matrix elements was significantly improved if the statistical properties of the surface profile function $\zeta(x_1)$ determined experimentally were used in the numerical simulation calculations instead of the commonly used assumption that $\zeta(x_1)$ is a stationary, zero-mean, Gaussian random process, with a Gaussian correlation function. Specifically, they found that while the probability density function (pdf) of $\zeta(x_1)$ for the surface studied was closely a Gaussian, with a correlation function that was also closely a Gaussian, the pdf of $\zeta'(x_1)$ was lower at the origin than predicted by a Gaussian expression, and the pdf of $\zeta''(x_1)$ was skewed in the direction of positive values of this function. By starting from a function $H(x_1)$ that is a stationary, zero-mean, Gaussian random process, with a Gaussian correlation function, we show how a surface profile function $\zeta(x_1)$ can be constructed in terms of $H(x_1)$ to have the statistical properties possessed by the surface studied by Knotts *et al.* Results of computer simulation calculations of the Stokes matrix elements on the basis of a surface defined by $H(x_1)$ and on the basis of the profile function $\zeta(x_1)$ obtained from it show that the latter is qualitatively and quantitatively in better agreement with the experimental results of Knotts *et al.* than the former.

B/F-6
1540

## RADAR SCATTER CROSS SECTIONS FOR TWO-DIMENSIONAL RANDOM ROUGH SURFACES USING THE FULL WAVE APPROACH -- THEORY AND EXPERIMENT

Ezekiel Bahar and Bom Son Lee
Electrical Engineering Department
University of Nebraska - Lincoln
Lincoln, Nebraska 68588-0511

Using the full wave approach, the bistatic radar scatter cross sections for two-dimensional random rough surfaces are obtained. The formal expression for the scattering cross sections for two-dimensional random rough surfaces involves 10- dimensional integrals (over the random surface heights, slopes and the surface variables at two points). At high frequencies and when the radii of curvature of the surface are large compared to the wavelength, it is shown that for isotropic rough surfaces, the 10-dimensional integral can be reduced to a 3-dimensional integral (over the slopes and the distance variable). This integral accounts for the height/slope correlation through the use of the conditional joint characteristic functions (Bahar and Lee, Radio Sci., Vol. 29, No. 2, 1994). These full wave results involving 3-dimensional integrals can be further simplified if the surface slopes are small. In this case, it can be assumed that the surface height and slopes are uncorrelated and the above 3-dimensional integral reduces to the product of a 2- and a 1-dimensional integral. Furthermore on applying a stationary phase (high frequency) approximation, the 3-dimensional integral reduces to a 1-dimensional (physical optics) integral or to a closed form (geometrical optics) expression.

These full wave results are compared with the associated small perturbation, physical/geometrical optics, and experimental results (O'Donnell and Mendez, J. Opt. Soc. Am. A, Vol. 4, No. 7, 1987). The full wave results are shown to reduce to the physical optics results in high frequency limit when the large radius of curvature assumption is made and to the small perturbation results when the rms height in wavelength is of the same order of smallness as the surface slopes. These results are also shown to be in good agreement with the experimental results.

B/F-7
1600

## NUMERICAL SIMULATIONS OF DIFFUSE SCATTERED FIELDS OF ONE DIMENSIONAL ROUGH SURFACES--FULL WAVE SOLUTIONS

Ezekiel Bahar and Yuzhi Zhang
Department of Electrical Engineering
University of Nebraska-Lincoln
Lincoln, NE 68588-0511

The full wave approach is based on the complete expansions of the electromagnetic fields and the imposition of the exact boundary conditions at rough surfaces. Maxwell's equations are transformed into a rigorous set of coupled first-order differential equations for the forward and backward traveling wave amplitudesgeneralized telegraphists' equations (E. Bahar, Can. J. Phys., vol. 50, no. 24, pp. 3123-3131, E. Bahar, Can. J. Phys., vol. 50, no. 24, pp. 3132- 3142). The generalized telegraphists' equations for the forward and backward travelling wave amplitudes are combined into a single integro-differential equation. A numerical method is derived to solve the total diffuse scattered radiation wave amplitudes from the integro- differential equation (E. Bahar and Y. Zhang, ISAE'93, Sept. 6-9, Nanjing, China, pp. 80-83, 1993). The singularities of the scattering coefficients are removed on integrating by parts. A stationary phase approximation is obtained for the far fields.

Numerical simulations are carried out for one dimensional deterministic and random rough surfaces. The Monte-carlo method is applied for the simulations of one dimensional random rough surfaces. For the deterministic sinusoidal surfaces, with maximum surface slope less than 30 degrees, the earlier single scatter analytical results are in good agreement with the numerical solutions for the total diffuse scattered fields derived here. The earlier solutions were based on assumption that the total field impressed upon rough surface is associated with the incident field only. The earlier results are in total agreement with the small perturbation results when the rough surface height and slopes are of the same order of smallness. The Monte-carlo simulations based on the numerical solutions derived here also support the results for deterministic rough surfaces.

B/F-8
1620

# SCATTERING OF A SCALAR WAVE FROM A TWO-DIMENSIONAL RANDOMLY ROUGH NEUMANN SURFACE

Rosa M. Fitzgerald and A. A. Maradudin
Department of Physics
University of California
Irvine, CA 92717
F. Pincemin
Laboratoire d'Energetique Moleculaire et Macroscopique
Combustion, Centre National de Recherche Scientifique
Ecole Centrale Paris
Chatenay Malabry, 92295 Cedex, France

We present a reciprocity and unitarity preserving formulation of the scattering of a scalar plane wave from a two-dimensional, randomly rough surface on which the Neumann boundary condition is satisfied. The theory is formulated on the basis of the Rayleigh hypothesis in terms of a single-particle Green's function $G(\vec{q}_{||}|\vec{k}_{||})$ for the surface electromagnetic waves that exist at the surface due to its roughness, where $\vec{k}_{||}$ and $\vec{q}_{||}$ are the projections on the mean scattering plane of the wave vectors of the incident and scattered waves, respectively. The specular scattering is expressed in terms of the average of this Green's function over the ensemble of realizations of the surface profile function $\langle G(\vec{q}_{||}|\vec{k}_{||})\rangle$. The Dyson equation satisfied by $\langle G(\vec{q}_{||}|\vec{k}_{||})\rangle$ is presented, and the properties of the solution are discussed, with particular attention to the proper self-energy in terms of which the averaged Green's function is expressed. The diffuse scattering is expressed in terms of the ensemble average of a two-particle Green's function, which is the squared modulus of the single-particle Green's function. The Bethe-Salpeter equation satisfied by $\langle|G(\vec{q}_{||}|\vec{k}_{||})|^2\rangle$ is presented, and properties of its solution are discussed. In the small roughness limit, and with the irreducible vertex function approximated by the sum of the contribution from the maximally-crossed diagrams, which represents the coherent interference between all time-reversed scattering sequences, the solution of the Bethe-Salpeter equation predicts the presence of enhanced backscattering in the angular dependence of the intensity of the waves scattered diffusely.

B/F-9
1640

# NUMERICAL SIMULATION STUDIES OF THE SCATTERING OF LIGHT FROM TWO-DIMENSIONAL RANDOMLY ROUGH METAL SURFACES

P. Tran
Code CO 2313
NAWC-WD
China Lake, CA 93555

A. A. Maradudin
Department of Physics
University of California
Irvine, CA 92717

We present results for the in-plane co- and cross-polarized scattering of p-polarized light incident normally on a two-dimensional, randomly rough, metal surface obtained by two different approaches. In the first a system of four coupled integral equations for the two independent components of the surface electric current and the two independent components of the surface magnetic current is derived from the Stratton-Chu formulas by means of the replacement of the surface charge densities by surface divergences of the surface current densities. This system of integrals is transformed into a system of matrix equations that is solved by Neumann-Liouville iteration. The scattered electric and magnetic fields are obtained from the solution.

In the second approach the system of four coupled integral equations for the independent components of the surface currents is reduced to a system of two coupled equations through the use of an impedance boundary condition for a two-dimensional rough metal surface.

The results obtained by both approaches are found to be in good agreement with our earlier results obtained on the basis of the six Stratton-Chu formulas (Opt. Commun. **110**, 269 (1994)).

D2-1
1340

## Optical Interconnects in VLSI Systems Using Polymer Waveguides and Switches

Jiong Ma and Alan R. Mickelson
Department of Electrical and Computer Engineering
University of Colorado
Boulder, Colorado 80309

Optical interconnects have some advantages over electronics, such as large bandwidth, no ground loop, small cross talk, immunity from electromagnetic interference, and reduced capacitive loading. The advantage of optical interconnect technology suggests a potential alternative for VLSI interconnections. The development of dye-doped polymer materials allows the fabrication of waveguides and active electro-optic waveguide components in layered structures in the same material system, the processing of the polymeric optical devices is compatible with standard packaging processing.

In this paper, comparison between chip-to-chip, and MCM-to-MCM interconnections for both the electrical and optical alternatives in terms of power dissipation, speed, and fanout capability will be discussed. The 0.8 $\mu m$ electrical interconnect model based on HSPICE simulation and CMOS compatible electro-optic interconnect model will be shown. The basis for the study will be the work on polymer waveguides and switches that is currently being performed here at the University of Colorado at Boulder.

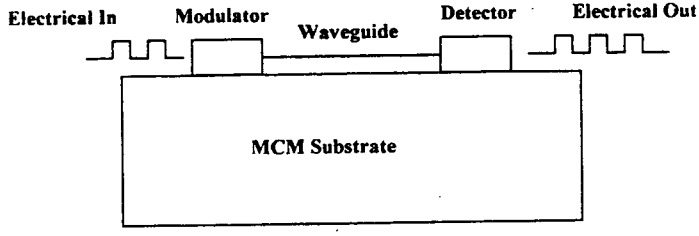


**Electro-optic Chip-tochip interconnection**

D2-2
1400

## CHANNEL WAVEGUIDE STUDIES IN *Mg-doped $LiNbO_3$*

Raghu Narayan and Prof. Alan Mickelson
Department of ECE, Campus Box 425
University of Colorado
Boulder, CO 80309-0425

Photorefractive damage is a serious concern for designers of active Integrated Optical(IO) devices. Magnesium doped Lithium Niobate(Mg:$LiNbO_3$) has been shown to have a very high optical damage threshold levels. One of the goals of this effort is to characterize this material sufficiently in order to fabricate low loss channel waveguides in them. In this talk, results from planar waveguide studies will be presented briefly. The technique, Annealed Proton Exchange(APE), used to fabricate channel waveguides will be overviewed(Refer Figure). Results of the annealing and its effect on the waveguide losses, index profile, hence its effect on the waveguide mode characteristics will be discussed. Preliminary results of channel waveguides in Neodymium indiffused Mg:$LiNbO_3$ using APE will also be presented.

**Proton Exchange Technique**

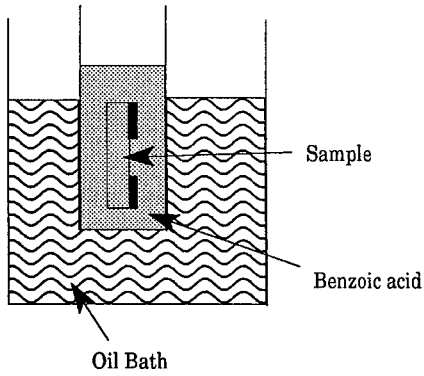


**Annealing**

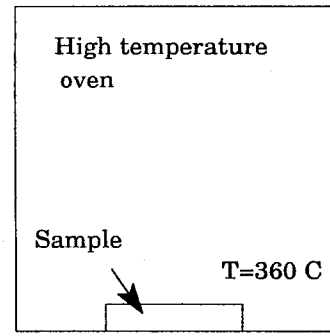

D2-3
1420

# CHARACTERIZATION OF HIGH PERFORMANCE PACKAGES: ELECTRICAL, THERMAL AND STRESS ISSUES

P. Tirkas, S. El-Ghazaly, S. Rajan, E. El-Sharawy, and C. Balanis
Telecommunications Research Center
College of Engineering and Applied Sciences
Arizona State University
Tempe, AZ 85287-7206

In recent years, packaging issues have been given greater attention mainly because the performance, reliability and cost of semiconductor chips are increasingly dictated by the choice and design of the package. While the trend in the eighties was to integrate different types of devices on relatively large chips to enhance overall performance, the emphasis in the nineties and well into the next century will be on reducing the overall cost with highly reliable packages. This may require having several chips with one type of device integrated on each chip. Microelectronic packaging design problems are not only characterized by multi-disciplinary issues but, more often, have several design alternatives all of which may be viable design options. In order to reduce the design iterations and meet increasingly stringent design standards, accurate and efficient integrated, multi-disciplinary analysis and design tools must be developed to address the needs of microelectronic packages.

The aim of this paper is to integrate different disciplines that affect the design and manufacturing of microelectronic packages, study their interaction and develop efficient and accurate analysis and design tools. The specific design issues addressed are thermal, stress, and electrical. This is achieved through a first-order analysis and design of a commonly used package, the flip-chip, that allows the direct attachment of the integrated circuits to ceramic chip carriers. The package is shown in Fig. 1. Results showing the package characteristics with and without an underfill will be presented. The electrical performance was analyzed via the finite difference time-domain technique. The thermal stress analysis was carried out using an elasto-plastic finite element formulation.

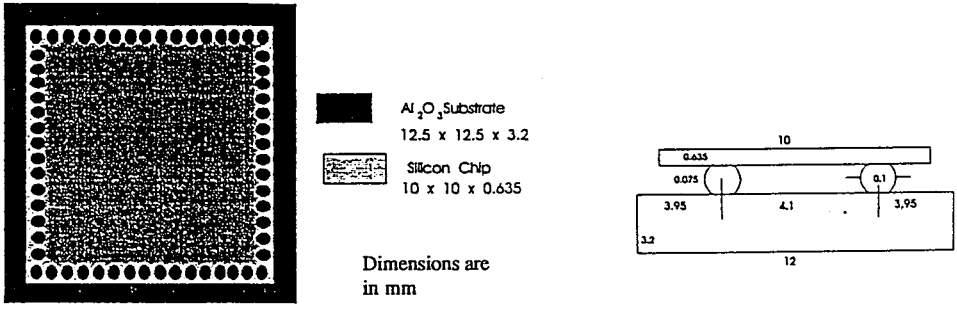


Fig. 1 (a) Flip-chip layout and (b) simplified model for analysis.

D2-4
1440

**OPTICAL SAMPLING FOR DETERMINATION OF MATERIAL CHARACTERISTICS**

Paul Biernacki , Henry Lee and Prof. Alan R. Mickelson
Department of Electrical & Computer Engineering
University of Colorado
Boulder, Colorado 80309-0425

The quality of Ohmic contacts can place limitations on device performance, especially on III-V semiconductors. Further, the process of Ohmic contact fabrication has been shown to allow long range transportation of atoms creating crystal defects and atom clusters which can possibly affect device performance (Fillard J P, et. al "Latest Results In Image Interface Reconstruction: Application To Ohmic Contact Inspection", DRIP V Conf., Santander, Spain 1993). Electro-optical sampling was used to measure the electrical anomalies produced by an in house fabricated Ohmic contact.

The device under test is shown in figure 1. The ohmic test device is a coplanar waveguide (CPW) constructed on electrooptic GaAs where part of the transmission line has been replaced by a heavily doped n++ strip. A standard GeAu/Ni/Au metalization mixture was brought to the eutectic temperature forming a distributed Ohmic contact along the CPW. High spatial resolution optical sampling was used to measure the electrical characteristics of the CPW and was correlated with IIR (Image Interface Reconstruction) microprecipitate images to provide a more thorough understanding of contact technology .

Preliminary results indicate that asymmetries present in the electrooptic sampling data may correspond to defect clusters created in the Ohmic contact process region and also possibly due to the crystal defect regions present in the bulk GaAs wafer. It may be possible to correlate defects produced in the contact process with their related local electrical perturbations.

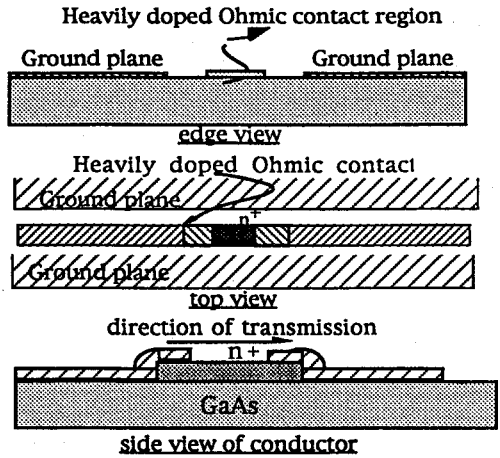


Figure 1 Coplanar transmission line with an ohmic contact

D2-5
1500

## Nd-CHELATE-DOPED POLYMER WAVEGUIDES FOR OPTICAL AMPLIFIERS

Sihan Lin and Alan R. Mickelson
Department of Electrical and Computer Engineering
University of Colorado
Boulder, CO 80309-0425

Loss in Polymer optical devices is still a major issue which limits their applications. One approach to this problem is to introduce polymer amplifiers which can be integrated with other optical devices on the same substrate to compensate the loss. By incorporating the rare-earth ions into polymers, optical amplifiers can be made. However, there is difficulty to dope rare-earth ions directly into nonpolar polymers, since solvents for these polymers can not dissolve rare-earth chlorides. We used organic rare-earth materials such as rare-earth chelates as dopants, which can be dissolved in the polymer solvents. By mixing rare-earth chelate with polymer solution we have doped rare-earth ions ($Nd^{3+}$, $Er^{3+}$) into nonpolar polymers such as electro-optic PMMA/DR1 and polyimides which have been widely used in electronics industry. The absorption measurements of these doped polymers showed the rare-earth signatures. We have observed photo-luminescence in Nd-chelate-doped polyimide channel waveguides. With 8 mW of pump power at 797 nm wavelength, we have seen luminescence at 1058 nm. Fig. 1 shows the photo-luminescence spectrum of a Nd-chelate-doped polyimide channel waveguide.

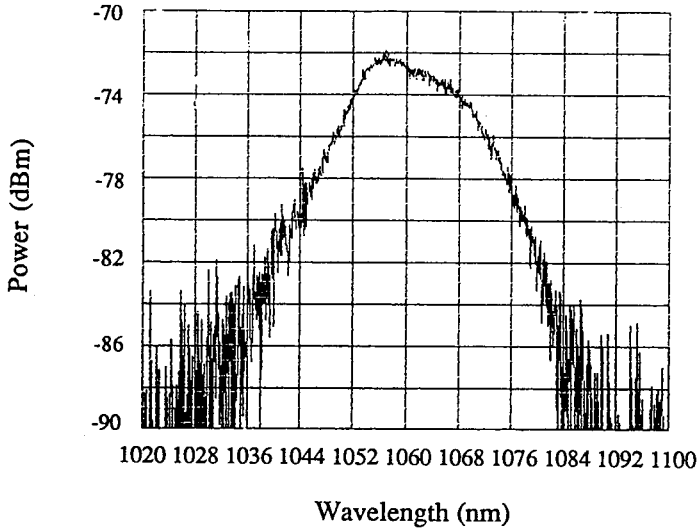


Fig. 1 The photo-luminescence spectrum of a Nd-chelate-doped polyimide channel waveguide. The waveguide was pumped by a 28 mW diode laser at 804 nm wavelength.

D2-6
1540

# INVESTIGATION OF MODELING TECHNIQUES FOR RADIATED EMISSIONS FROM PRINTED CIRCUIT BOARDS

**Vladan Jevremovic, Edward F. Kuester**
**Department of Electrical and Computer Engineering**
**University of Colorado at Boulder**
**Boulder, CO 80309-0425**

The scope of this paper is the accurate prediction of radiated emissions of Printed Circuit Boards (PCB) with the attached cables. The Printed Circuit Boards, in general, consist of traces of arbitrary complexity, passive lumped impedances and an RF source. In order to completely determine radiated emissions, it is required to compute radiation not only for fundamental, but for several harmonics as well. For practical applications, the PCB may often be considered electrically small with the respect to a wavelength corresponding to the fundamental frequency and the lower harmonics. A way of characterizing an electrically small PCB is to replace it with one or more small lengths of wire each oriented in a particular direction in addition to an equivalent RF source driving it. The orientation of wire(s) as well as the driving voltage of an equivalent RF source are determined by matching the far field radiation patterns of the corresponding structures, with the same attached cable present. We will show that the equivalent circuit (electrically small wire(s) and equivalent RF source) is largely independent of the orientation and the length of the cable, therefore eliminating the need to reanalyze the structure every time a new cable is attached to it. Furthermore, since the PCB is deemed to be electrically small for a certain frequency range, the quasi-static analysis may be employed, eliminating the need to recompute the radiation at each frequency using a full-wave approach. As an example, a simple PCB circuit in a free-space environment will be presented, and comparison between radiation from it and from an equivalent circuit as described above will be shown.

D2-7
1600

# WHAT LIMITS PASSIVE DIRECTIONAL COUPLER CROSSTALK

Darja Tomic, Sihan Lin, Wei Feng and Alan R. Mickelson
Department of Electrical and Computer Engineering
University of Colorado
Boulder, Colorado 80309

The crosstalk in passive directional couplers is limited to roughly -30 - (-35) dB. This limit on the crosstalk seems to be true for all devices independent of fabrication technology. Recent technologies, such proton exchange in $L_iN_bO_3$ or photobleaching in polymers have built in steps that can be used to "tune" a structure to achieve a desirable passive bias. Even after the tuning step these devices still exhibit a crosstalk which is about the same as the best achievable in $T_i : L_iN_bO_3$.

This theoretical analysis shows that finite loss is not a cause of the -30dB crosstalk limit. Several effects could be the limiting factors. One of the most imortant is asymmetry caused due to fabrication errors. Variations in $\Delta n \approx 10^{-4} - 10^{-5}$ will cause a -30dB limit, yet not be easily measurable. It is not possible by non invasive tests to determine which effect limits the crosstalk.

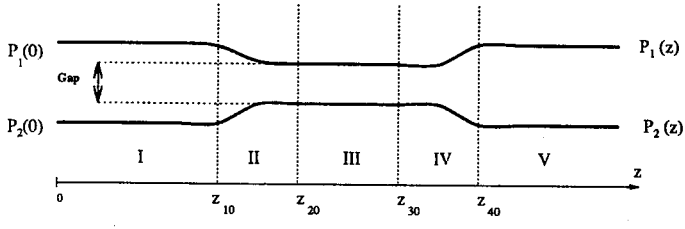


I,V - INDIVIDUAL WAVEGUIDES
II, IV - THE TRANSITION REGIONS
III - THE INTERACTION REGION

D2-8
1620

# POLYMERIC ELECTRO-OPTIC DEVICES

Wei Feng, R. Brian Hooker and Alan R. Mickelson
Department of Electrical and Computer Engineering
University of Colorado at Boulder
Campus Box 425
Boulder, CO 80309

Optical interconnects require basic components such as optical waveguides, electro-optic modulators and switches. Devices based on nonlinear optical (NLO) polymers are promising for these applications in that the materials have potentially large electro-optic coefficients, and low dielectric constant, and that the processing can be simple and compatible with processing in semiconductor industry. In this presentation, we report the results on polymeric electro-optic modulators and switches. The NLO polymer used is side-chained PMMA/DR1. The electro-optic modulators include straight channel phase modulators, and Mach-Zehnder intensity modulators. The electro-optic switches are based on directional coupler structures. In order to have NLO polymer exhibit macroscopic electro-optic effect, electrical poling has to be performed. We use parallel-plate electrodes for electrical poling, and coplanar electrodes for driving the devices. The material exhibits an effective electro-optic coefficient of 12 pm/V in the channel waveguide for a poling voltage of 600 V across the whole 13 μm structure. Characterizations of other device properties will also be presented. In addition, characterizations of optical losses of the waveguide bends and intersecting waveguides, and crosstalks of the intersecting waveguides, will be presented along with simulations on these structures for comparison.

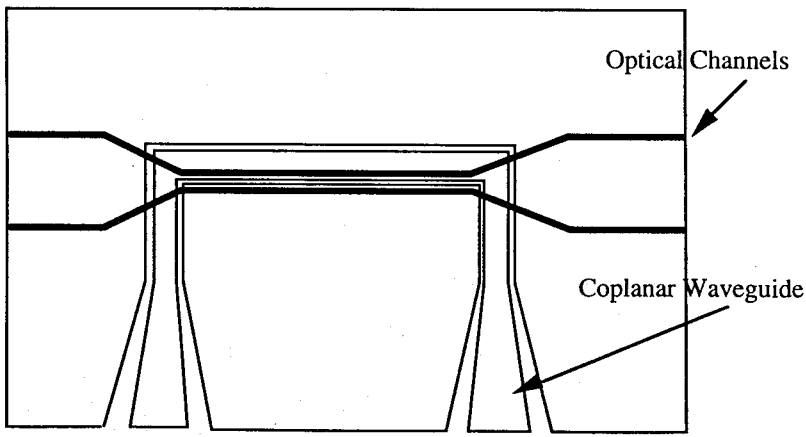

D2-9
1640

# DISK AND STRIPE CAPACITANCES

B. Gelmont, M. Shur, and R. J. Mattauch
Department of Electrical Engineering
University of Virginia
Charlottesville, VA 22903-2442

Maxwell and Kirchhoff were among the first to study the problem of the capacitance of a disk separated from the ground plane by a dielectric slab. Since that time, much effort has been devoted both to the numerical solutions and to the analytical approximations for this problem. We report on a new approach to the numerical solution of the problem of the disk capacitance. In our approach, the problem is reduced to the problem of solving the integral equation which already accounts for the proper boundary conditions. The integral equation which we derived can be easily solve by the Gauss' method. Based on the numerical solution, we propose a simple interpolation formula for different geometries and dielectric permittivities, with an accuracy sufficient for most engineering applications:

$$C_{appr} = \frac{2\pi(\varepsilon + \varepsilon_0)a}{\tan^{-1}\left(\frac{2b(\varepsilon + \varepsilon_0)}{a\varepsilon}\right)}$$

Here $a$ is the disk radius, $b$ is the thickness of the dielectric layer, $\varepsilon$ is the dielectric slab permittivity, and $\varepsilon_0$ is the dielectric permittivity of the surrounding medium. We also propose a much more accurate (but a more complicated) interpolation formula. Finally, we apply our method to the analysis of the capacitance of a metal stripe separated by a dielectric slab from the ground plane. With trivial changes in variables, the obtained results apply to the problem of a spreading contact resistance. These results can be used in the design of solid state devices and integrated circuits.

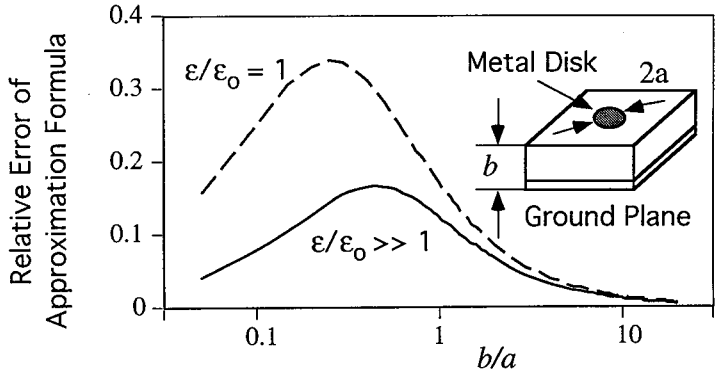

E2-1
1340

## PCS RADIO LINK DESIGN FOR INTEGRATED VOICE AND DATA

Richard A. Dean
National Security Agency
Attn: R22
9800 Savage Road
Ft. Meade, MD 20755

Personal Communications Services with the attendant wireless technologies represents a vision of information infrastructure that has captured the imagination of technologists, politicians and users. Each has a vision of services that these new technologies will support. Many of these visions include multimedia data and voice in support of government, business, and general users applications. The fusion of these services will require that many of the independent component technologies be reconciled with the realities of emerging wireless networks. This paper presents a perspective of the trade offs that are necessary to accommodate wireless integrated voice and data service.

Initially, a review is made of the characteristics of the services that are needed. A variety of existing or planned services are abstracted into categories (e.g., Circuit Switched, Interactive, Transactional, and Bulk Transfer). Each category of service can be further characterized by time constraint, error rate, bit rate variability, error control, flow control, and connection mode of the service.

It is critical to appreciate that the appropriate selection of radio interface depends on the ability to effectively trade off the properties of the various services. The choice depends on supporting the following set of properties:

(1) The radio interface should efficiently multiplex multiple users, service categories, control, and signalling.

(2) The radio interface should be channelized so as to make efficient use of channel capacity. Circuit switched users should be provided guaranteed bandwidth while packet switched users are offered bandwidth on demand.

(3) The radio interface should have minimum dependence on the bearer service.

The details of how industry standards activities support these trade offs will be discussed.

E2-2
1400

## A STATEWIDE SHARED DIGITAL WIRELESS INFRASTRUCTURE

Robert J. Matheson
National Telecommunications and Information Administration
Institute for Telecommunication Sciences
325 Broadway, ITS.S
Boulder, Colorado 80303
Mike Borrego
Colorado Division of Telecommunications
2452 W. 2nd Ave, #19
Denver, CO 80223

The technology of providing government employees with wireless connections to communications and databases is continually changing. Whereas a single radio channel between the user and his office using FM to carry an audio message was the best solution 30 years ago, a trunked digital system like APCO-25 seems to have major advantages today. This paper describes the development of a plan for the Colorado digital trunked radio system, a statewide system that is intended to include many state workers, and possibly substantial numbers of Federal and municipal personnel.

Though the field is still changing rapidly, it appears that a confluence of new technology has made it easier to share hardware (trunked base stations linked by a network), while keeping users services separated (definition of user call groups, encryption, independent selection of a wide variety of specific user services). In addition, the system could provide great robustness by diverting every-day capacity to high-priority emergency functions.

Although the prospect of an economical and efficient shared wireless infrastructure is technically very attractive, major uncertainties remain. The most important is how such a system can be managed, given the history of fierce independence of many of the agencies that would need to share the system.

E2-3
1420

## RADIO PROPAGATION ISSUES FOR WIRELESS ACCESS TO THE NII

Michael G. Laflin
U.S. Department of Commerce
National Telecommunications and
Information Administration
Institute for Telecommunication Sciences
Radio Research and Standards Group
Boulder, CO 80303

Wireless access to information is becoming ever more pervasive in modern society. With the advent of the National Information Infrastructure, requirements for wireless access are expected to increase dramatically. This wireless access will be provided through terrestrial based systems such as Personal Communications Services (PAS) and through various satellite based systems. Performance of these systems is very much a function of the environments in which they operate. It is essential that these environments be fully understood and characterized so that designers can build better systems and so that service providers can choose the systems best suited to meet their needs.

Much work on characterizing the radio environment has been conducted in the air interface standardization community. In particular, the Joint Technical Committee on Wireless Access (JTC) has developed a comprehensive set of propagation models dealing with both channel impulse response and transmission loss. The propagation models are then used in a model system deployment so that potential service providers can compare overall performance against a common set of measures. The JTC models are presented with a discussion of the rationale behind some of the choices that were made. Also presented is a brief overview of the seven candidate PAS technologies.

Additionally, candidates to support wireless services include satellite technologies. These include both Geostationary (GEO) and Low - Earth (LEO) technologies. A brief review is made comparing the propagation limiting factors (attenuation, delay, absorption etc.) which are of importance to establish both U.S. domestic and international wireless infrastructures.

E2-4
1440

## SHANNON CAPACITY OF CDMA SYSTEMS

Roger S Cheng
Department of Electrical and Computer Engineering
University of Colorado at Boulder
Boulder, CO 80309-0425

We consider direct-sequence code-division multiaccess (DS-CDMA) systems in additive white Gaussian noise (AWGN), Rayleigh fading, and multipath Rayleigh fading channels, respectively. In such systems, the overall bandwidth expansion factor, $N$, (the total bandwidth divided by the single-user data rate) is the product of two components: $N_1$, the expansion factor from DS spreading for alleviating inter-user interference; and $N_2$, the expansion factor from forward error correcting (FEC) code for background noise and any remaining inter-user interference.

Using Shannon capacity as the performance measure, we study, for a fixed value of $N = N_1 N_2$, the tradeoff between $N_1$ and $N_2$ and how sensitive the performance is relative to these parameters under various signal-to-noise ratios and various system configurations. We consider systems with single-user detectors as well as systems with multiuser detectors or equalizers; systems with fixed decoding complexities; and channels with and without multipath fading.

E2-5
1520

# CHARACTERISTICS OF VHF/UHF RADIO FREQUENCY INTERFERENCE (RFI) IMPORTANT TO ITS SUPPRESSION IN ULTRA-WIDE BAND RADAR RECEIVERS

Matthew Braunstein and James M. Ralston
Institute for Defense Analyses
1801 N. Beauregard Street
Alexandria, VA 22311

Ultra-wide band radars operate from 0.1 to 1.0 Ghz with a bandwidth of several hundred Mhz (M. I. Skolnik, "An Introduction to Impulse Radar", Naval Research Laboratory, NRL Memorandum Report 6755, November 20, 1990) and to date have been among the most promising techniques for underground and obscured object detection. These radars combine the penetration of low frequencies with the resolution of high absolute bandwidth. However, the same frequency range is used extensively by many broadcast services, including TV, radio and cellular telephone. The radio frequency interference (RFI) from these services effectively adds noise to the radar return and seriously impacts the sensitivity of many UWB radars (D. M. Sheen, R. H. Severtsen, J. M. Prince, K. C. Davis, and H. D. Collins, "Ultra-wide Band Clutter Measurement of Forested Terrain, 1991-1992", Pacific Northwest Laboratory, Richland, WA).

It is possible, however, to mitigate this interference by use of digital signal processing techniques which remove the offending RFI from the received signal (M. Braunstein, J. M. Ralston, and D. Sparrow, "Signal Processing Approaches to Radio Frequency Interference Suppression", SPIE Proceedings, volume 2230, p. 190, 1994). The success of these techniques depends on the characteristics of the RFI as well as the radar signal. Although frequency and bandwidth allocations and other information about the RFI emitters can be obtained from published sources, this information does not fully characterize the RFI nor does it reflect actual usage of typical broadcasters. In this paper, we present and analyze four different sets of measured radio frequency interference data in the 0.1 to 1 Ghz range in order to characterize actual signals to see how they can be most effectively removed from contaminated UWB radar signal returns. We will present data taken from rural and urban sites in different parts of the country measured in the time domain at rates fast enough and times long enough to capture most of the essential features of the different RFI. We will discuss these measurements in the context of possible RFI suppression algorithms for UWB radars, focusing on the important time constants in the radars and the RFI and how the RFI can be most easily suppressed with minimal loss to the uncontaminated radar signal return.

E2-6 1540 PERFORMANCE OF DIGITAL SIGNAL PROCESSING TECHNIQUES FOR SUPPRESSING RFI IN UWB VHF/UHF RADAR RECEIVERS

Matthew Braunstein and James M. Ralston
Institute for Defense Analyses
1801 N. Beauregard Street
Alexandria, VA 22311

Unlike their narrow-band counterparts, Ultra-Wideband (UWB) radars operating in the VHF/UHF frequency bands must share their spectrum with a wide variety of communications, radar, navigation and broadcast services. This not only increases the effective system noise level by an "RFI factor" but constrains the maximum power that UWB radars may employ under regulatory sanction. In order to minimize adverse impact on radar sensitivity it has been necessary to develop a variety of digital post-processing techniques for removing RFI from radar data. These techniques range from variously optimized and adapted non-coherent filters to more sophisticated (and computationally burdensome) methods for coherent estimation of narrow band interferers and subsequent cancellation. The rationale for these suppression options in terms of the known and measured characteristics of RFI sources is described in a companion paper (above).

In this paper we discuss the implementation and quantitative evaluation of several approaches to RFI suppression in UWB radar receivers including coherent subtraction of pure tones (P. Stoica, R.L.Moses, B. Friedlander, and T. Soderstrom, "Maximum Likelihood Estimation of teh Parameters of Multiple Sinusoids in Noisy Measurements," IEEE T-ASSP, vol. 37) and application of optimized spectral filters (J.G. Proakis and D. G. Manolakis, "Introduction to Digital Signal Processing," ch. 6, 1988). The most important application to date for UWB radar in the VHF/UHF bands has been airborne SAR. Consequently, we have taken airborne SAR imagery collected with VHF/UHF impulse radars as the standard of comparison. In all cases we seek to find the optimum compromise between two adverse effects on image quality: RFI, which leads to a general increase in measurement sensitivity floor, and filtering, which can degrade both the impulse response (IPR) and integrated sidelobe ratio (ISLR) of the processed image. Besides image quality, it is also necessary to consider the processing costs of the various suppression techniques, as well as their compatibility with the SAR waveforms employed (which are not generally impulsive) and the type of image processing used.

Session F-3, 1335-Wed., CR1-9
RADAR AND RADIOMETER MEASUREMENTS OF HYDROMETEORS
Chairperson and Organizer: Dusan S. Zrnic, National Severe Storms Lab., 1212 Halley Circle, Norman, OK 73069

F3-1
1340

## AN EVALUATION OF THE CLOUD DETECTION CAPABILITIES OF THE NOAA NETWORK WIND PROFILERS

Brad W. Orr, Brooks E. Martner, and Janet S. Gibson
NOAA/Environmental Technology Laboratory
Boulder, Colorado, 80303

The ability of wind profilers to detect layers of non-precipitating clouds has been the subject of debate. NOAA/ETL conducted a field experiment during the winter of 1993 to examine this question. A Ka-band (35 GHz) "cloud-sensing" Doppler radar was operated side-by-side with the NOAA Wind Profiler Demonstration Network 404 MHz system at Platteville, Colorado. A 915/924 MHz boundary layer wind profiler and a 50 MHz wind profiler also recorded data at the site.

The short wavelength, excellent sensitivity and range resolution of the Ka-band radar make it very well suited for detailed observations of non-precipitating and weakly precipitating clouds that are composed of small hydrometeors. Recent tests indicate that it can detect all but the most diaphanous visible clouds overhead. Thus, it provides a good basis against which the profiler data can be compared in this cloud detection test.

The instruments operated simultaneously for long continuous periods as multiple layers of clouds advected over the site. Profiles of signal-to-noise ratio and mean vertical Doppler velocity from the wind profilers are being compared with the concurrent reflectivity and Doppler measurements of the cloud-sensing radar during these periods. A primary goal is to determine general reflectivity thresholds at which the profiler data begin to indicate the presence cloud layers. The full spectrum of vertical Doppler velocities was also measured simultaneously on several occasions by the 404 and Ka-band systems. Results of the comparisons will be presented.

F3-2
1400

## INTERCOMPARISON OF RADAR AND AIRCRAFT MEASUREMENTS OF DROP SIZE DISTRIBUTIONS AND RAINFALL IN FLORIA STORMS: A CASE STUDY

L. Liu, V. N. Bringi, V. Chandrasekar and R. Xiao
Department of Electrical Engineering
Colorado State University
Fort Collins, CO 80523

The NCAR/CP2 dual-wavelength (S- and X-bands) radar was operated near Cape Kennedy during the summer of 1991, and several datasets were acquired in multi-cellular storms penetrated by King Air aircraft operated by NCAR and the University of Wyoming. Precipitation particles were imaged by the PMS probes on the aircraft enabling a detailed study of drop sizes,shapes and concentrations. These in-situ data are compared with radar measurements of reflectivity, differential reflectivity,linear depolarization ratio and X-band attenuation. The evolution of radar signatures associated with discrete rain "cells" are studied and compared with drop size distribution parameters from the PMS images. Several cells from 8 and 9 August,1991 are studied in detail and will be presented.

F3-3
1420

MULTIPARAMETER RADAR MEASUREMENT OF RAINFALL IN HAIL STORMS: A CASE STUDY

V.N.Bringi, L.Liu, K.Aydin and S.Bolen
Department of Electrical Engineering
Colorado State University
Fort Collins , CO 80523

The CSU-CHILL S-band radar located near Greeley, CO collected data in several storms on 20 June,1994 near Fort Collins,CO. One storm dumped marble-sized hail for 30 minutes associated with intense rainfall near the Department of Atmospheric Science at CSU. We study the evolution of multiparameter radar signatures for this storm including reflectivity at horizontal polarization, differential reflectivity, differential phase and copolar correlation coefficient. The accuracy of rainfall accumulations derived from specific differential phase is studied by comparison with raingage data, and these are also compared with NEXRAD rainfall algorithms based on Z-R relations.

F3-4
1440

# Multifrequency Radiometer and Radar-based Retrieval of Vertically Integrated Vapor, Cloud Water and Ice

J. Vivekanandan and Li Li
National Center for Atmospheric Research
P. O. Box 3000, Boulder, CO 80301
email: vivek@ncar.ucar.edu

With the advent of microwave radiometers, passive remote sensing of clouds and precipitation has become an indispensable tool in a variety of meteorological and oceanographical applications. There is wide interest in the quantitative retrieval of water vapor, cloud liquid and ice using brightness temperature observations in scientific studies such as earth's radiation budget and microphysical processes of winter and summer clouds. Emission and scattering characteristics of hydrometeors depend on the frequency of observation. Thus, a multifrequency radiometer has the capability of profiling cloud microphysics.

A novel neural network-based method to retrieve vertically integrated vapor, cloud water and ice is described. The results are compared with NOAA's statistical retrieval technique. Using three channel radiometer (20, 30 and 90 GHz) brightness temperatures, we have demonstrated a technique to infer ice in addition to the customary vapor and liquid quantities. Also, vertical profiles of ice microphysics such as mean bulk density, concentration and median diameter are obtained by combining radar and radiometer observations. The above discussed methods are applied to WISP data sets.

F3-5
1520

## HYDROMETEOR IDENTIFICATION WITH $K_a$-BAND MULTIPLE-POLARIZATION WEATHER RADAR

Roger F. Reinking,[1] Sergey Y. Matrosov,[2] and Robert A. Kropfli[1]
[1]Environmental Technology Laboratory
NOAA/ERL/ETL, R/E/ET6
325 Broadway
Boulder, Colorado 80303
[2]Cooperative Institute for Research in the Environmental Sciences
University of Colorado
Boulder, Colorado 80303

NOAA's Environmental Technology Laboratory has developed a variable dual polarization capability for its 8.66-mm ($K_a$-band) cloud-sensing Doppler radar. In 1993 and 1994 field studies of the Winter Icing and Storms Project (WISP), at the radar operator's discretion, polarizations were either fixed for range-height (RHI) scans, or cycled through a continuum of horizontal and elliptical states at each of three preselected elevation angles (e.g., 7.5°, 45°, and 90°) by rotating a phase-retarding plate. This plate induces a phase shift of 80°. The combination of varied polarization states and discrete viewing (elevation) angles provides information from which particle shape can be inferred.

Within shallow upslope winter storms, measurements were obtained for (a) planar crystals in large and small concentrations, (b) small and large aggregates of planar crystals, (c) columnar crystals, (d) graupel, (e) drizzle, and (f) raindrops. The radar data for some of these varied hydrometeors are examined for unique signatures, and the results are compared with theory.

F3-6
1540

## CLOUD DROPSIZE SPECTRA FROM DOPPLER RADARS

Earl E. Gossard
CIRES, University of Colorado / NOAA
Boulder, CO 80309-0429

In the large drop regime, where fall velocities are much greater than the turbulent velocity, the precipitation peak in the radar reflectivity spectrum is easily separated from the cloud (or clear-air) peak near zero velocity (typically used by clear-air wind profilers). This "clear-air" peak is used to remove any up/downdrafts in the medium, and the corrected fall velocity spectrum is then converted to dropsize distribution (e.g., Atlas et al, 1970). In this regime the reflectivity and the fall velocity are the important measureables.

On the other hand, as the droplets become small, their settling velocity becomes inseparable from the turbulent velocity of the medium, represented by the "air" peak near zero; i.e., the precipitation and the air peaks merge on any ordinary display of the velocity spectrum of reflectivity. The cloud droplets then serve mainly as tracers of the turbulent motion of the clear-air and their backscatter is not inherently distinguishable from clear-air return, based on velocity. In this regime the terminal fall velocity is not useful for deducing dropsize. This paper deals with this "cloud" regime where reflectivity and turbulence (i.e., turbulent spectral width) are the important measurables. In this regime turbulence strongly affects the spectral shape, so the "sedimentation" velocity (and size) information must be extracted by deconvolving the spectrum with the turbulent velocity PDF. A spectral "bulk" quantity ($Z/S_M$) is used to deduce the population size scale ($D_0$ or $D_M$, etc.) where $S_M$ is the spectral density ($mm^5\ m^{-3}$) at the maximum of the cloud reflectivity spectrum and is the total reflectivity under the cloud peak. The solution including the Stokes range is presented graphically. Accuracy and errors are discussed.

F3-7
1600

# ADVANTAGES OF RAIN MEASUREMENTS USING SPECIFIC DIFFERENTIAL PHASE.

Dusan S. Zrnic
Alexander V. Ryzhkov
National Severe Storms Laboratory
1212 Halley Circle
Norman, OK 73069

Because specific differential phase is obtained from phase estimates it does have several advantages over power measurements for estimation of rain rates in weather radars. These are: 1) It is independent of receiver and transmitter calibrations; 2) it is not affected by attenuation; 3) it is immune to beam blockage, 4) it is not affected by ground clutter cancelers; 5) it is not sensitive to variations in drop size distribution; 6) it is not sensitive to beam filling; 7) it is not biased by the presence of hail; 8) it provides signatures of anomalous propagation that can be filters out of the singnal. Advantages 1 through 4 are all rooted in the relative independence of phase measurements from amplitude of the signals. The remaining benefits are tied to physical principles. We quantify several of the listed advantages and show examples of measurements that corroborate theoretical expectation.

F3-8 1620 **Radar - Rain Gauge Comparisons for the Evaluation of Radar Measurements of Rainfall**

Robert K. Crane and Paul Robinson
University of Oklahoma

Abstract

Radar techniques for the estimation of rain accumulation over large areas have been sought for a number of years. With the advent of the WSR-88D (NEXRAD) radar, a well calibrated radar is available for rain accumulation measurements. Newer multiparameter radars may be available in the future that promise to provide even better rain rate estimates. For these radars, the question arises as to how well the radars perform. The only references available for comparison are rain gauge observations or measurements by other radars. In either case, the observations from the radar to be evaluated will not be made for the same spatial resolution volumes as the gauges or another radar. The spatial and/or temporal sampling problems are severe.

Recently, it has become evident that radar - rain gauge (or other radar) comparisons must be done statistically. The methods used often rely on a comparison between cumulative distributions of rain rate or rain accumulation over short periods. The compilation of a cumulative distribution from a volume scan of the radar or a single-storm case study does not mean that distribution represents a large number of statistically independent observations and that the comparison is based on a statistically large sample.

Rain accumulation measurements from over 100 gauges in the mesonet operated by the Oklahoma Climatological Survey were used to compile empirical distributions (cumulative) for intercomparison with each other and with simultaneous observations from a WSR-88D radar. The empirical distributions were used to estimate the statistical variability to be expected for the estimation of a single empirical distribution and the number of independent samples to be assigned to that distribution. The results show that although we may have used a large number of samples to compile a distribution, the inherent variability of the rain process and the correlations between observations (in space and/or time) conspire to reduce the statistical effectiveness of the distribution comparisons.

F3-9
1640

## DUAL MULTIPARAMETER RADAR OBERVATION OF RAINFALL

Abdullah Dobaie
Department of Electrical Engineering
Colorado State University
Fort Collins, CO 80523

Multiparameter measurements using polarization diversity have shown great potential in the area of remote monitoring of precipitation. In addition to the conventional radar reflectivity and other parameters used for rainfall measurements are the differential reflectivity (ZDR) and specific differential propagation phase (KDP). Data from two S-band multiparameter radars are used to map the rainfall distribution in 2D-space, in particular the 13 July 1993 case near Greely, Colorado. In addition to direct use of KDP, the cumulative differential propagation phase (phidp) profiles from two radars are used to construct the rainfall distribution in the region between the two radars.

G/H1a-1
1340

## LIGHTNING-IONOSPHERE INTERACTIONS

**U. S. Inan**
**Space, Telecommunications and Radioscience Laboratory**
**Stanford University**
**Stanford, CA 94305-4055**

During the past two years, an unusual surge of new scientific evidence has surfaced, which indicates strong electrodynamic coupling between phenomena occurring in the troposphere at altitudes of < 10 km and the mesosphere/lower ionosphere ranging in altitude up to 100 km. It is now known that energy released in lightning discharges can substantially heat the free electrons in the lower ionopshere, leading to the creation of new ionization and light emissions. Upward Lightning flashes, ranging from cloud-tops to altitudes possibly as high as 100 km, have been observed from the ground, from the Space Shuttle, and from aircraft. Gamma Ray bursts of atmospheric origin and associated with thunderstorm activity and possibly upward discharges have been observed. Other newly realized processes of electrodynamic coupling between thunderstorms and the overlying ionosphere include the heating of ions by whistler-excited lower-hybrid waves in the topside ionosphere and intense parallel electric fields and upward-accelerated electron beams observed at 300-500 km altitudes. In addition to these new means by which lightning interacts with the ionosphere, recent experiments have shown that lightning-induced electron precipitation might significantly affect radiation belt dynamics. A review of recent experimental and theoretical work will be presented.

G/H1a-2
1420

## IONOSPHERIC DISTURBANCES CAUSED BY LIGHTNING: RED SPRITES AND BLUE JETS

E.M. Wescott and D.D. Sentman
Geophysical Institute
University of Alaska
Fairbanks, AK 99775

We present results obtained during the Sprites94 campaign to study middle and upper atmospheric emissions associated with active mesoscale thunderstorm complexes. Two jet aircraft equipped with a variety of low light level color and B/W video cameras were employed to obtain simultaneous images of these remarkable events from widely spaced vantage points. Two types of emissions were recorded: (1) "Red sprites," or large red luminous D-region structures that appear to be excited by cloud lightning, and which stretch to terminal altitudes of 90-110 km within the lower E-region. These events appear suddenly on time scales of less than one video frame and decay in at most a few tens of ms. They often exhibit bluish tendrils reaching downward toward the underlying storm system. Sprites were observed above each of more than a dozen storms studied; several hundred were recorded during the campaign. (2) "Blue jets" that emerge from cloud tops and propagate upward within a narrow cone at speeds of 90+/-25 km/s. They appear to disperse at altitudes near 50 km at the base of the mesosphere. Fifty-seven blue jets were observed during the campaign, most of them during a single twenty minute interval above an intense thunderstorm over Arkansas.

The occurrence of lightning-driven sprites and jets in the middle and upper atmospheres suggests that thunderstorms may play a significant role in the electrodynamics and electrochemistry of this region, and may be a possible source of Sporadic-E.

G/H1a-3
1440

## OBSERVATIONS OF SPRITES ABOVE INTENSE THUNDERSTORMS DURING THE 1994 COLORADO SPRITE CAMPAIGN

**Walter A. Lyons**
**ASTeR, Inc.**
**46050 Weld County Road 13**
**Ft. Collins, CO 80524**

**The 1994 SPRITE Campaign was conducted from the Yucca Ridge site in Colorado during 75 days of the summer of 1994. Two dozen nights provided storms and viewing conditions allowing observations with low-light video systems and a suite of concurrently recorded VLF signals. Several nights have been selected for initial analysis. On 5-6 August, over 30 large sprites, some >60 km height and >50 km wide, were imaged along with a distinctive VLF signature (1-10 kHz and 1-100 kHz receivers). These originated from a mesoscale convective system (30,000 km$^2$) some 400 km distant. Over 90% of the sprites were time correlated to within 50 ms with positive CGs. The sprite-associated positive CG current amplitudes were generally 2 to 3 times more intense, some exceeding 150 kA, and were more likely to have multiple strokes. The associated cloud flash was often dramatically brighter than others, reminiscent of reports of lightning "superbolts." The "sprite zone" appeared fixed above a relatively small portion of the storm's anvil cloud and propagated with the storm. On this night, over a dozen sprites were visually observed. Several cases of sprites propagating in sync with extended horizontal flashes inside anvils were noted. Some events appeared as large horizontal glow discharges. On 11-12 July, over 40 large sprites were associated with intense cloud flashes, almost all reported as large positive CGs, some with amplitudes above 400 kA. There was also a very strong correlation between sprites and ELF Q-bursts detected by the MIT Schumann resonance station in Rhode Island. A large luminous region above the distant storm appearing on several nights is suspectedto be enhanced OH emissions due to thunderstorm-excited gravity waves. Smaller, highly electrically active storms with few or no +CGs and absent significant stratiform precipitation region generally produced few or no sprites. On another night, a singular observation of a translating, luminous column, extending perhaps to above 200 km, was noted.This was the one night on which whistlers were recorded. It may or may not be related to the sprite phenomena.**

G/H1a-4
1500

## LIGHTNING: A VIEW FROM THE SPACE SHUTTLE

Otha H. Vaughan, Jr.
Code ES-44
NASA Marshall Space Flight Center
Huntsville, Al. 35812
Telephone: 205 992 5893; Fax: 205 992 5723
E-mail Address: skeet@sferic.msfc.nasa.gov

An examination and analysis of video images of lightning, captured by the payload bay TV cameras of the space shuttle, has shown a variety of examples of lightning in the stratosphere above thunderstorms. These images were obtained on several recent shuttle flights while conducting the mesoscale lightning experiment(MLE). The images of stratospheric lightning illustrate the variety of filamentary and broad vertical discharges in the stratosphere that may accompany a lightning flash. A typical event is imaged as a single or multiple filament extending at least 30 to 40 kilometers above a thunderstorm that is illuminated by a series of lightning flashes. Examples have been found in temperate and tropical areas, over the oceans and over land areas. areas.

G/H1a-5 IONOSPHERIC DISTURBANCE AT ELF AND BELOW
1540

Leslie C. Hale
Communications and Space Sciences Laboratory
Department of Electrical Engineering
Penn State Univ., University Park, PA 16802

The highest lightning-related power coupled to the ionosphere is at VLF frequencies, and may generally be studied using half-space dipole (or multipole) moments, at least for the launching of transient waves, which may initiate non-linear phenomena such as "red sprites." This approach is invalid at lower frequencies where the launching of transients, which contain much of the total energy and nearly all of the related charge transfer, is strongly influenced by the presence of the ionosphere. "No-assumptions" computer modelling (Hale and Baginski, Nature 329. 814, 1987) has shown a unipolar pulse of current to the ionosphere having three timescales: 1) The longest, of 10's to 100's of seconds due to "monopole" decay, which transfers the most charge, 2) A ULF pulse of milliseconds to seconds due to a mechanism suggested by C. and P. Greifinger (JGR 81, 2237, 1976) which depends on the middle-atmosphere conductivity gradient, and 3) An unexpectedly large ELF (millisecond) pulse which contains most of the energy and may sustain phenomena initiated by the higher frequency "radiation."

This unipolar ELF pulse is now seen as necessary to establish the post-stroke "electrostatic" field, and releases about 10% of the total lightning charge onto the base of the ionosphere on a time scale too short to be immediately neutralized across the "transverse" conductivity in the magnetic field. Resulting transient effects in the ionosphere are related to the behavior of this "excess" charge, which violates the Lorentz "neutrality" hypothesis of plasma physics, and hence necessitates a return to basic fundamentals. The released charge will create more deeply penetrating effects if it is negative, corresponding to positive or intra-cloud lightning, propelling electrons upward along magnetic field lines by mutual repulsion. Subsequent to this initial interaction a somewhat longer (several milliseconds) unipolar radial TEM wavelet is launched in the earth-ionosphere transmission line. The polarity of this wavelet is reversed with respect to the directly coupled field (L. Hale, JGR, In press, 1994) so that the most deeply penetrating effects in the ionosphere due to the travelling unipolar wavelet are caused by "normal" cloud-to-surface lightning.

The scenario described above may have wider application, such as unexplained EMP effects and, when scaled to laptop computer dimensions, the excessive leakage of VHF transients.

G/H1a-6
1600

## LIGHTNIGN EMP AND PARAMETERS OF D REGION PERTURBATIONS OF ELECTRONS DEMSITY AND AIRGLOW

Y. N. Taranenko
NIS-1, MSD466
Los Alamos National Lab, NM 87545
U. S. Inan, and W. Sampson
Space, Telecommunications and Radioscience Laboratory
Stanford University
Stanford, CA 94305-4055

A new 2d model has been developed to study interaction of EMP from vertical tropospheric discharges with the lower ionosphere. The model considers propagation of EMP in the cylindrical geometry, ionization and currents are calculated on the basis of the experimental data. Intensities of optical emissions are obtained from a kinetic solution (Taranenko, Y.N., U.S. Inan, and T.F. Bell, *Geophys. Res. Lett.*, vol. 20, p. 2675, 1993). and propagating the optical pulse through the Rayleigh scattering atmosphere to the ground. We determine the horizontal extent of the perturbed region and study its parameters as a function of the pulse amplitude, duration, and shape. We provide a new interpretation of fast atmospheric pulsations (FAP) (Ogelman, H., *J. Geophys. Res.*, vol. 78, p. 3033, 1973). as optical emissions produced at altitudes around 90 km as a result of interaction of lightning EMP with the lower ionosphere. Our results show that experimentally observed variations in duration and intensity of lightning EMP are consistent with the hypothesis of FAP as being ionospheric-EMP-stimulated-optical emissions.

G/H1a-7
1620

## ON THE PHYSICS OF HIGH ENERGY PHENOMENA ASSOCIATED WITH LIGHTNING

G. Milikh and K. Papadopoulos
Departments of Physics and Astronomy
University of Maryland
College Park, MD 20742-3921

Recently discussed in the literature is the detection of brief and intense $\gamma$—ray flashes of terrestrial origin. The observed flashes appear to be correlated with the presence of giant thunderstorm clouds in the atmosphere. The detected spectra are hard, and indicative of bremsstrahlung from MeV electrons (G.J. Fishman et al., Science 264 1313-1318, 1994). Presented model of this process based on the "runaway discharge" mechanism, advanced recently (A.V. Gurevich et al., Phys. Lett. A 165, 463-468, 1992; R. Roussel-Dupre et al., Phys. Rev. 49E, 2257-2271, 1994). The mechanism relies in the presence of a seed population of runaway electrons (i.e. electrons with energy above 100 keV) in the region of the thunderstorm generated electric fields. The electric fields of amplitude as low as one tenth of the conventional air breakdown threshold are sufficient to generate a discharge that involves only energetic electrons, i.e. electrons with energies in the 100 keV to few MeV range. The process generates energetic electron beams which can produce the high energy photons. The proposed physical model relies in local generation of $\gamma$-rays at altitudes in excess of the required for photon escape through the atmosphere. While it retains key features of the "runaway discharge" including the presence of seed electrons, it does not rely on the direct multipolar electric fields produced by thunderclouds. Although the energy source is still due to space charge separation caused by the thunderstorm, the electric fields required for electron energization and discharge initiation, are attributed to the electromagnetic pulse induced when the thunderclouds discharge and create lightning. Contrary to most conventional lightning studies which focus on RF fields induced from cloud-to-ground discharges, the present model emphasizes fields induced directly and by ground reflection from cloud-to-cloud discharges.

A potentially correlated observation is a recent report that the Los Alamos operated ALEXIS satellite observed the radio pulses of thunderstorm origin, having pulse width of a few $\mu$s, with intensity $10^4$ larger than normally generated by thunderstorms (R.A. Kerr, Science 264, 1250-1251, 1994). One of the possible sources of such radio bursts could be the synchrotron radiation generated by the magnetized beam of relativistic electrons due to runaway breakdown caused by the low-altitude lightning discharge. The magnetization of the electron beam due to the runaway breakdown occurs at the height of excess of 15 km that the gyrofrequency of the relativistic electrons exceeds the electron collision frequency. We presenting model which allows to access the total intensity and spectrum of the synchrotron radiation due to the beam of runaway electrons and compare them with the measurements.

G/H1a-8
1640

## HEATING, IONIZATION AND UPWARD DISCHARGES IN THE MESOSPHERE DUE TO INTENSE QUASI-ELECTROSTATIC THUNDERCLOUD FIELDS

V. P. Pasko, U. S. Inan, Y. N. Taranenko*, T. F. Bell
Space, Telecommunications and Radioscience Laboratory
Stanford University
Stanford, CA 94305-4055
* NIS-1, MS: D466
Los Alamos National Laboratory
Los Alamos, NM 87545

Quasi-electrostatic fields that temporarily exist at high altitudes following the sudden removal (e.g., by lightning discharge) of separated charge at low altitudes are found to significantly heat mesospheric electrons. The optical emissions produced in this process can account for the observed features of the recently observed upward discharges. The intense electric fields heat the ambient electrons up to several eV and produce ionization due to conventional air breakdown. The temporal behavior of the electric field at each altitude depends upon the local rate of impact ionization of neutral molecules, the electron energy and the charge redistribution over different points of space. The calculated intensities of optical emissions for the cases of 100, 200 and 300 C charge placed at 10 km altitude equal or exceed the 10-50 kR observed in experiments. The typical time scale of electric field relaxation at 50 to 90 km altitudes (100 ms to 1 ms respectively) as well as geometrical shape, intensity and spectra of optical emissions produced by the quasi-static electric fields are found to be in good agreement with recent observations.

J1-1 THE NEW 45 GHZ SYSTEM ON THE VLA
1340

R. Sramek
National Radio Astronomy Observatory
P.O. Box O
Socorro, New Mexico 87801

Ten Antennas of the Very Large Array (VLA) radio telescope are now equipped with receivers that tune the 40 to 50 GHz band. This addition to the VLA was funded by the Mexican government through UNAM and opens a new area of observations. Thermal emission from young stars, proto-planetary systems, HII regions, SiO at 43 GHz, and perhaps CS at 49 GHz will be studied at the VLA in this new band. Although the highest frequency originally planned for the VLA was 24 GHz, the select group of ten antennas still provides 15% aperture efficiency at 45 GHz. Cryogenically cooled HFET amplifiers provide a receiver temperature of 61 K and a zenith system temperature of 94 K. The foremost problems remaining for observations in this band are pointing errors and deformation of the antenna and gain changes with elevation.

J1-2
1400

## THE BIMA MILLIMETER INTERFEROMETER UPGRADE

Wm. J. Welch
Radio Astronomy laboratory
University of California
Berkeley, California 94720

The BIMA array is currently undergoing an expansion in its number of antennas. With this increase in the number of antennas, there are a several other upgrades to the system. These include: (a) an increase in the overall IF bandwidth from 480 MHz to 830 MHz, (b) an increase in the maximum bandwidth of the spectral correlator from 320 MHz to 800 MHz and an increase in its flexibility, (c) improved antennas with better optics for higher sensitivity, (d) development of a receiver dewar with space for four receivers, (e) replacement of the cooled Shottky mixers with SIS mixers and the development of a temperature stable 3K Gifford-McMahon refrigerator to cool the receiver dewar, (f) the addition of two new stations along the North-South arm, increasing the length of that arm from 180m to 825m, (g) installation of fiber-optic connections and delay cables for the new longer baselines, and (h) the development of an entirely new data reduction package, MIRIAD, which runs efficiently on both work stations and main frame computers.

Further upgrades which are funded include baseline extensions to one km in both the East-West and North-South directions, the addition of of one millimeter receivers, and the further increase from nine to eleven antennas. The summary will conclude with discussion of recent experiments in antenna gain calibration, atmospheric phase stabilization, and, briefly, a few recent scientific results.

J1-3
1420

## THE CSO UPGRADE

Gene Serabyn
Caltech 320-47
Dept. of Physics, Mathematics and Astronomy
Pasadena, CA 91125

During the summer of 1994, a new chopping secondary mirror was installed at the Caltech Submillimeter Observatory. The new secondary is a carbon fiber mirror manufactured by MAN, with a surface rms error of about 9 microns. The secondary, the chopper driver, and the positioning control system were provided by the submillimeter group at the University of Chicago. The maximum off-axis chop angle is 4 minutes of arc.

As a result of this change to the optical system, the surface of the CSO primary was reset to minimize the errors in the primary/secondary combination. Using an upgraded version of the shearing interferometer we use to measure the surface figure, the primary panels were adjusted until the surface rms again reached a level of 15 microns rms at intermediate elevation angles. At very high and low elevations, the rms degrades to slightly over 20 microns rms. At the maximum chopper throw, an additional 17 microns rms due to coma is introduced. Subsequently, the high beam efficiency (0.54) measured on Mars at 490 GHz verified the surface setting, and work is proceeding on optimizing the illumination of the secondary by the receivers.

In the expectation that submillimeter arrays will soon be made use of at the CSO, a dual set of relay optics intended to provide for high quality, wide field imaging has been designed. At our shortest wavelength, 350 microns, a Strehl ratio of 0.9 has been exceeded over a field about 24 diffraction beams across.

J1-4
1440

## CURRENT CAPABILITIES AND FUTURE DEVELOPMENTS AT THE OWENS VALLEY MILLIMETER INTERFEROMETER ARRAY

David Woody
Owens Valley Radio Observatory
California Institute of Technology
P.O. Box 968
Big Pine, CA 93513

The Owens Valley millimeter interferometer array has recently been expanded from three to six telescopes. The telescopes are 10.4 meter diameter giving a net collecting area of 500 m**2. The array operates routinely at wavelengths as short as 1.1 mm with high aperture efficiency. The 200 m baselines provide 1 arcsec resolution at these short wavelengths. The optics are configured in a bent Naysmith configuration which polarization diplexes the beam to feed two receivers. The optical system is versatile and has accommodated nonstandard instruments such as tuneable polarizers and 26-36 GHz HEMT receivers. The primary receivers cover the 85-115 GHz and 210-270 GHz bands utilizing SIS mixers with backshort tuners. The 1 to 2 GHz IF bands from the two double sideband receivers are multiplexed onto one fiber optics cable. A combination of fiber and microwave analog delay lines are used. The backend consists of 2x15 baselines of 1 GHz bandwidth analog correlators for continuum observations plus a digital spectral line correlator. The digital correlator utilizes 256 MHz ECL gate arrays and can process 512 MHz of bandwidth. The whole system is operated by a distributed computer system with a very versatile and easy to use control and monitor program. A sophisticated error handling system is used to ensure the data integrity and locate hardware problems.

Instrument development is an important part of the effort at the Owens Valley Radio Observatory and the performance and capabilities of the millimeter array are constantly being improved. The mixer developments are aimed at achieving near quantum limited performance on the telescope, increasing the IF bandwidth and separating the sidebands. A sideband separation mixer can decrease the atmospheric emission contribution to the system noise without a loss of sensitivity or front end bandwidth. A system is also under development to measure the water vapor emission along the line of sight of each telescope for use in real time atmospheric phase correction.

J1-5
1500

# THE SUBMILLIMETER TELESCOPE

J.W.M. Baars and R.N. Martin
Submillimeter Telescope Observatory
University of Arizona, Tucson, AZ 85721

The Submillimeter Telescope (SMT) is a joined project of the Max-Planck-Institute for Radioastronomy, Bonn, Germany, and the Steward Observatory, University of Arizona, Tucson. The SMT has been specifically designed to operate at full capacity at the shortest wavelength of 0.3 mm, where the troposphere is sufficiently transparent under favourable atmospheric conditions. The SMT is located at 3200 m altitude on Mount Graham in Arizona, 150 miles from Tucson. Weather statistics indicate that during the 8 dry months of the year observations at 0.35 mm will be feasible for about one third of the time.

Extensive use of carbon-fiber reinforced plastic (CFRP) in the structure and reflector of the telescope minimizes deformations due to temperature variations to only a few micrometers. The space frame reflector support structure is extremely stiff and shows only about 5 micrometers rms deformation over the entire elevation range. The 60 composite (aluminium and CFRP) panels of the 10 m diameter reflector have been replicated with 6 micrometer accuracy from glass forms. The goal for the overall reflector accuracy is 15 micrometers, equally divided over structural deformations, accuracy of panel fabrication and measurement and setting of the panels, each being < 10 micrometers.

Construction of the SMT at the site started in Oct. 1992. A "holographic" method with the aid of a signal from the LES8 satellite at 38 GHz has been applied for the adjustment of the reflector. The presently achieved overall accuracy is about 30 micrometers, which we expect to improve to the stated goal in early 1995. The telescope is equipped with a high performance chopping secondary to suppress background fluctuations. The SMT will begin regular astronomical observing in Jan. 1995 at wavelenghts near 1.2, 0.8 and 0.6 mm with SIS-mixer receivers for spectroscopy and 1.2 and 0.35 mm with broadband bolometers in the continuum.

We shall present the salient and original features of the telescope's design, the measurement methods and the initial instrumentation. Some remarks on the further development of the facility will conclude the presentation. At its dedication last year the telescope was christened the Heinrich Hertz Telescope (HHT).

J1-6 STATUS OF THE GBT CONSTRUCTION PROJECT
1540 Roger D. Norrod
National Radio Astronomy Observatory
Green Bank, WV 24944

Under construction at the NRAO Green Bank facility is the GBT, a fully offset radio telescope with aperture diameter of 100 meters. In addition to its large collecting area and offset design, the antenna has a combination of features unusual in an instrument of its size, including an active primary reflector using actuators to correct for gravitational and thermal deformations, support for both prime and secondary focus receivers, and a large feed turntable allowing multiple on-line receivers ready for use. In addition, NRAO has under development ancillary equipment including broadband cryogenic receivers, a powerful new spectrometer, and laser-based ranging instruments intended to allow near real-time surface accuracy measurements and pointing determinations.

This presentation will review the design characteristics and goals of the GBT, and provide a construction status update of the antenna and related NRAO equipment.

J1-7
1600

# THE ARECIBO TELESCOPE UPGRADING PROJECT

Michael M. Davis, Arecibo Observatory,
Post Office Box 995, Arecibo, Puerto Rico 00613
Donald B.Campbell, National Astronomy and Ionosphere Center
& Dept. of Astronomy, Cornell University, Ithaca, NY 14853

Upgrading of the Arecibo 305m diameter radio telescope, presently under way, consists of three main tasks: 1) A 16m high wire mesh screen has been installed around the perimeter of the telescope's primary reflector. The expected reduction in system noise temperatures by shielding the focal area from thermal emission is confirmed by test measurements. 2) Most of the slotted waveguide feeds used in the past to correct for the spherical aberration inherent in the design of the telescope will be replaced with a wavelength independent and more efficient Gregorian secondary and tertiary subreflector system. 3) The power of the 2380 MHz transmitter used for planetary studies will be increased to 1.0 Mwatts. These changes will result in increased sensitivity at all frequencies above 1 GHz, large instantaneous bandwidths and increased frequency coverage from the current maximum of 2 to 3 GHz to about 8 GHz. Table I gives a detailed comparison of the expected performance of the new system compared with previous performance.

**TABLE I**

| Parameter | Present Performance | Expected Performance |
|---|---|---|
| Effective Aperture | 22,000 $m^2$ | 30,000 $m^2$ |
| Maximum Sensitivity | 8 K/Jy | 11 K/Jy |
| Best System Temperature | 35 K | 20 K |
| Transmitter Power | 0.42 MW | 1.0 MW |
| Maximum Frequency | 2.4 GHz | 8 GHz |
| Instantaneous Bandwidth | 40 MHz | $\geq$500 MHz |
| Minimum Beamwidth | 130 arcseconds | 40 arcseconds |
| Pointing Accuracy | 15 arcseconds | 5 arcseconds |

J1-8
1620

# THE SAO SUBMILLIMETERWAVE ARRAY

Colin R. Masson
Smithsonian Astrophysical Observatory
60 Garden Street
Cambridge, MA 02138

The Smithsonian Astrophysical Observatory (SAO), is currently building an interferometer to operate in the frequency range from 180 to 900 GHz. The principal goal of this instrument is to image regions of star formation in our own and in other galaxies, although it will be capable of a wide range of other observations. The SMA will be located near the summit of Mauna Kea, in Hawaii, a site with excellent atmospheric transparency in the submillimeter range.

The SMA will have 6 antennas, each of 6m diameter. The antennas have steel mounts, a carbon fiber backup structure with steel nodes, and machined aluminum surface panels. The surface accuracy is 12 microns rms, with an effective value of 15 microns when phase and pointing errors are included. Pads are provided for 4 scaled ring-like configurations, with a maximum baseline of 460 m. The antennas will be moved between the configurations by a rubber-tired transporter.

There will be 8 receivers in a single dewar in each antenna, cooled to 4K by a closed- cycle refrigerator. Two frequencies will be observable simultaneously, with one polarization at each frequency. The receivers will use waveguide mixer blocks and SIS junctions. The local oscillators will be multiplied Gunns, locked to reference signals transmitted over highly stable optical fiber links at frequencies near 7 GHz. The IF, in the band from 4-6 GHz, will also be transmitted over fibers.

The correlator is a hybrid digital design, with 24 chunks, each of width 104 MHz. The digital section is being built by Haystack Observatory, using a newly-designed chip which will provide 512 lags arranged in 16 sections of 32 lags each, and will operate at 64 MHz. Digital Signal Processors will be provided for each card of 32 chips, permitting fractional bit delay and residual fringe rate corrections to be performed by software. A total of 3072 channels is available for each receiver band, with very flexible configurations.

The instrument is designed for remote control, and the scheduling of observations will be adjusted according to the weather, to optimize the use of periods of good opacity.

The initial construction of all antennas is being carried out at Haystack Observatory in Massachusetts, to minimise the work to be carried out on top of the mountain. The pointing of the first mount will be tested in early 1995, and the surface will be tested holographically in mid 1995. Ground breaking in Hawaii is scheduled for Spring 1995, with first light for the completed array in 1997.

J1-9 THE LARGE MILLIMETER TELESCOPE
1640

N.R. Erickson, A.I. Harris, W.M. Irvine, C.R. Predmore
F.P. Schloerb, D.R. Smith*
Five College Radio Astronomy Observatory
619 Lederle Graduate Research Center
University of Massachusetts, Amherst MA 01003
* and Department of Mechanical Engineering
University of Massachusetts, Lowell MA 01854

The Large Millimeter Telescope (LMT) is a 50-meter diameter radome-enclosed, fully steerable millimeter-wave antenna system which will have the highest gain of any large-aperture millimeter antenna ever constructed. The LMT will operate with high efficiency at wavelengths as short as 1mm, requiring an overall effective system rms of 65-70 microns. In order to take advantage of the small beamsize at these wavelengths, pointing is a major challenge; the goal is an absolute pointing accuracy of 0.75 arcsecond and a relative pointing accuracy of 0.5 arcsecond. To meet these requirements the LMT includes the following design elements: 1) a primary reflector consisting of 126 actively controlled hexagonal segments which are continually adjusted in response to errors measured by sensors at the edges of the segments to maintain a precision paraboloid; 2) a radome enclosure with a very low loss membrane fabric to eliminate effects of wind on the antenna structure and pointing; and 3) a laser metrology system to measure and remove non-predictable structural effects related to pointing. Since a major scientific priority for the LMT will be rapid mapping of large areas of the sky, the telescope will be equipped with focal plane array receivers for both continuum and spectroscopic observations. The inherent flexibility of a large filled-aperture antenna will provide the ability to rapidly respond to targets of opportunity, as well as to ultimately install a radar astronomy facility at a frequency ten times higher than that currently available for planetary radar astronomy.

The LMT is a joint project of the University of Massachusetts and Mexico, with the lead Mexican institution being the Instituto Nacional de Astrofisica, Optica y Electronica, located near Puebla. The LMT will be located at one of several available high mountain sites in Mexico at an altitude of between 2800 and 4500 meters above sea level. An operational philosophy is planned which will both allow large programs which cannot conveniently be scheduled at national facilities and which will emphasize the training of students from universities in both the United States and Mexico.

Scientific priorities insofar as they can be forseen at this early date will include the study of both molecular and continuum emission from high redshift galaxies to probe the earliest stages of galaxy formation, analysis of the chemistry and physics of comets to study these relatively pristine solar system objects and their links to the interstellar medium, and processes of star formation in our own and in external galaxies.

J1-10 THE VLA UPGRADE
1700 T. S. Bastian
National Radio Astronomy Observatory
Socorro, NM, 87801

The Very Large Array is the most successful and productive radio telescope ever built, used by more than 600 investigators from more than 150 institutions every year. In the nearly fifteen years since it was commissioned, major technical improvements have been made in receiver components, correlator design, and the transmission of broadband signals, rendering many elements of the VLA obsolete. Greatly enhanced performance is both possible and highly desirable.

Planning has commenced for a significant upgrade to the VLA. As presently conceived it has three key elements: 1) replace most of the VLA receivers to achieve lower noise temperatures and a much wider bandwidth (1 GHz in each polarization), and add two new observing bands; 2) Replace the buried waveguide data transmission system with a fiber-optics system; 3) design and construct a new correlator to process both broadband continuum signals and to provide improved resolution and flexibility for spectral line work.

These, and additional features of the upgrade, will be reviewed.

J1-11
1720

## THE MILLIMETER ARRAY

Peter J. Napier
National Radio Astronomy Observatory
PO Box 0, Socorro, NM 87801

The Millimeter Array (MMA) is a major new radiotelescope which the National Radio Astronomy Observatory has proposed for funding to the National Science Foundation. The proposed instrument will support high resolution, high sensitivity observations at millimeter wavelengths in all atmospheric windows from 30 GHz to 360 GHz.

The basic concept for the MMA, which is still being refined, consists of 40 eight meter diameter antennas which can be moved into any one of four array configurations using an antenna transporter which runs on roads. The four arrays have diameters of 70m, 200m, 600m and 3000m. The site for the MMA has not yet been selected. Early site testing concentrated on sites in the White Mountains of Arizona and the Magdalena Mountains of New Mexico at elevations of 2800m and 3200m respectively. Currently, site studies are taking place on sites at elevations of 3700m and 4000m on Mt Mauna Kea in Hawaii and at 5000m in northern Chile.

The antenna specifications of 25 microns rms surface accuracy and 1 arcsecond rms pointing accuracy are demanding, as is the requirement for fast position switching to allow very frequent ( every 10 seconds of time) observations of phase calibration sources. To meet these requirements a novel antenna design using a slant-axis mount and an offset Open Cassegrain geometry is being considered, as well as a conventional antenna design.

Cryogenically cooled HEMT amplifier receivers are planned for frequencies up to 115 GHz with SIS mixers being used for all higher frequencies. The IF/LO transmission system will utilize optical fibers and the goals for the correlator include at least 2 GHz continuum bandwidth and spectral resolution of 2 MHz. An additional feature of the electronics system is a requirement to be able to measure total power accurately so that each antenna can be used as a single dish as well as an interferometer element.

During the talk the current status of the MMA Project will be discussed and some of the technical challenges will be described.

Session B-1, 0835-Thurs., CR2-28
EM THEORY
Chairperson: Steven L. Dvorak, ECE, Bldg. 104, Univ. of Arizona, Tucson, AZ 85721

B1-1
0840

## HOMOGENIZATION ANALYSIS OF AN ELECTROMAGNETIC STRIP GRATING WITH A PHASE SHIFT AND ITS APPLICATION

Tungyi Wu Edward F. Kuester
Electromagnetics Laboratory
Department of Electrical and Computer Engineering
Campus Box 425
University of Colorado at Boulder
Boulder, CO 80309

A periodic metal strip grating over a grounded dielectric slab can be applied in electronic-controlled antennas and filters when an active device is connected across the gap. To compute the propagation characteristics of guided waves efficiently, the "equivalent" or "average" boundary conditions can be employed to simplify the analysis.

The "equivalent" or "average" boundary conditions for the averaged fields at a metal strip grating lying on different media are investigated for the case when appreciable phase shift exists between adjacent strips of the grating. The method of homogenization based on the technique of multiple scales is applied for a periodic strip grating and the equivalent boundary conditions to the first-order which contain the Legendre polynomials of non-integer order are obtained. This analysis assumes that the grid period is much smaller than the wavelength of incident waves. The results modify the previously developed equivalent boundary conditions which did not account for the phase shift between adjacent strips (R. R. DeLyser *et al.*, *J. Electromag. Waves Appl.*, *5*, 1217-1236, 1991) and are identical to Ivanov's quasi-static approximation results when the grating lies in the air (V. N. Ivanov, *Radio Eng. Electron. Phys.*, *15*, 1365-1371, 1970).

In this presentation, the propagation of surface waves at an oblique angle with respect to the strips along a grounded slab covered by a strip grating is investigated in a simple manner. With the developed equivalent boundary conditions, determining eigenvalues of the dispersion equation for the propagation constant becomes analytically simple and computationally fast compared to the previous quasi-TEM Green's function method (J. A. Weiss, *IEEE Trans. MTT-22*, 1194-1201, 1974 and J. Crampagne *et al.*, *Int. J. Electron.*, *43*, 19-32, 1977). Computed results for the propagation constant versus propagation angle have been obtained and compare well with those of the quasi-TEM method.

B1-2
0900

# COMPUTATION OF ERROR BOUNDS TO THE EIGENVALUES OF ELECTROMAGNETIC WAVEGUIDES

Jeffrey A. Jargon
National Institute of Standards and Technology
Electromagnetic Fields Division, 813.06
325 Broadway, Boulder, CO 80303, U.S.A.

Edward F. Kuester
Electromagnetics Laboratory
Department of Electrical and Computer Engineering
Campus Box 425
University of Colorado at Boulder
Boulder, CO 80309

The well-known Rayleigh-Ritz method permits a relatively easy evaluation of the upper bounds for the eigenvalues (i. e., cutoff frequencies) of electromagnetic waveguides, but provides no way to compute lower bounds. In this paper, the Lehmann-Maehly method is applied to determine both upper and lower bounds to the eigenvalues, which are calculated using the finite element technique. The Lehmann-Maehly method as adapted for use in problems of elasticity (T. Chang and R. Craig, Jr., *International Journal for Numerical Methods in Engineering*, Vol. 6, 323-332, 1973) provides a systematic procedure for generating converging sequences of upper and lower bounds by varying a certain shifting constant. The method is based upon a formulation of the eigenvalue problem in terms of a self-adjoint (but not positive definite) matrix differential operator of first order.

Results will be presented for the resonant frequencies of a one-dimensional transmission-line resonator, although the technique may be generalized for two-dimensional waveguide cross-sections as well.

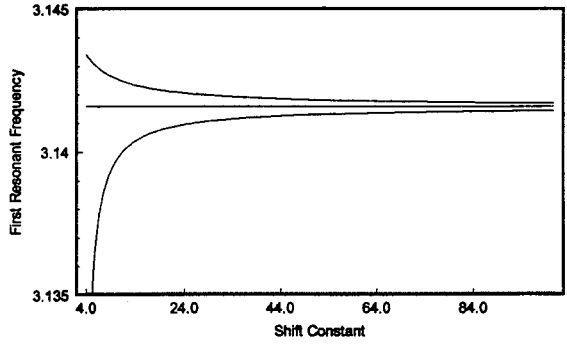


**Figure 1.** Bounds for the first resonant frequency of a one-dimensional, open-circuited, transmission-line resonator of length $l$ with $v_p/l=1$. The middle line is the exact solution.

B1-3
0920

# USE OF A NONLOCAL IMPEDANCE BOUNDARY CONDITION IN OBTAINING THE DISPERSION OF SURFACE POLARITONS ON A CLASSICAL GRATING

R. Garcia-Molina
Departamento de Fisica
Universidad de Murcia
Apdo. 4021
E-30080 Murcia, SPAIN

Rosa M. Fitzgerald and A. A. Maradudin
Department of Physics
University of California
Irvine, CA 92717

By the use of a recently derived impedance boundary condition for a p-polarized electromagnetic field at a one-dimensional, curved, metal surface that contains a nonlocal as well as a local contribution (Physica A**207**, 302 (1994)) we have calculated the dispersion curve of surface plasmon polaritons propagating normal to the grooves and ridges of a classical grating ruled on a metal surface. The period of the grating and the plasma frequency of the metal substrate have been chosen in such a way that the dispersion curve consists of two branches, separated by a gap, within the nonradiative region of the $(\omega, k)$-plane, where $\omega$ is the frequency of the surface plasmon polariton and $k$ is its wave number. The results obtained by the use of only the local impedance boundary condition, and with the inclusion of the nonlocal contribution to it are compared with the results of an exact calculation of the dispersion curve based on the extinction theorem (Phys. Rev. B**23**, 4965 (1981)). It is found that the inclusion of the nonlocal contribution to the impedance boundary condition improves the agreement between the approximate and exact results for the low frequency branch, but worsens it for the high frequency branch. A discussion of possible reasons for this result is presented.

B1-4
0940

# THEORY OF RECTANGULAR WAVEGUIDE FILLED WITH A MAGNETO-ELECTRIC MATERIAL

Taufik and P.L.E. Uslenghi
Department of Electrical Engineering and Computer Science
University of Illinois at Chicago
851 S. Morgan Street, Chicago, IL 60607-7053

A rectangular waveguide with perfectly conducting walls parallel to the (x,z) and (y,z) planes is considered. The waveguide is filled with a magneto-electric, or bianisotropic, material characterized in phasor domain by the constitutive relations

$$\underline{D} = \epsilon_0 (\bar{\bar{\varepsilon}}\,\underline{E} + \bar{\bar{\xi}}\, Z_0 \underline{H}) , \qquad \underline{B} = \mu_0 (\bar{\bar{\mu}}\,\underline{H} - \bar{\bar{\eta}}\, Y_0 \underline{E}) ,$$

where $\bar{\bar{\varepsilon}}$, $\bar{\bar{\mu}}$, $\bar{\bar{\xi}}$ and $\bar{\bar{\eta}}$ are four dimensionless tensors of the forms

$$\bar{\bar{\varepsilon}} = \begin{bmatrix} \varepsilon_1 & 0 & \varepsilon_8 \\ 0 & \varepsilon_2 & 0 \\ \varepsilon_9 & 0 & \varepsilon_3 \end{bmatrix}_{xyz} , \qquad \bar{\bar{\mu}} = \begin{bmatrix} \mu_1 & 0 & \mu_8 \\ 0 & \mu_2 & 0 \\ \mu_9 & 0 & \mu_3 \end{bmatrix}_{xyz} ,$$

$$\bar{\bar{\xi}} = \begin{bmatrix} 0 & \xi_4 & 0 \\ \xi_5 & 0 & \xi_6 \\ 0 & \xi_7 & 0 \end{bmatrix}_{xyz} , \qquad \bar{\bar{\eta}} = \begin{bmatrix} 0 & \eta_4 & 0 \\ \eta_5 & 0 & \eta_6 \\ 0 & \eta_7 & 0 \end{bmatrix}_{xyz} .$$

We prove that field decomposition into the sum of TE and TM modes occurs if

$$\frac{\mu_1}{\varepsilon_1} = \frac{\mu_2}{\varepsilon_2} = \frac{\mu_8}{\varepsilon_9} = \frac{\mu_9}{\varepsilon_8} = \alpha ,$$

where $\alpha$ is any constant, and

$$\xi_5 = -\xi_4 , \quad \xi_7 = -\xi_6 , \quad \eta_5 = -\eta_4 , \quad \eta_7 = -\eta_6 .$$

In imposing the boundary conditions, we obtain dispersion relations for the $TM_{mn}$ modes and $TE_{mn}$ modes that depend on the transversal dimensions of the guide and simplify to the well-known result for the case of an isotropic dielectric filling. In addition, however, another set of TE modes appears that depends only on one transversal dimension of the waveguide, and vanishes in the limiting case of dielectric filling. Dispersion relations for several modes are plotted and discussed.

B1-5
1000

# INTEGRAL EQUATION FORMULATION FOR INHOMOGENEOUS ANISOTROPIC MEDIA GREEN'S DYAD

George W. Hanson
Department of Electrical Engineering and Computer Science
University of Wisconsin-Milwaukee
Milwaukee, Wisconsin 53211

Integral equation (IE) techniques are very popular for determining propagation characteristics of transmission lines. The IE method provides physical insight, yields accurate results, and is usually straightforward once the Green's function for the surrounding environment is determined. Determination of the Green's function for multi-layered anisotropic media is extremely complicated, especially for biaxial media or when the principal axes of the material are not aligned with the waveguiding coordinate system.

This paper presents a simple numerical method for determining the complete Green's dyad in the spectral domain which accommodates multiple layers easily, allows for a full complex-valued matrix representation of the permittivity dyad, and yields results that are analytically integrable in directions transverse to the waveguiding axis. The method follows from a polarization-type IE using the relatively simple Green's function for two isotropic homogeneous half-spaces. The IE is solved at several points in the spectral plane and interpolated to provide efficient computation of the inversion integrals that are performed in solving for transmission line propagation characteristics. As an application, this technique is applied to the study of microstrip transmission lines on anisotropic substrates.

B1-6
1040 IMAGE SOLUTION FOR POISSON'S EQUATION IN PRESENCE OF DIELECTRIC WEDGE

Keijo Nikoskinen
Electromagnetics Laboratory
Helsinki University of Technology
Otakaari 5, FIN-02150 Espoo
Finland

Electromagnetic fields in the presence of a dielectric wedge is an important canonical problem since edges and corners are frequently encountered in practical structures. All aspects related to fields in this geometry have not been fully understood either for dynamic or static excitations.

The present paper is focused on Poisson's equation that is solved in dielectric wedge geometry by deriving a static image that corresponds to the potential contribution of the wedge. The problem is studied mainly in three dimensions but the solution for the analog two-dimensional problem is also provided. Since the analysis is based on an eigenfunction expansion for the unknown potential distribution, an analogous method is applicable to the two dimensional problem. The coefficients in the eigenfunction expansion are found by matching the boundary conditions at the flanks of the wedge and by demanding a correct singularity at the source point. However, the knowledge the eigenfunction expansion is not very useful in numerical computations for this problem at least in the three dimensional case. Therefore the contribution of the wedge to the potential is expressed in terms of image sources that are fairly easy to use in computations. The image sources are different for the interior and exterior problems and they depend on the position of the original source, the angle of the wedge and the permittivities of both media. Thus, the geometry and material parameters determine the form of the images that can be used like conventional sources to compute the potential everywhere by convolving them with the static Green's function. All known closed-form solutions in terms of elementary functions are derived for an electrically and magnetically conducting half plane.

B1-7
1100 PROPAGATION AND SCATTERING CHARACTERISTICS OF MICROSTRIP TRANSMISSION LINES ON ANISOTROPIC DIELECTRIC RIDGES

George W. Hanson
Department of Electrical Engineering and Computer Science
University of Wisconsin-Milwaukee
Milwaukee, Wisconsin 53211

Microstrip transmission lines residing on anisotropic dielectric ridges embedded in a multilayered environment are studied using a coupled set of integral equations (IE's). Microstrip ridge structures incorporating isotropic media have been recently studied [see Engel and Katehi, IEEE Trans. Microwave Theory Tech., 41, 1251-1261, 1993], yet no results are available for the anisotropic case.

This paper describes a theoretical formulation and numerical solution of a set of coupled integral equations which model the desired structure. The IE formulation was chosen since incorporation of anisotropy in the finite dielectric ridge can be accounted for easily by using equivalent polarization currents residing in a multilayered isotropic background. This technique allows for determination of propagation and scattering characteristics of relatively complicated structures. Results will be provided for single and coupled transmission lines on isotropic and anisotropic ridges. Scattering from the above structures will be examined in order to address interference issues, and results compared with transmission lines on infinite substrates.

B1-8 1120

## AN INVESTIGATION OF TRANSIENT PULSE FOCUSING BY A LENS

Steven L. Dvorak and Richard W. Ziolkowski
Department of Electrical and Computer Engineering
University of Arizona
Tucson, AZ 85721

The standard procedure for finding transient fields focused by a lens involves: 1) representing the frequency-domain fields by the Kirchhoff diffraction formula; 2) using either a two-dimensional (2d) spatial fast Fourier transform (FFT) or an asymptotic expression to compute the frequency-domain field for a number of frequencies; 3) employing a temporal FFT to transform the frequency-domain data to obtain the time-history of the pulse at the observation location. However, since the accurate computation of the frequency-domain field is challenging and computationally intensive, it is difficult to correctly compute the transient lens response. Purely numerical techniques such as the finite-difference time-domain technique can be employed (D. B. Davidson and R. W. Ziolkowski, J. Opt. Soc. Am. A, vol. 11(4), 1471-1490, 1994), but these technique suffer from the problems of large memory and computation time requirements. In order to study the focusing of pulses with a lens in more detail without these numerically imposed constraints, we have developed a new technique which allows for the accurate and efficient computation of the transient fields focused by a lens.

In a previous paper (G. E. Evans and S. L. Dvorak, submitted to J. Modern Optics), it was demonstrated that the paraxial approximation allows the frequency-domain Fresnel-zone fields to be represented in closed form in terms of incomplete Lipschitz-Hankel integral (ILHIs). In this presentation, we demonstrate that the transient Fresnel-zone fields can also be represented in closed form in terms of ILHIs. Convergent and asymptotic series expansions for the ILHIs are used to obtain accurate and efficient numerical results.

In order to demonstrate the usefulness of the new closed-form expressions, we investigate a problem of a Gaussian beam, which has either a double-exponential or continuous-wave time history, incident on a thin, non-dispersive lens. After validating our results by comparing with those obtained using a FFT approach, we use our algorithm to investigate the shape of the transient pulses in the vicinity of the focus. In addition, we will address further the enhancements in the intensity that can be obtained with focused pulsed-beams which were reported recently (R. W. Ziolkowski and D. B. Davidson, Optics Letters, Vol. 19(4), 284-286, 1994).

B1-9
1140

# EXACT, CLOSED-FORM FIELD EXPRESSIONS FOR TRANSIENT PLANE WAVES INCIDENT ON CONDUCTIVE MEDIA

H.-Y. Pao, S. L. Dvorak, and D. G. Dudley
Department of Electrical and Computer Engineering
University of Arizona
Tucson, AZ 85721

Because of applications in important problems such as stealth technologies, remote sensing, measurement of the electrical properties of dielectric substrates, geophysical probing, and subsurface communications, there has recently been a renewed interest in the interaction of transient electromagnetic pulses with lossy media. An understanding of the canonical problem involving the transmission and reflection of a transient plane wave obliquely incident on a lossy half space is crucial for such problems. This problem has been previously investigated by a number of authors, e.g., (D. G. Dudley et al., J. Appl. Phys., vol. 45, pp. 1171-1175, 1974) and (T. M. Papazoglou, J. Appl. Phys., vol. 46, pp. 3333-3341, 1975). Previous authors have expressed the transmitted and reflect fields as integrals. However, until now, no one has obtained an exact, closed-form solution for this important canonical problem.

In this presentation, we discuss a method which allows for the analytical evaluation of the inverse Laplace transform representations for the fields for a transient plane wave obliquely incident onto a conducting half-space. Starting with the equations for the reflected and transmitted waves in the Laplace-domain, the corresponding time-domain expressions are first represented as inverse Laplace transforms. We then demonstrate that the inverse Laplace transforms satisfy second-order, non-homogeneous, ordinary differential equations. The differential equations are solved analytically, yielding closed-form expressions involving incomplete Lipschitz-Hankel integral (ILHIs). The ILHIs are computed numerically using efficient convergent and asymptotic series expansions, thereby providing an efficient forward model for this dispersion problem. The exact, closed-form expressions are verified by comparing with results obtained by standard numerical integration.

B1-10
1200

## DIELECTRIC MIXTURE DATA PRESENTED WITHIN SELF-SIMILARITY AND EFFECTIVE MEDIUM TRAIT WINDOWS

Stephen Wallin and Steffan Scheibenstock
Department of Physics
University of Southern Colorado
Pueblo, CO 81001-4901

Selected permittivity data from dielectric mixtures are presented in terms of two basic traits derived from the 1) Lichtenecker's (self-similarity) and 2) effective medium (Bruggeman's symmetric) relations. At low permittivity contrast between mixture constituents the two relations are asymptotically congruent. However, at larger contrasts discrepancies occur which reflect different properties within the mixture types. The mixture traits remain basically real-valued even if the dielectric data is complex or lossy in the frequency domain. A brief historical background is included.

C1-1
0900

## SOLAR MODES OBSERVED BY ULYSSES; SOME IMPLICATIONS

**David J. Thomson,, L. J. Lanzerotti, and C. G. Maclennan**
AT&T Bell Labs, Murray Hill, NJ 07974

The study of solar modes observed in particle densities at *Ulysses* has been extended to include higher frequencies and comparisons with Gough's predictions of oscillation frequencies. In addition to the low-frequency g-modes previously reported we find the p-modes commonly measured by optical doppler techniques with frequencies agreeing with those measurements. Thus waves with periods of a few minutes are preserved to distances beyond 4 AU at easily detectable levels.

Agreement between the observed frequencies of the low-order modes and Gough's predictions are good for low-order modes, but less so for the higher-orders of g-modes.

In addition to being observable in particle densities the g-modes also appear to be present in Terrestrial magnetospheric variations.

C1-2
0920

## EARLY-TO-LATE-TIME SUPERRESOLUTION SIGNAL PROCESSING OF TIME-DOMAIN SCATTERING DATA

Robert C. Qiu and Lawrence Carin
Department of Electrical Engineering
Polytechnic University
333 Jay Street
Brooklyn, NY 11201
(718) 260-3876, FAX:(718) 260-3906,
Email: lcarin@stealth.poly.edu

A common practice in processing time-domain scattering data is to only consider the late-time response, which is described conveniently in terms of a compact set of aspect-independent resonances (modes). However, this technique has met with limited success because the late-time response often has a low signal-to-noise ratio (SNR). This paper examines the self-consistent use of both the early- and late-time scattered signal and demonstrates that the early-time signal contains an untapped reservoir of information.

The early-time response yields information about local portions of a given target. For example, the timing between the initial localized scatterings yields information concerning the target size and shape. We have learned in our initial studies that while the timing between returns from various scattering centers is initially aspect-dependent, the timing between multiple >reflections is aspect-independent and yields information about the target size. Further, the frequency-dependence (dispersion) associated with individual scattering centers is often aspect independent. Thus, the key in early-time processing is to distinguish individual scattered returns from multiple reflections involving two or more scattering centers. This can be accomplished by exploiting the unique frequency-dependent (dispersive) signature of returns from various common scattering centers (edges, corners, tips, cones, etc.). Moreover, the late-time signal has been shown previously to be built up by multiple reflections between scattering centers on the target, thus by tracking the multiple scatterings via superresolution schemes, we gain significant information concerning the target's resonant (modal) behavior. This early-to-late-time signal-processing strategy is novel and our initial results look promising.

We have applied superresolution signal-processing algorithms such as MUSIC, ARMA, and the matrix-pencil method to yield information about the timing (distance) between scattering centers. The advantage of these schemes is that because they are model-based, and hence not limited by Fourier transforms, we achieve better temporal resolution than is possible using the time-domain data directly. Further, the matrix-pencil method has been used with success to extract from data the dispersive nature of the scattering centers (useful for identification). Results of this early-to-late-time strategy are presented for several canonocal targets. Additionally, we place Cramer-Rao bounds on the accuracy one can anticipate from such a signal-processing strategy.

C1-3
0940

## DUAL POLARIZED LOW GRAZING ANGLE RADAR SEA SCATTER EXPERIMENTS DURING THE HIGH-RES II EXPERIMENT

Dennis B Trizna
Code 5303, Radar Scattering & Propagation Staff
Naval Research Laboratory
Washington, D.C. 20375-5000
James B. Edson
Woods Hole Oceanographic Institution
Woods Hole MA, 02543

Experiments were conducted with X-band marine radars using horizontal and vertical polarizations during the High-Res II experiment. The goal was to study the radar echo from submesoscale hydrodynamic surface features that provide a surface manifestation due to the generation of small scale roughness variation and wave breaking. The experiments were conducted aboard research vessels far offshore of Cape Hatteras, NC, where coastal processes mix cool shelf waters with warmer surface waters that impinge upon the shelf from the Gulf Stream. In this work we discuss the radar sea echo dependence on wind stress measured using the eddy correlation technique aboard ship, with corrections made for ship motions. Notable differences are found to occur between the two polarizations, and a scattering model is proposed to explain these differences.

C1-4
1000

# A STATISTICAL TECHNIQUE FOR THE DETECTION OF OUTLIERS IN MST RADAR WIND VELOCITY ESTIMATES

S E Palo[1], S K Avery[1,2]
[1]Department of Electrical and Computer Engineering
[2]Cooperative Institute for Research in Environmental Sciences
University of Colorado
Boulder, CO, 80309

The first step in the analysis of any mesosphere-stratosphere-troposphere (MST) radar data set involves the detection and elimination of signals which are not representative of the underlying wind field. This step is normally accomplished by thresholding the received signal to noise ratio and discarding any signals which fall below a predetermined threshold. The difficulty with such techniques is that they will not detect outliers which arise from strong interference signals and secondly they do not adapt to the variable nature of the received signal. Therefore, we have developed an algorithm which utilizes the horizontal velocities rather than the signal to noise ratio to detect outliers in the data.

To develop the detection routine we have exploited characteristics of both the underlying horizontal wind field and the Doppler frequency estimation techniques utilized by MST radars. Assuming the sampled time series of horizontal wind velocities can be modelled as the superposition of slowly varying signals relative to the sampling rate and non-white zero mean Gaussian noise the received signal can be high pass filtered to remove the slowly varying trend. The high pass filtering operation is accomplished through the use of an estimator based upon adaptively trimmed means, which is robust to outliers. The resulting high pass time series may be expressed as samples of a non-white zero mean Gaussian process. The variance of the sampled Gaussian process is estimated, and samples which are outliers are determined from a two-sided threshold test based upon the Lehmann-Scheffe theorem. As an additional data check we have also employed the use of a Kolmogorov-Smirnov test of empirical probability distribution functions in our algorithm. The Kolmogorov-Smirnov test has been added to determine when the MST frequency estimation algorithm is systematically failing. As MST systems employ a maximum likelihood style algorithm to estimate the Doppler frequency, systematic failures will occur at low signal to noise ratios resulting in velocity estimates which are approximately uniformly distributed.

The algorithm has been used to detect and remove outliers in ST wind data collected using the NOAA wind profiler located at Christmas Island. These results and a more detailed description of the algorithm will be presented.

Session D-3, 0835-Thurs., CR1-46
A TUTORIAL SESSION ON ACTIVE DEVICES
Chairperson: Robert Mattauch, Dept. of Electrical Engineering, Univ. of Virginia, Charlottesville, VA 22903-2442
Organizers: Michael Shur, Dept. of Electrical Engineering, Univ. of Virginia, Charlottesville, VA 22903; and Alan Mickelson, Univ. of Colorado at Boulder, Boulder, CO 80309

D3-1
0840

# HEMT AND HBT DEVICES AND CIRCUITS FOR SYSTEM APPLICATIONS

Dwight C. Streit
TRW Electronics and Technology Division
One Space Park, R6-2573
Redondo Beach, CA 90278

Recent improvements in the performance and reliability of high electron mobility transistors and heterojunction bipolar transistors have lead to both military and commercial insertion targets through W-band. Millimeter wave integrated circuits using these devices have recently demonstrated high-gain performance through D-band, making them useful for future insertion targets above 100 GHz.

GaAs-based 0.1 μm gate-length pseudomorphic InGaAs HEMTs are in production at TRW for 94 GHz applications that include passive millimeter wave imaging and automotive radar. The 94 GHz passive imaging system is targeted for all-weather battlefield observation and commercial aircraft landing systems. The 94 GHz automotive radar is based on a single-chip FMCW radar system for collision avoidance, air-bag deployment, and cruise-control applications. GaAs-based HBTs are in production at TRW for applications that include high speed digital to analog convertors, log amps, VCOs, and commercial PCS products,

The transition from GaAs- to InP-based HEMT and HBT devices has increased the circuit performance and frequency range of both types of products. For instance, we have recently demonstrated an InP-based pseudomorphic HEMT MMIC with 9 dB gain at 140 GHz. This 2-stage amplifier has over 12 dB gain at 120 GHz, and has applications for radio astronomy and earth observation. InP-based HBT circuits are attractive for both digital and analog applications due to their low Vbe and excellent high frequency performance, with power gain and cutoff frequencies exceeding those available with GaAs HBTs.

In this talk we will describe the design, performance, and application of HEMT and HBT devices and circuits for military and commercial applications. The design methodology, performance advantages, and system tradeoffs for each technology will be presented.

D3-2 ACTIVE QUASI-OPTICAL DEVICES

0920 Z. Popovic, S. Bundy, T. Mader,
J. Schoenberg, W. Shiroma, M. Markovic
Department of Electrical and Computer Engineering
University of Colorado
Boulder, CO 80309

An overview of work related to active quasi-optical devices done at the University of Colorado will be presented. In specific, the analysis, design and measurements of the following devices will be discussed: (1) quasi-optical two-level power combining subsystem at 10 GHz consisting of a PHEMT lens amplifier fed by a PHEMT grid oscillator, shown in Figure 1; (2) high-power slot antenna InP HBT X-band amplifier array; (3) three-dimensional Grid oscillator combiners; (4) free-space X-band digital phase modulator; and (5) monolithic V-band and Ka-band transmission wave amplifier designs.

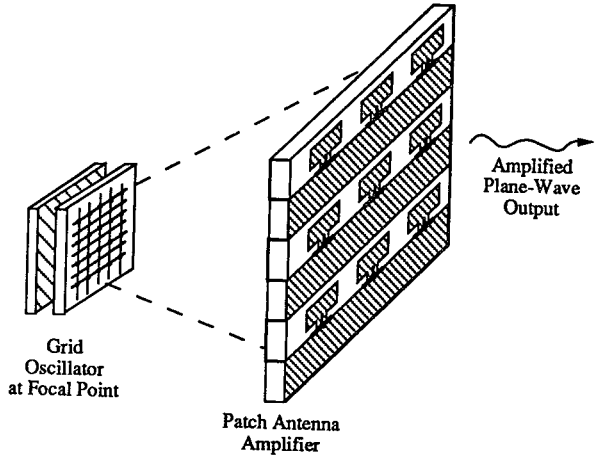


Figure 1: Quasi-optical transmission wave lens amplifier with patch input and output antennas is fed from a focal point by a grid oscillator. By moving the grid oscillator along a focal arc, beam-steering in both E and H plane is achieved.

D3-3
1020 COMPLEMENTARY HFET TECHNOLOGY: ISSUES AND PROGRESS

Fritz Schuermeyer
Wright Laboratory
Wright Patterson AFB, OH 45433-7319

Complementary heterostructure FET (C-HFET) technology has been developed to combine the high speed performance of heterostructure FETs with the low power, high integration capability and vast circuit design experience of complementary FET logic and memory. Critical issues in developing the C-HFET technology were the reduction of parasitic currents, especially of gate currents, hot carrier currents, and subthreshold currents. The most advanced technology is based on pseudomorphic channel AlGaAs/InGaAs/GaAs heterostructures. Other material systems studied includ InAlAs/InGaAs/InP and InAs/AlSb/GaSb heterostructures. Recently a new technique to evaluate the pseudomorphic heterostructure material and charge confinement was introduced, based on photo emission and conduction (PEC) using illumination from the back side of fully fabricated structures. C-HFET technology has set performance records, especiallyunmatched speeds were obtained at very low supply voltages.

D3-4
1100

## GaN/AlGaN HETEROSTRUCTURE FIELD EFFECT TRANSISTORS FOR HIGH TEMPERATURE MICROWAVE APPLICATIONS

Michael S. Shur* and M. Asif Khan**
*Department of Electrical Engineering
University of Virginia
Charlottesville, VA 22903-2442
**APA Optics, APA inc.,
2950 N. E. 84th Lane, Blaine, MN 55449
USA

Good transport properties, a wide band gap, and a respectable thermal conductivity (1.3 W/cmoC) of GaN make AlGaN/GaN Heterostructure Field Effect Transistors (HFETs) very promising devices for microwave applications at elevated temperatures. We will first discuss material and transport properties of GaN relevant to the device operation with emphasis on the properties which are dramatically different from those for more conventional semiconductor materials, such as Si or GaAs. We will then consider DC characteristics and microwave performance of AlGaN/GaN HFETs at room temperature and elevated temperatures based on the Universal Charge Control Model (UCCM) and review recently reported experimental data on the microwave operation of these devices at temperatures up to 300 oC. Our analysis shows that transconductances over a hundred mS/mm should be achievable in submicron AlN/GaN HFETs and that these devices can operate as power amplifiers well into the X-band.

F4-1
0840

## DETERMINATION OF NEAR-SEA SURFACE WIND VECTOR BY AZIMUTHAL AND POLARIZATION RADIOMETRIC MEASUREMENTS

V.Irisov
University of Colorado at Boulder/CIRES
NOAA/ERL/Environmental Technology Laboratory
325 Broadway, Boulder, CO 80303.

Spaceborne microwave radiometers compared to the scatterometers and radars have such advantages as low cost, low power consumption and long life time . On the basis of SSM/I data Wentz (*IEEE Trans. Geosci. Remote Sensing,* **17**(4), 960-972, 1992) showed that radiometers can be successfully used for wind speed and wind direction measurements.

In order to estimate the possibility of wind vector recovery, the microwave emission of a model sea surface is calculated using a small-slope approximation. The azimuthal dependencies of the first three Stokes's parameters at different viewing angles are considered. The full-polarization measurements give more information about sea waves, and hence about near-surface wind, than the traditional measurements of brightness temperatures at vertical and horizontal polarizations. In addition, the Stokes's parameters are less sensitive to the atmospheric radiation than the absolute brightness temperatures at any polarization.

The mechanism of rough surface radiation is different at different viewing angles, so the angle of observation is a very important parameter for data interpretation. Based on theoretical and experimental results the best choice of the angle and frequency for wind speed and direction determination is discussed . Different spaceborne scanning radiometric systems for the near-ocean wind remote sensing are compared.

F4-2
0900

## MODELLING OF PASSIVE MICROWAVE WIND DIRECTION SIGNATURES OVER THE OCEAN

D.B. Kunkee, A.J. Gasiewski
School of Electrical and Computer Engineering
Georgia Institute of Technology
Atlanta GA, 30332-0250

This paper investigates the geophysical origin of azimuthal radiometric brightness temperature variations over the open ocean and their relation to surface wind-driven anisotropies. Radiometric observations of the ocean surface made using a 92-GHz airborne polarimetric radiometer under light wind conditions have shown azimuthal variations in brightness temperature that are related to the wind direction. Variations of 1.0 K and 2.5 K in the vertical and horizontal brightness temperatures (respectively) were observed for an observation angle of 65 degrees from nadir. The data indicate an upwind/downwind asymmetry that is consistent with previous findings (F. Wentz, IEEE Trans. Geosci. Remote Sensing, 30, 960-972, 1992)using 19- and 37-GHz Special Sensor Microwave Imager (SSM/I) satellite observations.

The broadband nature of observed azimuthal brightness temperature variations suggest that they are caused by a frequency independent mechanism involving ocean-foam and scattering and emission from gravity ocean waves. To test this hypothesis, a Monte-Carlo ocean surface simulation and a geometrical optics (GO) model of the upwelling thermal radiation were used to simulate azimuthal signatures. Laboratory measurements of polarimetric emission at 92 GHz from small amplitude water waves corroborate the GO model. The shape of the simulated ocean surfaces was controlled by incorporating both amplitude and phase spectral information into each realization. Measured and simulated brightness temperature signatures were analyzed using azimuthal Fourier harmonics. The study shows that 19- and 37-GHz signatures at a wind speed of 7.9 m/s can be explained by ocean wave asymmetry and foam.

F4-3
0920

## A DUAL-FREQUENCY MILLIMETER-WAVE RADIOMETER ANTENNA FOR AIRBORNE REMOTE SENSING OF ATMOSPHERE AND OCEAN

Mark D. Jacobson[1], Leonard S. Fedor[1], Duane A. Hazen[1], William B. Madsen[1], Michael H. Francis[2] and Douglas P. Kremer[2]
[1] NOAA/ERL/ETL, R/E/ET5 and
[2] NIST/EFD/AMM, 813.08
325 Broadway
Boulder, CO 80303

Accurate multiwavelength radiometric remote sensing of the ocean and the atmosphere from an aircraft requires antennas with the same beamwidth at the various frequencies of operation (D. C. Hogg et al., "An Antenna for Dual-Wavelength Radiometry," IEEE Trans. Antennas Propagat., vol. 27, 764-771, 1979). Scientists at the National Oceanic and Atmospheric Administration designed an offset antenna with a pressure-compensating corrugated feed horn to meet this criterion (L. S. Fedor et al., "Dual-Channel Microwave Radiometer for Airborne Meteorological Applications," NOAA Tech. Memo., ERL 157, 1988). A specially designed fairing was incorporated into the antenna to optimize the aerodynamics and minimize the liquid buildup on the antenna surfaces. The antenna has two positions: the zenith (up) position and the nadir (down) position. The planar near-field facility at the National Institute of Standards and Technology was used to determine the far-field pattern of the antenna (A. C. Newell al., "Planar Near-Field Measurements o High Performance Arrayet Antennas," Natl. Bur. Stand. Interagency. Rept., NBSIR 74-380, 1974). The results show that the antenna beamwidths at 23.87 and 31.65 GHz are nearly the same as expected from the design criterion. This antenna was recently used in the recent San Clemente Ocean Probing Experiment (SCOPE). A few near-nadir measurements are compared with a new model.

F4-4
0940

## MEASUREMENTS DURING THE SCOPE EXPERIMENT FROM THE AIR/SEA INTERACTION ARRAY (ASIA) ABOARD FLIP TO PROVIDE GROUND TRUTH FOR REMOTE SENSOR MEASUREMENTS

Alfred J. Bedard, Jr. and Randall T. Nishiyama
NOAA/ERL/ETL CIRES/CU
325 Broadway, R/E/ET5
Boulder, Colorado USA 80303 3328

The ASIA system consists of three separate arrays to characterize the sea state: an underwater pressure array consisting of four pressure sensors provides directional spectra of gravity waves, a four-wire array using 1 cm wire spacings provides capillary wave directional spectra, and an array of four atmospheric pressure sensors directly above the gravity wave array elements provide directional spectra of atmospheric pressure disturbances. We review the data sets obtained and provide details of ASIA design, including calibration and data acquisition. Preliminary examples of observations from the three arrays show interesting results, including correlations between atmospheric pressure and gravity wave measurements. We will discuss potential uses of the data set for validating remote sensor measurements.

The entire data set has been processed and characterized in terms of the gravity waves and atmospheric pressure disturbances present. For example, the following situations are present in the data set:

- long periods when the gravity wave characteristics remain constant

- periods over which there is a transition in gravity wave amplitude, direction, and/or spectral content

- periods where there are gravity waves present from differing directions apparently producing local standing wave fields

- intervals of high correlation as well as low correlation between the gravity waves and atmospheric pressure disturbances (with a phase difference of about 180 degrees)

- time periods when unusual disturbances were detected; e.g., periodic bursts of high frequency energy, atmospheric acoustic waves, and a long period disturbance.

F4-5
1000

# COMPARISON OF FOURIER TRANSFORM SPECTROMETER AND FILTER RADIOMETER MEASUREMENTS OF IR ATMOSPHERIC BRIGHTNESS TEMPERATURES

Joseph A. Shaw, Jack B. Snider, James H. Churnside, and Mark D. Jacobson
NOAA Environmental Technology Lab.
325 Broadway
Boulder, Colorado 80303

We compare atmospheric brightness temperatures (Tb) measured in the field by a Fourier Transform InfraRed (FTIR) spectrometer and a single-band filter radiometer (PRT5). The PRT5 is a simple, relatively cheap instrument that is used widely for sensing cloud temperatures by measuring IR emission in a 1.5-μm-wide band centered near 10.6 μm. The FTIR measures emission in 1500 frequency bins from 5 to 20 μm. The measurements, when integrated to be equivalent temporally and spectrally, differ by only 1.5 K rms, with no bias, over the temperature range where both instruments are calibrated. Below the PRT5's cold calibration cutoff of 205 K the PRT5 measurements are too high.

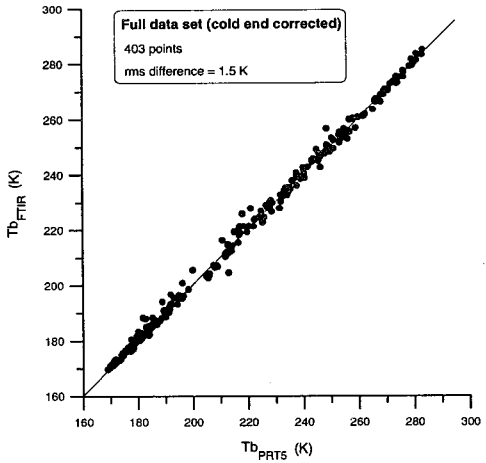


We corrected the cold PRT5 measurements using the FTIR data, which are calibrated over the entire range. The corrected data set shown in the scatter plot has an rms difference of 1.5 K. Three regions are evident: (1) stratus clouds (Tb > 265 K) with rms difference = 0.8 K; (2) variable clouds (180 < Tb ≤ 265 K) with rms difference = 2.4 K; and (3) clear skies (Tb ≤ 180 K) with rms difference = 0.5 K. All differences greater than the 1 K calibration uncertainty are within three standard deviations of the temporally integrated PRT5 values; 90% are within one standard deviation.

F4-6
1040

# AIR - WATER TEMPERATURE CONTRASTS DETERMINED BY A 5-MM MICROWAVE RADIOMETER

Yu.Trokhimovski
NOAA/ERL/ETL
325 Broadway, CO 80303

The 5-mm wavelengths band is usually used for the recovering of atmospheric temperature profiles. As was demonstrated by Trokhimovski and Leuski (IGARSS'93 Proceedings, pp.1625-1626) 5-mm radiometric measurements from a ship provide also an opportunity to determine the difference between water and air temperatures. In this report the comparison between in situ data and the 5-mm radiometer results is presented.

The experimental data have been obtained by scanning the 5-mm radiometer installed on the board of R/V "Akademik Ioffe" during the 1993 Joint US-Russia Internal Wave Experiment. Participants in the experiment included scientists from the Space Research Institute (Russia) and the Applied Physics Laboratory of Johns Hopkin's University. The radiometer's antenna beam was rotated in plane perpendicular to the ship 's axis with frequency of 1 Hz. The calibration was performed using brightness temperatures calculated from atmosphere temperature profiles. For analysis, the data obtained from 18 to 25 June 1992 were used. The brightness temperature in the horizontal direction was taken as equal to the air temperature at the level of radiometer location (8 m). The air - water temperature difference was determined using a best fit between the calculated and measured brightness temperatures of upwelling microwave radiation. The downwelling radiation was assumed in accordance with the experimental data. Waves were taken into account by means of a tangent slope approach.

Good agreement was obtained between air/water temperature contrasts as measured by the radiometer and by two sets of in situ measurements. The ship had instruments that measured air temperatures at 28 and 8 meters and water temperature at a depth of 2 meters. In addition, a small number of high vertical resolution (about 0.1 mm) measurements were made of temperature structure in a layer a few centimeters deep. The amplitude of contrasts determined by means of the remote sensing technique is 2-3 times smaller than was registered by temperature sensor at 2 meter depth. The small skin depth at wavelengths 5 mm (0.3 mm) explains this difference.

F4-7
1100

## DETERMINATION OF LOW-ALTITUDE AIR TEMPERATURE FROM A SCANNING SINGLE-CHANNEL MICROWAVE RADIOMETER

Y. Han, Y. G. Trokhimovski, and E. R. Westwater
NOAA/ERL/ETL
325 Broadway, CO 80303

During the 1993 Joint US/Russia internal wave EXperiment (JUSREX-93), a single-channel broad-band microwave radiometer (58GHz) was operated on a research ship. Many other sensors, including radiosonde release facility, were operated from the ship. The radiometric operation was intended to provide data for the study of air-sea temperature differences and the impact of the atmospheric stability on the ocean waves. The radiometer was operated in a circular scanning mode and it sequentially measured the sky and ocean brightness temperatures. In this presentation, we propose and evaluate a technique to derive low-altitude air temperature profiles from the atmospheric portion of the scanning brightness temperature measurements.

The proposed technique does not require absolute brightness temperature measurements. Instead, differences of the measurements at specified elevation angles from that at a reference angle are used. Thus, an absolute calibration of the radiometer is not required. Physically, such differential measurements contain information on profiles of temperature gradients. We applied Twomey-Tikhonov's inversion method to retrieve temperature gradient profiles and integrated the gradient profiles to obtain temperature profiles. The surface temperature, which is required in the integration, can be estimated from the brightness temperature measurements if their absolute accuracies are good or obtained from surface in-situ measurements.

This technique was tested and evaluated first by using simulated measurements from radiosondes and a radiative transfer model. Good agreement of the retrievals with radiosonde measurements was obtained from the surface to 300 to 400 m. Above that level the retrievals were poor. This technique is very promising in providing information on low-altitude air stability and a supplement to the temperature measurements by the wind profiler/Radio Acoustic Sounding System (RASS), which is unable to measure temperature below 200-500 m. The evaluation is being continued by using the observational data taken during the JUSREX-93 experiment.

F4-8
1120

STATISTICAL RETRIEVAL OF HUMIDITY PROFILES FROM PRECIPITABLE WATER VAPOR AND SURFACE MEASUREMENTS OF HUMIDITY AND TEMPERATURE.

Viatcheslav V. Tatarskii, Maia S. Tatarskaia,
University of Colorado/Cooperative Institute for Research in Enviromental Sciences, Boulder, Colorado
and NOAA/Enviromental Technology Laboratory.
Ed R.Westwater,
NOAA Enviromental Technology Laboratory

A new method is presented of statistical retrieval of humidity profiles based on measurements of surface temperature $\xi_1$, surface dewpoint $\xi_2$, and integrated water vapor $\xi_3$. In this method the retrieved values of humidity depend nonlinearly on predictors $\xi_{1,2,3}$. A self-training algorithm was developed to obtain the values of parameters that enter into the retrieval algorithm. The data from 2 years of measurements in eight different locations were used for training. The method was applied to an independent data set (including nonmonotonic profiles) of 1 month of surface measurements and integrated water vapor obtained from microwave radiometers. Three constraints were imposed: (1) the integrated retrieved humidity profiles had to be equal to the measured values $\xi_3$, (2) the retrieved surface humidity had to coincide with the measured value, and (3) the retrieved humidity had to be positive. The rms deviations of restored humidity values from measured profiles were approximately two times less than natural variations. A limited comparison with conventional linear statistical inversion showed that nonlinear method may improve the recovery of vertical structure.

Typical results are shown in Figure 1. In cases of monotonic profiles both methods lead to approximately similar results, although the results indicated in Figure 1 B showed an approximately 20 to 30 % improvement in the nonlinear over the linear method. But the linear method was unable to retrieve nonmonotonic profiles, whereas the method developed here does. (e.g.Fig. 1 A). This difference is significant, because nonmonotonic profiles are frequently related to special weather conditions.

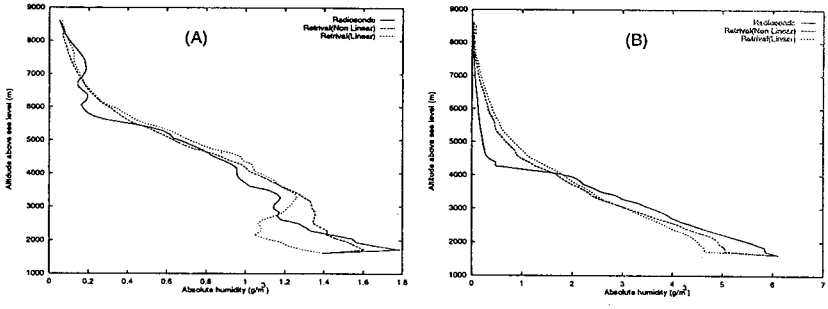


Figure 1. Comparison of linear and nonlinear retrievals of the vertical humidity profile for a case of nonmonotonic vertical dependence for Denver, by statistically independent data A) 2305 UTC 17 March 1991, B) 0205 UTC 05 March 1992

F4-9
1140

## DESIGN OF TUNEABLE MICROWAVE RADIOMETERS FOR PROFILING OF TEMPERATURE AND HUMIDITY

Fredrick Solheim
Radiometrics Corporation
2760 29th Street #200
Boulder, CO 80301
solheim@radiometrics.com

Millimeter wave radiometers traditionally utilize Gunn local oscillators. Complexity and cost therefore limit the number of frequencies observed. Additionally, Gunn oscillators drift in frequency, introducing noise into the observations.

A temperature profiling radiometer based on a highly stable synthesizer, rather than traditionally used Gunn oscillators, has been designed and fabricated under contract to White Sands Missile Range. This profiler is capable of tuning a user-selected ensemble of frequencies in the range of 52.85 to 58.8 GHz. It weighs 30 kg and consumes 120 watts. Because of the frequency stability of the receiver, and because of the large number of observing frequencies possible, improved profile accuracy and resolution is expected over Gunn-based temperature profilers.

Preliminary design work has also been accomplished on a portable (35 kg) water vapor profiling radiometer. This radiometer is to utilize a stable synthesizer to map pressure broadening by tuning over a 6 GHz width across the 22 GHz water vapor line. We expect accuracies of better than 0.8 mm total water vapor and .04 mm total liquid water, with correspondingly good accuracies along the water vapor profiles.

An inexpensive, simple, and accurate calibration target system that includes the antenna system has been developed for mm wave radiometers. Tests with a Radiometrics water vapor radiometer have demonstrated stability of 0.1K over 6 hours. The calibration target can be loaded with liquid nitrogen or other cryogenic liquids, thereby giving a reference in the range of sky observables. The cryogenic liquid temperature can be known by its boiling point to within several hundredths of a Kelvin by a simple barometric pressure measurement.

F4-10
1200

## USE OF A NOVEL NON-LINEAR DECONVOLUTION ALGORITHM FOR WATER VAPOR RETRIEVALS

A. K. AL-Khalaf, G. R. Markowski, and T. T. Wilheit
Department of Meteorology
Texas A & M University
College Station, TX 77843-3150

Water vapor is one of the most important constituents in the earth's atmosphere. It is the greenhouse gas which plays the most important role in its radiative balance. A non-linear general deconvolution algorithm, STWOM (G. R. Markowski, Aerosol Sci. Technol., 7, 127-141, 1987), has been adapted for retrieving atmospheric water vapor profiles data from the Special Sensor Microwave/Temperature-2 (SSM/T2) instrument on the Defense Meteorological Satellite launched November, 1991. This instrument has 3 channels near the strong water vapor absorption line at 183 GHz, a window channel at 91.655 GHz and an intermediate channel at 150 GHz. A major advantage of STWOM is that it allows retrieval of relative humidity as a function of altitude without reference to statistical data; thus, it is expected to provide a more accurate measure of atmospheric water vapor than methods which depend on other than direct measurements.

Advantages of STWOM are: a) its solution is independent of functional form; b) it is insensitive to numerical instabilities; c) high frequency instabilities are automatically eliminated; d) the number of calculated points in the solution is not limited to the number of measurements; and, e) its resolution is usually enhanced over matrix inversion and entropy minimization approaches--typically, several times more output points than the number of input data points are needed to take full advantage of the resolution it gives. STWOM's improved resolution results partly from its constraints: positive definiteness and smoothness with respect to high frequencies. Other constraints may be straightforwardly added. STWOM is easily capable of deriving smooth water vapor profiles whose calculated brightness temperatures are within the noise of the measured microwave values.

STWOM has been included in a physical relaxation water vapor retrieval algorithm which includes a forward radiative transfer model (A. K. AL-Khalaf, D. Conlee, and T. T. Wilheit, "Retrieval of Atmospheric Water Vapor Profiles from SSM/T2 Microwave Radiances", 7th Conference on Satellite Meteorology and Oceanography, June 6-10, 1994, Monterey, CA). We compare retrievals of water vapor over ocean and land surfaces integrated over 5 layers (SFC-850 mb, 850-700 mb, 700-500 mb 500-400 mb and above 400 mb) with ground truth using global operational radiosondes and ECMWF analyses. The results presented here show good agreement with ground truth and appear to be an improvement over statistical methods. The retrieved relative humidity profiles also show good agreement with the radiosonde measurements, except that the STWOM profiles are substantially smoother than the radiosonde profiles. The smoother profiles likely reflect the much larger measurement area seen by the SSM/T-2 sensors (approximately a circle 50 km in diameter) compared to the radiosonde, which samples a much smaller volume of the atmosphere, in addition to the limitations inherent in passive sensing. Because this is the first use of STWOM in this application, further improvements are likely.

Session F/G/H-1a, 1015-Thurs., CR2-6
ACTIVE REMOTE SENSING-I
Chairperson and Organizer: Susan Avery, CIRES, Campus Box 261, Univ. of Colorado at Boulder, Boulder, CO 80309

F/G/H1a-1
1020

## DOPPLER LIDAR PROBING OF THE ATMOSPHERE: COMPARISONS AND SYNERGISMS WITH RADAR TECHNIQUES

R. Michael Hardesty
NOAA Environmental Technology Laboratory
325 Broadway, Boulder, Colorado 80303

Although similar to Doppler radar in concept, Doppler lidar probing of the atmosphere differs in many respects because of the much shorter wavelength of the transmitted radiation (at least 3 orders of magnitude). The wavelength difference affects most of the key parameters that characterize system performance, including transmission, scattering, antenna characteristics, transmitter design, and signal processing methodology. For many applications, Doppler radar and lidar are synergistic, in that a lidar can observe aspects of a phenomena that are not well-observed by a radar (and vice versa).

Doppler lidars are most effective probing the optically clear air, and suffer significant attenuation in clouds or heavy precipitation. Because an optical beam is characterized by minimal broadening and no sidelobes, measurements of complex wind and turbulence flows near the ground or in the vicinity of complex terrain are particularly well-suited to lidar techniques. The NOAA Doppler lidar has been used to great benefit in several regional air quality or mesoscale studies, including an experiment at the Grand Canyon, for flow characterization and model validation.

Simultaneous deployment of a Doppler radar and lidar has produced useful results in studies aimed at observation of cirrus cloud microphysical properties, detection of thunderstorm microbursts, and characterization of the cloud-topped marine boundary layer. For cloud studies, sensitivity of the instruments to different size particles enables information on effective particle size, ice water content, and total number density to be estimated. In the boundary layer, radar and lidar systems are used effectively to interrogate different regimes: clear air (lidar) and cloud and precipitation (radar). Combining the results of such multi-wavelength probing produces a picture of the total scene that generally cannot be obtained using a single instrument.

F/G/H1a-2
1100

## REMOTE SENSING OF THE UPPER ATMOSPHERE WITH OPTICAL EMISSIONS EXCITED BY HIGH POWER RADIO WAVES

P.A. Bernhardt
Beam Physics Branch Naval Research Laboratory
Washington, DC 20375-5320

New techniques have been developed to measure the properties of the earth's upper atmosphere using optical detection and active radio probes. These techniques are based on transmissions of radio waves with enough power to produce electron energization and density fluctuations in the ionosphere. At high powers, electromagnetic waves near the plasma frequency cause several nonlinear effects in the plasma including (1) formation of large scale (1-30 km) density irregularities driven by thermal pressure gradients, (2) acceleration of electrons by Langmuir waves, and (3) large (factors of 3 to 10) increases in electron temperatures by absorption. One technique uses large scale irregularities that are visibly outlined as energetic electrons collide with ambient atomic oxygen. The motions of these irregularities is recorded with low-light-level cameras. These images provide a visual tracer of the $\mathbf{E} \times \mathbf{B}$ drift of the plasma. Another technique uses satellite images of infrared emissions from hot minor species in the mesosphere to provide estimates of neutral densities, velocities, and temperatures. These new diagnostic tools may provide better spatial and temporal sensitivities than other passive or low-power methods.

F/G/H1a-3
1120

## TECHNIQUES TO ANALYZE SIGNALS FROM SPACED ANTENNA WIND PROFILERS

Christopher L. Holloway1*, Richard J. Doviak2,
Rich J. Lataitis3, Steve A. Cohn4 and Joel Van Baelen5
1 Institude for Telecommunication Sciences/NTIA, Boulder, CO
2 National Severe Storms Laboratory/NOAA, Norman, OK
3 Environmental Technology Laboratory/NOAA, Boulder, CO
4 National Center for Atmospheric Research, Boulder, CO
5 CNRS-Meteo France/CNRM, Toulouse, France

Spaced antenna (SA) systems have been used for some time to estimate the 3-D wind vectors in the atmosphere. The analysis of signals from these multiple receiver systems can be carried out in either the lag-time domain (correlation analysis) or the frequency domain (spectral analysis). When turbulence effects are not taken into account, the correlation and spectral analyses will over-estimate the true wind speed. A procedure known as the Full Correlation Analysis (FCA) has been used to extract unbiased wind estimates in the presence of turbulence, as well as the diffraction pattern's correlation parameters. The implementation of this technique can be involved and estimated winds have shown considerable differences from the winds measured with other independent techniques.

Recently we have developed a theoretical scattering model for a turbulent atmosphere (Doviak, Holloway, and Lataitis, Third International Symposium on Tropospheric Profiling, Hamburg, Germany, 274-277, 1994 and Doviak, Holloway, Lataitis, and Van Baelen, Radio Sci, Submitted, 1994). This model has allowed us to relate the cross-correlation and cross-spectrum of the echoes from a SA system to the properties of the refraction index field and its flow (e.g., laminar, turbulent). For cases of practical interest the cross-correlation and cross-spectrum reduce to simple analytic forms which allow physical interpretation of measurements in terms of SA parameters and the properties of the scattering medium. These simple analytic expressions have allowed us to developed four new techniques (three time-domain and one frequency-domain) for determining unbiased estimates of the wind in the presents of turbulence.

In this talk we will introduce these four new techniques, discuss their limitations, and show calculations of the wind based on these four techniques using data from NCARS unique 33 cm wavelength SA wind profiler. We will also show comparisons of these techniques to both the conventional Doppler Beam Swinging (DBS) technique and to rawinsonde measurements.

F/G/H1a-4
1140

## MEASUREMENT OF REFRACTIVE INDEX GRADIENTS ALOFT WITH GROUND-BASED DOPPLER RADARS

Earl E. Gossard, Richard G. Strauch and B. Boba Stankov
CIRES, University of Colorado / NOAA
Boulder, CO 80309-0429

Using the zero, 1st and 2nd moments of the Doppler Spectrum of clear-air reflectivity, it is possible to calculate the height-gradient of refractive index (RI) in each range gate of a surface-based radar. The primary uncertainties in the method arise from uncertainty in the accuracy of the 2nd moment and from contamination of the 0 moment by clouds and insects. In this paper we examine the accuracy of $C_w^2$ provided by the spectral 2nd moment and calculate the R. I. gradients in elevated layers. It is also shown that the method yields the humidity gradient, if the temperature gradient is provided by RASS.

F/G/H1a-5
1200

## RECENT CLOUD OBSERVATIONS WITH AIRBORNE, POLARIMETRIC 95 GHZ RADAR

Robert D. Kelly[1], Gabor Vali[1], John Galloway[2], Andrew Pazmany[2], and Robert E. McIntosh[2]
[1]Department of Atmospheric Science
University of Wyoming
[2]Microwave Remote Sensing Laboratory
University of Massachusetts

Using a 95 GHz, polarimetric, Doppler radar designed and constructed at the University of Massachusetts and mounted on the University of Wyoming King Air research aircraft, measurements in a variety of cloud types and conditions were gathered in 1992 and 1994 (WISP94), all in southeastern Wyoming and northeastern Colorado. With a movable, flat-plate reflector mounted just outside the lens antenna, both vertical and horizontal view angles are possible. The radar pulses were transmitted in tight clusters of four (HHVV), for the polarimetry, and the clusters, in turn, were transmitted with a repetition frequency of about 1000 Hz. By averaging 100 clusters per recorded profile, cloud features as small as 10-20 m along the flight path could be resolved. Similar resolution normal to the flight path was obtained by using pulse lengths of 30 m. For analysis and interpretation the radar data are combined with data from in-situ cloud particle and air-motion sensors on the aircraft.

Examples will be shown of reflectivity, Doppler, and polarimetric measurements from various cloud and precipitation situations, including: 1) polarimetric signatures of pristine stellar and needle crystals, 2) VAD-style wind profile retrieval, from data taken during constant bank-angle turns, and 3) small-scale cloud features from cumulo-nimbus, nimbo-stratus, and lenticular wave clouds.

G2a-1
0840

## ON THE SEEDING OF PLASMA BUBBLES BY LARGE-SCALE WAVES IN THE EQUATORIAL IONOSPHERE

R. T. Tsunoda, W. B. Hanson, T. L. Aggson
Geoscience and Engineering Center
SRI International
Menlo Park, CA 94025

The role of seeding in the day-to-day variability in occurrence of equatorial spread *F* is examined. Using electric field and ion density measurements made from the San Marco-D satellite in conjunction with ground-based measurements from the Kwajalein Atoll, Marshall Islands, we show that electric-field perturbations that occur in the pre-sunset period play a role in the development of plasma bubbles. Perturbations in the eastward electric-field component with amplitudes as large as 0.9 mV/m (i.e., 30 m/s upward) were found to exist in the absence of corresponding perturbations in the vertical electric-field component and in plasma density. We interpret these results as indicating that the dynamo source of the perturbation electric field was not located where the measurements were made. This observation combined with the fact that these perturbations occurred prior to *E*-region sunset is consistent with the hypothesis that the perturbations develop in the *E* region and are mapped up to the *F* layer, a situation that is more favorable during sunlit conditions. We further show that these electric-field perturbations can occur under both quiet and active magnetic conditions.

G2a-2 GPS OBSERVATIONS DURING SEVERE EQUATORIAL SPREAD F
0900

T.L. Beach, M.C. Kelley and P.M. Kintner
School of Electrical Engineering
Cornell University
Ithaca, NY 14853

S. Musman
Geosciences Laboratory
National Oceanic and Atmospheric Administration
Silver Spring, MD 20910

During August 1990, GPS measurements of Total Electron Content (TEC) were made with a Trimble 4000 receiver from the island of Kwajalein. The period was also one of nearly continuous VHF radar observations in support of a NASA rocket campaign and occasional Altair radar and rocket-borne measurements. We report here on two days of GPS observations from four satellites during periods of UHF and VHF radar scattering observations. One day, August 15, was relatively quiet while August 14 was quite active with numerous spread F plumes intercepting the line of sight to GPS. The most serious disruptions were clearly coincident with the plume passages. Precursor TEC variations also seem to occur prior to the severe disruptions.

G2a-3
0920

## CHEMICAL RELEASE EXPERIMENTS TO ARTIFICIALLY INDUCE EQUATORIAL SPREAD-F

Peter J. Sultan, Michael Mendillo, Roland Tsunoda
Phillips Laboratory/GPIA
29 Randolph Road
Hanscom AFB, MA 01731

The physics of the generally accepted Rayleigh-Taylor mechanism for the initiation of equatorial spread $F$ (ESF) can be tested experimentally by the deliberate creation of low-density plasma bubbles in ambient ionospheres that are deemed susceptible to the R-T instability. Two such artificial seed perturbations were generated during the 1990 NASA/Boston University CRRES-at-Kwajalein campaign, when clouds of sulfur hexafluoride ($SF_6$) were released by sounding rockets to initiate plasma recombinations near the bottomside of the equatorial ionosphere. Multiple diagnostics (incoherent scatter radar, high frequency radar, airborne and ground-based optics and a satellite polarimeter chain) were used to monitor the pre-launch status of the ionosphere and the electron depleted regions that resulted from the chemical releases. Small patches of $F$ region irregularities were observed to form in the vicinity of the artificial perturbation during both experiments. The successes in being able to initiate ESF artificially lend support to the physical model adopted for the instability mechanism, and open up new avenues of research into ESF predictability on a night-to-night, and even an hour-to-hour, basis.

G2a-4
0940

## ON THE RELATIONSHIP OF SPORADIC-*E* ECHOES OVER KWAJALEIN AND 150-KM ECHOES OVER THE DIP EQUATOR

R. T. Tsunoda
Geoscience and Engineering Center
SRI International
Menlo Park, CA 94025

We present the first evidence of enhanced irregularity-drift velocities and a velocity shear in the daytime *E* region at 4.3° N dip latitude. These features, found in radar measurements from Kwajalein during q-type sporadic *E* events, are interpreted in terms of a polarization electric field that develops in response to the presence of latitudinal gradients in field-line-integrated conductivity caused by sporadic-*E* layers. Because the *E* region over Kwajalein connects directly to 150-km altitude over the magnetic dip equator, we suggest that a similar polarization process is responsible for the so-called 150-km echoes that have been observed routinely by the Jicamarca radar.

G2a-5
1000

## MULTIPLE BEAM MEASUREMENTS OF EQUATORIAL 150 KM ECHOES AT JICAMARCA

Patricia Franke, Julio Urbina,
Clint Fawcett and Erhan Kudeki
University of Illinois, Aeronomy Laboratory

During the recent CADRE campaign conducted at Jicamarca, backscatter from 150 km irregularities were monitored with a multibeam radar configuration. During this campaign the radar was configured with four beams, each 2.5 degrees off zenith, in the east, west, north, and south directions. The resulting data set, including ten days of observations, will be used to explore the characteristics of the irregularities. Backscatter intensity maps of the region show regions of strong signal return arranged in very distinct layers that exhibit a morning descent followed by an afternoon ascent. Superimposed upon the layers, which appear in all of the data sets encompassing data from different years and seasons, are periodic structures with periods from 3-20 minutes. The periodic structures show up in two different ways i) a displacement of the layers, and ii) vertical structures which change phase as they span a layer.

Results from the CADRE campaign will be presented showing the basic structure and characteristics of the irregularity echoes. Zonal and vertical drift estimates, backscattered power plot comparisons between beams, and numerical simulation of gravity wave generated structure, are some of the analysis results to be shown. Possible generation mechanisms including gravity wave effects (Kudeki, E. and Fawcett, C., High resolution observations of 150 km echoes at Jicamarca, GRL, Vol. 20., No. 18, 1987-1990, Sept. 1993) and E-region coupling (Tsunoda, R. T., Enhanced Velocities and a shear in daytime Esq over Kwajalein and their relationship to 150 km echoes over the dip equator., GRL 1994) will be discussed in light of the observations.

G2a-6
1040

## CHANNEL PROBE MEASUREMENTS OF SPREAD F EFFECTS ON A TRANSEQUATORIAL HF PATH

T. Joseph Fitzgerald
Space and Atmospheric Sciences Group
MS D466
Los Alamos National Laboratory
Los Alamos, NM 87545

The ionospheric phenomenon called Equatorial Spread F encompasses a variety of effects associated with plasma irregularities occurring in the post-sunset and nighttime ionosphere near the magnetic equator. These irregularities can seriously degrade the performance of systems which involve either of necessity or inadvertently radio propagation through the equatorial ionosphere. One such system is Over-the-Horizon(OTH) radars which operate in the high-frequency (hf) band and use ionospheric reflection for forward and backscatter propagation to ranges of thousands of kilometers. When such radars are directed towards the equator, Spread F irregularities can cause scintillation effects which may be aliased into the ranges of interest and have the effect of causing excess clutter in which targets may be hidden. In January, 1994 Los Alamos participated in a campaign to measure Spread F effects on OTH propagation from the United States looking towards South America in conjunction with local diagnostics in Peru. During the campaign Los Alamos fielded a 1600 km bistatic path between Piura, Peru, and Arequipa, Peru; the one-hop reflection region for this path was near the magnetic equator. We obtained four types of measurements: an oblique ionogram between Piura and Arequipa every three minutes; Doppler spread and spatial correlation for a single frequency cw path between Piura and Arequipa; Doppler spread, time-delay spread, and spatial coherence for a 10 kHz bandwidth path between Piura and Arequipa; and Doppler spread and time-delay spread for the one-way path between the AVA radar in New York and Arequipa, Peru. We describe the diagnostic experiments that we carried out and summarize the statistics of Doppler spread, time-delay spread, and spatial coherence that we observed.

G2a-7
1100

## PRODUCTION OF IONOSPHERIC IRREGULARITIES BY TURBULENT DRIFTS: TRANSFORMATION OF CHAOTIC CHARACTERISTICS

S. V. Fridman, O. V. Fridman, S. J. Franke
University of Illinois
Electrical and Computer Engineering Dept.
322 CSRL
1308 W. Main St.,
Urbana, IL 61801-2307

Evidence has been reported in the literature showing that small-scale density irregularities of the ionospheric F-region sometimes demonstrate signatures of a chaotic deterministic behavior (A. Bhattacharya, K. C. Yeh, and S. J. Franke, Space Sci. Rev., 61, 335, 1992;. V. N. Zvezdin and S. V. Fridman, J. Atmos. Terr. Phys., 54, 957, 1992). In particular, the observations indicate that the fractal dimensionality of the process of scintillations is finite in some experiments. If this is actually so, then, according to the theory of nonlinear dynamical processes, it may be concluded that the dynamics of corresponding ionospheric turbulent motions should posses a finite dimensionality.

We suggest a scenario for formation of small- scale irregularities with chaotic dynamic behavior in the midlatitude ionosphere. According to this scenario the chaos originates from atmospheric turbulent vortices or convective cells existing below the turbopause. These atmospheric motions generate electric fields in the E-region that are transmitted into the F-region. These fields cause vortex-like chaotic motions in the F-region. The typical scale of the motions is of the order of 10 km or more (the lower bound of the scale is defined by the penetration conditions of the electric field from the E- to F-region). Finally, the small scale irregularities are produced as a result of the mixing of ionospheric layers by the vortical motions.

We have carried out numerical modeling of ionospheric irregularities generated by chaotic vortices. The vortex velocity field was simulated in the spirit of the Lorentz (J. Atmos. Sci., 20, 130, 1963) model of a convective cell. A uniform horizontal drift of ionospheric plasma was imposed on the vortical motion. In such a configuration a trail of small-scale density irregularities is created downstream of the vortex. This study has shown that the above scenario is capable of producing irregularities with scales as small as several hundred meters. The irregularities demonstrate much more complex dynamical behavior than the original chaotic flow. It can be said that the mixing amplifies the chaos. The fractal dimensionality of the process of density fluctuations appears to be higher than the dimensionality of the vortex flow. The association between spectral and dimensional characteristics of the density irregularities produced by this mechanism is discussed. The question of estimation of dimensionality of the atmospheric turbulence from ionospheric observations is also addressed.

G2a-8
1120

## INVESTIGATIONS OF QUASI-PERIODIC ECHOES IN MIDLATITUDE SPORADIC-*E* USING THE MU RADAR AND THE FREQUENCY-AGILE RADAR (FAR)

R. T. Tsunoda, S. Fukao, M. Yamamoto, K. Igarashi, T. Ogawa
Geoscience and Engineering Center
SRI International
Menlo Park, CA 94025

One of the growing areas of irregularity research has to do with quasi-periodic echoes that occur from field-aligned irregularities imbedded in nighttime sporadic-*E* layers. These echoes are interesting because they reveal not only a large-scale, wavelike nature suggesting atmospheric gravity waves as the source, but also enhanced irregularity drift velocities and shears that suggest the presence of a polarization process. Results from the MU radar measurements and from a joint radar experiment between the MU radar and the SRI frequency-agile radar are presented. The latter experiment, conducted from 26 May to 26 July 1993 in Japan, was designed to shed light on the three-dimensional spatial distribution and propagation characteristics of the field-aligned irregularities. We show that the preferred direction of group velocity is toward the southwest, a direction that is consistent with recently proposed models of these quasi-periodic echoes.

G2a-9
1140

## COORDINATED DIGISONDE AND INCOHERENT SCATTER RADAR F-REGION DRIFT MEASUREMENTS AT SONDRE STROMFJORD

J. L., Scali[1], B. W. Reinisch[1], C. J. Heinselman[2] and T. W. Bullett[3]
[1]University of Massachusetts Lowell
Center for Atmospheric Research, Lowell, MA
[2]SRI International, Menlo park, CA
[3]Phillips Laboratory, Geophysics Directorate
Hanscom, AFB.

Comparison of drift measurements made at Sondre Stromfjord show that the apparent velocities measured by the Digisonde are in good agreement with the drift velocities observed by the co-located Incoherent Scatter Radar (ISR). Data for 5 to 9 December 1991, show the mean DGS velocities to be within 50m/s of the ISR velocities, i.e. within the uncertainty levels of each instrument. The analysis highlights the dominance of the electric field in controlling the plasma motions since the measured velocities are generally height independent as would be expected for an E-field mapped along the magnetic field lines from high altitudes to ionospheric heights. The comparative analysis is used to study an ionospheric event where a large section of ionization was removed from the daytime cusp region by a strong anti-sunward drift when the IMF Bz component changed orientation.

G/H1b-1
0840

## SATELLITE OBSERVATIONS OF TRANSIONOSPHERIC PULSE PAIRS

D. N. Holden
Space and Atmospheric Sciences Group NIS-1, MS D466, Los Alamos National Laboratory, Los Alamos, NM 87545; 505-667-3406; e-mail: dholden@lanl.gov

The Blackbeard instrument aboard the ALEXIS satellite has been recording data for over one year. Blackbeard is in a 70 degree low earth orbit at 800 kilometers altitude. The principal features of the Blackbeard instrument are: 150 Msample/sec digitizer, 2 receiving bands: a "low" band of 28-95 MHz and a "high" band of 108-166 MHz, 16 Mbytes of memory, wide field of view antenna and photo diode array. So far during the mission, several hundred unusual radio emissions have been recorded. These emissions have a short duration of approximately 10 $\mu$sec, are 20 to 40 dB brighter than the average background, and occur in pairs separated by typically 50 $\mu$sec. They exhibit dispersion that is consistent with one pass through the earth's ionosphere and with the local time at the sub-satellite point. Some of these emissions exhibit O and X mode splitting which implies that the radiation has a component of linear polarization. We have dubbed these emissions "TransIonospheric Pulse Pairs" or TIPP events. We have observed them in both our low and high bands with very little diminution of signal strength as a function of frequency. When a TIPP event is detected, usually there is no other broad band emissions within the 100 msec record. The optical data that we have recorded simultaneously with the broad band RF data have not yet shown any coincidence which might link these pulses with lightning. TIPP events have been recorded when the satellite is over Africa and most of the equator during northern hemisphere winter, and over North America during the summer. The statistics of the local time at the sub-satellite point when TIPP events are detected suggest a relation to thunderstorms.

G/H1b-2
0900

## PHENOMENOLOGY OF IMPULSIVE RADIO EMISSIONS FROM THE MYSTERY PLANET EARTH.

R. S. Massey and D. N. Holden
Space and Atmospheric Sciences Group, MS-D466, Los Alamos National Laboratory, Los Alamos, NM 87545; (505)667-0014; rmassey@lanl.gov

The Blackbeard instrument on the ALEXIS satellite has recently observed powerful trans-ionospheric radio impulses that seem to occur only in pairs. In this paper, we analyze 84 of these events, called TlPPs. We compute several parameters that describe the events: the location and local time of the satellite at the time of reception, the energy in each pulse, the separation between pulses, the duration of each pulse, and the dispersion of each pulse. The statistical distributions of these parameters provide clues to and constraints on possible source mechanisms.

TlPPs appear to be a global phenomenon of natural, subionospheric origin. They have been observed at all longitudes near the equator, over the US, and elsewhere. Their power spectral density is roughly uniform from 25-75 MHz, up to about 10 nJ/Hz (effective isotropic), which is at or above the upper end of estimates from ground-based observations of spherics. Individual pulses last a few μs (first and second pulses generally have the same duration), and the pairs are separated by as much as 110 μs, with a median of 50 μs. The first pulse is usually, but not always, the more energetic. TlPPs appear in isolation, not as part of a long burst of radiation.

The possibility that the pulses might be the direct and reflected signals from a high-altitude source is evaluated by using simple models for sources, and comparing measured and modeled distributions.

Thunderstorms are probably in view for all events, and some electrical discharge in these storms seems a likely source candidate, but we have no direct evidence linking the pulses to thunderstorm emissions.

G/H1b-3 0920

SPORADIC E AND LIGHTNING -- WHAT IS THE CONNECTION?

C. Miller, J. Rosado-Roman, W. Swartz, M. Kelley
School of Electrical Engineering
M. Wysocki
Soil, Crop, and Atmospheric Sciences
Cornell University
Ithaca, NY 14853

The connection between lightning and ionization of the upper atmosphere was first suggested by Wilson in 1925. The first recorded observation of a connection between ionospheric ionization and thunderstorm activity was recorded in 1929 by Appleton, Naismith, and Hollingsworth. Between 1929 and 1972, numerous authors published reports of direct correlations between thunderstorm activity and sporadic E. In this paper, we ``rediscover" this historical literature and suggest how lightning may help explain three well known deficiencies of the wind shear theory of sporadic E formation: 1) the correlation between thunderstorms and sporadic E itself; 2) the diurnal, seasonal, and geographic morphology of sporadic E; and 3) the existence of highly localized, extremely dense patches of E region ionization. We end by suggesting that research into the connection between lightning and sporadic E may also help illuminate broader questions regarding the electrodynamic coupling of the troposphere and ionosphere.

G/H1b-4
0940

"Ionospheric Disturbances Caused by Lightning-induced Whistler Waves"

M.C. Lee(1,2), D.T. Moriarty(1), S.M. Murphy(1), R. Riddolls(1)
M.J. Starks(2), K.M. Groves(3), S.P. Kuo(4), M.J. Sulzer(5)
1. MIT Plasma Fusion Center, Cambridge, MA 02139
2. BU ECS Engineering Dept., Boston, MA 02215
3. Air Force Phillips Laboratory, Bedford, MA 01731
4. Polytechnic University, New York, NY 11735
5. Arecibo Observatory, Arecibo, Puerto Rico 00613

Lightning-induced gravity waves, transient electric field, and electromagnetic emissions (primarily whistler waves) can be the potential sources causing significant ionospheric disturbances. This paper will ceter on the discussion of several prominent ionospheric phenomena which are believed to be produced by the lightning-induced whistler waves. The lightning-induced whistler waves with intensities exceeding 40 mv/m were measured in the ionosphere by rocket-borne instruments. These intense whistler waves, appearing typically in the range of 5-10 kHz, can excite both lower hybrid waves and field-aligned zero frequency density striations in the ionosphere. These excited electrostatic modes have short scales, field-aligned nature, and large growth rates. They have been detected by ground-based radars as rapidly growing, short-lived ionospheric disturbances. This process detected by satellites, gives rise to two lower hybrid sideband modes and a low-frequency mode because of the Doppler effect. The lightning-induced whistler waves with higher frequencies, for example, tens of kHz have much less intensities and they cannot excite lower hybrid waves via plasma instabilities. However, these relatively weak whistler waves can still produce weak lower hybrid waves in the presence of naturally occurring ionospheric density irregularities. Briefly speaking, the existing density fluctuations can nonlinearly scatter the whistler waves into lower hybrid waves. This process generates a broad spectrum of lower hybrid waves in the ionosphere. The appearance of these weak broad-band lower hybrid waves can lead to the spectral broadening of the naturally-occurring Langmuir waves produced by photo-electrons. This spectral broadening process seems to have occurred in our ionospheric heating experiments at Arecibo, Puerto Rico.

J2-1 0840

## NNLS DECONVOLUTION AND SELF CALIBRATION

Daniel Briggs, NRL Research Associate
NRL/USNO Optical Interferometer Project
Center for Advanced Space Sensing
Naval Research Laboratory
Code 4215
Washington, DC 20375

A new deconvolver has been developed which greatly outperforms CLEAN or MEM on compact sources. It is based on a preexisting Non Negative Least Squares matrix inversion algorithm. NNLS deconvolution is somewhat slower than existing algorithms for slightly resolved sources, and very much slower for extended objects. Memory is the limiting factor to the source size that can be deconvolved. A map with approximately 6000 pixels of significant emission and high SNR can be deconvolved in several hours on an IBM RS/6000-560 workstation with 128MB of memory. The solution degrades with increasing source size. At the present computational limit it is roughly comparable in deconvolution fidelity to existing algorithms.

NNLS deconvolution is particularly well suited for use in the self calibration loop. It is somewhat more forgiving than CLEAN to wide support windows, and multiple iterations can be run without human intervention. Unlike CLEAN, NNLS is not spatially iterative and there is no arbitrary cutoff criterion needed. Windowing information enters the solution in a global manner which prevents the ringing instability around resolved peaks seen in CLEAN. Unlike MEM, NNLS is not biased against compact structure and the residual deconvolution errors are largely uncorrelated.

VLBA observations have been made of the slightly resolved source DA193. The best self calibrated maps using CLEAN as the deconvolver yielded a peak to offsource RMS dynamic range of 9400, well under the theoretical 28000, and an extended halo at the .2% level. The best maps using NNLS as the deconvolver achieved the theoretical dynamic range and produced no halo. Realistic simulations have shown CLEAN to be quite capable of generating artifacts at this level, and NNLS capable of detecting such a halo were it present. The halo is believed non-physical. Residual calibration errors are partially responsible for the CLEAN limitations, as the CLEAN solution improved to 14000 dynamic range and .05% halo when run on the NNLS calibrated data.

J2-2
0900

## FRINGE FITTING FOR VLBI POLARIZATION

Chris Flatters
National Radio Astronomy Observatory
P.O. Box 0
Socorro, NM 87801

Differences between the frequency standards at different antennae in a VLBI array lead to delay and rate errors which must be removed from the data. Their values may be estimated by searching for the peak of the correlation function as a function of delay and rate. This procedure is known as fringe fitting. Fringe fitting may be performed by Fourier transforming a short segment of data into delay-rate space and searching for the peak or by modelling the phase of the data as a function of delay and rate and finding the values that produce the best fit to the observed data; in practice the two methods are usually combined.

Fringe fitting can not be carried out in cases where the signal-to-noise ratio is low. This presents a problem for polarization observations since the linear polarization signal is usually much weaker then the total intensity signal. In practice the delays and rates for the cross-polarization correlations (which supply the linear polarization information) are wholly determined from the antenna-based delays and rates for each hand of polarization and the offsets between the delays and rates for each hand of polarization at each antenna. The antenna-based quantities may be determined by global fringe-fitting algorithms while the offsets at the reference antenna can be determined from the cross-polarized signal from a strong source on a single baseline. If a stable antenna is chosen as the reference antenna and the time-variable effects due to the changing parallactic angle and ionospheric Faraday rotation are removed then the offsets between the opposite hands of polarization should be constant over the duration of an observing run and can be determined from a single measurement.

J2-3 SPECTRAL LINE POLARIZATION VLBI
0920 Dr A.J. Kemball
National Radio Astronomy Observatory
Socorro, NM 87801

Data reduction techniques are described for the full polarization imaging of spectral line sources observed using Very Long Baseline Interferometry (VLBI). The instrumental and propagation effects that need to be removed in the course of calibrating such observations are discussed. General methods are presented for antenna-based amplitude, phase and instrumental polarization calibration that allow an arbitrary degree of circular polarization in the source. Several approaches to instrumental polarization calibration are discussed, including the use of spectral line sources with moderate linear polarization.

J2-4 POLARIZATION SELF-CALIBRATION
0940
K. J. Leppanen, J. A. Zensus, P. J. Diamond
National Radio Astronomy Observatory, Socorro, NM
kleppane@aoc.nrao.edu

We discuss a novel technique of determining the instrumental polarization parameters of a VLBI array, with the goal of imaging the linear polarization structure of compact radio sources. We use the source to be imaged in this calibration, avoiding the need for extensive observations of a polarization calibrator source. The technique is applicable to both line (masers) and continuum sources, is completely insensitive to circular polarization, and allows high levels of linear polarization in the source. Simulations indicate that an average parallactic angle coverage of 50 degrees is adequate for a good solution of the instrumental parameters.

The technique employs a non-iterative linear least-squares algorithm, and is based on the assumption that the linearly polarized emission has the same support as the total intensity emission (a physical necessity). This is a very strong constraint, since the parallactic angle rotation spreads the spurious emission due to uncorrected polarization leakage in the feeds unphysically over the polarization image. The algorithm requires a total intensity model for the source, which can be obtained from the standard gain self-calibration preceding the polarization self-calibration.

We have used this approach to calibrate 22~GHz observations with the VLBA and we present images of the polarization structure of three quasars and two masers. Finally, we discuss the calibration of e-vector position angle in VLBA observations.

J2-5
1000

# FEED POLARIZATION EFFECTS ON GEODETIC VLBI

Robert Potash
NVI Inc.
code 926.9
NASA GSFC
Greenbelt MD 20771

Geodetic vlbi normally observes using RCP feeds. Unwanted pickup of LCPradiation by the RCP feeds causes fringe phase changes, both from response to linearly polarized radiation and from the second order LCP-LCP response. When this unwanted pickup, or polarization leakage, varies with frequency, the group delay is perturbed as well. The effects depend on the feed orientation relative to the source, so they will vary systematically across the sky and alias into baseline determinations. These errors are likely to be larger in geodetic than in astronomical receivers because the geodetic systems are dual frequency, wide bandwidth, compact in size, and at some sites are periodically dismounted and re-mounted. But if the leakage coefficients are less than about 10% (-20 dB power) in all frequency channels at all sites, then the effect on the geodetic observables should be small enough to neglect.

In July 1994 we performed an experiment designed to determine the instrumental polarization (leakage) parameters of several geodetic vlbi stations. Two VLBA stations - Owens Valley and Pie Town - observed on the same day as a NASA geodetic experiment, performed between Kokee, Fairbanks, Westford, Onsala, Wettzell, Los Alamos and Fort Davis. The geodetic stations observed in their standard configuration and followed their normal schedule. Owens Valley and Pie Town observed both LCP and RCP simultaneously, sampling eight of the frequency channels in the geodetic experiment, ranging from 8212 to 8932 MHz at X-band and 2220 to 2345 MHz at S-band. Owens Valley and Pie Town spent about half the session tracking four calibrator sources - 3C84, OQ208, DA267 and DA193 - through transit at both sites. For the remaining time they followed the ongoing geodetic schedule, but using dual polarization.

To date (mid September) half of the calibrator data has been correlated. Analysis of the fringe amplitude ratios shows instances where the net total cross-hand response is 10% of the parallel hand response. This response apears to vary with parallactic, and sometimes differs significantly in different frequency channels. The cross-polarization may be caused in part by the dichroic system, which is not present for normal astronomical observing.

The remainder of the experiment will be correlated in October, and it is expected that non-vlba sites will show instances of more severe cross-polarization.

J2-6
1040

## MILLIMETER VLBI FRINGE DETECTION AND FITTING

Alan E.E. Rogers and Sheperd S. Doeleman
MIT Haystack Observatory, Westford, MA 01886
James M. Moran, Center for Astrophysics and
Harvard University, Cambridge, MA 02138

In mm-VLBI observations, atmospheric turbulence and local oscillator phase noise often limit the coherence time to a few seconds. When such coherence losses severely limit the integration time, detection thresholds rise and weak sources cannot be detected. Under these conditions, the detection methods and measurements of visibility amplitude and phase can be reformulated in terms of incoherently averaged quantities. To prepare mm-VLBI data for entry into the standard radio interferometry imaging software, a global fringe search is first performed on incoherently averaged data to determine the station clock offsets and rates. Then, using the clock information from the search, the data for each baseline is segmented with segment length shorter than the coherence time. The fringe amplitudes for each baseline are then derived from the incoherent average of segments for each baseline. Closure phases for all possible triangles of baselines are determined by averaging the bispectrum for each triangle over all segments in a scan. Individual baseline phases are assigned using a weighted least squares fit to the closure phases. Incoherent averaging is found to be more effective than previously recognized. The detection threshold for M segments improve with $M^{0.4}$ dependence for small M tending to the slower $M^{1/4}$ dependence for large M.

J2-7 AUTOMATIC IMAGING, INCLUDING SELF-CALIBRATION
1100 Dr. M. C. Shepherd
Department of Radio Astronomy 105-24,
California Institute of Technology,
Pasadena, CA 91125

This talk centers on recent experiments in "hands-off" processing of visibility data to generate astronomical images from radio interferometer measurements. Improved interferometers, software, and computer hardware are now making this an attractive alternative to the painstaking and all-too subjective black-art employed by human experts. Sample results from a couple of survey experiments are presented to demonstrate that all but a small fraction of the resulting maps rival those made by hand, and that the remainder are also amenable to the same procedure but required small adjustments to the initial running parameters. When pipelined to process multiple observations from surveys, the automatic procedure is also shown to be on the order of 300 times faster at producing maps than manual procedures. The tools used in Difmap to construct automatic mapping procedures are discussed, along with an outline of the two procedures used so far.

J2-8
1120

## IF BANDPASS CORRECTION FOR DATA FROM THE VLBA CORRELATOR

Dr. P. J. Diamond
National Radio Astronomy Observatory
P.O. Box 0
Socorro
NM 87801

The VLBA FX correlator uses an earth-centered geometrical delay and delay rate model. This has many advantages over the baseline-based model used in MkIII and MkII correlators. However one problem that is exacerbated by the use of such a model is bandpass calibration. Astronomers observe bright continuum radio sources for the purposes of bandpass calibration, these sources are often many degrees distant from the source of interest. In such a case the natural geometrical fringe rate for the bandpass calibrator and program source are very different, the result being that the bandpass calibrator is shifted in frequency from the program source.

I shall describe a technique that has been developed to correct for this frequency shift and to produce flat, bandpass-corrected spectra.

J2-9
1140

## B-FACTOR OF A FX CORRELATOR FOR DIFFERENT PAIRS OF DIGITIZERS (TWO AND FOUR LEVELS QUANTIZATION).

L. Kogan
National Radio Astronomy Observatory,
PO Box 0, Socorro, NM 87801

The B-factor of a FX correlator has been analized for different pairs of digitizers (two and four levels) and for different tapering functions at the FFT stage. Problem of reconstructing of the original analog signals' spectrum from a FX correlator measurements in the case of strong correlation (auto correlation in particular) is formulated. It is shown that zero padding can not be just an option of a FX correlator but *must* be applied in the high correlation coefficient case (auto correlation in particular).

J2-10
1200

# A TEST OF WVR-BASED TROPOSPHERE DELAY CALIBRATION USING VLBI OBSERVATIONS ON A 20 KM BASELINE

L.P. Teitelbaum, S.J. Keihm, M.J. Mahoney,
R.P. Linfield, G.M Resch, R.N. Treuhaft
Jet Propulsion Laboratory
California Institute of Technology
4800 Oak Grove Drive
Pasadena, CA 91109-8099

Dual frequency (S/X band) Very Long Baseline Interferometry (VLBI) observations over a 20 km baseline at Goldstone, CA were conducted in order to test troposphere delay calibration by Water Vapor Radiometers (WVRs). The initial data were taken in April and May 1993 and a follow-up experiment was performed in June and September 1994.

Analysis of the 1993 data is complete. Determinations of the structure function of the VLBI residual phase delay over few-hundred second time scales indicate that the residual phase delay is mainly due to the troposphere for time intervals $10 < \Delta t < 300$ s. However, model calculations of tropospheric turbulence fluctuations show that the spring 1993 Goldstone troposphere was exceptionally quiet. Comparison of the VLBI and WVR measurements shows a statistical agreement on time scales $< 700$ s. But on longer time scales, VLBI instrumental errors which could not be calibrated became important. The improvement in VLBI post-fit residual delays from the application of the WVR calibration was consistent with the measured level of tropospheric fluctuations.

The 1994 observations used a new 34 m beam waveguide antenna at one end of the 20 km baseline. Preliminary analysis of the 1994 data indicates that the VLBI instrumental errors were smaller, that the troposphere was much more active, and exhibits a strong correlation between VLBI and WVR estimates of the wet delay.

J2-11
1220

# AMPLITUDE CALIBRATION INCLUDING ATMOSPHERE

R. C. Walker
National Radio Astronomy Observatory
PO Box O
Socorro, NM 87801

It should be possible to obtain apriori amplitude calibration of VLBI observations accurate a couple of percent at most frequencies without recourse to amplitude calibrators. This is significantly better than traditional practice. It has been common to make amplitude adjustments of several percent to factors of a few, based on calibrators or self-calibration, after apriori calibration. For the VLBA, apriori amplitude calibration can approach the above accuracy goal, as will be described. This can significantly improve both the ease of the imaging process and, in some cases, the quality of the final results.

The high quality calibration available on the VLBA is the result of several factors. Antenna gains and gain curves are measured frequently and with large amounts of data. Gain curves are only needed at the highest frequencies. System temperatures are measured continuously on all channels during observations. Weather data is monitored and can be used as an aid in editing data and in making adjustments for opacity. Finally, the pointing at most frequencies is good enough that the amplitudes are not degraded significantly.

The gain curves that are traditionally provided by VLBI observatories are actually combined gain and opacity curves. While the gain portion is likely to be constant, the opacity is not. For the VLBA, the gains and gain curves delivered to users do not include opacity so explicit opacity corrections should be made. The system temperature, after subtraction of the receiver temperature and spillover, can be divided by an atmosphere temperature to obtain a reasonable measure of the instantaneous opacity. The atmosphere temperature can be determined from the weather data, adjusting for the fact that most of the absorption will occur well above the antenna location. An opacity determined in this way also accounts, to first order, for absorption due to water on the feeds and due to partial aperture blockage at low elevations when the local horizon is close.

Amplitudes calibrated using antenna gains determined with single dish observations and using system temperatures depend on accurate knowledge of all scaling applied by the correlator and reduction software and of all losses due to sampling effects etc. For the VLBA, with its large number of recording and processing modes, getting this right requires some care.

Session B/D-2, 1355-Thurs., CR2-28
APPLICATIONS OF NEW MATERIALS FOR ELECTRONICS, DEVICES, AND SYSTEMS
Chairperson: S.A. Long, Dept. of Electrical and Computer Engineering, Univ. of Houston, Houston, TX 77004
Organizers: S.A. Long, Univ. of Houston; and J.W. Mink, Army Research Office

B/D2-1
1400

## MODELING OF SUPERCONDUCTING TRANSMISSION LINES FOR MICROWAVE CIRCUIT APPLICATIONS

Jeffrey M. Pond
Microwave Technology Branch
Naval Research Laboratory
Washington, DC 20375

Accurate and efficient modeling of superconducting transmission lines is needed in order to fully exploit the advantages of high-temperature superconductors (HTS) for microwave circuit applications. One of the principle microwave application areas that should benefit from HTS technology is that of very narrow bandwidth (<1%) filters. Microwave losses of thin-film-based distributed filters fabricated using HTS as opposed to normal metals can have insertion losses of approximately 1 dB instead of more than 10 dB when the bandwidth is small (A. Fathy, et. al., 1993 IEEE MTT-S IMS Digest, 3, 1277-1280, 1993). Of course, in order to fabricate such a filter and have it work according to design it is necessary to be able to design the resonant elements to very tight tolerances. Although narrowband filters have been fabricated which have very good pass band shapes, present computer aided design techniques are, in general, unable to account for the internal fields of the superconductor and hence it is very difficult to design for a precise center frequency.

Computational considerations limit the use of electromagnetic field solvers to relatively simple geometries since the fields internal to the superconducting films as well as the external fields must be modeled. Obviously, considerable computational efficiency can be gained if the internal fields of the superconductor do not need to be solved and yet the affects of the superconductor can still be retained. A surface impedance description is insufficient because the thickness of most high quality HTS films is on the order of the superconducting penetration depth. However, another approximate boundary condition, the resistive boundary condition (T. B. A. Senior, Radio Sci., 10, 645-650, 1975), can be used in conjunction with other electromagnetic modeling approaches such as the spectral domain technique. This approach was first applied in the case of very thin superconducting films where the approximate boundary condition is well defined (J. M. Pond, et. al., IEEE Trans. on MTT, 37, 181-190, 1989). It is shown that an extension of this approach to thicker films, on the order of a penetration depth thick, is valid for most transmission line topologies of interest. Combining this approximate boundary condition with the spectral domain technique is computationally efficient and gives excellent agreement with measured results obtained from a set of HTS coplanar waveguide resonators.

B/D2-2
1420

# A Circularly Polarized YBaCuO Microstrip Antenna Array

*Jarrett D. Morrow, Jeffery T. Williams, Matthew F. Davis*
*Darian Licon, Stuart A. Long,* and *John C. Wolfe*

Applied Electromagnetics Laboratory
Department of Electrical and Computer Engineering
University of Houston
Houston, TX 77204-4793

The primary advantage of using superconducting materials in antenna systems is the reduction of the loss associated with transmission line matching circuits and feed networks, particularly at microwave and millimeter-wave frequencies where the ohmic losses begin to significantly affect the system performance. For large antenna arrays with long, elaborate corporate feed networks, the use of high temperature superconducting (HTS) transmission lines can substantially increase the gain of the array. These benefits become more apparent as the number of radiating elements in the array increases. In addition to the feed line losses, the losses associated with the individual radiators must also be included to obtain the overall efficiency of the antenna array. In general, the efficiency of a microstrip patch antenna is limited by the power dissipated by ohmic losses in the patch element and the ground plane, dielectric loss in the supporting substrate, and undesirable excitation of surface-wave radiation. Thin substrate patch antennas have lower antenna efficiencies due to conductor and dielectric loss and lower impedance bandwidths. It has been demonstrated that the conductor losses can be significantly reduced by constructing the antenna from HTS thin films since these materials have microwave surface resistances that are one to two orders of magnitude less than that of copper at 77K.

$\tan\delta = 10^{-4}$ or $10^{-5}$

In this presentation we will discuss the fabrication and testing of a four-element 20 GHz, circularly polarized $YBa_2Cu_3O_x$ microstrip antenna array on a $LaAlO_3$ substrate. Typical antenna feed designs are not feasible on the high dielectric constant substrates upon which the high temperature superconductors are deposited. Therefore, we considered an array of *gap-coupled* circularly polarized elements. We were able to experimentally determine the gap size necessary to achieve a good match between the feed line and the patch. Then we fabricated and tested circularly polarized elements and four-element arrays on LaAlO using sputtered copper films. These antennas were found to perform well, with relatively good circular polarization. Using the design established in copper, we constructed a YBaCuO array and measured its patterns and gain relative to the room temperature copper array. Below the transition temperature of the film, the YBaCuO antenna array operated well. The patterns were essentially the same as those for the copper array and the measured gain of the YBaCuO array was greater than that for the room temperature copper array, as predicted.

He @ 15K
Gain relative to Cu array (2×2) is
+2dB at 75K and +4dB @ 25K
Resonant freq shifts with temp because
of dielectric and penetration into metal patch
($\epsilon_r \approx 24$)

B/D2-3
1440

## DESIGN AND MEASUREMENT OF ELECTRICALLY SMALL, SUPERCONDUCTING HALF LOOP AND SPIRAL ANTENNAS

Donald R. Bowling and Michael M. Neel
Weapons Division
Naval Air Warfare Center
China Lake, California

Recent developments in high temperature superconducting (HTS) thin film materials and processing technology have made possible the fabrication of printed circuit antennas and integrated matching networks. The extremely low loss properties of HTS materials can be utilized to design electrically small resonant antennas whose radiation efficiency is not degraded by conductor losses. HTS low loss properties also make possible the use of electrically small travelling wave antennas, and "supergain arrays" where the electrical spacings are less than a few tenths of a wavelength. The near absence of any resistive loss improves the efficiency of both antenna radiating and matching structures enabling the feasibility of previously inefficient designs.

For the case of a half loop resonant antenna, the design and application considerations along with test results of the antenna built at China Lake will be presented. Efficiency-bandwidth considerations will be discussed. Effects of normal conducting groundplane losses upon the effciency of both single element and superdirective arrays will also be discussed. Data comparing patterns and efficiency for a three element superdirective array fabricated from both gold and HTS will be presented. Specific problems encountered during the design and fabrication will also be addressed.

For the case of an archimedean spiral antenna, the design and application considerations for an integrated feed line, 3 inch diameter design will be presented along with current test results. The increase in gain at frequencies below the conventional limit will be discussed, along with analysis performed to understand these antennas behavior better.

B/D2-4
1500

# A Monolithic High-Gain Superconducting Antenna

*Jagannath Poosarla, Jeffery T. Williams,* and *David R. Jackson*
Applied Electromagnetics Laboratory
Department of Electrical and Computer Engineering
University of Houston
Houston, TX 77204-4793

We have developed a new leaky-wave antenna that requires the use of high temperature superconducting (HTS) materials for its operation. An advantage of this antenna design is that it is an extremely simple monolithic structure. It consists of a substrate backed by an HTS ground plane that is covered by a thin film of HTS material, fed from behind the ground plane by a simple waveguide feed. The design is most appropriate for the millimeter-wave frequency range because high gains can be obtained using thin, small diameter (< 5cm) substrates; therefore, a design frequency of 94 GHz will be used for the results to be discussed. In the presentation we will summarize the analysis of this antenna with respect to the different parameters of interest for a leaky-wave antenna: the propagation constant, radiation efficiency, radiation patterns, directivity, and bandwidth. We will evaluate the performance of this antenna with respect to variations in the superconducting $YBa_2Cu_3O_x$ film and ground plane and the $LaAlO_3$ substrate, and the geometrical parameters of the antenna. We will present results for the case of broadside radiation (as shown in the figure) and will show that high gain performance is more easily realized using high temperature superconductors, as opposed by low temperature superconductors, since higher antenna efficiencies are obtained at temperature substantially below $T_c$. We will also demonstrate that for a 94 GHz antenna optimal gain (~ 30 dB) is achieved with a cover layer thickness of approximately 260 Å.

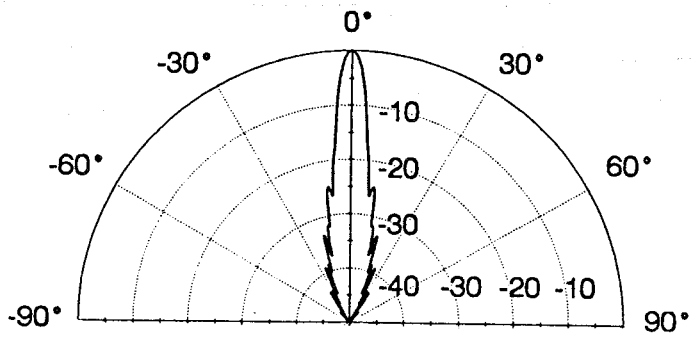


Theoretical E-plane radiation pattern for a YBaCuO antenna on a 5 cm diameter LaAlO substrate.

Substrate: $LaAlO_3$
$\epsilon_r = 23$ $\tan\delta = 10^{-5}$
Need SC groundplane for decent $\epsilon_r$

B/D2-5 1540 DEVICE APPLICATION ISSUES FOR HIGH-Tc PASSIVE MICROWAVE CIRCUITS

W. Gregory Lyons
Lincoln Laboratory
Massachusetts Institute of Technology
Lexington, MA 02173

The integration of high-Tc superconductor (HTS) passive components into microwave receiver subsystems for actual field demonstrations has begun, and convincing applications are promised within this decade. Both general and application-specific challenges exist for each type of passive microwave device or network presently envisioned. General challenges include the quality of the HTS thin films, cryogenic cooling of the devices for field use, patterning the HTS films in a reliable and accurate fashion without damaging the films, and packaging HTS devices to achieve long-term reliability. Every type of passive HTS microwave device would benefit from improvements in material quality of the films, which would in turn result in low surface resistance at both low and high microwave current levels. These improvements would enable higher Q's and higher power-handling levels, respectively. Higher power-handling levels would also lead to reduced spurious nonlinear signals from intermodulation and harmonic generation as well as reduced power dissipated in the device by maintaining a low surface resistance. An overview will be given of present approaches towards overcoming these general challenges.

A summary of the specific issues and research directions that relate to each type of HTS passive microwave circuit will also be presented. Resonator-based high-Q filters store large circulating currents and therefore stress the power-handling capability of HTS films. Accuracy is also a key issue in producing planar HTS filters that do not require tuning as replacements for high-performance low-loss dielectric filters, which must be tuned. Long low-loss low-dispersion electromagnetic HTS delay lines and tapped delay lines have no real equivalent counterpart in conventional technology. Challenges for HTS delay lines are the requirement of large-area films (2-in-diam. minimum) and the possibility of spurious modes. Antenna arrays with low-loss HTS feed networks are attractive as alternatives to active MMIC phased arrays. Very large area films are required (3-in-diam. minimum), Butler-matrix crossovers are a challenge in HTS, and cryogenic cooling of an array that must radiate into free space is difficult. Matching networks for superdirective arrays are also a possibility, but stress the accurate layout of the structure. Resonator-stabilized oscillators suffer from phase noise added by the HTS films. Hybrid semiconductor/HTS signal-conditioning networks present a packaging problem because of the chemical sensitivity of the HTS films. These challenges are being met in a variety of ways as HTS devices move into actual application environments.

B/D2-6 THE NEW SUPERCONDUCTING DIGITAL ELECTRONICS
1600

Marc J. Feldman
Department of Electrical Engineering
University of Rochester
Rochester, NY 14627

An increasingly widespread research effort to use superconducting circuitry for high-speed digital computation is based on the "RSFQ" (Rapid Single Flux Quantum) logic system developed at Moscow State University. In this scheme, digital information is coded in quanta of magnetic flux, which are the natural excitations in superconducting circuits. (Earlier research, which used dc voltage levels to code information in emulation of semiconductor computation, in spite of the fact that superconducting circuits do not readily support a dc voltage, largely came to a dead-end.) The magnetic flux quanta can be generated and processed by simple Josephson junction circuits at very high speed. A full logic family now exists. There is now no evident barrier to constructing complex RSFQ circuits which operate at clock speeds of more than 100 GHz, in the near future.

In this talk I will discuss the basis and the potential of RSFQ logic, and research accomplishments around the world. I will describe recent work at the University of Rochester in this area, including the development of a logic simulator and design tool for large-scale pulse-based circuits, the design and simulation results for an LSI RSFQ digital decimation filter, and experimental tests of various RSFQ circuits including components of the decimation filter.

Research supported by the Rochester University Research Initiative sponsored by Army Research Office grant No. DAAL03-92-G-0112.

B/D2-7 FIRST OBSERVATION OF SFQ PULSES

1620 C.-C. Wang, M. Currie, D. Jacobs-Perkins, R. Sobolewski, T.Y. Hsiang, and M.J. Feldman
Department of Electrical Engineering and Laboratory for Laser Energetics
University of Rochester
Rochester, NY 14627

The superconducting single-flux-quantum (SFQ) pulse is the basic information "bit" of several new families of digital logic. SFQ logic promises LSI clock rates of hundreds of GHz, much faster than semiconductor logic, with negligible heat generated by the circuitry.

An SFQ voltage pulse is generated when a quantum of magnetic flux, a fundamental "particle," passes through a Josephson junction. The pulse area is quantized: the integral of the voltage over time is exactly equal to h/2e, which is 2.07 mV x ps. Because of this small amplitude and picosecond timescale, an SFQ pulse has never been observed, i.e. mapped out and delineated. Nevertheless, SFQ pulses are standardly generated, processed, and detected in many different superconducting circuits, digital and analog.

We have made the first observation of superconducting SFQ pulses, using a cryogenic electro-optic sampling system. The experimental results were unambiguous. The pulse height was typically 0.7 mV with a pulse width of 3 ps, while the rms noise of the measurement was less than 70 microV and the time resolution was 350 femtoseconds.

The SFQ pulses were generated by using a planar interdigitated Nb/Si/Nb metal-semiconductor-metal photodiode as an optoelectronic switch on superconducting microstrip line, to drive a "pulse shaper" consisting of two Nb/Al2O3/Nb Josephson junctions. The resulting SFQ pulses were launched onto another superconducting microstrip and were detected with the sampling system by a non-invasive measurement of the fringe field of the microstrip.

The observed SFQ pulses agreed well with simulations. However, several surprising and as yet unexplained results seen in some experiments will also be presented.

These experiments set the stage for a great variety of future work, including non-invasive optical probing of functional and dysfunctional SFQ digital circuits, detailed measurements of the timing parameters of SFQ subcircuits, and leading to the integration of optical--superconducting systems.

Research supported by the Rochester University Research Initiative sponsored by Army Research Office grant No. DAAL03-92-G-0112.

B/D2-8 Roundtable Discussion
1640

Session C-2, 1355-Thurs., CR1-42
DETECTION AND ESTIMATION
Chairperson: David J. Thomson, AT&T Bell Laboratories, Murray Hill, NJ 07974
Organizers: David J. Thomson and Louis L. Scharf, Dept. of Electrical and Computer Engineering, Univ. of Colorado at Boulder, Boulder, CO 80309

C2-1
1400

## MULTI-WINDOW ESTIMATORS OF CORRELATION

L. Todd McWhorter and L.L. Scharf
Electrical and Computer Engineering
University of Colorado
Boulder, CO 80309

In this presentation we discuss multi-window estimators of correlation matrices and correlation sequences. Adaptive filtering, source coding, and a variety of array processing algorithms are examples of signal processing techniques which implicitly or explicitly use estimators of correlation. Typically, these and other algorithms use single-window or sum of lagged products estimators. We state and prove a representation theorem for all estimators of the correlation matrix which are Toeplitz, non-negative definite, quadratic in the data, and modulation invariant. The representation theorem admits estimators which use multi-windowed copies of the time series data. We then show that multi-window estimators of the correlation matrix can have smaller mean-squared error than the conventional single-window estimators. We conclude by describing, and discussing the properties of, an adaptive LMS algorithm which uses multi-window estimators of the correlation matrix.

C2-2
1440

## KARHUNEN-LOEVE EXPANSIONS and QUADRATIC INVERSE THEORY

**David J. Thomson**
AT&T Bell Laboratories, Murray Hill, N.J. 07974

Multiple-window spectrum estimation methods (Proc.IEEE **70,** pp 1055-96, 1982) derive from a frequency-localized least-squares solution of the first-kind Fredholm equation connecting the Fourier transform of a short sample of a stationary process with the Cramer spectral representation of the process. Quadratic-inverse spectrum estimates ( *Phil. Trans. R. Soc. Lond. A* **332,** pp 539-97, 1990.) extend this theory to give optimum estimates of the second moments by decomposing the covariance matrix of the multiple-window eigencoefficients into a components-of-variance like series of known basis matrices with scalar coefficients. In this talk, I describe some relations of quadratic-inverse theory to and Karhunen-Loeve expansions, to maximum-likelihood estimates, and to covariance extension models.

C2-3 1540

# Neural Network-based Radar Target Detection System

Simon Haykin and Tarun Bhattacharya
McMaster University
Communications Research Laboratory
Hamilton, Ontario, Canada L8S 4K1

## Abstract

In this paper we present a novel adaptive (intelligent) system for the detection of a radar target in a clutter-dominated environment. The system consists of three basic components:

1. Nonlinear time-frequency analysis, based on the Wigner-Ville distribution.
2. Feature extractor, based on principal components analysis.
3. Pattern classification, using a multilayer perceptron.

The last two components are implemented using self organized and supervised neural networks, respectively. Examples representative of a radar system operating in an ocean environment are used to do the training.

The distinguishing features of the new target detection system include the following:

* Weak statistical assumptions.
* Distributed nonlinearity, accounting for the nonlinear dynamic process responsible for the generation of clutter.
* Learning capability, accounting for the nonstationary nature of the radar clutter.

Experimental results, based on ground-truthed and calibrated real-life radar data, are presented, which demonstrate the superior performance of the new detection system over a conventional Doppler CFAR processor.

C2-4
1620

## Data Adaptive Low Rank Modelling

Louis L. Scharf
John Thomas
Electrical and Computer Engineering
University of Colorado
Boulder, CO 80309

How does one adaptively split a measurement subspace into signal and orthogonal subspaces of reduced rank so that detectors, estimators, and quantizers may be adaptively designed from experimental data? We provide some answers to this question by decomposing experimental correlations into their Wishart distributed Schur complements and showing how these distributions may be used to identify subspaces.

Session F-5, 1335-Thurs., CR1-9
PROPAGATION MEASUREMENTS FROM THE
ADVANCED COMMUNICATIONS TECHNOLOGY SATELLITE (ACTS)
Chairperson and Organizer: Faramaz Davarian, Jet Propulsion Lab, MST708, 4800 Oak Grove Dr., Pasadena, CA 91109

F5-1
1340

## ACTS Ka-BAND MEASUREMENTS IN FLORIDA

Professor Henry Helmken (Florida Atlantic University) and
Professor Rudolf Henning (University of South Florida)
Department of Electrical Engineering
Florida Atlantic University, M.S. SE-456
777 West Glades Road
Boca Raton, Florida 33431

NASA's Advanced Communications Technology Satellite (ACTS) was developed to assist the creation and validation of communication technology as it expands into the millimeter region. One vital program element is providing the needed propagation data base for Ka Band (20/30 GHz) commercial communication system development. At these frequencies, reliable signal transmission system design relies heavily on validated models of channel characterization and propagation statistics. The Space Communications Technology Center, a NASA sponsored Center for the Commercial Development of Space (CCDS) headquartered at Florida Atlantic University, is developing systems for digital satellite communication of voice, data and video via Ka-band and thus very dependent on accurate propagation information.

An ACTS Propagation Terminal (APT) has been established by NASA at the University of South Florida in Tampa, supporting both the ACTS program and the CCDS mission. This terminal, one of the seven strategically placed in North America (from Alaska to Florida), has been acquiring propagation and related data since December 1993; its initial year's data has been processed. Preliminary results of concurrently observed ACTS beacon signal path attenuations variations and radiometer data will be presented.

First results will focus on individual CDF distributions and relative comparisons such as Beacon 20 GHz vis-a-vis Radiometer 20 GHz. A comparison will also be made to the CCIR and Global models using a JPL-developed propagation program and both dry and rainy season data. Also included will be a preliminary report of fading statistics during the year's Florida sub-tropical dry and rainy seasons.This information will be compared to OLYMPUS satellite fading statistics reported by Stutzman.

In addition, a more detailed analysis of radiometer data will be presented. Interest here is in determining under what conditions and to what accuracy will radiometer measurements provide actual path loss variations? Also, to what extent, if any, is there a radiometer data fine structure that correlates with scintillation-caused path attenuation variations?

F5-2
1400

## Ka BAND PROPAGATION STATISTICS AT WHITE SANDS NEW MEXICO

Glenn Feldhake[1], Dr. Louis Ippolito[2] and Dr. Stephen Horan1
[1]New Mexico State University
Department of Electrical and Computer Engineering
Box 30001, Dept. 3-O
Las Cruces, NM 88003-0001
[2]Stanford Telecommunications Inc.
1760 Business Center Drive
Reston, VA 22090

The increased demand for communication capacity over the last several years has led to more spectral bandwidth being allocated for private use. Before communication activities take place, users must characterize the propagation properties of both the frequencies used and meteorological conditions governing the transmission space. This paper discusses preliminary findings of a Ka band propagation experiment using the Advanced Communications Technology Satellite (ACTS). Signal fade and rain attenuation statistics are the primary variables measured. Monthly and yearly breakdowns are compiled. All data were collected at the Seconds TDRSS ground station near White Sands New Mexico during 1993 and 1994. Frequently used models also generate expected statistics for the area. Comparisons of predicted and observed data show discrepancies. Possible causes of these discrepancies, including the geography of the area, are discussed.

F5-3 Evaluation of Open-loop Up-link Power Control Using ACTS
1420 Asoka Dissanayake
COMSAT Laboratories
Clarksburg MD 20871

Propagation impairments originating in the troposphere, such as rain attenuation and tropospheric scintillations, impose a limit on the use of the 20/30 GHz frequency band for satellite communication applications. Development of useful techniques to ameliorate these impairments are of considerable importance for the successful exploitation of the frequency band. One such technique, open-loop up-link power control, has been evaluated using the Advanced Communication Technology satellite (ACTS).

Open-loop power control entails the estimation of the up-link fade at an earth station using a down-link signal and increasing the transmit power of the carrier to compensate for the up-link fade. Although other forms of power control such as closed-lop control can be considered, the open-loop scheme has the advantage of having the least implementation complexity in a satellite network. Power control is effective not only in fade situations, but also under signal enhancements experienced during tropospheric scintillations that can generate undesired interference to other satellite users.

Two key factors which determines the effectiveness of the open-loop power control are the detection of the correct down-link signal fade/enhancement and the frequency translation of this value to the up-link frequency. Errors in the fade detection arise due to equipment limitations; sources contributing to this error include gain variations in the ground station receive chain and the diurnal effects at the satellite. Frequency translation errors are brought about by the random nature of the propagation phenomena; this is exacerbated by the large frequency separation between the up- and down-link frequencies in the Ka-band. Inhomogeneity of rain along the propagation path, which include variations in the rain drop size distribution and the rain temperature, largely determines the frequency scaling error.

An experiment was conducted using the ACTS satellite to investigate the limitations of the open-loop power control technique. A power controlled pilot carrier was transmitted from the NASA ground station in Cleveland, OH, and received at COMSAT Laboratories in Clarksburg, MD. The power control algorithm takes account of equipment induced errors as well as those due to the propagation environment. Preliminary results of the experiment indicate that open-loop control can be applied to compensate fade levels up to about 15 dB. Additionally, the control error can be maintained within about ±2 dB under most situations.

F5-4
1420

## Ka-BAND PROPAGATION STUDIES USING THE ACTS PROPAGATION TERMINAL AND THE CSU-SCHIL MULTIPARAMETER, DOPPLER RADAR

J, Beaver, J. Turk, and V.N. Bringi
Dept. of Electrical Engineering
Colorado State University, Fort Collins, CO 80521
(303)491-7678; FAX (303)491-2249
jb686028@long.lance.colostate.edu

In September 1993, the National Aeronautics and Space Administration's (NASA) Advanced Communications Technology Satellite (ACTS) was deployed into geostationary orbit, near 100 degrees west longitude. The ACTS satellite employs two Ka-band beacons, one at 20.185 GHz and another at 27.505 GHz, where impairments due to rain attenuation and tropospheric scintillations will significantly affect new technologies for this spectrum. Heavy rain at Ka-band can easily produce 35 dB of attenuation along the propagation path. Propagation experiments, being con-ducted in seven different climatic zones, involve multi-year attenuation measurements along the satellite-Earth slant path. Measurements in the B2 climatic zone are made with Colorado State's ACTS propagation terminal (APT) located in northeast Colorado. The APT is designed to collect both beacon signals and radiometric sky noise brightness temperatures. For path attenuations under approximately 10 dB, the brightness temperatures can be related to the attenuation, and this is used to set the "clear sky" attenuation reference level. The main goal of the ACTS propagation experiments is to obtain monthly and annual attenuation statistics at 20 and 27 GHz.

In order to gain more understanding about the physical processes that are responsible for Ka-band attenuation, the CSU-CHILL polarimetric radar is used to take radar measurements along the slant path. The Colorado Front Range experiences a variety of weather conditions throughout the year, ranging from upslope rain conditions to winter storms. To date, several "bright band" cases have been observed and a strong convective case where the 27 GHz attenuation exceeded 35 dB. The polarimetric radar data will be used to initialize a radar driven propagation model that incorporates the Mueller and extinction matrices. Concurrent data from the APT and SCU-CHILL radar will be shown for a bright band and a convective case. In addition, preliminary modelling esults will be presented.

F5-5
1500

# One Year of the ACTS Propagation Experiment in Oklahoma

Robert K. Crane and Xuhe Wang
University of Oklahoma

Abstract

The NASA Advanced Communications Technology Satellite (ACTS) Propagation Experiment in Oklahoma started over a year ago with the advent of beacon data from the satellite. Simultaneous radiometer observations of sky brightness temperature and beacon received power level measurements at 20 Ghz and 27 Ghz have been made since September 23, 1993. The reference levels for beacon attenuation measurements were obtained from a least squares fit to attenuation estimates obtained from the radiometer measurements. The radiometer system was calibrated by comparison to theoretical calculations of sky brightness temperature using profile data from nearby radiosonde soundings. The one second average total attenuation values estimated from the beacon measurements and from the radiometer measurements were used to compile cumulative attenuation distributions for each month and for a year.

Supporting meteorological data were obtained from mesonet stations operated by the Oklahoma Climatological Survey. Rain-rate measurements were obtained from a site near the beacon receiver terminal and from over 100 additional locations throughout Oklahoma. These data were used for propagation modeling and to compile rain-rate distributions for comparison with the attenuation distributions.

Attenuation distributions were compiled for all the data and for observations by propagation phenomenon. Attenuation by rain was predominant but a significant number of occurrences of attenuation by dew on the antenna surface were recorded. During the summer and fall a number of instances of measurable scintillation by clear-air turbulence were also detected. In addition, where possible, attenuation events caused by non-precipitating clouds were identified and used to tabulate an attenuation by cloud distribution.

F6-1
1540

## ACTS 20 GHZ MOBILE PROPAGATION MEASUREMENTS

Julius Goldhirsh
Applied Physics Laboratory
The Johns Hopkins University
Johns Hopkins Road, Laurel, MD 20723-6099

Wolfhard J. Vogel
Electrical Engineering Research Laboratory
The University of Texas at Austin
Austin, Texas 78758-4497

During the first six months of 1994, four mobile propagation measurement campaigns at 20 GHz using transmissions from the Advanced Communications Technology Satellite (ACTS) were executed. The 20 GHz transmissions were received at a mobile van having a tracking antenna on its roof and a receiver/data acquisition system in its interior. The field tests were undertaken in Austin, Texas (elevation angle of 55°) during winter and spring periods when the deciduous trees were bare and in full blossom, respectively. Other tests were performed in Central Maryland and in Fairbanks Alaska (elevation angles of 39° and 8°, respectively). In this paper we report on fading effects for the following mobile scenarios: roadside trees in rural regions for deciduous trees with and without leaves, highway obstacles, and buildings in urban regions.

Preliminary results as of this writing are showing that fade margins between 15-25 dB at 20 GHz should enable a 90% connectivity for a roadside tree with-leaf environment. Only 7-11 dB are required when trees are without leaves. The cumulative fade distributions show two characteristic segments separated by distinct curve inflections at an approximate 3 dB fade. Fade levels smaller than 3 dB are attributable to multipath fading, whereas larger fading is representative of attenuation due to shadowing. Large differences in the cumulative distributions were observed for the same tree runs during different seasons in which the trees were devoid of leaves and were in full blossom. For percentages of 50% and smaller, the fading levels with leaves were more than double relative to those without leaves. This result is in contradistinction to the UHF case (870 MHz) where the foliage case resulted in a 25% increase relative to the non-foliage case (J. Goldhirsh, W. J. Vogel, IEEE Trans. Ant. and Prop., 37/4, 489-498, 1989). These differences are explained in terms of the relative wavelength size and the spacing between branches and leaves.

F6-2
1600

# K-BAND MOBILE SATELLITE PROPAGATION CHARACTERISTICS USING ACTS

Michael Rice
Dept. of Electrical & Computer Engineering
Brigham Young University
Provo, UT 84602

Deborah Pinck
Jet Propulsion Laboratory
4800 Oak Grove Drive
Pasadena, CA 91109

The Advanced Communication Technologies Satellite (ACTS) provides a stationary K/Ka-band platform ideally suited to the measurement of K-band propagation characteristics in a land mobile satellite application. Field tests conducted in the Pasadena, California area during the first seven months of 1994 using the ACTS Mobile Terminal (AMT) developed by JPL provide channel characterization data. A pilot tone was transmitted from the NASA Lewis Research Center in Cleveland, Ohio to ACTS and downlinked at 20 GHz in the Southern California spot beam. The AMT was equipped with a narrow beam, high gain antenna which tracked the satellite signal in azimuth for a fixed elevation angle (A. Densmore and V. Jamnejad, IEEE Transactions on Vehicular Technology 24, 502-513, 1993) which, in this case, was 46 degrees.

The field tests were conducted in three basic environments: 1) rural freeway which was free of obstructions except for occasional over passes, 2) lightly shadowed suburban environments with occasional obstructions from buildings, utility poles, and trees, and 3) heavy shadowed suburban environments. The predominant vegetation in catagories 2 and 3 was a mixture of palm, oak, pine, Eucalyptus, and olive trees.

Frequency histograms of cumulative fade distributions display characteristics similar to those reported by Goldhirsh and Vogel for ACTS field tests conducted in Texas and Maryland (J. Goldhirsh and W. Vogel, Proceedings of Eighteenth NASAPropagation Experimenters Meeting (NAPEX XVIII), JPL Pub 94-19, 135–150, 1994.) The shape of the histogram is typical of mobile satellite channels: the slope from the reference level to 2-3 dB below is steep and consistent with a Ricean characteristic. A transistion region or "knee" (at 3-5 dB fade levels) preceeds a less steep curve for the deeper fades. This shallow curve is characteristic of heavy shadowing. A quantitative description of these results is given by the 1% fade level and outlined in the table below.

| ROUTE | 1% FADE LEVEL | NOTES |
|---|---|---|
| rural freeway | 1 dB | |
| broad suburban road | 8 dB<br>27 - 30 dB | in good lane<br>in bad lane |
| canopied suburban road | >> 30 dB | |

The preliminary results of these field tests indicate very little multipath in rural environments and when an LOS path exists (which is to be expected with a narrow beam antenna). Fades were very deep in shadowed areas, especially those with tree canopies covering the road and blocking the LOS signal. This characteristic magnifies the importance of so-called "lane-diversity."

F6-3
1620

# INTERFERENCE ON MOBILE SATELLITE LINKS DUE TO HYDROMETEOR SCATTER

R.A. Hulays and M.M.Z. Kharadly
Department of Electrical Engineering
University of British Columbia
2356 Main Mall
Vancouver, B.C., Canada V6T 1Z4

While interference caused by precipitation has received considerable attention for fixed services applications, there appears to be little done on its effect on mobile systems. In this paper, we estimate the interference level at a typical mobile terminal in the vicinity of a transmitting earth station.

The geometry considered assumes a high directivity earth station with 30 degrees elevation angle transmitting to a satellite. A mobile terminal, which receives a satellite signal at the same frequency, is in the vicinity of the earth station and has an elevation angle of 25 degrees. The mobile antenna has a gain of 28.5 dB and half-beam width of 7.2°; its sidelobes are assumed to have a gaussian shape with half-beam width 3.675 times that of the main lobe at -17 dB. A fixed Capsoni-type rain cell is assumed, with and without melting-snow layer presence.

Assuming the satellite EIRP to be 30 dBW and that of the transmitting station 80 dBW, the interference signal level, relative to that of the desired signal, is calculated for different mobile-terminal and rain-cell positions, for a range of rain rates between 0.25 and 30.0 mm/h with the melting layer present, and up to 150.0 mm/h for rain only. A frequency range between 1.0 and 40.0 GHz is examined.

The results of these computations show that the interference signal could be significantly higher than the desired signal. For example, in the near backward scattering direction, at a rain rate of 30 mm/h and a frequency of 20 GHz, the interference signal is about 4 dB higher than the desired signal at a separation distance of 80 km from the transmitting station; the two signals are about equal at 120 km and, at 160 km, the interference level falls to approximately 4 dB below the desired signal level. Generally, the interference level increases with increasing rain rate or frequency; the presence of a melting layer tends to enhance interference at lower frequencies and to decrease it at higher frequencies.

It is also found that interference coupling is mainly due to the sidelobe characteristics of the receiving antenna and, with higher receiver antenna gain (e.g., 35 dB gain and 2.8° degree half-beam width), the interference level is sharply reduced, 43 dB below the desired signal at 80 km. This result indicates a need for more accurate modeling of the receiving antenna radiation pattern.

F6-4
1640

# FADE PERFORMANCE OF SPREAD AND UNSPREAD MODULATION SYSTEMS IN MULTIPATH ENVIRONMENTS

Jeffrey D. Jenkins
Department of Electrical and Computer Engineering
New Mexico State University, Las Cruces, NM 88003

Multipath fading is a known problem in mobile communications systems. One proposed solution to minimize the effects of multipath fades is to employ spread spectrum modulation. By employing spread modulation, multipath signals whose excess path delay is greater than the chip duration of the spreading function may be separated, eliminating their contribution to fading. The underlying issue is whether or not the excess path delays are large enough to be separable in typical urban multipath environments. This paper will describe a program of research underway at New Mexico State University which will answer this question. The experiment employs a dual-beacon transmitter located on an airborn platform. One beacon transmits a CW pilot tone, while the second transmits a spread spectrum signal having an 8 MHz chip rate. The transmitter is flown in 5-mile diameter circles around the target city's downtown area, and measurements collected in a mobile receiver are processed into cumulative fade statistics. By comparing the fade statistics of the spread and unspread modulation schemes, the relative performance improvement from the spread modulation technique may be observed. While this research is not scheduled to be completed until early February, preliminary results for one city are presented in this paper.

F6-5
1700

## PHOTOGRAMMETRIC MOBILE SATELLITE SERVICE PREDICTION

Riza Akturan and Wolfhard J. Vogel
Electrical Engineering Research Laboratory
The University of Texas at Austin
Austin, Texas 78758-4497

To predict the performance of mobile and portable personal satellite communication systems in rural, suburban, and urban environments, engineers have relied on propagation measurements carried out with the help of satellites, airplanes, helicopters, or balloons. Such measurement campaigns are labor-intensive to carry out, making the data very expensive. This is the reason why data usually are obtained in only a small sample of many possible representative locations. Potential customers of satellite systems consequently are concerned whether the results can be applied to their own operating region. Even more difficult is the prediction of satellite diversity gain, involving either extrapolations from single source measurements or dual source experiments. To test a completely new prediction approach, photographic images of the sky were taken with a camera through a fisheye lens with a 180° field-of-view. The images, acquired in rural, suburban, and urban Austin, Texas and urban San Antonio, Texas, were processed on a computer to derive quantitative information about the elevation angles at which the sky becomes visible, i.e., the skyline was determined. The 90th percentile elevation angle of the skyline was found to be at about 10°, 17°, and 51° in the three environments. For elevation angles above 8°, an average of 87%, 86%, 69% and 58% of the sky was visible in the four locations, respectively. The skyline autocorrelation fell to 1/e with a 28° azimuth separation in the average and with a 54° azimuth separation at the 90th percentile with only small differentiation for environment type. Mean estimation errors are below 4°. A discussion of how the optical data will be used for satellite service prediction is included.

F6-6
1720

# INITIAL STUDY OF THE LOCAL MULTIPOINT DISTRIBUTION SYSTEM RADIO CHANNEL

Peter B. Papazian*, Mike Roadifer, and George A. Hufford

Institute for Telecommunication Sciences
National Telecommunications and Information Administration
U.S. Department of Commerce
NTIA/ITS.S3, 325 Broadway, Boulder, CO 80303, USA

Sergio Aguirre

U S WEST Advanced Technologies
4001 Discovery Drive
Boulder, CO 80303

A broadband millimeter wave propagation study was completed to characterize the radio channel for Local Multipoint Distribution Systems(LMDS). Area coverage statistics were collected in a suburban environment in Boulder, Colorado using two transmitter heights.

The study, which closely matched proposed carrier frequency and receive antenna beamwidth, provided multipath and signal loss data for single and multiple family dwellings. A 500 MB/s pseudo noise code was transmitted at 30.3 GHz. After correlation at the receiver, multipath delays could be resolved to 2 ns. The transmitter was a 26 degree beamwidth standard gain horn. It was positioned at 16 and 40 meters height in a 13 story apartment building. The receive antennas were 5.5 degree beamwidth horns aligned to receive vertically and horizontally polarizated signals. Forty five receive locations were occupied for both transmitter heights. At these locations, the mast mounted antennas were raised 1 meter above roof height for single family houses and up to a maximum of 8.5 meters for multistory townhouses and apartments. The signal level was then peaked using and azimuth/elevation controller. By utilizing a wideband system, the frequency response of ten 20 MHz channels could be measured simultaneously.

Distributions of delay spread, frequency selective fading and scatter plots of signal loss are presented. The median signal loss for the 40 m transmitter was 15 dB and for the 16 meter height was 18 dB. This consistent with previous measurements at for mm-wave propagation through 1 to 4 trees with no leaves. The maximum delay spreads were below 10 ns and the average value was less than 1 ns. Cross polarization for a flat plate reflector operating at 28.8 GHz was measured and was between 18 and 35 dB. The study concluded that vegetation losses and signal shadowing by buildings are the major impediments to the LMDS service.

Session F/G/H-1b, 1335-Thurs., CR2-6
ACTIVE REMOTE SENSING-II
Chairperson and Organizer: Susan Avery, CIRES, Campus Box 261, Univ. of Colorado at Boulder, Boulder, CO 80309

F/G/H1b-1
1340

## DEVELOPMENTS IN VHF AND HF RADAR TECHNIQUES FOR STUDIES OF WINDS AND WAVES IN THE TROPOSPHERE, STRATOSPHERE, AND MESOSPHERE

Steven J. Franke
Department of Electrical and Computer Engineering
University of Ilinois, 319 CSRL, 1308 W. Main Street,
Urbana, IL 61801-2307

The status and recent development of radar techniques for studies of winds and waves in the lower and middle atmosphere will be reviewed. Principles and limitations of single-observation-site wind and momentum flux measurements will be described, and particular attention will be paid to limitations imposed by spatially inhomogeneous wind and reflectivity fields which inevitably arise when the wind and reflectivity are modulated by wave motions. Implications for radar and lidar estimation of horizontal and vertical winds in the troposphere, stratosphere, and mesosphere will be stressed. This discussion will include a summary of the current status of efforts to understand apparent discrepancies between incoherent scatter and Medium Frequency (MF) radar measurements of mesospheric winds observed in AIDA campaign results from Arecibo.

F/G/H1b-2
1420

## SENSING THE EARTH'S THERMOSPHERE BY INCOHERENT SCATTER RADAR

Joseph E. Salah
Haystack Observatory
Massachusetts Institute of Technology
Westford, MA 018856-1299

Incoherent scatter radar observations of the earth's ionospheric plasma can be used, under suitable assumptions, to determine the structure and dynamics of the thermosphere, a region of the neutral atmosphere spanning altitudes between about 100 and 500 km. In particular, the incoherent scatter radar technique provides unique information about the complex interactions that take place in the lower thermosphere region, between about 100 and 150 km. This region has been hitherto inaccessible to satellite observations, a remote sensing techniques are best suited to study the coupling that takes place between the thermosphere and the middle atmosphere, through the propagation of waves on tidal time scales.

The methods used to determine neutral temperature and winds in the thermosphere are described, together with the underlying assumptions and limitations of the technique. Recent results from incoherent scatter radar observations at Millstone Hill are presented, showing the dominance of diurnally driven oscillations in the upper thermosphere, and semidiurnal tide oscillations in the lower thermosphere with apparent large variability. Comparisons with observations of winds in the mesosphere made by meteor wind and HF radars at midlatitudes reveal the changing character of the wind fields in the lower thermosphere.

F/G/H1b-3
1440

## RADIO SOUNDING OF THE EARTH'S MAGNETOSPHERE

W. Calvert, R. F. Benson, D. L. Carpenter, S. F. Fung, D. L. Gallagher, J. L. Green, D. M. Haines, P. H. Reiff, B. W. Reinisch, M. F. Smith, and W. W. L. Taylor
c/o W. Calvert
Department of Physics and Astronomy
University of Iowa,
Iowa City, IA 52242

Radio sounding in the Earth's magnetosphere would provide remote density measurements of unprecedented precision and coverage, yielding important new information about the structure, relationship, and variations of its different plasma regions. Using ray tracing and wave theory, we have investigated the echo properties of the magnetosphere for a satellite radio sounder located in the magnetospheric cavity outside the plasmasphere. We have constructed density models for the plasmasphere, magnetopause, and cusp based on previous satellite measurements of local density, and calculated the direction, echo power flux, and delay of the echoes which they produce at frequencies of 30 to 300 kHz. We have also analyzed focusing and defocusing by curved surfaces, investigated the echoes produced by large-scale density irregularities at the magnetopause, and examined the nature of spread echoes at the plasmapause and magnetopause.

For a sounder using three orthogonal antennas to measure echo directions, the angular precision, in radians, equals twice the reciprocal signal-to-noise ratio, and as a consequence, the volume resolution remains constant as the pulse length and bandwidth are varied to change the range resolution. Using pulse compression and spectral integration, a 10-watt sounder with 500-meter transmitting antennas would produce a signal-to-noise ratio of a hundred or more for echoes from the magnetopause, plasmapause, and plasmasphere at 30 to 300 kHz in about 3 minutes, using 5% frequency steps, a 300 Hz receiver bandwidth, and 3.3 msec sounding pulses. This then implies $1^{\circ}$ angular precision, and hence 500 km spatial resolution in all three directions at a distance of 4 Earth radii.

F/G/H1b-4
1500

# IONOSONDE SIGNATURES OF DUCTING IN THE BOTTOMSIDE F REGION

H. G. James
Communications Research Centre
P. O. Box 11490, Station "H"
Ottawa, Ontario K2H 8S2
Canada

High-frequency waves guided by cylindrical irregularities aligned with the magnetic field (**B**) in the ionosphere execute ray paths whose projections on the plane perpendicular to **B** resemble the motion of a particle in a central field. The inclusion of a **B**-aligned density gradient in a ray-tracing model gives some indication of what happens to guided waves in the ionospheric F region. An ionospheric density depletion irradiated from the bottomside of the F region by O- and X-mode waves from a high-latitude ionosonde has been analyzed assuming that the density dependence along the **B** direction is parabolic with distance. The possibility of complete traces in ionograms has been examined. A cylindrical depletion irregularity is placed throughout a matrix of points north-south and east-west of the ionosonde, and the ionogram trace computed in each case. It is found that the duct can return more or less complete traces from a considerably greater solid angle than that obtained for reflection from a horizontally stratified F layer. In comparison with the ionogram trace for horizontal stratification, the ducted traces exhibit some broadening and are at somewhat greater apparent heights.

F/G/H1b-5
1540

# THE SØNDRE STRØMFJORD METEOR RADAR: SYSTEM DESCRIPTION AND INITIAL RESULTS

T A Valentic[1], S K Avery[1,2], J P Avery[1]
[1]Department of Electrical and Computer Engineering
[2]Cooperative Institute for Research in Environmental Sciences
University of Colorado
Boulder, CO, 80309

The University of Colorado, Clemson University and SRI International have undertaken a joint project to observe upper atmosphere dynamics at Søndre Strømfjord, Greenland. During the fall of the 1993, SRI's frequency agile radar (FAR) was installed along with two separate antenna arrays. The site became operational in the May of 1994 and data was collected continuously through August of the same year. Operation is interlaced between a 28MHz meteor scatter and a 2MHz spaced antenna MF mode. This paper will concentrate on the meteor system.

The meteor data is collected with the University of Colorado's meteor echo detection and collection (MEDAC) system. The time series data associated with each meteor echo is recorded, from which the direction of arrival and doppler information are extracted. All-sky coverage is provided through an antenna array consisting of five crossed dipoles arranged as an interferometer. A self-survey calibration technique was employed to measure the system delays and antenna orientation. An initial presentation of the data will be made, showing echo collection statistics and mean wind profiles.

F/G/H1b-6
1600

## A COMPARISON OF METEOR RADAR DETECTION SYSTEMS

J P Avery[1], S K Avery[1,2], T A Valentic[1]
[1]Department of Electrical and Computer Engineering
[2]Cooperative Institute for Research in Environmental Sciences
University of Colorado
Boulder, CO, 80309
M A Cervera, R A Vincent, I M Reid
University of Adelaide
Adelaide, South Australia

Both the University of Colorado and the University of Adelaide have developed systems that allow the detection of meteor echoes on radars designed for lower atmospheric wind profiling. The doppler shift of the backscatter from the ionization trails left by the meteors gives a measure of the wind at the location of the trail, which is typically in the 80-110 km height region.

During a recent sabbatical leave, a group from the University of Colorado was able to work with the designers of the Adelaide system, and joint experiments were conducted on the two systems at the Buckland Park installation. Despite having been developed independently, the two systems share many common characteristics. The differences are significant, however, and have led to interesting improvements in the detection and processing of the meteor data. These improvements are being incorporated into both the Colorado MEDAC system and the Adelaide Buckland Park system.

We will present an overview of the two systems, the theory used in the detection and processing of echoes, and the results of a series of side-by-side trials of the two systems performed at the University of Adelaide's Buckland Park research station. Results from the meteor radars will also be compared with winds recorded by the Buckland Park MF radar, which was operating during the trials.

F/G/H1b-7
1620

# A THREE YEAR GRAVITY WAVE CLIMATOLOGY OF THE MESOSPHERE AND LOWER THERMOSPHERE OVER KAUAI

L. N. Connor[1] and S. K. Avery[1,2]
[1]Department of Electrical and Computer Engineering
[2]Cooperative Institute for Research in Environmental Sciences
University of Colorado
Boulder, CO 80309

A three year study, covering 1991, 1992, and 1993, is conducted using horizontal wind measurements collected by a partial reflection MF radar located on the island of Kauai, Hawaii. High echo return rates between 72 km and 98 km provided ample time resolution for the study of gravity wave variability in this height range. Horizontal wind measurements are band pass filtered for periods between 20 minutes and 6 hours, establishing a gravity wave band time series. Gravity wave variance calculations are carried out over various time frames and examined with regard to their response to season and background environment. Among the more interesting observed phenomenon are the semi-annual oscillation in the gravity wave variances and the extended enhancement of these variances during the latter half of the El Niño year of 1992.

F/G/H1b-8
1640

# INITIAL MODEL RESULTS RELATING THE SENSITIVITY OF THE QUASI-TWO DAY WAVE TO CHANGES IN THE EQUATORIAL ZONAL MEAN WIND FIELD

S E Palo[1], S K Avery[1,2]
[1]Department of Electrical and Computer Engineering
[2]Cooperative Institute for Research in Environmental Sciences
University of Colorado
Boulder, CO, 80309
M E Hagan[3], W J Randel[4]
[3]High Altitude Observatory, National Center for Atmospheric Research
[4]Atmospheric Chemistry Division, National Center for Atmospheric Research
Boulder, CO, 80307-3000

Observations of the equatorial mesospheric and lower thermospheric wind fields, collected at Christmas Island (1.95°N, 157.30°W), exhibit the presence of a quasi-two day wave. The observed quasi-two day wave peaks in late January with amplitudes of 40 to 60 $ms^{-1}$ in the meridional wind field and has a dominant period close to 48 hours. Theoretical results have indicated that the quasi-two day wave is a manifestation of the (3,0) Rossby normal mode in a linearized, windless, isothermal atmosphere. Additionally, recent numerical simulations have shown that both the amplitude and resonant period of the quasi-two day wave are profoundly dependent on the prevailing zonal mean wind field.

We will present the results of a numerical study conducted to determine the sensitivity of the quasi-two day wave to variations in the equatorial zonal mean wind field during January. Four zonal wind conditions are discussed. The first is a control case consisting of both geostrophic winds derived from the MSISE-90 global temperature profile and empirical models of the zonal wind field. The other zonal wind conditions consist of the control case modified by the observed tropospheric/lower stratospheric and upper mesospheric/lower thermospheric Christmas Island winds from 1989, 1991 and 1992. The results of our analysis indicate that changes in the equatorial zonal wind field will induce global changes in both the amplitude and resonant response of the quasi-two day wave.

GH2-1 ICY PLASMA PHYSICS IN THE SUMMER POLAR MESOSPHERE
1340 M.C. Kelley
School of Electrical Engineering
Cornell University
Ithaca, NY 14853

The earth's summer polar mesosphere is a fascinating region for many reasons. It is by far the coldest part of our atmosphere, sinking to less than 100 K, and has the highest clouds on the planet. The region also has a very large radar scattering cross section at VHF frequencies, some 5-7 orders of magnitude higher than other locations and seasons. This scattering has been explained as due to the presence of charged ice crystals and their subsequent effect on the plasma dynamics, particularly the diffusion coefficient. At UHF frequencies, scattering is also enhanced, but a new explanation seems necessary - one related to an enhancement of the incoherent scattering of a medium which has multiply charged dust or ice particles. The region thus provides a near-earth dusty (icy) plasma suitable for study via rockets and remote sensing. There may also be some interest in active experiments in this research area, for example, releases of dust particles from a rocket.

GH2-2
1420

## DUST PLASMA INTERACTIONS IN NEAR EARTH SPACE

D.A. Mendis
Department of Electrical and Computer Engineering
University of California, San Diego
La Jolla, CA 92093 U.S.A.

Dust grains in the near earth environment are immersed in a plasma and radiative environment. Consequently these grains are electrically charged and thereby coupled to the plasma via electric and magnetic fields, the coupling becoming stronger as the grain size decreases. Here I first consider the electric potential acquired by a dust grain with respect to the ambient plasma in various regions of the ionosphere and magnetosphere, as well as its diurnal variations. I will then proceed to discuss the physical and dynamical consequences of this charging on the dust grains. Special attention will be paid to the role of charging in polar mesospheric and noctitucent clouds.

GH2-3
1440

## WAVES IN DUSTY PLASMAS: APPLICATION TO NEAR EARTH SPACE

M. Rosenberg
Department of Electrical and Computer Engineering
University of California, San Diego
La Jolla, CA 92093 U.S.A.

Dust grains, or solid particles of micron to submicron size, are observed in space plasma environments such as planetary atmospheres and rings, asteroid zones, comets, and noctilucent clouds and polar mesospheric clouds in the Earth's ionosphere. The grains can be electrically charged by various mechanisms such as plasma current collection, secondary emission, or photoemission. The mixture of charged dust grains, electrons, ions, and neutrals typical of space plasmas is loosely referred to as a "dusty plasma". Here, the behavior of various low frequency waves in dusty magnetized plasmas are considered with attention given to parameter regimes representative of dusty regions in the mesopause. Several electrostatic instabilities, such as two-stream and drift instabilities, that may be relevant to dusty space plasmas are discussed, and applications to regions of near-Earth space are considered.

GH2-4 1500 THE IMPORTANCE OF THE HELICON MODE ON THE PHYSICS OF THE LOWER IONOSPHERE

Dr. Dennis Papadopoulos
University of Maryland
Department of Physics
College Park, MD 20742

The low altitude ionosphere in the range of 70--130 km contains an unconventional plasma. The electron-neutral collision frequency is much smaller than the electron cyclotron frequency, while the ion-neutral collision frequency exceeds to ion collision frequency. As a result the electron response is that of magnetized particles at any frequency smaller than the electron cyclotron frequency, while the ions are strongly coupled to the neutrals responding as "infinite mass" particles. In this respect this region of the ionosphere resembles a strongly magnetized n-semiconductor plasma. As discussed in the early 1960's (P. Aigrain, Proc. International Conference on Semicond. Phys., Prague, 1960, Academic, New York, 1961 p. 224; O.V. Konstantinov and V.I. Perel, Sov. Phys. JETP 11, 117, 1960) in this case the eigenmode of the plasma is the "helicon" wave. The helicon wave is similar to the whistler wave but its frequency range extends to frequencies much lower than the nominal ion cyclotron frequency, all the way to zero frequency. The helicon wave has the important property of being able to carry large amounts of field aligned currents. In this paper we will first review the key properties of the helicon wave for parameters relevant to those of the lower ionosphere, and then present a series of important applications related to the natural and disturbed environment.

Work supported by the Office of Naval Research.

GH2-5 RESEARCH ON REMEDIATION OF OZONE DEPLETION
1540

Alfred Y. Wong
Department of Physics
& HIPAS Observatory,
UCLA, Los Angles, CA 90024-1547.

Laboratory and field experiments[A.Y.Wong et al Phys. Rev Lett v72, 3124(1994); Phys. Lett.A v168, 423(1992)] including computer modeling are presented to describe how atmospheric charging might remediate the problem of ozone depletion.

In the stratosphere the catalytic destruction of ozone by chlorine can be slowed considerably by conversion to negative chlorine ion,especially in a denitrified environment. The negative chlorine ion will be collected by a positively charged electrode before charge transfer to other molecules with higher affinity but less mobility takes place.

In the troposhere CFC can be dissociated by low energy electrons and negative ions through the dissociation attachment process with a large cross section, which has been measured by laboratory experiments. This mitigation process does not require the collection of dissociated products because they are very reactive and readily form products with other atmospheric constituents. CFC will not reform.

Methods of charging a middle atmosphere source region by uv irradiation and field emission with subsequent dispersal of charges over a large volume will be presented. For those negatively charges which can make it to the upper atmosphere, a method of accelerating selective ions using ion cyclotron waves excited by ionospheric modification in the polar region will be described.

In our proposed concept to treat the vast region of atmosphere, the use of natural free energy sources - solar uv and auroral precipitation - is emphasized.

Work performed with Drs R. Wuerker and C. Hendricks of UCLA and Prof J. Grabowski of U of Pittsburg, Dr Darwin Ho of LLNL.

GH2-6
1600

## ARTIFICIAL DUSTY PLASMA EXPERIMENTS USING SPACE SHUTTLE EXHAUST

P.A. Bernhardt[1], G. Ganguli[1], M.C. Kelly[2], W.E. Swartz[2]
[1]Beam Physics Branch, Plasma Physics Division
Naval Research Laboratory Washington, DC 2037505320
[2]Cornell University School of Electrical Engineering Ithaca, NY 14853

The Shuttle Ionospheric Modification with Pulsed Localized Exhaust (SIMPLEX) experiments are designed to investigate the scatter of electromagnetic waves from artificially created dusty plasmas. The SIMPLEX experiments are an extension of the Spacelab 2 experiment over the Arecibo Ionospheric Observatory on 30 July 1985. During the Spacelab 2 experiment, the nighttime burn of the Orbital Maneuvering Subsystem (OMS) engines was observed with the 430 MHz incoherent scatter (ISR) from Arecibo. Within 1 km of the exhaust trail, the ISR backscatter was enhanced by 5 dB. One source for the enhanced radar echo could be "dressed aerosol scatter" from charged ice that forms as the exhaust vapors condense. Ground-based ISR systems at Jicamarca, Peru; Kwajalein, Marshall Islands; and Arecibo, Puerto Rico will record radar echoes from dusty plasmas created by the Space Shuttle during the SIMPLEX program. The measurements will be used to test recent theories on enhanced radar scatter over the 50 MHz to 430 MHz frequency range. Both nighttime and daytime experiments will be conducted to distinguish the effects of charge density variations. Optical techniques will be used to estimate the size of the ice particles. SIMPLEX will be supported with numerical simulations of dusty plasma creation, charge accumulation, and electromagnetic wave scattering.

GH2-7
1620

## ICE-DUST-GAS INJECTED PLASMA EXPERIMENTS

B. H. Ripin, D. N. Walker, J. Bowles,[1] W. E. Amatucci,[2]
J. Antoniades, C. Siefring, G. Ganguli, D. Duncan,[3]
and J. Stracka
Plasma Physics Division
Naval Research Laboratory
Washington, DC 20375

The D-region is the host for noctilucent clouds and it also exhibits very large radar scattering cross sections that have been ascribed to the presence of a dusty (charged ice crystal) plasma environment. Ice and gas laden plasmaregions are also formed in space by rocket and spacecraft emissions. Water/ice is also a major constituent of the plasma surrounding comet heads and in their tails. We will describe an experimental apparatus designed to inject gas or fluid aerosols into a laboratory plasma and, eventually, into space on a rocket or spacecraft for active experiments. Initial laboratory experiments will be performed in the NRL Space Physics Simulation Chamber (SPSC) in which nominal D-region parameters can be easily set up. Various gases and fluids can be injected into a microwave produced plasma, with density in the 103 to 107 electron/cc range and electron temperature from 0.5 to 2 eV, with a specially designed fast fuel-injector valve and nozzle. A background atmosphere can also be adjusted to levels found in the D-region and an adjustable magneticfield can be applied. Ice crystals are formed by spraying water through the valve/nozzle assembly into the vacuum region. The nozzle is designed to operate sub- or supersonically allowing an adjustable injection velocity. Particulates can be loaded into the fluid or gas for coinjection in order to examine condensation effects, such as might occur with meteor dust or rocket exhaust effluents. We plan to produce gas, ice, and dust laden plasma in the laboratory to study their physical and chemical properties and dynamics applicable to space situations, such as in the D-region, and to help eventually design in-situ experiments. Work funded by the Office of Naval Research.
[1]ONR Postdoc. [2]NRC Postdoc. [3]Sachs Freeman Associates, Inc.

GH2-8 LABORATORY EXPERIMENTS IN DUSTY PLASMAS

1640 Robert L. Merlino
Department of Physics and Astronomy
The University of Iowa
Iowa City, IA 52242-1479

We have recently described a rotating-drum dust-dispersal device (Xu at al, Rev. Sci. Instr. 63, 5266, 1992) which we have used to produce extended, steady-state, magnetized dusty plasma columns. The device surrounds a Q-machine plasma column over a length of 30 cm and disperses micron-sized dust grains (aluminum silicate) into the plasma. The grains acquire a negative charge corresponding to several hundred to a few thousand electrons. Using Langmuir probes it is possible to determine how the negative charge in the plasma is divided between free electrons and negatively charged dust grains.

This talk will review three experiments that we performed in this dusty plasma device:

(1) The effect of closely packed dust grains: When the intergrain spacing becomes comparable to the plasma Debye length the charge Q on a dust grain is reduced compared to the value for an isolated dust grain (Xu et al, J. Geophys. Res. 98, 7843, 1993).

(2) Electrostatic ion cyclotron (EIC) waves in a dusty plasma: A substantial amount of negative dust in the plasma makes the plasma more unstable to the EIC instability.

(3) Confinement of a Coulomb dust cloud in a double layer: An electrostatic double layer was used to trap and levitate a dust cloud in the plasma. The negatively charged dust grains organize into an almost spherical three-dimensional structure.

Work supported by ONR.
In collaboration with A. Barkan, N. D'Angelo, B. Song, and W. Xu.

J3-1 **THE ON-THE-FLY OBSERVING TECHNIQUE**

1340 D. T. Emerson & P. R. Jewell
National Radio Astronomy Observatory[1]
Campus Building 65
949 N. Cherry Ave.
Tucson, AZ 85721-0655

Mapping observations made with single-dish radio telescopes often include many thousands of independent pixels. Conventionally, maps have been built up rather painstakingly, pixel by pixel. With the current generation of sensitive radio telescope receivers, the required integration time per independent map point may only be a few seconds, but it may take several seconds for a telescope to move to and stabilize on each new pixel; the total overhead in observing time can be considerable. During a lengthy map coverage, many instrumental parameters may change. Particularly important at mm wavelengths, the prevailing atmospheric conditions may change, and the intervening atmospheric path length, strongly affecting system noise temperatures, may change dramatically as the source elevation changes. The end effect is that the quality of the map may vary appreciably between the starting and ending points.

With the On-The-Fly technique, the telescope is driven very rapidly across the source, whilst recording data at high speed. Most telescope acceleration and deceleration overhead is removed, and a full coverage of a given field may be completed quite quickly. If greater sensitivity, and hence integration time is required, the entire mapping process may be repeated many times and data averaged until the background noise level is sufficiently reduced, giving a very much more uniform quality of data. Systematic errors, caused by drifts in the telescope instrumentation or changing weather conditions, will be uncorrelated between individual coverages, and so will also average down together with the random noise. Relative pointing drifts can be corrected on individual coverages before combining the data sets. The observing is more efficient, and the final data of much higher quality.

The technique has been used at some observatories, particularly for radio continuum observations, for many years. However only recently has available computing power allowed its application conveniently to thousand-channel spectral line observations. Earlier implementations have often assumed perfect telescope tracking in position and velocity. At the NRAO 12-m telescope position information is recorded along with each data sample, and software correctly regrids the raw data. Useful data can be recorded even while the telescope is accelerating or decelerating, and otherwise excessively stringent demands on the telescope tracking servos are relaxed.

Examples are presented of data obtained in this way at the NRAO 12-m telescope at Kitt Peak, with some discussion of critical aspects of the technique, and of possible future extensions of the observing mode.

---

[1]The National Radio Astronomy Observatory (NRAO) is operated by Associated Universities, Inc., under cooperative agreement with the National Science Foundation.

J3-2
1400

## EFFECTS OF ANTENNA GEOMETRY ON PERFORMANCE

Roger D. Norrod[1] and S. Srikanth[2]
[1]National Radio Astronomy Observatory
Green Bank, WV 24944
[2]National Radio Astronomy Observatory
Charlottesville, VA 22903

This presentation will review and summarize a number of studies which have been done during the course of the Green Bank Telescope (GBT) antenna design. These studies concerned antenna performance in the context of radio astronomy observations and the effects of antenna geometry on performance. The GBT, which is presently under construction at the NRAO site in West Virginia, uses a double-offset design providing an aperture completely free of blockage. This choice leads to reduced sidelobes, higher gain, lower system temperature, and negligible standing waves as compared to a conventional on-axis telescope. However, numerous tradeoffs were made during the design process, and this presentation will discuss some of these.

In most cases, the offset geometry offers inferior polarization performance from prime focus. Use of an aperture matched feed [1] can enhance the polarization performance but only over limited bandwiths. From secondary focus the polarization characteristics of the antenna can be superior to that of an on-axis antenna with proper choice of geometry [2]. However, because of gravitational forces, the idealized geometry is realized only at certain elevations. Like most large antennas, the GBT subreflector can be translated and rotated to compensate for structural deformations, but residual alignment errors will be present at most observing elevations. Various factors led to the selection of a Gregorian secondary for the GBT, and it was realized that diffraction loss for an ellipsoidal reflector is higher than a comparable hyperboloidal reflector. As a result the Gregorian geometry can result in higher system temperatures. The multiple reflections between the feed and aperture blockage present in an on-axis antenna is absent for the offset design. However, scattering from the gaps between panels on the surface can become dominant in an offset reflector, and some results will be presented on this topic.

[1] A. W. Rudge and N. A. Adatia, "Offset-Parabolic-Reflector Antennas: A Review", Proceedings of the IEEE, vol. 66, no. 12, pp. 1592-1618, December 1978.

[2] Y. Mizugutch, M. Alagawa and H. Yokoi, "Offset Dual Reflector Antenna", in IEEE Int. Symp. AP-S, Amherst, MA, pp. 2-5, October 1976.

J3-3
1420

## OBSERVATIONAL TECHNIQUES FOR MILLIMETER POLARIMETRY

C. Read Predmore, G. C. McIntosh[1] and Richard Barvainis[2]
Five College Radio Astronomy Observatory,
Department of Physics and Astronomy
University of Massachusetts,
Amherst, Massachusetts 01003
[1] Division of Science and Mathematics
University of Minnesota Morris, Morris, MN 56267
[2] Haystack Observatory, NEROC, Westford, MA 01886

Polarization measurements at millimeter wavelengths are important for studying astrophysical phenomena which are not accessible from unpolarized observations. Included in these phenomena are the magnetic field directions and strengths measured by linear and circular polarization observations of astronomical masers such as SiO (Barvainis, R., and Predmore, C.R., *Astrophys. J.*, **288**, pp. 694-702, 1985; Barvainis, R., McIntosh, G. and Predmore, C.R., *Nature*, **Vol. 329**, pp. 613, 1987). Also included are continuum polarization observations of quasars and active galactic nuclei where the polarization varies on a rapid time scale of days.

The observational and data analysis techniques required to make sensitive polarization observations in the millimeter wavelength range are discussed along with an error analysis for the various types of observations. In particular, spectral line linear and circular polarization observations are discussed as well as continuum linear polarization observations.

The design of polarizer plates for millimeter wavelengths involves several factors such as insertion loss, matching, cost and ease of fabrication. Dielectric vane, metallic vane and bi-refringent crystal polarizer plates will be compared for use at millimeter wavelengths. Fabrication techniques will also be discussed.

Observations of linearly polarized spectral lines require special observing procedures and data analysis to eliminate systematic effects. The Stokes parameters I, Q and U are measured using a $\lambda/2$ polarizer plate. The total intensity I is measured using a standard position switched spectral line observation. Each of the Q and U Stokes parameters are measured by switching between two angles of the polarizer plate such that the position angle on the sky differs by 90°. A second set of observations is then taken to cancel the $\cos(2\theta)$ systematic effect in the receiver temperature, where $\theta$ is the polarizer plate angle.

Circular polarization observations of spectral lines are done with a $\lambda/4$ polarizer plate and a $\lambda/2$ polarizer plate. The Stokes V parameter is measured by switching the $\lambda/4$ polarizer plate at fixed position of the $\lambda/2$ polarizer plate. Then the $\lambda/2$ plate is rotated 90° and the V measurement repeated to cancel out systematic effects.

J3-4
1440

## ADAPTATION OF RADIO ASTRONOMY TECHNIQUES FOR MEASUREMENTS OF OZONE AND TRACE CONSTITUENTS IN THE STRATOSPHERE

Dr. Alan Parrish
Millitech Corp, also Univ. of Mass.
Box 109
South Deerfield, MA 01373

Radio astronomers have observed, from time to time, spectral lines of ozone and other constituents in the Earth's upper atmosphere. (The first published microwave observation of stratospheric ozone appeared in the Astrophysical Journal - Caton, et al., Ap. J., L151-L153, 1968.) While the spectroscopic physics is the same and the instrumentation is very similar to that used for observations of molecular spectral lines in the interstellar medium, the observing techniques have to be adapted to the observational geometry with some care if high quality measurements are to be made. The intensity of atmospheric spectral lines, observed in emission, varies only slowly with the zenith angle of observation, prohibiting the use of the azimuthal beam switching technique often used with celestial sources. The quality of load or frequency switched observations is apt to suffer from standing wave or other instrumental artifacts, limiting the utility of these techniques. This paper describes a beam switching technique developed to meet the needs of atmospheric observations, and describes several instruments in which this technique has been used. Some results are shown, in particular results from a long term intercomparison of microwave measurements of the stratospheric ozone distribution with measurements made by a co-located lidar and a satellite-borne UV absorption experiment (SAGE-II). This intercomparison (Tsou, et al., J. Geophys. Res., in press) showed that measurement accuracies of the order of 5% are obtainable using the technique described herein.

J3-5
1500

## OBSERVING THE COSMIC MICROWAVE BACKGROUND: DESIGN AND PERFORMANCE OF THE OWENS VALLEY 5.5M TELESCOPE

Dr. Thomas Herbig[1], Dr. C. R. Lawrence[2],
Dr. S. Gulkis[2], Prof. A. C. S. Readhead[3],
Dr. H. E. Hardebeck[3], and Dr. M. W. Hodges[3]
[1]Princeton University, Physics Department, Jadwin Hall Princeton, NJ 08544-0708
[2]Jet Propulsion Laboratory,
California Institute of Technology
[3]Owens Valley Radio Observatory
California Institute of Technology

The 5.5m radio telescope at the Owens Valley Radio Observatory is designed for observations of the cosmic microwave background radiation (CMB). Such observations require statistical errors of 10 microkelvin or less, and must be free from systematic effects at a similar level. This implies that the telescope must achieve very high sensitivity while providing an isolation of at least 70dB from its surroundings.

The 5.5m telescope is an on-axis Cassegrain system with a dual-feed receiver operating at a frequency of 32GHz with a bandwidth of 5.7GHz. The input of the cryogenic HEMT amplifier is switched at 500Hz between two corrugated horns that produce two beams of 7.3 arcminutes width separated by 22.2 arcminutes on the sky. The receiver noise temperature of 33K permits a total system temperature of 52K at the zenith. The receiver backend is fully digital to minimize pickup and to permit thorough testing of the entire system.

As with most CMB telescopes, pickup of ground radiation is one of the telescope's most serious systematic effects. In the original configuration of the secondary reflector's support structure, the total ground pickup was 27K, and the double-switched ground pickup reached a maximum of 4.3 millikelvin at some zenith angles. A modification of this structure reduced the total pickup to 9K and the peak double-switched pickup to 140 microkelvin (C. R. Lawrence, T. Herbig, and A. C. S. Readhead, Proc. IEEE, 82, 763-767, 1994).

To control the remainder of this systematic effect, we adopted a triple switching technique, in which standard double switching is performed on the field of interest, as well as on leading and trailing blank reference fields. Observations of these fields are alternated every 15 minutes and are synchronized such that the main and reference fields cover precisely the same track with respect to the ground.

J3-6
1540

# STANDING WAVES IN SPECTRA CAUSED BY SCATTERED GROUND RADIATION: THE ARECIBO MINI-GREGORIAN EXPERIENCE

Michael M. Davis (mdavis@naic.edu)
Arecibo Observatory, Post Office Box 995
Arecibo, Puerto Rico 00613-0995

Strong continuum sources frequently cause baseline undulations in sensitive radio spectra. Some of the radiation scattered from structures near the telescope focus makes an extra round trip to the reflector or other scattering object before entering the feed. The direct and scattered radiation combine in and out of phase as the path length difference, measured in wavelengths, moves through whole and half-integers. The characteristic distance between peaks (1.1 MHz at Arecibo) is c/(2D) for a round trip path length of 2D. Scattered radiation frequently sets the limit on achievable sensitivity, particularly for broad, weak features in the spectrum. The effect is well known, and can be reduced by limiting the effective scattering cross section of receiver housings, feed support legs and the like. Observations taken out of focus by + and - 1/8 wavelength can be combined to further suppress the undesired baseline variations. The Arecibo line feeds, while limited in other ways, produced nearly no standing waves as they had very poor on-axis illumination of the area directly below them.

The new Gregorian subreflector system at Arecibo will have a normal illumination pattern, so standing waves are a potential concern. Experience gained with the mini-Gregorian feed system has already proven valuable in identifying a source of standing waves not normally discussed -- scattered ground radiation. The mini-Gregorian served as a prototype of the full Gregorian dual-reflector system but illuminated an aperture of only 107 m diameter. Hence the aperture blockage of the mini by the feed platform was about 15%, and led to a system temperature increase from ground radiation scattered off the feed platform of ~16K. About 0.1% of this radiation made one extra round trip to the feed, causing standing waves with 10 to 20 mK amplitude in the spectra.

Standing waves are expected to be much reduced with the Gregorian, as the blockage will be <4% and the effective aperture more than four times greater. Nevertheless the mini-Gregorian experience predicts standing waves from scattered ground radiation with amplitudes up to 1 mJy. As a result the cable system has been redesigned to maintain the feed platform orientation fixed within ~1 mm for long periods. This will stabilize the standing wave structure, and permit accurate cancellation by using identical tracks for target and reference spectra.

J3-7
1600

## HOLOGRAPHIC MEASUREMENT AND SETTING OF THE SUBMILLIMETER TELESCOPE REFLECTOR SURFACE

R. N. Martin, J. W. M. Baars, J. G. Mangum,
G. Narayanan, and W. L. Peters
SMTO/Steward Observatory
University of Arizona
Tucson, AZ 85721

Using the LES-8 satellite beacon at 38 GHz, the reflector surface of the Submillimeter Telescope has been iteratively measured and set. We have adapted a receiver on loan from the NRAO Tucson to the prime focus location of the SMT reflector. The phase reference signal is obtained through a lens/horn combination at the rear side of the prime focus box. The two phase synchronous IF signals are fed into a digital signal processor box built specially for this experiment. To reach the target surface accuracy of 15 microns rms for this telescope surface, we must extend the measurement accuracy of LES-8 holography method to limits which exceed other, previous experiments. Results of the recent experiments will be presented along with a discussion of the residual surface errors and the measurement limitations.

J3-8 A NEW DIGITAL FILTER BANK BASED PULSAR MACHINE
1620

Roger S. Foster
Remote Sensing Division
Code 7210
Naval Research Laboratory
Washington, DC 20375

With the recent upgrade of the Arecibo telescope and the construction of the Green Bank Telescope the opportunity to conduct pulsar observations over very large bandwidths (~500 MHz) at frequencies above 1 GHz has occurred. The primary limitation to these observations is the availability of a backend processor with the necessary time and frequency resolution for both pulsar searching and timing. The Naval Research Laboratory in conjunction with the U.S. Naval Observatory is building a pulsar processor for rapid deployment based on an existing VME digital filter board built at the University of California at Berkeley and a data interface developed for the Penn State Pulsar Machine (PSPM). The Naval instrument for pulsar processing will be a dual polarization 96 channel device with a nominal frequency resolution of 2 MHz per channel adjustable downward in bandwidth by steps of sqrt(2). A single 9UVME crate will be capable of processing 192 MHz of total bandwidth in six independent 32 MHz bands. The system will be able to record data continuously at 0.8 Mbytes/s with dual high density 8mm tape drives. A ten gigabyte disk array will allow for the accumulation of data at even faster rates for up to several hours. The design is modular and capable of being upgraded either through the addition of multiple VME crates or by increasing hardware bandwidth. The initial configuration will be able to to record 4 bit data sampled at 50 us in search mode, while in timing mode, the machine will have a 5 us time resolution. The first planned use of the machine will be in a Galactic plane survey for sub-millisecond pulsars with the Nancay telescope in the late summer or fall of 1995.

J3-9
1640

# LIMITS ON THE SENSITIVITY OF A RADIO TELESCOPE IMPOSED BY A RADOME

Alan E.E. Rogers, MIT Haystack Observatory
Westford, MA 01886

While a radome protects an antenna from the weather, provides an excellent thermal environment, and eliminates wind loading, it reduces the sensitivity by aperture blockage, increased ground pick-up and membrane losses. For a large millimeter telescope the elimination of wind loading is probably an overriding advantage in favor of a radome. However radio astronomy at millimeter wavelength typically involves very large receiver bandwidths so that the effects of granularity in the ground noise scatter and multiple reflections from the radome membrane can limit sensitivity. At 3mm wavelength the 37-m antenna of the Haystack Observatory, radome ground scatter granularity is $\approx 50$ mK and radome reflection granularity $\approx 5$ mK when observing with a beam switched radiometer with 0.12° separation of the beams. The ground scatter granularity is broadband and effects continuum observations while the radome reflections produce ripple in the spectrum and limit spectral line observations. The ground scatter granularity can be reduced by retracing the same region of the radome in a comparison scan. Radome reflection ripples also vary with pointing and are reduced by averaging. Another problem introduced by the radome is granularity in the pick-up from the sun. For the Haystack antenna most of the radome ground noise granularity, solar pick-up granularity, and radome reflection ripple comes from sidelobes of the feed which spill over the subreflector and illuminate the radome. New antenna and radome designs for radio astronomy need to take these effects into account in order to optimize performance.

*Friday Morning, 6 January, 0835-1200*

Session B-2, 0855-Fri., CR2-28
ANTENNAS
Chairperson: Chalmers M. Butler, Dept. of Electrical and Computer Engineering, Clemson Univ., Clemson, SC 29634-0915

B2-1
0900

## A RECONFIGURABLE REFLECTOR WITH AUTONOMOUS NULLING CAPABILITY

Tony A.D. Monk and P.J.B. Clarricoats,
Dept. of Electronic Engineering, Queen Mary & Westfield College,
University of London, Mile End Road, London E1 4NS,
United Kingdom

3 wanted
1 unwanted

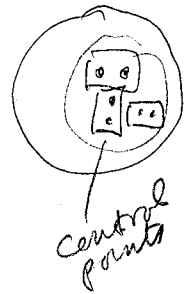


### Introduction

The reconfigurable reflector was devised at Queen Mary and Westfield College in 1988 and the means by which it can be used to generate shaped beams described (P.J.B. Clarricoats et al. Proc. IEE Part H 138 No. 6, 485-496, 1991), also an extension enabling the generation of either spot-beams or shaped-beams has been given (P.J.B. Clarricoats, A.D. Monk and Zhou Hai, USNC/URSI Symposium 1994). The ability to form pattern nulls given *a priori* knowledge was first shown in 1991 by the above authors while this paper describes the first known results whereby a reflector antenna produces nulls *autonomously* in response to unwanted signals appearing within the sidelobe region of the pattern.

### Principle of Operation

The nulling scheme used here follows a preliminary study made with a linear phased array (A.D. Monk and P.J.B. Clarricoats, Proceedings IEE ICAP, 979-982, 1993). In the formation of a null, small groups of actuators are powered which cause the surface to change locally. The movement of a mesh control point (associated with a given actuator) gives rise to a local change in aperture phase. Thus the movement of a mesh control point is closely equivalent to the perturbation of the phase of an array element.

### Antenna Operation

The QMW offset reconfigurable antenna has an aperture diameter of approximately 30 wavelengths and the gold-plated molybdenum mesh surface is controlled through 52 actuators which can be activated simultaneously. The motor drive and control circuitry, control software and electrical interface allow real time adjustment of the mesh profile via an IEEE-488 bus. A separate PC acts as controller on the same bus and associated equipment runs the adaptive algorithm. For each iteration new mesh settings are sent to the antenna in response to a digitised sample of the interference power level coupled into the antenna. The antenna has been tested using the QMW Compact Antenna Test Range which has been modified to allow for multiple feeds arrayed across the focal plane of the CATR thus simulating multiple far-field sources. The system performs as predicted rapidly forming deep nulls in the directions of interference. In the paper results will be shown for nulls formed in association with both pencil-beam and shaped-beam patterns. Minimum degradation of the wanted pattern is also demonstrated.

Early application for this antenna was for a prime-focus, offset, shaped-beam space reflector.
QMW Compact antenna Test Range operates to 600 GHz

Future work: a reconfigurable subreflector to control pattern 237 in a dual reflector. (nulling and reshaping pattern).

B2-2
0920 PREDICTION OF DIFFRACTION LOSSES IN MULTI-REFLECTOR ANTENNAS BY TRACINGTRANSITION REGIONS VIA REFLECTORS

Per-Simon Kildal,
Antenna group
Department of Microwave Technology
Chalmers University of Technology
412 96 Gothenburg
SWEDEN

The major effect of edge diffraction is to remove the discontinuities of the geometrical optics (GO) fields at the shadow boundaries. The slope of the total field at a GO boundary is determined by the width of the transition region of the edge diffraction field. The presentation will show how can be calculated from the principle wavefront curvatures associated with both the GO and edge diffracted ray fields at the GO boundary. These formulas also allow tracing of via reflectors, without tracing more diffracted rays than that coinciding with the GO boundary. (P-S. Kildal, J. Stamnes, IEEE Trans. Antennas Propagat., Vol. 38, 1350 - 1358, 1990).

Thereafter, the paper will show how can be used to predict the spillover and reduction in efficiency of a multi-reflector system (P-S. Kildal, IEEE AP Trans. 38, 1359-1365, 1990).

Finally, the paper will show the application of the theory to the design of dual-reflector antennas and of the Gregorian dual-reflector feed for the radio telescope in Arecibo. These asymptotic results are in both cases verified by numerical computations using physical optics integration.

B2-3
0940

# A DUAL REFLECTOR SHAPING METHOD BASED ON VECTOR DIFFERENTIAL CALCULUS

Lynn Baker
National Astronomy and Ionosphere Center
Cornell University
Ithaca N.Y.

This paper will present a dual reflector shaping method which gives maximal control of the aperture distribution. The technique defines a three dimensional normal vector field using ray tracing techniques. The ray trace utilizes constant path length and a mapping from the input wavefront (horn pattern) to the output wavefront (aperture plane). This mapping is initially unknown. A theorem from vector differential calculus applied to this normal field produces a first order linear partial differential equation for the unknown mapping. This PDE leaves considerable flexibility in specifying the mapping. The PDE and the normal field are simultaneously integrated to produce the reflector shapes and the complete mapping. The method is mathematically rigorous and numerically fast.

Dual reflectors permit mapping of feed coordinates into aperture coor. (e.g. amplitude control).

a surface that is everywhere $\perp$ to the vector field $\vec{N}$ satisfies $\vec{N} \cdot \nabla \times \vec{N} = 0$

B2-4
1000

## PLANAR INVERTED F ANTENNA (PIFA): CHARACTERIZATION AND PERFORMANCE VISUALIZATION

Y. Rahmat-Samii, K. Virga, R. Hodges, and M. Jensen
Department of Electrical Engineering
University of California, Los Angeles
Los Angeles, CA 90024-1594

The modern age of personal and wireless communications has created great opportunity for antenna designers to seek for novel antenna solutions and designs. Antennas mounted on the hand-held unit play an important role in an overall optimum design of the communication link. Among various antenna configurations, Planar Inverted F Antennas (PIFA) have many desirable features. The PIFA is a compact low-profile antenna structure which can be readily integrated on the hand-held unit. The PIFA consists of a rectangular patch element (typically air suspended), small ground plane (body of the hand-held unit), and a shorting pin. This antenna can be designed to match very well to a standard 50 ohms coaxial line feed.

The objective of this presentation is to critically examine the performance characteristics of this antenna by using both the surface integral equation and FDTD techniques. The emphasis of this presentation will be on the unique visualization of the amplitude and phase of the surface currents on each segment of the antenna. This will provide an insight into the radiation mechanism of the PIFA. In particular, the important features of the small ground plane, the shorting pin and the patch element will be characterized.

Results will be shown for various geometrical configurations of this antenna, input impedance, bandwidth characteristics, radiation patterns and polarization properties. The performance of the PIFA will also be compared versus other commonly used antennas such as monopole antennas.

B2-5
1040

# SAMPLING IN PLANE-POLAR COORDINATES

Arthur D. Yaghjian and Margaret B. Woodworth
Electromagnetics Directorate
RL/ERCT, Hanscom AFB, MA 01731, USA

A number of points needing clarification have been brought to our attention since the publication of "Antenna Coupling and Near-Field Sampling in Plane-Polar Coordinates" (A.D. Yaghjian, *IEEE Trans. Antennas Propagation*, **40**, 304-312, 1992). They involve the co-rotation of the probe, the bandlimit on the number of angular modes representing the measured data, the bandlimit on the spatial frequency spectrum of the extended measured data, and the computation of the many zeros of integer-order Bessel functions needed to apply the rigorous sampling-reconstruction algorithm to electrically large, asymmetric antennas. We clarify these points in this paper, and apply the sampling-reconstruction algorithm to the plane-polar scanning of a circular aperture test antenna whose center is offset from the plane-polar axis of rotation, so that a large number of angular modes are necessary to represent the fields of the test antenna.

We begin by giving a simplified proof of the result that the vector response of the probe that scans the test antenna in plane-polar coordinates is unchanged by rotation about its axis if the complex receiving pattern of the probe antenna has only first-order angular dependence. Secondly, a tighter bandlimit is determined for the number of angular modes required to represent the measured plane-polar data. Thirdly, we prove that the plane-polar data, analytically continued from $0 < \rho < \infty$ to $-\infty < \rho < \infty$, has the same spatial frequency content as plane-rectangular data on a rectilinear near-field coordinate from $-\infty < \rho < \infty$. In other words, its Fourier spectrum is bandlimited to approximately $\pm k$, when the test and probe antennas lie outside each others reactive fields. Fourthly, the algorithm is described for computing accurately and rapidly the many zeros of integer-order Bessel functions needed to represent the fields of electrically large antennas. Lastly, the errors between the exact far fields and those computed from the rigorous sampling-reconstruction summations and from the nonrigorous direct summation are shown for the offset circular-aperture test antenna.

B2-6
1100

# EXACT EXPRESSIONS FOR THE VECTOR POTENTIAL AND ELECTROMAGNETIC FIELDS OF A UNIFORM CURRENT CIRCULAR LOOP ANTENNA

D. H. Werner
The Pennsylvania State University
Applied Research Laboratory
P.O. Box 30
State College, PA 16804

Exact expressions for the vector potential and corresponding electromagnetic field integrals have not been available for the uniform current circular loop antenna. In the past, various assumptions have been made in order to obtain closed form approximations to these integrals. Analytical techniques originally developed for evaluating the cylindrical wire kernel integral (D. H. Werner, IEEE Trans. Antennas Propagat., 41, 1009-1018, 1993) have been successfully applied to solving the vector potential integral associated with a uniform current circular loop antenna. The integral form of the vector potential for a circular loop with radius $a$ and an assumed uniform current distribution of $I_o$ is given by (C. A. Balanis, Antenna Theory, Harper & Row, New York, Ch. 5, 1982)

$$A_\phi = \frac{a\mu I_o}{4\pi} \int_0^{2\pi} \cos\phi' \, \frac{e^{-j\beta R}}{R} \, d\phi'$$

where

$$R = \sqrt{r^2 + a^2 - 2ar\sin\theta\cos\phi'}$$

The derivation of an exact series expansion for the uniform current circular loop vector potential will be presented in this paper. The resulting series representation will be shown to have the form

$$A_\phi = \frac{\beta a\mu I_o}{2j} \sum_{n=1}^{\infty} \frac{(\beta^2 ar\sin\theta/2)^{2n-1}}{n!\,(n-1)!} \, \frac{h_{2n-1}^{(2)}(\beta R_o)}{(\beta R_o)^{2n-1}}$$

where

$$R_o = \sqrt{r^2 + a^2}$$

and $h_{2n-1}^{(2)}$ are spherical Hankel functions of the second kind of order 2n-1. Exact expressions for the electromagnetic field components will also be derived by making use of the above expansion for the vector potential. Finally, it will be demonstrated that the familiar small-loop approximations as well as the classical far-field expression may be obtained as limiting cases of the more general exact series solution of the vector potential integral.

B2-7
1120

# DESIGN AND ANALYSIS OF STRIPLINE-FED SLOT ANTENNAS

Catherine L. Levinson and Chalmers M. Butler
ECE Department
Clemson University
Clemson, SC 29634-0915

The stripline-fed slot array is one type of low-profile antenna. If the stripline is enclosed by a rectangular waveguide below cutoff whose axis of propagation is transverse to the stripline, the unwanted pararallel plate waveguide modes in the stripline that are excited by the slot and by possible bottom feeds will be cutoff. The antenna input admittance and radiation pattern can be determined by solving for the current induced on the feed and the electric field induced in the slot for a given voltage excitation at the feed point. The Method of Moments is applied to the integral equations for the unknown currents on the stripline, feeds, and in the slot.

The Green's functions for the rectangular waveguide behind the slot can be represented as a doubly infinite sum of modes, as a doubly infinite sum of images, or as a singly infinite sum of mixed mode and image terms. The relative convergence of these series depends on the electrical dimensions of the cavity and the electrical distance between the source and observation points at which they are evaluated. Many techniques have been developed to accelerate the convergence of these series and make them more tractable in computer applications. Several of these techniques will be described and compared for accuracy and speed.

The design of an array of stripline-fed slot elements can be enhanced by integration of the interelement mutual coupling and of the microwave feed circuit definition in the solution matrix. Measurements and MoM results will be presented for a stripline-fed slot and an array of slots for a variety of feed and array configurations. Input admittance and radiation pattern results, as well as slot electric field and stripline currents, will be presented.

B2-8
1140

# OPTIMAL CURRENT DISTRIBUTION FOR A CONFORMAL ANTENNA AT HIGH FREQUENCIES

T. S. Angell[1] R. E. Kleinman[1] and B. Vainberg[2]
[1]Center for the Mathematics of Waves
University of Delaware
Newark, Delaware 19716
[2]Department of Mathematical Sciences
University of North Carolina
Charlotte, North Carolina 28223

The problem under consideration is that of finding the current distribution on a smooth surface which optimizes the power radiated in a prescribed angular sector. In previous work we have provided constructive methods for finding optimal current distributions at low and intermediate frequencies (T. S. Angell and R. E. Kleinman, J. Optimization Theory Appl., 37, 469-497, 1982). Here we find explicit asymptotic solutions at high frequencies.

Specifically we treat the two dimensional TM problem where the non-vanishing component of electric field satisfies the Helmholtz equation and its normal derivative is proportional to the surface current. The optimization problem is that of determining this current, subject to a boundedness constraint, which produces a radiation pattern which maximizes power in some preassigned angular sector.

The analysis involves a related non-stationary problem and a limiting amplitude principle to obtain an explicit characterization of the Neumann-to-Dirichlet map at high frequencies. With this we are able to explicitly characterize the optimal current in terms of the Gaussian curvature of the surface.

B/D3-1
0840

## SIMULATION OF MICROWAVE CIRCUITS BY FDTD METHOD

C.N. Kuo(1), B. Houshmand(2), and T. Itoh(1)
(1) Department of Electrical Engineering
University of California
Los Angles, CA 90024-1595
(2) Jet Propulsion Laboratory
Oak Grove Drive
Pasadena, CA 91109

This paper presents the application of the Finite-Difference Time-Domain (FDTD) method to microwave circuits such as microwave oscillators and amplifiers. Such structures include active devices which can be nonlinear such as resonant tunneling diode (RTD) and three terminal devices such as Field Effect transistors (FET), in addition to passive microwave structures such as transmission lines and matching stubs. This method provides a full vector electromagnetic analysis of wave interaction with microwave circuit. Traditionally, simulation of these structures are carried out into two steps. First, the passive structure is replaced by its equivalent circuit. The second step is to combine the device model and the equivalent passive structure for circuit simulation. This type of analysis, in effect, discards higher order electromagnetic interactions such as coupling and radiation. While this approach is adequate for low frequency applications, with increasing the operating frequencies and reduction of circuit size, electromagnetic effects should be included in the circuit simulation.

In this presentation the FDTD method is applied to microwave circuits which include three terminal devices such as FET and BJT transistors. The active device is characterized by its equivalent circuit model and treated as a lumped element. The interaction of the passive structure and active devices are accounted for by simultaneous solution of the Maxwell's equations via the FDTD method and the device equation. In order to assess the accuracy of the FDTD simulator, a number of amplifier circuits are simulated using the above FDTD method, Touchstone, and Microwave device simulator (MDS). Touchstone is microwave circuit simulator where the passive microwave components are modeled as lumped elements. MDS includes the higher order effects to some extend by using precalculated data. For above simulations, the FDTD method agrees more closely to MDS than Touchstone. Clearly, for these type of configurations and operating frequencies the electromagnetic interactions should be included in themicrowave circuit simulations.

B/D3-2
0920

# USING THE INTEGRAL FORM OF MAXWELL'S EQUATIONS TO MODIFY AND IMPROVE THE FD-TD (2,4) SCHEME

Mohammed F. Hadi
Prof. Melinda Piket-May
Department of Electrical Engineering
University of Colorado at Boulder
Boulder, CO 80309-0425

We have observed that applying finite-difference time-domain analysis to the integral forms of Maxwell's equations provides a more accurate model than with the differential forms. This is especially true when we encounter sub-cell material variations.

Based on this observation we succeeded in starting with the standard (2,4) scheme (second-order finite differences in time and fourth-order finite differences in space) which was derived using the differential Maxwell's equations, and modifying it to provide a more accurate representation of the integral Maxwell's equations. The end result being a marked improvement in the spacial dispersion behavior over the standard (2,4) scheme as shown in Fig. 1.

Fig. 1a compares the dispersion error-grid resolution relation of the modified (2,4) scheme with the standard (2,2) and (2,4) schemes. In Fig. 1, $\nu$ is the courant number which is defined as $\Delta t_{\max}/\Delta t$. For the standard (2,4) scheme, $\nu = 1$ is no longer the optimum value, an unpleasant computational drawback which is eliminated by the modified (2,4) scheme.

Fig. 1b shows the needed grid resolutions by the different schemes to provide a maximum specified dispersion error. Note that for the standard (2,4) scheme, having a resolution of $\lambda/16$ with an optimum $\nu = 5.826$ is equivalent (from a computational point of view) to a resolution of $\lambda/(16\sqrt{5.826}) \simeq \lambda/39$.

*Fig. 1a: Dispersion Error Comparison with Optimum $\nu$,* error $= \frac{2}{\pi}\int_0^{\pi/2}\left[\frac{\tilde{k}(\alpha)-k}{k}\right]^2 d\alpha$

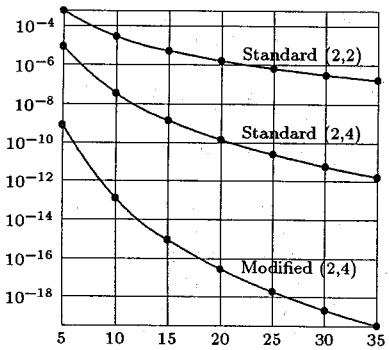


*Fig. 1b: An Error Envelope of ±4 parts per 100,000,* error $= \frac{\tilde{k}-k}{k}$
*A. Modified (2,4),* $\lambda/5$, $\nu = 1$
*B. Standard (2,4),* $\lambda/16$, $\nu = 5.826$
*C. Standard (2,2),* $\lambda/142$, $\nu = 1$

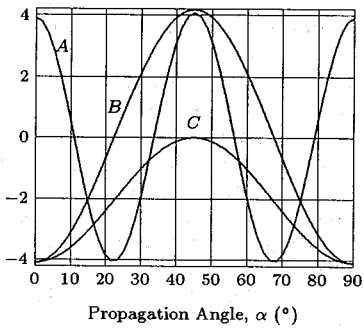

B/D3-3
1020

# NUMERICAL MODELING OF THE INTERACTIONS OF CONTINUOUS WAVE AND ULTRASHORT OPTICAL PULSES WITH RESONANT MATERIALS AND STRUCTURES

Richard W. Ziolkowski
Electromagnetics Laboratory
Department of Electrical and Computer Engineering
The University of Arizona, Tucson, AZ 85721 USA
(602) 621-6173 (Office) ziolkowski@ece.arizona.edu

We are developing full-wave, vector Maxwell equation solvers for use in studying the physics and engineering of linear and nonlinear integrated photonics systems. These simulators and their applications will be described. Particular emphasis will be given to the interaction of ultra-short optical pulses with nonresonant and resonant optical materials and structures. Results will be presented that simulate the interaction of ultrashort pulses with corrugated waveguide sections filled with either linear or nonlinear materials and the scattering from structures coated with thin films designed from materials exhibiting resonant loss or gain. Interest in these problems follows from our desire to design micron-sized linear and nonlinear guided wave couplers, modulators, and beam steerers.

These problems pose severe difficulties to numerical modeling because of the many time and length scales involved. For instance, we have developed a hybrid simulator which couples Maxwell's equations with Lorentz linear dispersion and with Raman and instantaneous nonlinear materials models to describe locally both linear and nonlinear finite length corrugated optical waveguides, with a near-to-far-field transform capability to generate the global far-field patterns associated with these structures. We are also developing simulators which combine a multi-level atom materials model with our Maxwell's equations simulator to model self-induced transparency and gain medium effects. This Maxwell-Bloch model requires a careful marriage between a microscopic (quantum mechanical) materials model of the resonant material system and the macroscopic Maxwell's equations solver. Examples from our efforts will be given to illustrate the design and control of both of these different types of large scale structures.

B/D3-4
1100

# SIMULATION AND MEASUREMENT OF HIGH SPEED DIGITAL TEST MODULES

Prof. M. Piket-May, J. Mix, and D. Barnhart
Department of Electrical Engineering
University of Colorado at Boulder
Boulder, CO 80309-0425
Roger Gravrok
Cray Research Inc.
Development Building
Chippewa Falls, WI 54729

In an effort to validate various measurement and computational methods, simple circuit board test modules were developed at Cray Research. These modules are meant to help us understand some of the fundamental physics involved in high speed digital circuit design. Measurements of the test modules were made using a time domain reflectometer (TDR). It has been shown (B.M. Oliver, "Time Domain Reflectometry," Hewlett Packard Journal, Vol. 15, No. 6, Feb. 1964: hp, Palo Alto, CA) that the area of a reflection in a TDR waveform is related to the impedance of the corresponding discontinuity. Models of the TDR measurements using lumped elements in HSPICE were constructed in an attempt to replicate the waveforms produced by the measurements, and validate the relation between the area of the reflection in the TDR waveform and the theoretical values of the impedance of each discontinuity. However, HSPICE only provides lossless transmission line models. Therefore, a second computational technique was investigated; the Finite-Difference Time-Domain technique (FD-TD) was used to analyze a model of the physical structure. A comparison between the TDR measurements and FD-TD simulations is made.

B/D3-5
1140

# RECENT PROGRESS IN FD-TD MODELING OF PASSIVE AND ACTIVE OPTICAL MICROSTRUCTURES

Rose M. Joseph, Susan C. Hagness, and Allen Taflove
Department of Electrical Engineering and Computer Science
McCormick School of Engineering
Northwestern University
Evanston, IL 60208

As increasingly complex optical structures are proposed, some with dimensions that span only a few microns, the need arises for detailed two- and three-dimensional modeling of the electromagnetic wave characteristics of these devices. We are exploring the use of the finite-difference time-domain (FD-TD) method for this purpose. Since FD-TD makes no assumptions about pulse bandwidth or preferred direction of scattering, and can account for material properties that vary on a sub-wavelength scale, it can provide optical design engineers with models having an unprecedented level of detailed field information, including pulse dynamics.

We have recently demonstrated the ability of FD-TD to model the dynamics of nonlinear active optical devices such as semiconductor lasers. This paper reports our latest work, including:

1. Characterization of reflection, transmission, and scattering loss of photonic bandgap structures and nonlinear Bragg gratings, which can propagate gap solitons.

2. Time-domain analysis of the nonlinear electromagnetic behavior of laser diodes consisting of nearly homogeneously broadened gain media.

3. Time-domain simulation of various feedback mechanisms in semiconductor lasers such as distributed Bragg reflectors and coupled cavities.

As part of the discussion, we will report fundamental advances in FD-TD modeling techniques that are central to the modeling of these phenomena and devices. These advances include a novel Lorentzian (frequency-dispersive) field amplification model and the Berenger PML absorbing boundary condition.

F7-1
0840

## DIRECT MEASUREMENT OF RF PROPAGATION IN THE LOW ELEVATION REGION OVER VARYING RANGE

S. S. Kang and J. K. Stapleton
Naval Surface Warfare Center
Dahlgren Division, Code F42
Dahlgren, VA 22446

RF propagation in the lower ten meters above the sea surface has been noted to vary with altitude, range, time and frequency. Under generally enhanced propagation conditions, deep nulls have been observed with widths less than 3 feet having varying temporal and spatial characteristics. In order to assess the actual performance of next generation sensors designed to detect low flying threats, direct RF propagation measurement in this low altitude region is required. As a part of the Multisensor Integration Test, a single frequency RF propagation measurement system operating at 13.95 GHz has been developed to probe the propagation profile dependence on range. With the receiver at a fixed height, the transmitter is mounted on a moving shuttle to simulate different antenna heights. The tower that supports the moving transmitter is placed on a boat that makes an outbound run on a fixed radial from the receiver until the signal is undetectable. Data is presented from tests conducted during June and July 1993 on the Potomac River near Naval Surface Warfare Center, Dahlgren, VA, and during March 1994 at Naval Surface Warfare Center Detachment, Wallops Island, VA. Data from the Potomac River has shown experimentally, for the first time, the presence of horizontal fade as predicted by G. D. Dockery at the Johns Hopkins University Applied Physics Laboratory as early as 1988.

F7-2 0900 DIRECT MEASUREMENT OF RF PROPAGATION IN THE LOW ELEVATION REGION FOR 2 TO 18 GHZ

J.K. Stapleton and Steve Kang
Naval Surface Warfare Center
Dahlgren Division, Code F42
Dahlgren, VA 22448

Detection of low flying sea skimming threats is dominated by the affects of the RF propagation environment. It has been observed that propagation in the lower ten meters above the sea surface can be highly variable both temporally and spatially with significant changes occurring in tens of seconds and in less than one meter vertically. The testing of next generation sensors designed to detect these sea skimming threats mandates the need for propagation ground truth measurements so that actual performance can be assessed. Likewise, the design of future sensors benefits greatly from the characterization of this low elevation propagation region. An RF propagation measurement system has been developed to directly measure RF propagation for targets at one to ten meters in altitude (using an array of 10 transmitters) and for four radar heights of interest (using four receivers), and covering 2 to 18 GHz in frequency with 16 definable frequencies in 8 seconds. An innovative frequency modulation approach allows separation of the propagation paths such that measurements are made simultaneously per carrier frequency with the carrier frequency being changed at a 2 Hz rate. Data is presented from tests conducted during January through April 1994 where the transmitter array was located on Parramore Island, Virginia and the receivers located 16 nmi north along the Virginia coast at Wallops Island Virginia. These unique measurements reveal aspects of frequency, temporal, and height structure not previously reported.

F7-3
0920

## NEAR-GRAZING PROPAGATION AND SHADOWING ABOVE LARGE-SCALE ROUGH SURFACES

Donald E. Barrick
CODAR Ocean Sensors
1000 Fremont Avenue
Los Altos, CA 94024

An exact, unified, computationally efficient, modal methodology is used to study fields and/or currents excited by a near-grazing plane wave over a periodic ocean-like surface. Results are given for both polarizations, for perfectly conducting as well as finitely conducting impedance boundaries like the ocean. Steep, long-period swell profiles of both sinusoidal and Stokes/trochoidal shapes are examined, for frequencies from HF (4 MHz) through microwave (4 GHz). This study is motivated by the failure of approximation techniques (perturbation and optics approaches) over most of this band for the difficult region near grazing.

The suggestion of a sharp 'optical-like' shadow simply does not hold; this is especially true for vertical polarization. Even for peak-trough occluded regions behind the wave as much as 36 wavelengths deep, the ratio of max/min illumination over the surface is only a factor of five in field strength for vertical polarization, increasing to fifty for horizontal. The current or field strength exhibits a spatially oscillatory behavior on the forward face of the wave for a perfectly conducting profile at high frequencies and vertical polarization. These oscillations become damped when sea-water properties are used; no oscillation at all is seen for horizontal polarization. The field strength is lower by about a factor of three for vertical polarization for a finite vs infinite sea-surface conductivity at 300 MHz; on horizontal poiarization, there is no difference.

Finally, we show how expressions for radiation and propagation near the sea surface can be modified to account for the roughness, as a change in the effective surface impedance. This construct has heretofore been applied successfully at HF, where perturbation theory is applicable. The present work shows how this can be extended to VHF and UHF, when the surface height is no longer small in terms of the radio wavelength, by using our unified modal methodology and defining the effective surface impedance in terms of the modified Fresnel specular reflection coefficient.

F7-4
0940

## THE THEORY OF WAVE PROPAGATION THROUGH INTERMITTENTLY RANDOM MEDIA

Dr. J. Gozani
Cooperative Institute for Research in
Environmental Sciences
University of Colorado at Boulder
Boulder, Colorado 80309-0449

This paper provides formulations for propagation through locally homogeneous [J. Gozani, Opt. Lett. 17, 559 (1992)], as well as strictly inhomogeneous media [J. Gozani, Proceedings of the NASA-UCLA Workshop on Laser Propagation in Atmospheric Turbulence, February, 1994. Editors: A.V. Balakrishnan and R. Butts]. The underlying assumption is that the medium is non-Gaussian, and longitudinally correlated. The formulations, which are exact, include functional path integrals and partial-differential equations for suitable conditions.

The presentation will convey the importance and potential implicit in propagation through intermittently random medium. This topic is of a great educational importance: (1) In reality, it is not always possible to eliminate inhomogeneous data, hence the necessity to include them. (2) It is a considerable generalization of the theory of propagation through homogeneously random media. (3) The analysis shows what actually needs to be measured to define the propagation; it can predict salient effects, and asymptotic propagation regimes where inhomgeneity is not crucial [J. Gozani, SPIE, Vol. 1971, 15 (1992)]. Finally, (4) The phenomena calls for new measurements techniques.

F7-5
1020

# COMPARISON OF ELECTROMAGNETIC WAVE PROPAGATION COMPUTER PROGRAMS.

Stephen A. Fast
Applied Research Laboratories University of Texas at Austin
10,000 Burnet Road
Austin, Tx 78758

Glen E. Evans
Hughes Aircraft Company
Aerospace and Defense Sector
2000 E. Imperial Hwy
El Segundo, CA 90245

Many propagation programs have been used to model radio wave propagation over terrain. Various knife edge methods, uniform theory of diffraction, and the parabolic equation approximation are applied in the propagation programs. Each program has it advantages and applicable range.

The purpose of this paper is to demonstrate the differences and similarities of each propagation program and highlight typical terrain features ignored by the programs. Graphics presented show the terrain features ignored by the models and the differences between the programs.

We have compared the following programs: the British Broadcasting Corporation program, GTD Estimated Loss due to Terrain (GELTI) developed by R. Luebbers and K. Chamberlin, the Communications Research Centre program developed by J. Whitteker, Smooth Earth Knife Edge (SEKE) developed by S. Ayasli, Terrain Integrated Rough Earth Model developed by the Electromagnetic Compatibility Analysis Center, Institute for Telecommunication Sciences' Irregular Terrain Model (ITM), Variable Terrain Radio Parabolic Equation (VTRPE) developed by F. Ryan, and Terrain Parabolic Equation Model developed by A. Barrios. The set of terrain features chosen is the result of discussion with the developers and is an attempt to define a standard set of terrain features for propagation program testing. The terrain features were chosen to stress each propagation program and highlight their differences. Each terrain profile was evaluated using a phase map to determine the significant contributions to the Helmholtz integral. By identifying the significant terrain features and comparing them to model results, we were able to determine if a model neglected to consider the effects caused by a significant terrain feature.

F7-6
1040

## EXTRACTING VEGETATION TOPOGRAPHIC AND SCATTERING CHARACTERISTICS FROM INTERFEROMETRIC SAR

Robert N. Treuhaft, Mahta Moghaddam, Eric Rignot,
Sasan S. Saatchi, and Jakob J. van Zyl
Jet Propulsion Laboratory, MS 300-235
California Institute of Technology
4800 Oak Grove Drive
Pasadena, California 91109

The effect of vegetation canopies on interferometric synthetic aperture radar (INSAR) can be viewed both as a vegetation signature to be extracted from the data and a bias in INSAR-determined altitudes. In this paper, we describe a statistical estimation approach in which both vegetation and topographic parameters are simultaneously estimated from INSAR data. Using a coherent field approach (e.g. R. H. Lang, Radio Sci. 16, 15-30, 1981), and assuming that the radar return is dominated by canopy volume scattering, we parameterize the INSAR cross-correlation in terms of the altitude of the top of the canopy, the canopy depth, the extinction coefficient (attenuation per unit length), and a multiplicative constant depending on the density and scattering amplitude of backscatterers in the vegetation. We outline the nonlinear estimation procedures necessary to extract these four parameters from the INSAR cross-correlation amplitude, phase, and the total SAR backscattered power. Because we initially envision extracting 4 parameters, and because each INSAR observation contains the above 3 independent pieces of information per incidence angle, per frequency, per pixel, we describe optimal multiple-incidence-angle and multiple-frequency configurations for parameter estimation.

As a first test of the feasibility of this estimation approach, we will demonstrate the degree to which C-band INSAR data taken over the Bonanza Creek Experimental Forest are described by the above parameterization, using ground truth data to generate the expected INSAR observations. Because the Bonanza Creek INSAR data were taken at a single incidence angle and frequency, ground truth data will be used to constrain some linear combination of the 4 parameters, while estimating orthogonal linear combinations. Another approach to be demonstrated is to use ground truth to constrain the relative values of some of the parameters for nearby pixels, and estimate the pixel-to-pixel differences in the remaining parameters. Primarily flat terrain with homogeneous vegetation will be studied first in this proof-of-concept demonstration. We will describe some additional parameters, for example ground roughness and dielectric constant, and possibly vertical attenuation profile parameters, which may be required for multiple-frequency work in which other mechanisms besides homogeneous-canopy volume scattering contribute to the INSAR data.

F7-7
1100

## A REVIEW OF ICE DEPTH MAPPING USING VLF SURFACE IMPEDANCE MEASUREMENTS IN THE ANTARCTIC

David V. Thiel, Daniel James and Peter Johnson
Radio Science Laboratory
Faculty of Science and Technology
Griffith University, Qld. Australia 4111

Many techniques used for the determination of ice thickness are based on electromagnetic techniques. Examples include surface mounted and airborne ice radar operating in the frequency range 80-200MHz, surface mounted and airborne multicoil induction methods operating in the frequency range of 1-10kHz, and surface impedance methods operating in the frequency range 10-25kHz. While radar and induction methods require the control of a local generator, the surface impedance method uses transmissions from the global network of navigation transmitters, ie it is a passive technique. A dual channel VLF receiver monitors the horizontal magnetic field component perpendicular to the plane of incidence (a measure of the signal strength) and the horizontal electric field in the plane of incidence which is directly influenced by the ground depth-conductivity profile. The instrumentation is quite small (40cm x 30cm x 20cm) and portable, and the complete system requires very little power. (Thiel, 1986, J. Glaciology 32(112) pp 376-382; Thiel & Neall, 1989, J. Glaciology 35(120) pp 197-200).

In the summers of 1987-88, 1990-91 and 1993-94, VLF surface impedance measurements were made on ice sheets in the Antarctic. The most recent survey was conducted along a major traverse from Mawson to Law Base around the Lambert Glacier, where the distance from the coast line reached 1000km, and ice depths of almost 3000 metres were encountered. During this traverse, and where possible in other areas, results have been compared directly with ice radar data. In this paper the effectiveness of the technique and the interpretation of results in terms of ice thickness will be presented. The effects of cravasses, surface conditions, subsurface moraines and the transition from fresh water ice to sea ice will be presented. The possibility of using the technique to measure the thickness of sea ice beneath a floating ice shelf will discussed.

Session G-3, 0855-Fri., CR2-26
NATURAL AND SHUTTLE-INDUCED IONOSPHERIC VARIABILITY
Chairperson: Ken Davies, NOAA/SEL, Boulder, CO 80303

G3-1 0900 A COMPARISON OF IONOSPHERIC TOTAL ELECTRON CONTENT MEASURED BY GPS AND GOES-2 AT BOULDER, COLORADO

K. Davies
NOAA/SEL, 325 Broadway, Boulder, CO 80303, USA
FAX (303) 497-3645, email kdavies@selvax,sel,bldrdoc.gov

Hourly measurements of TEC from the time delays on GPS-L1 made at the National Institute of Standards and Technology, Boulder, are compared with Faraday measurements of 136 MHz beacon onboard the GOES-2 geosynchronous satellite near 135 West. The observations were made during the early months of 1994. The night values of TEC-GPS are larger than the TEC-GOES are expected. The day-to-day variations are similar. Some reasons for these difference are discussed including the role of the plasmasphere.

G3-2
0920 DETECTION OF AURORAL ACTIVITY USING GPS SATELLITES

Clayton Coker
Applied Research Laboratories,
The University of Texas at Austin, Austin, TX 78713-8029
Robert Hunsucker
RP Consultants,1618 Scenic Loop
Fairbanks, AK 99709-6734
Gus Lott
Naval Postgraduate School
Monterey, CA 93943

An experiment is presently underway using GPS (Global Positioning System) satellites and a receiver located at Fairbanks Alaska to detect auroral activity. From this experiment, we have examined 90 passes of GPS satellites whose E-layer penetration points lie close to the reflection point of a propagation path from Wales, Alaska to Fairbanks, Alaska. When sufficiently dense auroral-E ionization (AEI) is present at the reflection point, a 25.5 MHz signal transmitted from Wales is received at Fairbanks. AEI, as indicated by the 25.5 MHz propagation, is strongly correlated with variations in the TEC (total electron content) data.

Additionally, the feasibility of using multiple satellites to locate and distinguish between different types of activity in the auroral ionosphere is investigated. We present TEC data associated with auroral substorms. During quiet periods, weak TEC variations exist poleward from Fairbanks. During auroral substorms, an intensification and equatorward motion of auroral activity is seen in the data as well as a subsequent poleward motion and lessening of auroral activity. These results are compared with magnetometer data from College, Alaska and a model of the auroral oval.

G3-3
0940

## USE OF GROUND FACILITIES COMPLEX FOR OBSERVATIONS OF HIGH-LATITUDE IONOSPHERE

Sergei M. Chernyakov, Nina V. Shulgina
Polar Geophysical Institute
15 Khalturina St., Murmansk 183010, Russia

The complex of traditional ground observations methods (a vertical sounding ionosonde and magnetometers) situated near Murmansk (polar latitudes) was supplemented with measurements of total electron content (TEC) by means of navigational satellite signals. The measurements of satellite Doppler signals were carried out at spaced points which were located in the auroral and subauroral zones. Availability of two independent Doppler measurements gives an opportunity to obtain TEC values which can be used for investigation of ionosphere structures and their dynamics in conditions of distubance. Use of ground data permitted to interpret structural variations of latitudinal profiles of vertical electron content, in particular, a phenomenon of creation and change of ionosphere troughs.

G3-4
1000

# VARIABILITY INDICES FOR THE MID-LATITUDE F-REGION

Adolf K. Paul
7455 Brockway Dr.
Boulder, Colorado 80303
AND
Richard Sprague
NCCOSC RDTE DIV, CODE 542
SAN DIEGO, CA 92152-5235

The variability index of a F-region parameter as a function of time is defined as the absolute value of its temporal derivative approximated by the divided differences of consecutive data for an individual day or the median value of this quantity obtained over a period of one month.

The median values for a variety of F-region parameters were calculated for a period of two years using the high temporal resolution data ( 5 minute interval ) produced by the San Diego Dynasonde.

During the winter months the critical frequencies and the MUF3000 show very similar behavior - low at night and higher during the day. The height variability index shows almost the opposite behavior, it is higher at night than during the day.

During the summer months there is little or no difference between day and night for the height and for the frequency variability.

G3-5
1020

## OBSERVING SHUTTLE-GENERATED IONOSPHERIC TEC FLUCTUATIONS USING VHF RADIO INTERFEROMETRY TECHNIQUES

D M Suszcynsky, W T Armstrong, R C Carlos, R. Massey, C P Munson, G. Wu, H. DeHaven, A. Rose, M. Ierkic*
Space and Atmospheric Sciences Group, MS D466, Los Alamos National Laboratory, Los Alamos, NM 87545
*Electrical and Computer Engineering Dept., University of Puerto Rico, Mayaguez, PR 00681-5000

VHF radio interferometry systems have been deployed in Western Puerto Rico and on the East Coast of the U.S. to detect acoustic and gravity wave activity generated by the space shuttle's exhaust plume during several launches over the past few years. The shuttles are usually launched at inclinations of 28° (due east) or 57° and dump approximately 1.5 tons of propellant per second into the 105 - 115 km altitude range for about a 200 second period. The impulsive insertion of this mass into the ionosphere can produce acoustic and gravity waves that collisionally couple to the ionosphere and produce perturbations to the ionospheric electron density. Two types of interferometry systems have been deployed to detect these perturbations. The first type consists of (1) a ground-based pod of three VHF transmitters operating in CW mode in a 100 kHz bandwidth centered at 149.22 MHz with transmitters located at Ramey, Mayaguez, and Arecibo, PR, (2) the use of a VHF transponder aboard the ATS-3 NASA satellite, and (3) a VHF receiver operating in the AM mode at 135.60 MHz (400 Hz bandwidth) at Los Alamos, NM to receive the downlinked signal. Propagating wavefronts are detected and characterized by measuring fluctuations in the Total Electron Content (TEC) along the transmitter-satellite paths. The second type is a similar system (R. Carlos, R. Massey, and A. Jacobson, IEEE Trans. Geosci. Remote. Sens., 32, 954, 1994) that has been primarily deployed along the east coast of the U.S. and measures TEC fluctuations in VHF signals transmitted from GOES-2, ATS-3, and ATS-1 satellite beacons to ground receivers.

Collectively, the two systems have allowed us to study both shuttle-generated and naturally occurring acoustic and gravity waves under a variety of observing conditions. These conditions are quantitatively described by a figure of merit that gauges the degree to which the neutral acoustic wave couples to the ionosphere and also the viewing efficiency or extent to which the line-of-sight parallels wavefronts. Details of such system design considerations and an overview of the systems operations and goals will be discussed. Analysis results from campaigns designed to study near and far field phenomena will be presented in the accompanying papers by Munson et al., and Carlos et al. in this session.

G3-6
1100

## SHOCK WAVES IN THE IONOSPHERE FROM SPACE SHUTTLE LAUNCHES IN THE NEAR FIELD

Ya Qi Li, R.C. Carlos, A.R. Jacobson, G. Wu, R.S. Massey, H.V. DeHaven, and T.C. Rose (Los Alamos National Lab, Los Alamos, NM, 87544; 505-667-6367; e-mail rcarlos@lanl.gov
M. Ierkec, University of Puerto Rico at Mayaguez

From 200 to 500 seconds after lift-off, the Space Shuttle main engines burn 1.5 tons of fuel per second in nearly horizontal flight at an altitude of 100-110 km. This is a large perturbation and a good altitude to launch an acoustic wave into the ionosphere.

Three stations, and a fourth for reference, were set up in West Virginia, Kentucky, and Indiana to monitor a Marecs-B CW beacon. Marecs-B is an ESA geosynchronus satellite at 15 degrees west longitude. The stations' lines-of-sight were nearly orthogonal to the shuttle's path on 57 degree inclination launches. Three launches have been observed. The lines-of-sight passed over the shuttle's path at altitudes ranging from 130 km to 240 km. The acoustic pulse can be observed to grow as it rises in altitude. There was also a second pulse, 1200 seconds after the first and of equal strength, in every observation. It has been tentatively identified as a ground reflection, pending verification by modeling.

We also have observations with other geometries of shuttle launches both closer to the path and further away, but still in the near field of the launch. Period stretching is very apparent over the range of observations.

G3-7
1120

## ANALYSIS OF SHUTTLE GENERATED IONOSPHERIC TEC PERTURBATIONS IN THE FAR FIELD

C. P. Munson, W.T. Armstrong, and D.M. Suszcynsky
Los Alamos National Laboratory, NIS-1, Mail Stop D466, Los Alamos, NM 87545

Utilizing VHF RF interferometric techniques described in the paper by Suszcynsky (Suszcynsky, et al, this meeting), measurements were performed from Puerto Rico of the long range ( > 1000 km from the source ) perturbations induced in the ionospheric Total Electron Content (TEC) by ducted acoustic waves generated during the launch of the Space Shuttle (STS-65), on July 8, 1994.

Two independent sets of data have been examined. The primary data set was collected by transmitting CW signals from three stations located in Puerto Rico, through a VHF transponder on board the ATS-3 satellite, to a receiver located in Los Alamos. Differences in the TEC on the upward portion of these paths produce phase variations between the three signals, while phase variations induced on the downward leg are common to all three signals, and are removed. The second data set was collected in Puerto Rico by receiving VHF signals at each of the three stations from transmitter beacons on board the GOES-2 and ATS-3 satellites. In addition to the paths which are common to the transponder and beacon data for the ATS-3 satellite and the ground stations, this provides a measurement set on the paths from GOES-2 to the ground stations.

Data analysis consists of sequential application of doppler corrections (to compensate for the relative motion of the satellites with respect to the ground stations), band-pass filtering (to limit the system response to the ducted acoustic wave regime), and cross- and multi-variate correlation techniques (to limit the system response to propagating waves). These techniques allow the detection of ionospheric perturbations which are propagating past the ground stations, along with determination of wave characteristics such as period, phase velocity, and propagation direction. By proper restriction of the wave periods examined (in this case 40 to 250 sec.), signals which are attributed to the STS-65 launch have been identified at a distance in excess of 1000 km. This data, along with background data on both acoustic and gravity wave activity will be presented.

G3-8
1140

## STATISTICS OF TRAVELING IONOSPHERIC DISTURBANCES OBSERVED BY THE NORTHERN NEW MEXICO SATELLITE BEACON INTERFEROMETER

R.C. Carlos, A.R. Jacobson, R.S. Massey, G. Wu (Los Alamos National Lab, Los Alamos NM, 87544; 505-667-6367; e-mail rcarlos@lanl.gov)

A phase-coherent 70-km triangular array of VHF beacon receivers has been in continuous operation, less unavoidable downtime, for two years now and has observed many thousands of TIDs. Two satellites at different longitude, GOES-2 and ATS-3, were observed, and well as ATS-1 as it drifted east from 110 to 60 degrees longitude. Two more receiver stations have been added near the center of the array in the last six months to extend the array's sensitivity to shorter wavelength TID's. We have statistics of speed, direction, and amplitude as a function of time-of-day, season, and satellite azimuth and elevation.

A quick explanation of the theory and operation of the array will be given, including the problems of phase-coherency and daily data collection over large distances.

G3-9
1200

# WHAT HAPPENED ON NOVEMBER 18, 1993 IN THE F-region

Adolf K. Paul
7455 Brockway Dr.
Boulder, Colorado 80303

On November 18, 1993 the processed data of the San Diego Dynasonde showed an extreme rapid descent of the height of maximum of the F2 layer from about 620 km to approximately 270 km over a period of two hours between 9 and 11 hours local standard time. The fastest vertical velocity exceeded 300 km/hour. This decrease of the height was accompanied by a large increase of the maximum electron density by almost a factor four. Rapid changes of the height of the F-layer maximum are quite common during the night, but are very rare during the daytime.

At the same time a significant increase followed by a large decrease of the magnetic declination at Tuscon, Fresno and Boulder was observed.

A comparison of the San Diego ionograms ( taken in 5 minute intervals) with Boulder ionograms ( taken in 15 minute intervals) shows very close simularity.

The simularity of the ionograms and of the variations of the magnetic declination indicate an effect of large horizontal dimension. The coarse temporal resolution of the Boulder ionograms and the lack of ionosondes between the two stations do not permit an estimate of a potential time delay or of a horizontal propagation velocity component in the San Diego - Boulder direction.

Session G/H-3a, 0855-Fri., CR2-6
IONOSPHERIC MODIFICATION WITH HIGH POWER RADIO WAVE-I
Chairperson: Lewis Duncan, Univ. of Tulsa, 600 S. College Avenue, Tulsa, OK 74104
Organizers: Don Dubois, Complex Systems Group, Los Alamos National Laboratory, Los Alamos, NM 87545; and Frank Djuth, Geospace Research, Inc., 550 N. Continental Blvd., Suite 110, El Segundo, CA 90245

G/H3a-1
0900

## STATUS OF THE THEORY OF HF-INDUCED IONOSPHERIC TURBULENCE

D.F. DuBois, ** Complex Systems Group, B213
Los Alamos National Laboratory, Los Alamos, NM 87545

The observations of Sulzer an Fejer (J. Geophys. Res., 13, 333, 1994) of the temporally and spatially resolved HF-induced plasma line (HFPL) spectrum in the preconditioned, nighttime, ionosphere at Arecibo are in substantial agreement, during the first tens of milliseconds following HF turn-on, with the predictions of the so-called strong Langmuir turbulence (SLT) theory. These are the only observations for which we confidently know the initial conditions of the background ionospheric plasma. In this early time regime the conventional weak turbulence approximation completely fails to describe the observations. There seems to be general agreement that density irregularities must be present for heating times greater than 30-50ms at Arecibo and in preconditioned regimes at Arecibo and Tromsoe. Modification of the election velocity distribution in these regimes must also be important. SLT theory appears to predict field-aligned density depressions that trap the decay Langmuir and ion waves and which may be the seeds for the short scale striations which are observed to be correlated with the HFPL enhancement. The ponderomotive pressure of the turbulence at the heater interference maxima may produce horizontally stratified density depletions. This talk will concentrate on the challenges associated with applying SLT theory to these more complex regimes.

* Research supported by the US DOE
** In collaboration with D. Russell and H.A. Rose

G/H3a-2
0940

## HF DRIVEN LANGMUIR TURBULENCE INCLUDING THE EXTERNAL MAGNETIC FIELD

E. Helmersen and E. Mjølhus
Institute of Mathematical and Physical Sciences
University of Tromsø, N–9037 Tromsø, Norway

It is now well established theoretically, from studies of one–dimensional models, that the character of the HF driven turbulence is of a cavitation type when $\Delta\Omega = \omega_0 - \omega_c$ is small (or slightly negative), and of a cascading type when $\Delta\Omega$ is large. Here $\omega_c$ is the cutoff frequency of the high frequency electrostatic waves and $\omega_0$ the applied frequency. Thus, for an unmagnetized plasma, $\omega_c$ is equal to the electron plasma frequency $\omega_{pe}$. For a magnetized plasma, $\Delta\Omega$ becomes direction dependent: $\Delta\Omega(\theta) = \omega_0 - \omega_c(\theta)$, $\omega_c = (\omega_{pe}^2 + \Omega_{ce}^2 \sin^2\theta)^{1/2}$, where $\Omega_{ce}$ is the electron cyclotron frequency and $\theta$ is the angle between the magnetic field and the actual wave vector. Thus, situations may occur which are in the cavitation range with respect to some range of directions and in the cascading range with respect to some other range of directions. The character of the excited turbulence will then also depend on the angle between the driving electric field and the magnetic field. We will present results from new 2D numerical simulations where we study the effect this has on the observed turbulence.

G/H3a-3
1000

## FORMATION OF ELECTRON TAILS IN 1-D VLASOV SIMULATIONS OF LANGMUIR TURBULENCE IN THE HEATED IONOSPHERE

Dr. Jin-Gen Wang, Dr. David L. Newman and Prof. Martin V. Goldman
Department of Astrophysical, Planetary, and Atmospheric Sciences
University of Colorado
Boulder, CO 80309-0391

Electron and ion Vlasov equations are numerically integrated in 1-D while driven by a constant-amplitude clamped electric-field near the plasma frequency. Plasma and pump parameters are chosen to model typical conditions at and below the critical heater reflection altitude for ionospheric-modification experiments at Arecibo. Following initial transients, steady state turbulence is attained. Close to the critical altitude the turbulence is characterized by coherent wavepackets, which nonlinearly self-focus and collapse to small spatial scales where they transfer energy to electrons thereby forming a tail on the distribution. Damping rates inferred from these tails will be used in more computationally efficient Zakharov equation simulations of Langmuir turbulence in the heated ionosphere, which can also be performed in 2 and 3 dimensions. The electron distributions produced by these simulations can be used as seed distributions that freely propagate along magnetic field lines outside the heated region to lower altitudes where they serve as a source for atomic excitations that result in observed airglow (Paul A. Bernhardt, Lewis M. Duncan and C. A. Tepley, Science 242, 1022, 1988).

G/H3a-4
1040

## RECENT EISCAT HEATING RESULTS USING CHIRPED ISR

B. Isham[1], C. La Hoz[2], T. Hagfors[3] and H. Kohl[3],
T. B. Leyser[4], M. T. Rietveld[5]
[1]Arecibo Observatory
Arecibo, PR 00613-0995, USA
[2]The Auroral Observatory
N-9037 Tromsoe, Norway
[3]Max-Planck-Institut fuer Aeronomie
D-37189 Katlenburg-Lindau, Germany
[4]Swedish Institute of Space Physics
S-981 28 Kiruna, Sweden
[5]EISCAT Scientific Association
N-9027 Ramfjordbotn, Norway

The chirp technique has recently become fully operational on the EISCAT 931-MHz radar system and has been used for daytime observations of the HF-modified ionosphere over Ramfjordmoen in November 1992, March 1993, and May 1994. During certain periods these observations show a difference in the frequencies of the photoelectron-enhanced plasma line (PEPL) and the HF-enhanced plasma line (HFPL) similar to the one seen during chirp observations of heating at Arecibo. The frequency difference seen at EISCAT, however, varied dramatically with time and sometimes vanished completely, which was not the case at Arecibo. This frequency difference indicates that the HFPL source region is located several kilometers above the height where the linear Langmuir dispersion equation indicates a resonance should occur at the HF pump frequency. Simultaneous long-pulse measurements of the HFPL spectrum show a cascade-type structure in the HFPL spectra which, according to current theories, indicates that the HFPL must follow the Langmuir dispersion relation. This may be interpreted to mean that the HF-induced plasma waves are excited within plasma density depletions whenever the frequency difference is present.

UHF observations sometimes show an additional feature in the HF-modified plasma line spectrum which appears to be the same as that observed in an experiment performed at EISCAT in August 1986 (B. Isham et al., Radio Sci., 25, 251-262, 1990). This new feature has been dubbed the "outshifted" line as it appears downshifted (upshifted) from the heating frequency in the downshifted (upshifted) plasma line spectrum. The magnitude of the shift is in the range of 100 to 300 kHz. A similar feature has been observed with the EISCAT VHF radar, although the measurement was made on a different day. In the VHF case, the feature was observed superimposed on the usual HF-induced plasma line. We attempt to explain the differences in the VHF and UHF spectra by speculating that this new feature may be due to HF-enhanced natural Langmuir oscillations.

G/H3a-5
1100

## DIAGNOSTICS OF ARTIFICIAL IONOSPHERIC DISTURBANCES ABOVE KHARKOV BY USING INCOHERENT SCATTER RADARS

Taran V.I., Goncharenko L.P.,
Bogovsky V.K., Pulyaev V.A.
Institute of the Ionosphere
Kharkov State Polytechnical University
Kharkov, Ukraine

In the Institute of Ionosphere, Ukraine, experiments aimed at causing artificial ionospheric disturbances through the use of a heating facility have been carried out for several years.

Data on the temporal variability of artificially enhanced ion and plasma lines, the dependence of the intensity and plasma line spectra upon the power and operating modes of the heating facility were obtained. Using the fully steerable antenna, measurements were made of the size and configuration of the disturbed region.

In the course of nighttime experiments, the electron temperature, as affected by the pump wave, showed a 30-50% increase. The propagation of a thermal disturbances along the magnetic field lines was recorded.

G/H3a-6
1120

# DUCTING OF WAVES FROM AN IONOSPHERIC HEATER AT HIGH LATITUDE

H. G. James
Communications Research Centre
P. O. Box 11490, Station "H"
Ottawa, Ontario K2H 8S2
Canada

High-frequency waves guided by cylindrical irregularities aligned with the magnetic field (**B**) in the ionosphere execute raypaths whose projections on the plane perpendicular to **B** resemble the motion of a particle in a central field. The inclusion of a **B**-aligned density gradient in a ray-tracing model has permitted the study of wave ducting in the ionospheric F region. An ionospheric density depletion irradiated from the bottomside of the F region with O-mode waves from a high-latitude ionospheric heater is considered, assuming that the density varies linearly with distance along **B**. The focussing and reflection of radio waves under the Wentzel-Kramers-Brillouin approximation is used to locate areas of nonlinear modification of the plasma. Because ray tracing keeps track of the wave-vector (**k**) history, it is used to predict where the EISCAT ground-based radars would detect the parametric decay instability in an irregularity whose lower end is located vertically above the EISCAT Heating facility. Regions of **k**-vector matching for both the 224 MHz and 933 MHz radars are located on conical surfaces parallel to the conical, constant-density surfaces. The separation at right angles to the constant-density surfaces of the regions of radar matching are similar to what is observed in a horizontally stratified ionosphere. The three-dimensional nature of the model leads to north-south asymmetries in the distribution of locations of radar-detectable modification.

G/H3a-7
1140

## SELF-FOCUSSING INSTABILITY IN THE PRESENCE OF IONOSPHERIC IRREGULARITIES IN HF HEATING EXPERIMENTS

M. J. Keskinen[1], H. L. Rowland[1]
S. L. Ossakow[2], and P. Bernhardt[1]
[1] Beam Physics Branch
[2] Plasma Physics Division
Naval Research Laboratory
Washington, DC 20375-5346
P. N. Guzdar and P. K. Chaturvedi
University of Maryland
College Park, MD 20742

The evolution of the self-focussing instability driven by high power radio waves in the presence of ionospheric density irregularities is studied both analytically and numerically. In contrast to previous work, the role of pre-existing finite amplitude density irregularities, which are always present in the instability region, especially at high latitudes, is investigated. We find that the effect of ambient density irregularities acts to destabilize self-focussing instability-driven small-scale perturbations which would normally be stable in a uniform ionosphere. Comparison with observations is made.

J4-1
0840

## THE NRAO VLA SKY SURVEY

W. D. Cotton, J. J. Condon,
E. W. Greisen, Q. F. Yin,
National Radio Astronomy Observatory
520 Edgemont Road, Charlottesville, VA 22903-2475
R. A. Perley,
National Radio Astronomy Observatory
Post Office Box 0, Socorro, NM 87801-0387
and J. J. Broderick
Physics Department
Virginia Tech, Blacksburg, VA 24061

The National Radio Astronomy Observatory (NRAO) is currently producing the NRAO VLA Sky Survey (NVSS) which will map the entire sky north of a declination of -40 deg at 1.4 GHz producing a set of 2326 4 degree square sky images in each of the Stokes parameters I, Q, and U. This survey, made with the Very Large Array (VLA), has 45 arcsec. FWHM resolution and a nearly uniform 5 sigma detection limit of approximately 2.5 mJy/beam which corresponds to 0.75 K. The rms position uncertainties range from <1" for S > 10 mJy to approximately 5" at S = 2.5 mJy. The sources included in this survey are mostly extragalactic, including most luminous radio galaxies and quasars in the universe, most of the galaxies found by IRAS at 60 micrometers, ultraluminous starburst galaxies and protogalaxies even at cosmological distances, as well as statistically useful numbers of nearby low-luminosity AGNs.

Identification of nearby, low luminosity AGNs should aid in their investigation at other wavelengths. Comparison of NVSS results with those of IRAS should distinguish between monsters and starburst galaxies; the NVSS should produce approximately 2 million monsters and approximately 100,000 starburst galaxies.

FITS images and source catalogs are being released via anonymous ftp (ftp 192.33.115.53, login anonymous, password = your name, cd vlass) as soon as they are made. To date about one third of the survey region has been observed. Most of these observations should be reduced and publically available in early 1995.

The NRAO is operated by Associated Universities, Inc., under cooperative agreement with the National Science Foundation.

J4-2 0900 The FIRST Survey: Faint Images of the Radio Sky at Twenty-cm

Dr. Robert H Becker
Physics Dept
University of California
Davis, CA 95616

The FIRST survey is a high sensitivity, high angular resolution survey of 10,000 square degrees centered on the north GalactiC pole and coincident with the Sloan Digital Sky Survey area. Using the B configuration of the VLA, the survey will generate a catalog of one million sources with a flux limit below a mJy and with positional accuracy of 1 arcsec(90% confidence). The data from the initial observing run of spring, 1993 are now fully analyzed and the resulting images as well as a catalog of discrete sources extracted from the images are available via world wide web( see http://sundog.stsci.edu/ for details). A comparison of the FIRST catalog with a catalog based on the Palomar Sky Survey( the APM catalog from Cambridge Univ supplied by Richard McMahon) finds optical counterparts for15% of the radio sources. Results demonstrating the accuracy and reliability of FIRST data will be presented.

J4-3
0920

# THE WESTERBORK NORTHERN SKY SURVEY (WENSS)

A.G. de Bruyn (ger@nfra.nl)
Netherlands Foundation for Research in Astronomy
Postbus 2
7990 AA Dwingeloo
THE NETHERLANDS

The Westerbork Northern Sky Survey (WENSS) is a large-sky survey being carried out at 92 and 49 cm with the Westerbork Synthesis Radio Telescope (WSRT), an east-west synthesis array. The survey uses a mozaicing technique to cover large regions of sky within a basic time unit of 12 hours, yielding both excellent uv-coverage and high efficiency. At 92 cm WENSS will cover the sky north of declination 30 deg (an area of 10,000 square degrees) to a limiting flux density (5 sigma) of 15-20 mJy. The resolution will be about 1 arcmin. At 49 cm about a third of this area will be covered to approximately the same limiting flux density. The resulting catalogue will contain about 300,000 sources at 92 cm and 60,000 sources at 49 cm.

WENSS will provide (i) radio spectra for a large number of radio sources, (ii) positional information sufficient for optical identification purposes for most of the catalogue sources, (iii) information on the linear polarization of a huge sample of discrete radio sources as well as that of the galactic diffuse emission and (iv) limited data on the low-frequency variability of sources over time-scales from hours to years.

By the end of 1994 80% of the 92cm data will be available; the remaining observations will be taken in 1995. The data reduction should be finished by the end of 1996. We expect that the first results of the survey will become available to the astronomical community sometime in 1995.

The WENSS product will consist of a catalogue of radio sources extracted from the survey and a set of FITS images (each 1024x1024 pixels covering 6x6 degrees at 92cm). We plan to make these available in both digital (DAT/CD-ROM) as well as graphical form (atlas). Images will be centered at the locations for the new Palomar Observatory Sky Survey plates. Special technical and dataprocessing aspects of the survey will be highlighted. A selection of scientific results of the survey will also be presented.

J4-4
0940

# THE PARKES-MIT-NRAO (PMN) SURVEY OF THE SOUTHERN SKY

B.F. Burke*, R.D. Ekers+, M.R. Griffith** and Alan E Wright++
*Dept. of Physics,26-335
MIT, Cambridge, MA 02139, USA
+Australia Telescope National Facility
CSIRO,Epping, NSW, Australia
**Dept. of Astronomy, U of Wash.,
FM-20, Seattle, WA 98195 USA
++Australia Telescope National Facility, CSIRO, Parkes, NSW, Australia

We present a catalog of radio sources discovered at a frequency of 4850 MH3 in the Southern Hemisphere, using the Parkes 64-m telescope and the NRAO 14 channel receiver. The survey is in 4 parts: The southern survey, (-87.5x<k<-37x), the zenith survey (-37x<k<30x), the tropical survey (-30x<k-9x) and the equatorial survey (-9x<k<+10x). The complete survey increases the number of known southern-hemisphere by a factor of 5. In comparing the tropical and southern surveys, it is clear that the fundamental flux standards in the southern sky are in error by comparison to the northern sky; below declination -30x, all fluxes based on the Kuhrs survey must be raised by 1.07. In conjunction with the GB87 survey of Condon et al, meaningful statistical studies of the whole sky can now be made. (note: \370=degree symbol \353=delta symbol)

J4-5 A MICROJANSKY RADIO SOURCE SURVEY

1000 E. B. Fomalont and K. I. Kellermann
National Radio Astronomy Observatory
Charlottesville, VA 22903

We have used the VLA in the D configuration at 8.4 GHz (3.6 cm) to survey a field centered at $13^h$ +43°. The field-of-view is set by the primary beamwidth of the individual antenna elements which is 5.2 arcmin between half power points. The synthesized beamwidth is 10 arc seconds. We observed for a total of 104 hours spread over 15 nights between October 1993 and January 1994. About 20 hours of data were excluded due to poor weather conditions. The remaining 84 hours of data were used to make an image with the NRAO AIPS reduction package. The rms noise level in the resulting map is 1.97 microjanskys, close to the value expected from consideration of the average receiver noise temperature and antenna gain.

We found 28 radio features above a 4.5 sigma completeness level of 9 microjanskeys. Comparison of the VLA radio image with an optical image from the HST Medium Deep Survey shows a remarkable coincidence between radio and optical features. All but 1 of the brightest 16 radio features in the region common to the two surveys have optical counterparts with faint galaxies, pairs or groups of galaxies, or quasars. In addition to the discrete radio features the survey shows a 20 by 40 arcsec negative feature which we cannot explain as a result of noise or other artifact, and which may be the result of absorption of the 2.7 K CBR by the Sunyaev-Zeldovich effect.

With the 10 arcsec resolution of the VLA D-configuration, our radio image is confusion limited and it is difficult to make quantitative statements about individual sources and their statistics. C-configuration observations scheduled for late 1994 will decrease the synthesized beam area by a factor of 9 and decrease the rms noise on the map to 1.4 microjansky. This will allow us to study individual sources as weak as 6 microjanskeys.

J4-6
1040

## REQUIREMENTS FOR A WIDE FIELD LOW FREQUENCY IMAGING SURVEY

Namir E. Kassim, Roger S. Foster, and Scott C. Lundgren
Remote Sensing Division
Code 7210
Naval Research Laboratory
Washington, DC 20375-5351

Standard aperture synthesis techniques of two-dimensional Fourier imaging are inadequate for generating high dynamic range, high resolution, wide-field images at long wavelengths with a non-coplanar antenna array. In response to this challenge, special 3-dimensional imaging algorithms have been developed and applied successfully to 330 MHz data from the Very Large Array (VLA). Unfortunately, the required algorithms are extremely CPU intensive, with the compute time being a strong function of maximum interferometer baseline length. As a result, wide field imaging algorithms have been applied only to baselines up to ~10 km in length (VLA B array). The lack of compute power to handle longer baseline data (e.g. VLA A array, maximum baselines ~30 km) has limited the angular resolution which can be achieved on wide-field images made at 330 MHz. We are currently porting the wide-field imaging algorithms to a powerful, symmetric multi-processing computer in order to demonstrate that high dynamic range images can be achieved at the maximum possible angular resolution permitted by the VLA geometry (~6" at 330 MHz). We explore the requirements to make wide-field images and to possibly conduct a large sky survey with the VLA at 330 MHz. Such a survey would provide the highest brightness sensitivity and angular resolution ever achieved at a frequency below 1 GHz.

J4-7 1100 THE LEIDEN/DWINGELOO SURVEY OF GALACTIC ATOMIC NEUTRAL HYDROGEN

Dap Hartmann
Leiden Observatory, P.O. Box 9513, 2300 RA Leiden, The Netherlands
(after 1-dec-94)
Center for Astrophysics, 60 Garden Street, Cambridge, MA 02138, USA

The Leiden/Dwingeloo survey of galactic neutral hydrogen was observed over a 5-year period using the world's oldest still-functioning fully-steerable radio telescope, the Dwingeloo 25-m telescope. We observed some 350,000 spectra of 1024 channels at 1420 MHz with a bandwidth of 5 MHz. The sky was sampled at delta-l and delta-b of 0.5 degrees (true-angle) with a 1 km/s velocity resolution. The entire sky north of declination -30 degrees was covered. The integration time was 3 minutes per spectrum; the sensitivity is of the order sigma <= 0.07 K.

All profiles in the survey were corrected for stray radiation which enters the receiver from directions outside of the main beam. We used holographic measurements of the Westerbork Synthesis Radio Telescope (WSRT) dishes as an estimate for the near sidelobes (theta <= 16 degrees) of the Dwingeloo dish. The far sidelobes (theta >= 16 degrees) were modelled using antenna-pattern measurements made in the late 1960's. These measurements served as a finding chart for characteristic features in the antenna pattern such as the spill-over ring, and the stray cones from the feed-support legs. Because the feed support structures was modified in the 1970's we created a model from the new geometry. Frequent observations towards the same direction in the sky provided abundant material to tune the model. A program was developed to visually inspect the behaviour of the convolution process, integrated over different velocity intervals.

The correction procedure employed was the algorithm developed by Kalberla (see Kalberla, Mebold, & Reich 1980, A&A, 82, 275) for the Effelsberg 100-m telescope. We modified the algorithm to correct the Dwingeloo data for stray radiation. The basic procedure is to convolve the antenna pattern outside the main beam with a model of the HI sky at the time of observing. We used a re-binned version of the (uncorrected) Leiden/Dwingeloo survey as the model input sky. The stray radiation was calculated separately for the near- and far-sidelobes, using a slightly different (computational) approach. The velocity range over which the corrections were computed was |v_lsr| <= 264 km/s. The computation of the stray radiation for a single observation required about one second of CPU time on a 150 MHz Alpha-APX workstation, and involved more than a million coordinate transformations.

The results show a dramatic improvement in the quality of the data, especially at high latitudes. There, the amount of stray radiation subtracted from the measured profile amounts to up to 50% of the emission.

J4-8
1120

## WIDE FIELD IMAGING OF THE MOLECULAR ISM

Dr. Mark H. Heyer
Five College Radio Astronomy Observatory
Lederle Research Building
University of Massachusetts
Amherst, MA 01003

The development of sensitive detectors and focal plane array receivers at mm wavelengths has greatly increased the ability of astronomers to spectroscopically image the molecular interstellar medium with high spatial dynamic range. Such large scale imagery provides critical information to the ongoing physical processes within the interstellar medium and to place individual features into a larger, environmental context.

Images are presented from targeted studies of individual molecular clouds, the Galactic Center and initial results of a survey of CO J=1-0 emission from the outer Galaxy obtained with the 15 element focal plane array receiver of the Five College Radio Astronomy Observatory. The reconnaissance of the molecular cloud environment reveals rings, shells, and filaments which can be attributed to the energetic activities associated with the star formation process such as stellar winds and HII regions.

General techniques for the analysis of 3 dimensional data cubes are discussed. Multivariate statistical tools such as Principle Component Analysis provide a powerful means to decompose a cloud with complicated velocity structure without prior assumptions or to simultaneously find associated structures from 1 or more data cubes.

J4-9 1140 MOSAICING OF INTERFEROMETRIC AND SINGLE DISH DATA

M.A. Holdaway
National Radio Astronomy Observatory
Socorro, NM 87801

Maximum entropy (MEM) based mosaicing tasks allow synthesis of an image from data obtained from multiple sky pointings and multiple instruments, correctly weighted by signal to noise. For extended, complicated sources, MEM produces images which are far superior to the CLEAN deconvolution. Further, since total power data (required for most mosaic observations) can be added quite painlessly and naturally, MEM is the mosaicing algorithm of choice.

Since mosaicing is more complicated than single pointing interferometry, it is important to understand the errors which can occur. Mosaicing exacts more stringent requirements for antenna pointing errors and primary beam model accuracy than single pointing interferometry does, and we discuss how these requirements guide the design of new mosaicing instruments. Bright point sources exacerbate these errors and scatter flux throughout the image unless they are removed from each pointing's data in a consistent manner prior to mosaicing. The observing strategy is very important for mosaicing: sample the image properly with pointings spaced by $\lambda/2D$, observe each sky position with several short snapshots spaced in hour angle to achieve better $(u, v)$ coverage, include a guard band of pointings around the region of interest, and observe a larger guard band with the single dish.

We also discuss these more advanced topics:

- linear and circular polarization mosaicing in the presence of beam squint.
- mosaicing and pointing self-calibration.
- high resolution mosaicing with incomplete $(u, v)$ coverage.
- imaging objects which continue beyond the image plane coverage.
- foreground estimation.
- mosaicing with continuous scanning antennas.

We present spectral line and continuum mosaic images made with the VLA as well as simulated mosaics which address some of these technical problems. Finally, we look ahead to the future and briefly discuss what science mosaicing is opening up to interferometers, the mosaicing possibilities for the VLA D Array Sky Survey data, a possible VLA E configuration which may be included in a VLA upgrade, and the proposed Millimeter Array.

J4-10
1200

## MISSING SHORT SPACINGS AT MM WAVELENGTHS

David J. Wilner
Harvard-Smithsonian Center for Astrophysics
60 Garden St.
Cambridge, MA 01238

A basic restriction of single pointing interferometry is that the largest structures accurately imaged are limited by the finite size of the array elements. For the radio interferometers currently operating at millimeter (and short centimeter) wavelengths, the largest observable structures are significantly smaller than many astronomical sources of interest, including galaxies, molecular clouds, evolved star atmospheres, and planets. We present a simple calculation to quantify the effect of the central "hole" in the (u,v) sampling for axisymmetric brightness distributions (D.J. Wilner and W.J. Welch, ApJ, 427, 898, 1994). Although interferometer observations are often said to be "sensitive" to structures on scales $\lambda/S_{min}$, where $\lambda$ is the observing wavelength and $S_{min}$ the minimum baseline length, the sensitivity to these size scales is very low. For example, the central brightness recovered for a Gaussian distribution characterized by $\theta_{fwhm}=\lambda/S_{min}$ is only about 3%.

The uncertainties introduced by missing low spatial frequency information can be the limiting factor in the interpretation of interferometer data. Several methods have been developed to obtain improved short spacing sampling: (1) use of a large single antenna, (2) observations with a multi-size array, and (3) scanning with a homogeneous array. Each of these methods, while straightforward in concept, involves a series of alternative procedures to arrive at final images. We describe practical implementations of some of these alternatives, drawing on recent molecular line observations from the BIMA array and NRAO 12 meter telescope, and from the VLA and Effelsberg 100 meter telescope.

J4-11 1220 MAGELLAN MISSION REPORT : THE FINAL CHAPTER

Thomas.W. Thompson and Magellan Flight Team
Jet Propulsion Laboratory
California Institute of Technology
Pasadena, CA 91109

The Magellan spacecraft which has been orbiting Venus since August 10, 1990 will be deliberately plunged into the Venusian atmosphere in October 1994. Magellan had the objectives of (1) improving the knowledge of the geological processes, surface properties and geologic history of Venus by analysis of surface radar characteristics, topography and morphology and (2) improving the knowledge of the geophysics of Venus by analysis of Venusian gravity.

The first objective was supported by radar imaging, altimetric and radiometric mapping of the Venusian surface from September 1990 until September 1992 (mission cycles 1,2,3). Some 98 percent of the surface has been mapped with radar resolution on the order of 120 meters. Over 1200 radar image products are available as analog photographs and digital compact disks (CD-ROMs) at the National Space Science Data Center (NSSDC), Goddard Space Flight Center. In addition, the altimetric and radiometric data products from MIT and the cartographic maps from USGS are available at the NSSDC. A contact for these Magellan data products is the PDS Geosciences Node at Washington University, St. Louis, Missouri (e-mail slavney@wunder.wustl.edu).

The second objective was supported by high resolution Doppler tracking of the spacecraft from September 1992 October 1994 (mission cycles 4,5,6). Some 950 orbits of high-resolution gravity observations were obtained between September 1992 and May 1993 while Magellan was in an elliptical orbit with a periapsis near 175 kilometers and an appoapsis near 8,000 kilometers. An additional 1500 orbits will likely be obtained since orbit-circularization in mid-1993. These data exist as a 75 degree-by 75-degree harmonic field produced by Bill Sjogren of JPL. This and other Magellan gravity products are available at NSSDC also.

Magellan has also provided information about the Venusian atmosphere. The high effective power of the Magellan downlink radio system enabled the deepest probing of the Venusian atmosphere by occultation. Also, atmospheric drag measurements, particularly during aerobraking and in this October's final plunge into the Venusian atmosphere, have expanded upon those originally obtained with the Pioneer-Venus spacecraft and have validated the Venus International Reference Atmosphere (VIRA).

Session B-3, 1355-Fri., CR2-28
FINITE METHODS
Chairperson: J.L. Volakis, Dept. of Electrical Engineering and Computer Science, Univ. of Michigan, Ann Arbor, Michigan 48109-2122

B3-1
1400

# ANALYSIS OF TE SCATTERING BY A FILLED GROOVE IN AN IMPEDANCE PLANE VIA THE FE-BI METHOD

Sunil S. Bindiganavale and John L. Volakis
Radiation Laboratory
Department of Electrical Engineering and Computer Science
The University of Michigan
Ann Arbor, Michigan 48109-2122

The finite element-boundary integral (FE-BI) method is employed to analyse the two-dimensional scattering from an arbitrarily shaped groove in an otherwise uniform impedance plane (see Fig 1). The finite element method, which is well suited for dealing with material inhomogeneity and geometry irregularity, is employed to formulate the fields within the groove and establish a relationship with the external fields at the aperture. The fields external to the slit are constructed via the boundary integral equation involving an integral expression of the fields over the aperture. A system is then derived by enforcing field continuity across the aperture. The boundary integral equation employs the impedance plane Green's function derived using the exact image theory. The proposed technique involves only a modification of the boundary integral from a previous analysis applicable to grooves in PEC ground planes (Jin & Volakis, IEEE AP, vol.38, Aug.1990) and could thus be easily extended to more complicated cavity geometries and gratings on imperfect surfaces. The resulting solution is validated by comparison with a finite element/moment method solution for cavities in coated planes and a high frequency solution.

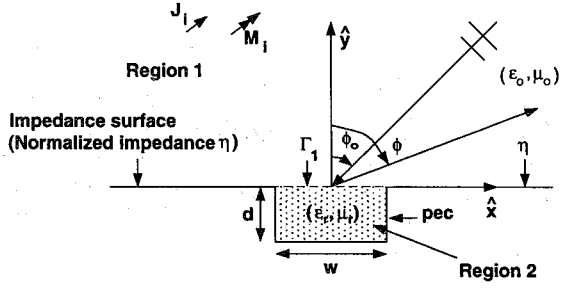


Figure 1: Geometry of the groove in an impedance plane

B3-2
1420

# STRIPLINE RESONATOR ANALYSIS USING FINITE ELEMENT CODES

Chriss A. Jones, Lorant Muth, James Baker-Jarvis, Yehuda Kantor
National Institute of Standards and Technology
Electromagnetic Fields Division
325 Broadway
M/S 813.08
Boulder, CO 80303

John DeFord, Patrick Wallen
The MacNeal Schwendler Corporation
Electromagnetics Development Branch
4300 W. Brown Deer Rd.
Suite 300
Milwaukee, WI 53223

A large stripline resonator, used to measure the electromagnetic properties of materials from 150 MHz to 2 GHz, was studied using finite element codes. These codes were used to analyze effects that could not be addressed using conformal mapping techniques. These effects are in order of interest: (1) radiation of fields from resonator when a dielectric sample is inserted, (2) field distribution inside samples of various sizes, and (3) computed characteristics of both low-loss and high-loss dielectric and magnetic samples at three frequencies. Details of the numerical modeling will also be discussed, such as higher-order modal analysis, application of finite conductivity to the model, boundary conditions and errors associated with the modeling. The computed permittivity and permeability for the dielectric and magnetic samples will be compared to measured values. All other data will be used to obtain further insight into the behavior of the fields inside this particular resonator.

B3-3
1440

# INFLUENCE OF PROXIMITY OF ABSORBING BOUNDARY CONDITIONS TO ANTENNA IN FDTD PREDICTIONS

A D Olver, M Rayner and A D Monk
Queen Mary & Westfield College
Mile End Road
London E1 4NS
United Kingdom

The Finite Difference Time Domain technique is a powerful but computational intensive method for predicting the radiation characteristics of small antennas which are close to conducting or dielectric structures. The antenna must be surrounded by absorbing boundaries to simulate the far-field radiation conditions. Ideally the absorbing boundary conditions should be positioned as near to the antenna as possible to reduce the size of the FDTD. This is particularly important for three dimensional grids. This paper studies the influence that the closeness of the boundary surfaces next to an antenna will have on its radiation characteristics.

The antenna and supporting structure are defined inside a 3D FDTD space which is constructed using standard Yee cells. The source excitations are ramped amplitude sinusoid's since results are only required at a few specific frequencies. The FDTD time marching algorithm is then applied in conjunction with the Courant stability condition to calculate the fields over the problem space. At two time steps, the near-fields are interpolated onto a spherical surface for the implementation of a Time-Domain to Frequency-Domain transformation. The derived near-fields over a spherical surface are then converted to equivalent currents in order to calculate the far-field radiation patterns using an integral transformation.

The proximity of the absorbing boundary conditions to the antenna can have a significant effect on the far-field radiation patterns. Results have been obtained to assess the influence of several types of absorbing boundary conditions (Mur 1st order, Mur 2nd order, Taflove and Brodwin formulations) upon the calculated radiation patterns of a number of small antennas. These show that care must be taken to avoid placing the near-field to far-field integration surface closer than about 0.5 wavelengths to the antenna or structure. In this region the electric and magnetic fields can vary rapidly. The surface should also not be too close to the absorbing boundaries where field deformations occur. Despite this it has been shown to be possible to position the surface as close as 0.2 wavelengths from the antenna. This leads to an overall reduction in the required grid size and hence a shorter computation time.

B3-4
1500

## APPLICATION OF FDTD TO PERIODIC STRUCTURES

B. Houshmand
Jet Propulsion Laboratory
4800 Oak Grove Drive
Pasadena CA, 91109

The finite-difference time-domain algorithm is applied to periodic structures such as slotted antennas and peridic surfaces. An important issue for this type of problems is the termination of the computation space. Here a periodic absorbing condition is used to preserve the periodic nature of the problem. As a results the computation domain can be reduced.

In this talk, the above method is applied to radiation and scattering problems. The radiation charactristics of waveguides with periodic gratings are numerically evaluated. For this type of structure, the propagating mode in the wavegide is coupled to a finite set of radiating modes or radiation directions. The effect of periodic geometery on the coupling efficiency and near field distribution is evaluated. Scattering from periodic surfaces is also examined. The FDTD computed scattering cross sections are compared with the frequecy domain methods, and numerical performace of this method with respect to surface representation and direction of incidence is evaluated.

B4-1
1500

## AN INCREMENTAL THEORY OF DIFFRACTION FORMULATION FOR ARBITRARY INCIDENT FIELDS

Roberto TIBERIO[2], Stefano MACI[1],
Alberto TOCCAFONDI[2], Filippo CAPOLINO[1]
[1] *Dept. of Electronic Engineering, Univ. of Florence, via S. Marta 3, Florence 50123*
[2] *College of Engineering, Univ. of Siena, via Roma 56, Siena 53100*

Recently, an Incremental Theory of Diffraction (ITD) has been introduced [R. Tiberio, S. Maci, IEEE Trans. on Antennas and Propagat, Vol. 42, n. 5, 1994], which provides a self-consistent, high-frequency description of a wide class of scattering phenomena within a unified framework. This method is based on an appropriate use of local canonical configurations, that have a uniform, cylindrical shape with arbitrary cross-section. The application of a generalized localization process leads to define local incremental field contributions that are adiabatically distributed either on the edge discontinuity and shadow boundary lines of the actual scatterer. Within this framework, ITD explicit formulations have been obtained for plane wave illumination of wedge shaped configurations.

In this paper, the case is examined of a point source with an arbitrary pattern, which is placed at a finite distance from the scatterer. To this end, the plane wave spectrum of the source is weighted by the incremental, plane wave response of the local configuration. The asymptotic analysis provides uniform, high-frequency expressions for the distributed contributions of the local, incremental diffraction coefficients. High-frequency field contributions are also introduced that may occur when the local incident field exhibits rapid spatial variations. Augmentations of the above leading contributions are deduced by a slope diffraction procedure. The final expression involves standard transition functions with a distance parameter which is explicitly symmetric with respect to the source and the observation points.

This representation of the field is applied to several plate configurations and their complementary aperture problems. Applications of this same technique to calculate the radiation of open-ended circular pipes are shown and discussed.

Comparisons of numerical results with those obtained from other methods have shown that this formulation may provide surprisingly accurate results even very close to and at the edge. They suggest useful applications to improve weighted aperture integration procedures.

B4-2
1540

# A COMPARISON OF TWO TECHNIQUES FOR PREDICTING FAR FIELD RADAR CROSS-SECTION (RCS) FROM NEAR FIELD MEASUREMENTS

Ivan J. LaHaie and Joseph W. Burns
Environmental Research Institute of Michigan
P.O. Box 134001
Ann Arbor, MI 48113-4001

It is well-known that the far-field scattering (and hence RCS) of a target can be rigorously extrapolated from near field measurements on planar (Dinallo, Proc. AMTA, San Diego, CA, 1984) or spherical (Wacker, IEEE Trans. AP-29, 342-351, 1981) scanning surfaces **provided full bistatic data are collected.** These bistatic collections make implementation of the rigorous near field to far field transformation (NFFFT) impractical for all but the smallest targets. ERIM has developed two approximate, **monostatic-only,** spherical NFFFT algorithms which offer the potential for practical implementation. The first, called the baseline algorithm, uses the monostatic-bistatic equivalence theorem to replace the bistatic near field measurements with equivalent monostatic, multifrequency data, and then inputs these to the rigorous NFFFT. The second approach evokes a reflectivity model commonly used in ISAR imaging to derive a new relationship between the near zone and far zone fields. The resulting algorithm, called the image-based NFFFT, also requires only monostatic near field data.

This paper will compare and contrast the two techniques, both analytically and with numerically-simulated data. We will show that despite their differences in formulation, their RCS predictions are remarkably similar.

B4-3
1600

## ON THE HIGH FREQUENCY ASYMPTOTIC EVALUATION OF THE POTENTIALS OF ELEMENTAL SOURCES ON AN ANISOTROPIC IMPEDANCE CYLINDER

Ronald J. Pogorzelski
Jet Propulsion Laboratory
California Institute of Technology
Pasadena, CA 91109

The high frequency surface fields of a uniform magnetic line source on an impedance cylinder have been studied by Paknys and Wang [IEEE Trans. AP-35, March 1987, 293-298]. The approach is similar to that in Chang, Felsen, and Hessel's treatment of the general ray direction case for axial and azimuthal magnetic sources [PINY Final Report, Sept. 1975 - Feb. 1976, AD A033544] in that for large distances the relevant integral is evaluated as a residue series and for small distances it is expressed as a power series. Paknys and Wang have shown that, for the examples discussed, twelve power series terms are required to achieve an approximation which agrees with the residue series at intermediate distances when two residue terms are retained. On the other hand, Wait [J. Res. NBS, Vol. 56, No. 4, April 1956, 237-243] and Hill and Wait [Radio Science Vol. 15, No. 3, May-June 1980, 637-643] have exploited an early suggestion of Bremmer, which he later published [IRE Trans. AP-9, July 1958, 267-272], to compute a small curvature approximation which agrees with the two term residue series at intermediate distances using only three terms.

The present work extends the work of Hill and Wait to the general case treated by Pearson [IEEE Trans. AP-35, June 1987, 698-707] accommodating both electric and magnetic sources and general ray propagation directions on the surface. It is verified that for large distances the residue series is convenient. For small distances, however, the power series representation is not very useful in that the many terms required are impractically cumbersome. In this work the small curvature approximation is generalized to non- azimuthal ray directions by means of a partial fraction expansion of a large argument approximation of the relevant integrand. This results in a practically useful approximation complementing the residue series and these two approximations thus provide representations valid throughout the entire range of distances.

B4-4
1620

# THE HALF-PLANE REVISITED

P.L.E. Uslenghi
Department of Electrical Engineering and Computer Science
University of Illinois at Chicago
851 South Morgan Street, Chicago, IL 60607-7053

A novel approach is developed to obtaining the canonical solution to the scattering of a plane wave by a perfectly conducting half-plane. The optical result, consisting of incident and reflected waves, is introduced at the onset. Next, the abrupt field transitions across the two optical boundaries are smoothed over by adding a diverging cylindrical wave to the optical solution, that emanates from the edge and has an angular dependence determined by separation of variables in the wave equation. Some simple algebraic manipulations lead to the standard exact solution in terms of Fresnel integrals.

The novelty of the above approach consists in introducing an asymptotic solution as the initial step, and then obtaining the exact solution to the scattering problem as a "refinement" of the asymptotic solution, thereby reversing the usual process. A crucial step in this new approach is the assumption, based on simple physical considerations of conservation of energy, that the fields associated with the cylindrical wave outgoing from the edge depend on a variable which is the product of the square root of the distance from the edge times a function of the angular coordinate. A discussion is given on possible extensions of this concept of "interior separability" to other boundary-value problems.

B4-5
1640

# BACKSCATTERING FROM APERIODIC RESISTIVE GRIDS USING PHYSICAL OPTICS

**Randy L. Haupt**
**Department of Electrical Engineering**
**2354 Fairchild Dr, Suite 2F6**
**USAF Academy, CO 80840-6236**

Optimizing the strip resistivities and spacings of an aperiodic grid for a desired backscattering response requires many numerical evaluations of the backscattering pattern. Using the physical optics (PO) formulation to evaluate the backscattering from the strips is much faster than using method of moments (MOM). Unfortunately, PO does not model backscattering from grids very well.

This presentation compares the PO and MOM formulations for representing the backscattering from an aperiodic grid of resistive strips. Although there is a large discrepancy between the PO and MOM formulations, the relative backscattering patterns are usually very similar. For instance, a 10 strip array with spacings of -1.3, -0.9, -0.7, -0.3, -0.1, 0.1, 0.3, 0.7, 0.9, 1.3$\lambda$ and normalized resistivities of 1.1, 0.9, 0.75, 0.25, 0.1, 0.1, 0.25, 0.75, 0.9, 1.1 has the relative MOM and PO scattering patterns shown below. Thus, PO can be used in optimization problems that optimize the relative pattern characteristics.

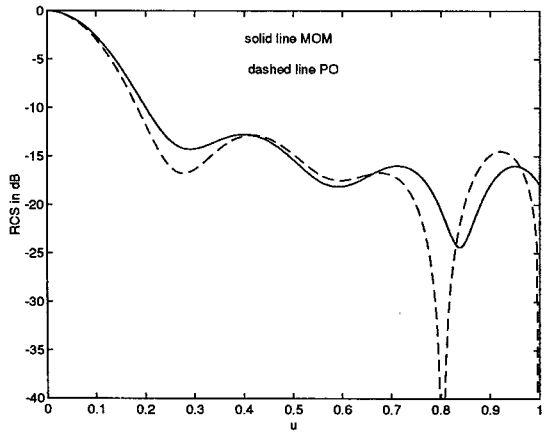


**Figure 1** PO and MOM relative backscattering patterns from an aperiodic resistive grid of 10 strips.

G2b-1
1600

# CORRECTIONS FOR IONOSPHERIC PROFILE EFFECTS IN DIRECT IONOGRAM RANGE CONVERSION

K. J. W. Lynn [1] and L. F. McNamara [2]
[1] Communications Division, Defence Science and Technology Organisation, PO Box 1500, Salisbury 5108, Australia
[2] 9038 Oakpath Lane, Dallas, Texas 75243

Converting ionograms (either oblique or vertical) to the equivalent ionograms expected over a path of different range is proving a useful technique in practical applications such as the Real Time Frequency Management (RTFM) of HF communications as well as in solving propagation problems associated with Over-The-Horizon (OTH) radar. The basic technique involved is accurate only for a curved earth with a flat ionosphere or for small path differences. The curved ionosphere results in a profile and range-dependent frequency error which becomes significant beyond some 500 km in range at F region heights. This error is traditionally corrected by the k factor. There is an associated time-delay correction factor (tentatively called the j factor) which has hitherto been ignored but is of importance in radar applications.

This paper explores the dependence of the k factor on the electron density profile with a view to improving the errors associated with simple range-dependent algorithms for k. Possible corrections for the time delay are also examined. The sensitivity of ionogram conversion to residual errors in the various components of the range conversion process is discussed, as is the effect of the earth's magnetic field. Results are illustrated with both real and simulated ionograms.

G2b-2
1620

## CORRELATIONS BETWEEN F2-LAYER PEAK PARAMETERS

R. O. Conkright [1] and L. F. McNamara [2]
[1] NOAA/NGDC 325 South Broadway, Boulder CO 80303
[2] 9038 Oakpath Lane, Dallas TX 75243

The F2-layer parameters foF2 and M(3000)F2 are normally considered to be uncorrelated. However, extensive analysis of scaled values from different sites has revealed strong positive correlations at some sites in summer months , and strong negative correlations in winter months. These correlations have implications for world-wide mapping of foF2 and M(3000)F2 as independent parameters, for real-time HF frequency management using effective indices, for HF propagation simulation using monthly median ionospheres, and for the values of upper and lower MUF deciles normally provided by HF propagation prediction programs. The correlations will be illustrated for typical locations, and their implications discussed.

Session G-4, 1335-Fri., CR2-26
TOMOGRAPHIC TECHNIQUES APPLED TO THE UPPER ATMOSPHERE
Chairperson and Organizer: Helen Na, Univ. of Iowa, Dept. of Electrical and Computer Engineering, Iowa City, Iowa, 52242

G4-1
1340

## AN ITERATIVE ALGORITHM FOR IONOSPHERIC RECONSTRUCTION USING ORTHOGONAL DECOMPOSITION

Eric Sutton and Helen Na
University of Iowa
Department of Electrical and Computer Engineering
Iowa City, Iowa 52242

A vertical cross section of the ionospheric electron density can be obtained by applying tomographic techniques to data collected by several ground stations tracking a single satellite pass. The principle difficulty associated with ionospheric tomography is that the vertical distributions of the ionospheric electron density are not well defined by the data. Most current ionospheric tomography algorithms use a priori information on the vertical distribution of electron density to improve vertical resolution. However, the optimal method for incorporating a priori information is still a topic of current research.

This paper presents a new iterative reconstruction algorithm based upon the Orthogonal Decomposition Algorithm (ODA) which incorporates a priori information through the use of model ionospheres in the selection of image domain basis functions. This algorithm constrains the image to lie in the space spanned by the basis functions, but is not weighted toward any particular solution. This allows the algorithm to utilize to the maximum extent possible the small amount of vertical information contained in the data.

In ODA, solving for the weights associated with each basis function means finding the least squares solution to a set of linear equations. The poor vertical resolution of the imaging system translates into poor numerical conditioning of the least squares problem. This new iterative algorithm avoids this problem by partitioning the ill-conditioned problem into a set of well-conditioned problems in solving for the weights associated with the basis functions. The rapid convergence of this algorithm will also be demonstrated in this paper.

G4-2
1400

# TOMOGRAPHIC METHODS FOR THE DETERMINATION OF THE "CONSTANT OF INTEGRATION"

D. L. Page and J. R. Austen
Department of Electrical Engineering
Tennessee Technological University
Box 5004
Cookeville, TN 38505

Computerized Ionospheric Tomography (CIT) is emerging as a promising research tool for studying ionospheric physics and monitoring propagation characteristics of the ionosphere. The CIT algorithms use multiple total electron content (TEC) measurements to reconstruct a two-dimensional image of the electron density in the ionosphere. A problem associated with these measurements is an unknown constant that is added to the data. This constant which is referred to as the "constant of integration" introduces artifacts into the reconstructed image. Using computerized tomography and image processing techniques, a priori information about these artifacts can be used to resolve the unknown constants. This procedure and results will be presented.

G4-3
1420

## THE EFFECT OF CONTINUITY, SMOOTHNESS AND OTHER CONSTRAINTS ON TOMOGRAPHIC RECONSTRUCTIONS OF EXPERIMENTAL DATA

T. D. Raymund
Applied Research Laboratories
University of Texas at Austin
P.O. Box 8029
Austin, TX 78713-8029

It is well known that ionospheric tomography requires additional constraints or information beyond the observations in order for a unique solution to be specified. Several recent presentations suggest that constraints like continuity and smoothness may play significant roles as additional information. These types of constraints are implemented as additional information in the tomography reconstruction and the results compared and contrasted with earlier reconstructions. The test cases are selected from data recorded during the MACE '93 campaign (when nine receivers were deployed along -98 E longitude between 26.06 N and 44.18 N latitude). The selected passes coincide with the operational window of the Russian American Tomography Experiment, particularly passes recorded during a geomagnetic storm on November 4, 1993.

G4-4
1440

## PARAMETER ESTIMATIONS OF TIDS USING MACE '93 DATA

Sigrid Close[1], Gary S. Bust[1], Jeffrey A. Cook[1]
and Ethan T. Vishniac[2]
[1]Applied Research Laboratories
The University of Texas at Austin
[2]The University of Texas at Austin,
Astronomy Department

Analysis of the total electron content (TEC) data and reconstructed tomographic images from the Mid-America CIT (computerized ionospheric tomography) Experiment (MACE '93) is presented with the intent ofcharacterizing traveling ionospheric disturbances (TIDs) and atmosphericgravity waves (AGWs). Examination of consecutive passes of filtered TEC data indicate a spectral evolution of the TID and AGW properties. Filteredtomographic images of the ionosphere are fit to an analytic model of TIDs. Parameters estimated include horizontal and vertical wave number, frequencyand perturbation amplitude of the number density. The temporal and spatialevolution of the irregularities is also examined utilizing sequentialsatellite passes.

G4-5
1500

## INVESTIGATION OF THE STRUCTURE AND DYNAMICS OF THE MID-LATITUDE TROUGH USING CIT MACE'93 DATA

Gary Bust and Steve Ward
Applied Research Laboratories
The University of Texas at Austin
(ARL:UT) P.O. Box 8029
Austin, Texas 78713-8029

MACE'93 cit reconstructions are used to investigate the structureand dynamics of the mid-latitude trough. Particular attention is payed to storm-time trough structure and diurnal evolution. Parameters calculated from the cit data include troughlocation, the steepness of the poleward and equatorial sides of thetrough, and percent depletion. The trough structure and location is correlated with Kp index and magnetic local time (MLT). Initial determination of the qualitative effects of large scale convective motions on the trough structure is deduced from the data.

G4-6
1540 IMAGING THE MID-LATITUDE IONOSPHERE WITH RADIOTOMOGRAPHY AND INCOHERENT SCATTER RADAR DURING GEOMAGNETIC STORM ONSET

J. C. Foster
MIT Haystack Observatory
Westford, MA 01886
T. D. Raymond
University of Texas
Austin, TX
V. E. Kunitsyn
Moscow State University
Moscow, Russia

Meridian-plane elevation scans with the Millstone Hill incoherent scatter radar provide evidence of a strong perturbation of the coupled magnetosphere-ionosphere system during the early phases of a geomagnetic storm on November 4, 1993. Near the equatorward edge of auroral latitudes, a narrow ionospheric trough formed at L=3.5 in the pre-midnight sector and particle precipitation produced elevated electron temperatures and enhanced ionization immediately poleward of the trough, at L=4. We have intercompared total-phase and phase-difference techniques of reconstructing tomographic images with the direct observations of ionospheric density and structure obtained by the radar during this event. An array of four receiving stations was set up in the northeastern United States and eastern Canada as a part of the Russian-American Tomography Experiment and data from both Russian and US navigation satellites were recorded. The most-pronounced ionospheric response to the event was a brief (20-min) uplifting of the F region equatorward of the trough, such that the peak altitude increased with distance away from the trough. Magnetospheric observations made during satellite overflights contribute to the interpretation of the mid-latitude ionospheric perturbation identified by the ground-based observations.

G4-7
1600

## EQUATORIAL ANOMALY OBSERVATIONS WITH A LOW-LATITUDE IONOSPHERIC TOMOGRAPHY NETWORK

A.V.Izotov, S.J.Franke, H.C.Yeh, K.C.Yeh, C.H.Liu, T.D.Raymund, H.H. Chen, J.Y.Liu, J. Wu, K.H.Lin, S.W. Chen

We report the first results obtained using the Low-latitudeIonospheric Tomography Network (LITN) along Taiwan meridian (app. 120deg East). LITN represents an array of receiving stations, specificallydesigned to receive and process signals from NNSS, which spans thelatitude range from Manila (14.5N) to Shanghai (31.5N). Firstcollections of data are analyzed, and attempts to investigate thediurnal development and dynamics of the equatorial anomaly are made. Further possible applications of LITN are outlined.

G4-8
1620

## GLOBAL RADIOWAVE TOMOGRAPHY OF THE IONOSPHERE AND PLASMASPHERE

Y. T. Chiu, D. R. Schropp, Jr., M. A. Rinaldi
Lockheed Palo Alto Research Laboratory, O/91-20 B/255
3251 Hanover St.
Palo Alto, CA 94304

Resolution of space science issues addressing global and magnetospheric scales require data sampling on space-time scales commensurate with magnetosphere phenomena. This requires remote sensing of the ionospheric and magnetospheric plasma environments. A well-developed method is to detect ion and neutral atom emissions stimulated by ionospheric and solar processes, which are subject to or require simultaneous detection of the variations in the stimulating agent. A complementary technique, free of such calibration difficulties, is to focus on deconvolving collective effects of refraction by the plasma upon the phase and group properties of radio waves propagating through the plasma medium. Such a remote sensing technique requires active precision radiowave sources distributed on a scale commensurate with the ionosphere and magnetosphere. Such a source exists -- it is called the Global Positioning System. This paper discusses the implications of using the GPS radio signals as ionospheric and plasmaspheric remote sensing media on a space-based system. Further, we shall show how such a radio wave data base can be interpreted in terms of global three-dimensional tomography of the ionsophere and plasmasphere. An end-to-end simulation of this space-based remote-sensing scheme and tomographic retrieval will be demonstrated.

G4-9 1640 COMPARISON OF SPACE AND GROUND BASED IONOSPHERIC TOMOGRAPHY

G.A. Hajj, L.J. Romans, E.R. Kursinski
Jet Propulsion Lab
California Institute of Technology
4800 Oak Grove Drive
Pasadena, CA. 91109

In the past several years, ionospheric tomography has been investigated through simulation and field experiments by numerous investigators. Nearly all of these studies however concentrated on ionospheric tomography obtained from a set of ground receivers tracking one or several satellites in low earth orbit (LEO). With this type of ground-based tomography it has been shown that a key factor for obtaining reasonable reconstructions of large scale structures in the ionosphere is the use of proper apriori information on the vertical structure. This is due to the insensitivity of the ground links to the vertical structure, which in turn is due to the lack of links that cross the ionosphere in a tangential geometry. These links can only be provided by an occultation geometry, in which a transmitting satellite is setting or rising behind the Earth's atmosphere as seen by a receiver in space.

The strength of data obtained from space in an occultation geometry over those obtained from the ground is examined through covariance analysis and simulation in 2-D. Other means of analyzing occultation data when there are not sufficient intersecting links to do a full tomographic reconstruction are presented.

One possible way of obtaining occultation data is through use of signals transmitted by satellites of the Global Positioning System (GPS) and received by one or more other satellites in LEO. A single LEO satellite tracking the 24 GPS satellites will provide 500-700 globally distributed occultations daily. The first opportunity to make occultation observations from space will come with GPS-MET, a prototype orbiting occultation mission scheduled to launch late 1994. Future potential missions include having GPS receivers on a large constellation of communication satellites such as Teledesic, Iridium, Orbcom and Globalstar. Coverage and potential 3-D tomography with the Iridium constellation (which consists of 66 LEO satellites in 6 polar orbital planes) are discussed.

GH3b-1
1400

## A GENERATION MECHANISM FOR THE DOWNSHIFTED PEAK IN STIMULATED ELECTROMAGNETIC EMISSION SPECTRUM

J. Huang and S. P. Kuo
Weber Research Institute
Polytechnic University
Route 110, Farmingdale, NY 11735

In the recent ionospheric heating experiments, some secondary electromagnetic waves which cover a frequency band of the order of 100 KHz around the pump frequency has been measured directly on the ground. The spectrum of these waves, so called stimulated electromagnetic emissions (SEEs), are richly structured and very sensitive to the electron cyclotron harmonic resonances. A classification of these spectral features is given in detail by Stubbe et al. (J. Geophys. Res., 89, 7523 1984).

The spectral feature investigated in the present work is known as the downshifted peak (DP). It appears when the heater wave frequency $f_0$ is close to the third harmonic of electron cyclotron frequency $f_c$, and when the down shifted maximum (DM) is quenched. Its offset frequency (1~3 KHz) decreases as $f_0$ is increased toward $3f_c$ (Stubbe et al., J. Geophys. Res., 99, 6233, 1994). Sometimes a second downshifted peak (2DP) with offset frequency twice that of the DP feature and an upshifted peak (UP) located in the mirror position of the DP feature can also be observed.

In the present work, a generation mechanism for the DP feature is proposed as follows: The heater excited electron Bernstein pump wave first decays into a backward propagating electron Bernstein wave and a nearly perpendicularly propagating ion acoustic wave (i.e., electrostatic ion cyclotron wave). The sideband electron Bernstein wave, having a frequency downshifted from the HF heater wave by an amount of $f_{ia}$, can scatter off field-aligned density irregularities to produce the DP emission line. The 2DP and UP lines can also be generated through further cascading and multiple scattering processes. It is found that the instability threshold field can be readily exceeded by the present heating power in a very small frequency range near $3f_c$, and the offset frequency of the DP feature decreases as $f_0$ increases toward $3f_c$, consistent with the experimental observations.

GH3b-2
1420

## STIMULATED ELECTROMAGNETIC EMISSIONS EXCITED BY HIGH POWER RADIO WAVES

P.A. Bernhardt[1], L.S. Wagner[2], J. Goldstein[2], V.Yu. Trakhtengerts[3], E.N. Ermakova[3], V.O. Rapoport[4], G.P. Komrakov[4]
[1]Plasma Physics Division, Naval Research Laboratory
Washington, DC 20375-5320
[2]Information Technology Division Naval Research Laboratory
Washington, DC 20375-5320
[3]Institute of Applied Physics Nizhniy Novgorod, Russia
[4]Radiophysical Research Institute Nizhniy Novgorod, Russia

Stimulated electromagnetic emissions (SEE) have been generated by high power transmissions from the SURA facility in Russia by research groups from Russia, Sweden and the United States. The origin of these emissions may be (1) upper hybrid waves that parametrically decay to electromagnetic (EM) emissions, (2) Langmuir waves that are mode converted into EM waves, or (3) waves excited by electron beams that are produced by electron acceleration from the HF wave interaction regions. Multiple frequency heating experiments have been designed to distinguish between these various excitation processes. In March 1993, two powerful waves with frequency separations greater than 0.5 MHz are simultaneously transmitted at the SURA facility. The large frequency difference permitted excitation of two widely spaced altitudes near where each of the two waves reflected in the F-region. The results of the experiments showed that the SEE was enhanced at one frequency when a second, higher frequency wave was turned on. If the second powerful wave was lower in frequency, then the SEE enhancement was not recorded. The results of these experiments can be attributed to direct ponderomotive effects of one powerful wave on the other and they seem to eliminate the effects of field-aligned irregularities or electron beams on the SEE enhancements.

GH3b-3
1440

## CONVECTIVE SATURATION OF LANGMUIR WAVES DURING IONOSPHERIC MODIFICATION OF A BARIUM CLOUD

Prof. Martin V. Goldman and Dr. David L. Newman
Department of Astrophysical, Planetary, and Atmospheric Sciences
University of Colorado
Boulder, CO 80309-0391

Dr. R. Paul Drake and Dr. B.B. Afeyan
Lawrence Livermore National Laboratory
Plasma Physics Research Institute
PO Box 808
Livermore, CA 94550

In recent experiments (F.T. Djuth, M.P. Sulzer, J.H. Elder and K.M. Groves, "The CRRES AA-2 Release; HF Wave-Plasma Interactions in a Dense BA+ Cloud", submitted to Journal of Geophysical Research, December, 1993), a parametric electron-ion decay instability was excited by an ordinary-wave HF pump during an ionospheric chemical release from a rocket over Arecibo, PR, which created an artifical "barium ionosphere," with peak plasma frequency above the pump frequency, and a density gradient with a (short) 5 km scale length. Simultaneous incoherent scattering measurements revealed a strong initial asymmetry in the amplitudes of almost vertically upgoing versus downgoing measured plasma waves. We account for this asymmetry in terms of linear convective saturation of parametrically unstable plasma waves originating from a range of altitudes. The more intense measured downgoing wave receives contributions from initially upgoing waves which are doubly amplified - both before and after reflection. The less intense measured upgoing wave, originating from lower altitudes, is only singly amplified.

GH3b-4 VERY LOW FREQUENCY AND HIGH FREQUENCY WAVES
1500 GENERATED BY A MODULATED ELECTRON BEAM

N. B. Myers and J. Ernstmeyer
Rome Laboratory/ERCP
31 Grenier St
Hanscom AFB, MA 01731-3010
W. J. Raitt
Utah State University
Physics Department
Logan, UT 84322

The CHARGE-2B sounding rocket launched March 28, 1992, was the first space experiment with the primary objective of generating waves using an electron beam as a virtual antenna. The payload carried an electron gun capable of modulating the beam current between 4 and 19 kHz. A free-flying sub-payload obtained measurements of the three-axis electric and magnetic wave fields at distances of up to 2 km. The electron beam current was sinusoidally modulated, and proved to be very effective at generating VLF waves at the fundamental modulation frequency. In addition, higher harmonics were often generated, and HF waves were stimulated. A neutral gas release system was flown to determine the effects of vehicle potential on the wave generation capabilities of the electron beam.

GH3b-5 "Studies of Plasma Turbulence with the Versatile Toroidal
1520 Facility (VTF) for Ionospheric Plasma Modification"
D.T. Moriarty, S.M. Murphy, R. Riddolls, M.C. Lee
Plasma Fusion Center
Massachusetts Institute of Technology
Cambridge, Massachusetts 02139

Laboratory experiments have been conducted with the Versatile Toroidal Facility (VTF) to investigate plasma turbulence, aimed at simulating the ionospheric plasma environment and cross-checking some ionospheric heating experiments. VTF is a large plasma device which can generate magnetized plasmas with sharp density gradients and intense magnetic field-aligned currents. The VTF plasmas have the key characteristics of ionospheric plasmas, especially in the auroral region. Short and long pulses of electron beams are injected into the VTF to study the excited plasma waves. Our experiments show that the VTF plasma turbulence is structured with both high-frequency and low-frequency wave modes. Such a plasma turbulence can be similarly produced by sharp plasma density gradients and/or field-aligned currents in the ionospheric F region and in the topside ionosphere. The results of the VTF laboratory experiments are compared with those of rocket experiments in space. We show that VTF can adequately simulate the naturally occurring plasma turbulence in the auroral ionosphere and complement the active ionospheric plasma experiments.

Session G-5, 0900-Sat., CR2-26
RADAR TECHNIQUES WORKSHOP
Chairperson and Organizer: John C. Foster, MIT Haystack Observatory, Route 40, Westford, MA 01886

INDEX

**Thursday, 5 January (cont.)**

*1015-1220*

| | | |
|---|---|---|
| F/G/H-1a | ACTIVE REMOTE SENSING-I | CR2-6 |

*1335-1520*

| | | |
|---|---|---|
| F-5 | PROPAGATION MEASUREMENTS FROM THE ADVANCED COMMUNICATIONS TECHNOLOGY SATELLITE (ACTS) | CR1-9 |

*1335-1700*

| | | |
|---|---|---|
| F/G/H-1b | ACTIVE REMOTE SENSING-II | CR2-6 |
| G/H-2 | INVESTIGATIONS OF DUSTY PLASMAS AND POLAR MESOSPHERE SUMMER ECHOES | CR2-26 |
| J-3 | INSTRUMENTAL LIMITS AND OBSERVING TECHNIQUES | CR0-30 |

*1355*

| | | |
|---|---|---|
| B/D-2 | APPLICATIONS OF NEW MATERIALS FOR ELECTRONICS, DEVICES, AND SYSTEMS | CR2-28 |
| C-2 | DETECTION AND ESTIMATION | CR1-42 |

*1535-1740*

| | | |
|---|---|---|
| F-6 | MOBILE AND PERSONAL ACCESS RADIO PROPAGATION | CR1-9 |

*1700-1800*

| | |
|---|---|
| Commission B Business Meeting | CR2-28 |
| Commission C Business Meeting | CR1-42 |
| Commission G Business Meeting | CR2-6 |
| Commission J Business Meeting | CR0-30 |

**Friday, 6 January**

*0835-1200*

| | | |
|---|---|---|
| B/D-3 | TUTORIAL SESSION ON FINITE DIFFERENCE TIME DOMAIN TECHNIQUES | CR1-46 |
| F-7 | PROPAGATION, SCATTERING, AND EXTRACTING SURFACE FEATURES | CR1-9 |
| J-4 | WIDE FIELD MAPPING AND SURVEYS | CR0-30 |

*0855-1200*

| | | |
|---|---|---|
| B-2 | ANTENNAS | CR2-28 |
| G-3 | NATURAL AND SHUTTLE-INDUCED IONOSPHERIC VARIABILITY | CR2-26 |
| G/H-3a | IONOSPHERIC MODIFICATION WITH HIGH POWER RADIO WAVE-I | CR2-6 |

*1335-1700*

| | | |
|---|---|---|
| G-4 | TOMOGRAPHIC TECHNIQUES APPLED TO THE UPPER ATMOSPHERE | CR2-26 |

*1355-1520*

| | | |
|---|---|---|
| B-3 | FINITE METHODS | CR2-28 |

*1355-1540*

| | | |
|---|---|---|
| G/H-3b | IONOSPHERIC MODIFICATION WITH HIGH POWER RADIO WAVES | CR 2-6 |

*1455-1700*

| | | |
|---|---|---|
| B-4 | HIGH-FREQUENCY METHODS | CR1-46 |

*1555-1640*

| | | |
|---|---|---|
| G-2b | E- AND F-REGION IRREGULARITIES | CR2-6 |

**Saturday, 7 January**

*0900-1700*

| | | |
|---|---|---|
| G-5 | RADAR TECHNIQUES WORKSHOP | CR2-26 |